University of Milan

Doctorate School in Chemical Sciences and Technology

Chemistry Department

Course of Industrial Chemistry, XXVII Cycle

Synthesis of Nitrogen-Containing Compounds via Nitrene-Transfer Catalysed by Porphyrin Complexes

CHIM/03

Doctorate Thesis of

Paolo Zardi R09613

Tutor: Prof. Emma Gallo

Co-Tutor: Dott. Alessandro Caselli

Coordinator: Prof. Dominique Roberto

Academic Year 2013/2014

Summary

1. Introduction

1.1. The Porphyrin Ligand

1.1.1. Structure of the porphyrin ring

Porphyrin ligands are a class of heterocyclic macrocycles composed by four pyrrole units interconnected at the α carbons by methine bridges. Porphyrins are aromatic compounds since 26 π-electrons are delocalized all over the macrocyclic ring[1], thus respecting the Hückel rule (4*n*+2). Hence, the macrocycle forms a rigid and planar structure in which the four pyrrolic rings lay on an equatorial plane. Porphine is the parent porphyrin compound and its structure is represented in *Figure 1* along with the classification of the positions (α, β and *meso*).
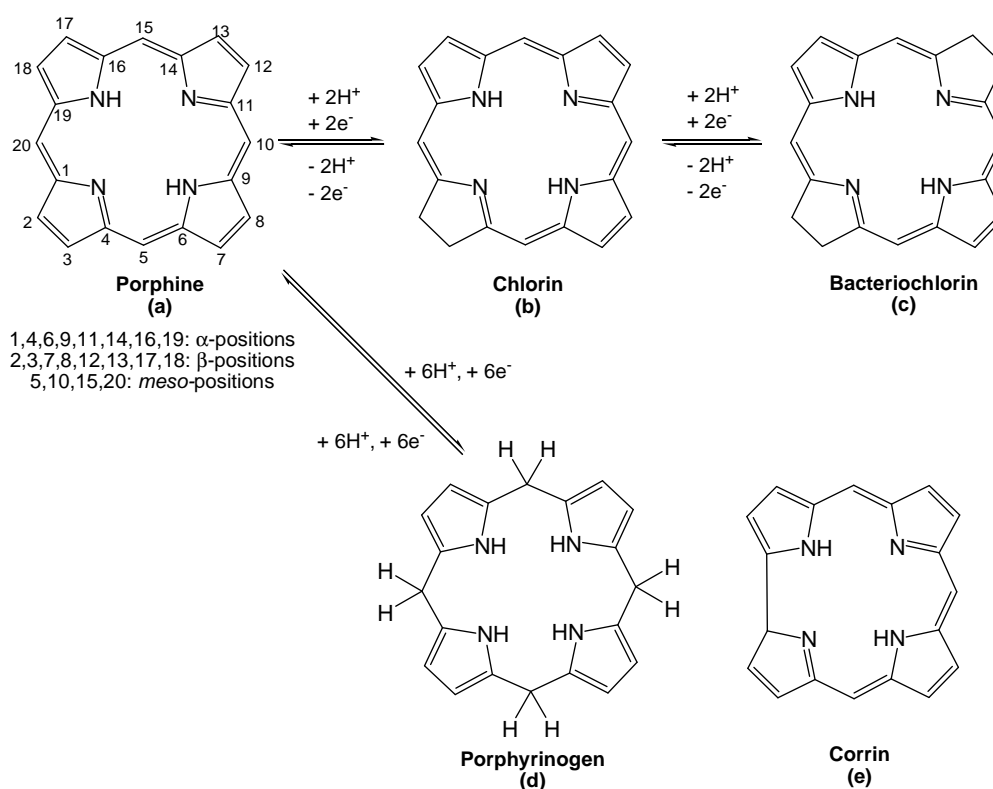
Figure 1. Porphine and other related tetrapyrrolic macrocycles.

Together with their reduced-aromatic forms (chlorins and bacteriochlorins in *Figure 1*) porphyrins and other tetrapyrroles derivatives are very recurrent compounds in all organisms. Among the most famous examples there are heme-proteins whose iron-porphyrin core is essential for their activity in a wide variety of biochemical processes and vitamin B_{12} which is based on a corrin macrocycle (*Figure 1*). These highly coloured ligands, due to their fundamental biological importance, have been named "the pigments of life".[2]

1.1.2 Synthesis of porphyrins

The first synthesis of a porphyrin was reported in 1926 by Hans Fischer[3] by using dipyrromethanes as starting materials. This synthetic strategy allowed the synthesis of the natural compound Protoporphyrin IX that was pivotal for Fischer's 1930 Nobel Prize award.

After this pioneering work, new routes for the synthesis of *meso*-substituted porphyrins were developed by Rothemund, who first investigated the synthesis of *meso*-tetramethylporphyrin by the reaction between pyrrole and acetaldehyde in 1935.[4]

This protocol was improved by Adler and Longo[5] who found that porphyrins can be synthesised reacting benzaldehydes and pyrrole in refluxing propionic acid (***Scheme 1***). This reaction allows the conversion of a wide variety of benzaldehydes in the corresponding *meso*-substituted porphyrins in yields up to 20%. This method is still one of the most convenient to rapidly obtain a good amount of crystalline and relatively pure material, however, the harsh reaction conditions do not allow the synthesis of derivatives carrying sensitive functional groups and the purification may be difficult since a large amount of by-products is obtained. To limit these problems minor modifications may be applied, such as the use of a reaction solvent with a lower boiling point (e.g. acetic acid, nitrobenzene/acetic acid mixture) or the use of microwave irradiations.[6]
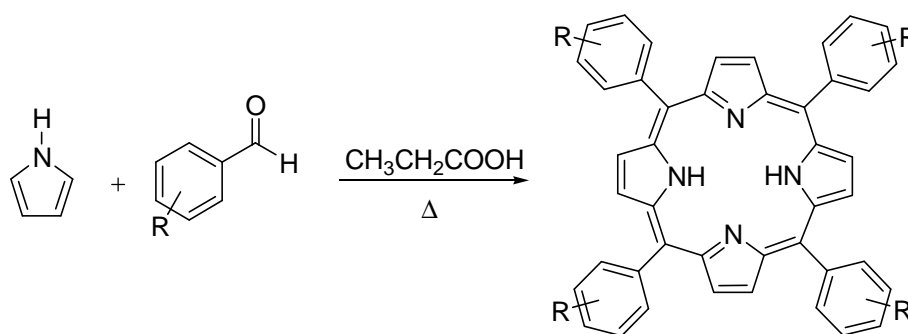
Scheme 1. *The classical Adler and Longo's synthetic methodology for meso-tetraarylporphyrins.*

In 1987 Lindsey and co-workers proposed a porphyrin synthesis at milder reactions conditions via porphyrinogen[7] (***Scheme 2).*** In this method a pyrrole and an aromatic aldehyde react at room temperature under anaerobic conditions in the presence of an acid catalyst (e.g. $BF_3 \cdot Et_2O$) establishing an equilibrium with the porphyrinogen species, then after the addition of an oxidizing agent, such as 2,3-dichloro-5,6-dicyano-1,4-benzochinone (DDQ), the porphyrinogen undergoes oxidative aromatisation to give the porphyrin. This method has the advantage that sensitive aldehydes can be employed for porphyrin synthesis, the final product has an easier purification and

it is obtained in good yields (30-40%). However, the Lindsey method requires diluted solutions (10^{-2} M) to optimize the porphyrinogen formation, thus making more difficult the reactions on a large scale.
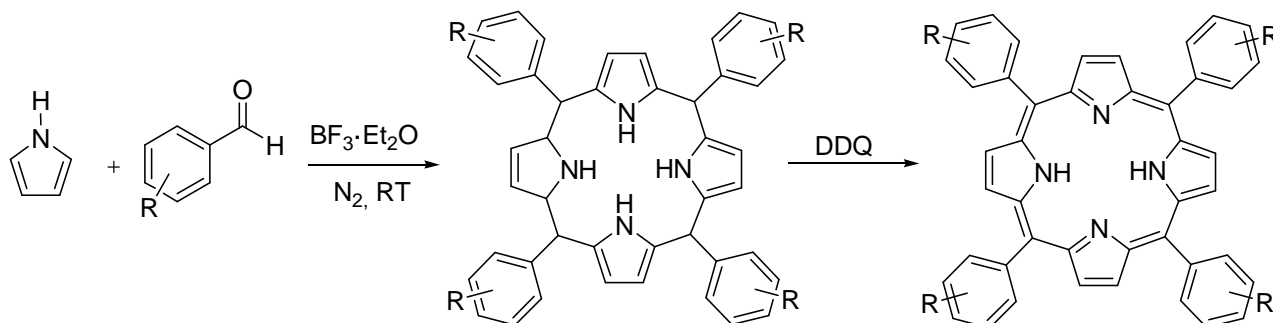
Scheme 2. Lindsey's methodology.

Adler's and Lindsey's methodologies, and all their modifications and improvements in the recent years, are useful strategies to synthesise a large variety of porphyrins carrying identical substituents at the *meso* and/or β positions with a plethora of possible structural and electronic properties.

Many other synthetic strategies to synthesise asymmetric porphyrins, that for example carry different groups at the *meso* positions or differently substituted pyrrole units, were developed but these methods will not be discussed since these compounds were not employed in the present thesis.

1.2. Porphyrin Complexes

The majority of elements in the periodic table form complexes with porphyrins, the highly stable macrocyclic ring and the rigid structure make these compounds a unique class of ligands. Porphyrins are called "free-base" in their neutral form, with two protonated pyrrolic units, when these protons are removed the porphyrin becomes a tetradentate dianionic ligand capable to coordinate a metal ion in the central cavity of the macrocycle.

Metal fragments bonded to the porphyrin ligand can exist in a wide range of oxidation number, electronic and spin state. Their stability to demetalation varies depending on many factors. The empirical stability is defined on acid resistance: the most stable metalloporphyrins are fully resistant to 100% sulphuric acid while the least stable are demetalated by neutral water.

The ion size is an important factor for metalloporphyrins, if the metal atom fits reasonably well into the central cavity, as generally late transition metals do, only two mutually *trans* sites are available and a great control over the coordination environment is achieved (***Figure 2,*** entry a). Conversely, early transition metals tend to be too large to fit in the central cavity, so they coordinate at one side of the porphyrin and have additional ligands placed *cis* (***Figure 2,*** entry b).
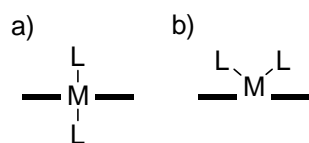
Figure 2. *General coordination mode for porphyrin complexes.*

1.2.1 Synthesis of Metalloporphyrins

Different routes have been employed for the insertion of a metal or a M-L$_n$ fragment into a porphyrin ring, mostly depending on the nature of the metal source. In the present thesis two main synthetic strategies were employed:

A) Coordination of a metal from a M(II) salt: the synthetic procedure simply consists in allowing the free-base and a divalent metal salt to react in the opportune solvent, in order to get the porphyrin ligand and the metallic reagent simultaneously in the solution under reactive conditions. Usually, good solvents for porphyrins in their neutral forms are generally poor solvents for simple metallic ions and vice versa. Adler and co-workers[8] proved that refluxing *N,N*-dimethylformamide (DMF)

is a useful reaction solvent, the desired M(porphyrin) complex is obtained in short reaction times with good to excellent yields for a number of bivalent metals (M = Zn, Co, Cu, Ni, Fe, Cr, Mn, Pb, Pd, Hg, Cd etc.) (**Scheme 3**). The addition of a weak Brønsted base promotes the reaction rate by removing the two pyrrolic protons of the free base.

$$Zn^{II}(OAc)_2 + LH_2 \xrightarrow{\text{DMF}} Zn^{II}(L) + 2\ AcOH$$

$$Co^{II}Cl_2 + LH_2 \xrightarrow{\text{DMF}} Co^{II}(L) + 2\ HCl$$

L = porphyrin ligand
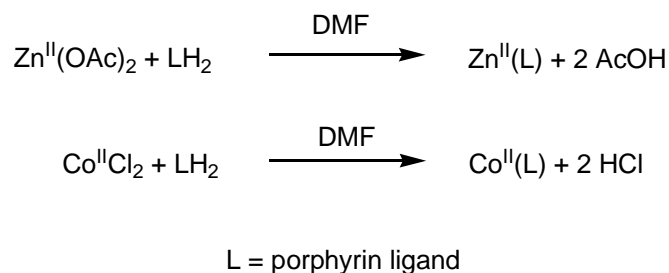
Scheme 3. *Synthesis of metalloporphyrins via a metathesis reaction.*

B) Coordination/oxidation of the metal source: In some cases, an external oxidant has to be added to the reaction mixture to promote the variation of the metal oxidation state in order to have an isolable and stable product. For example, using a Fe^{II} metal source initially an iron(II) porphyrin intermediate is formed, then it is oxidized to the more stable iron(III) complex during the work-up in air and in the presence of a donor ligand (for example Cl^- from aqueous HCl solution). For other metals stronger oxidants are necessary to promote the formation of the product, for example, the insertion of rhodium as Rh^{III} in a porphyrin ligand is accomplished starting from a carbonyl complex of Rh(I) ($[Rh(CO)_2Cl]_2$) in the presence of molecular iodine as the oxidant.

Spontaneous oxidation can occur when a M(0) clusters are used as metal sources. The more extensively reported way for the preparation of ruthenium(II)-carbonyl and osmium(II)-carbonyl complexes[9] involves the reaction between the free-base porphyrin and the neutral metal cluster $M_3(CO)_{12}$ in a high-boiling solvent, such as decahydronaphthalene or diethylen glycol monomethyl ether. In these cases a spontaneous oxidation of the metal from 0 to +2 occurs, formally promoted by the two protons displaced from the free-base as molecular hydrogen.

$$Fe^{II}Br_2 + LH_2 \xrightarrow[O_2]{Cl^-} Fe^{III}(L)(Cl) + 2H^+$$

$$1/2\ [Rh^I(CO)_2Cl]_2 + LH_2 \xrightarrow{+\ 1/2\ I_2} Rh^{III}(L)(I) + 2CO + 2H^+ + I^- + Cl^-$$

$$1/3\ Ru_3{}^0(CO)_{12} + LH_2 \longrightarrow Ru^{II}(L)(CO) + 3CO + H_2$$

L = porphyrin ligand
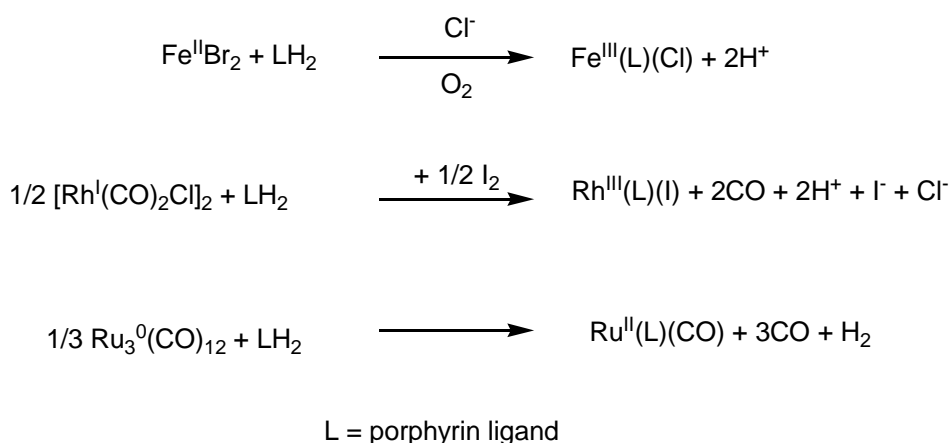
Scheme 4. *Synthesis of metalloporphyrins through the coordination/oxidation protocol.*

1.2.2. Catalytic Activity of Metalloporphyrins in Nature

The most naturally abundant metalloporphyrin is the iron complex of protoporphyrin IX (***Figure 3***). The porphyrin ligand is peripherally substituted by an alkyl or an alkenyl residue at each *β* position, as observed for most natural occurring species. Heme B and its derivatives are the prosthetic group for a large number of biological active proteins with many different functions. Among the most studied heme-containing systems, cytochromes P-450 occupy a prominent role. The P-450 domain is present in many monooxygenase, important enzymes for many metabolic pathways, whose function is to insert a hydroxyl moiety in a determined organic substrate. The oxidation of nonactivated hydrocarbons is promoted by members of the cytochromes P450 family at physiological temperature by the activation of molecular oxygen.
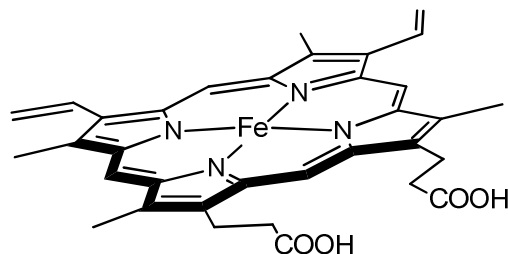
Figure 3. *Iron(II) protoporphyrin IX complex also known as Heme B.*

The best structurally and biochemically characterized P450 is the soluble protein P-450cam, which is able to promote the regioselective camphor hydroxylation at 5-*exo* position and was studied to model the catalytic activity of cythochromes P450.[10] The catalytic cycle is described in ***Scheme 5***.

The resting state is the hexacoordinated iron(III) complex **A** that is activated by the removal of the sixth ligand and one-electron reduction from a coenzyme to give a pentacoordinated iron(II) complex **B** that is able to coordinate molecular oxygen. The O_2 activation occurs through the cleavage of the O=O bond by addition of one electron from a coenzyme and of two protons to release a water molecule. A very reactive Fe^V=O intermediate is formed and it is stabilized by the donation of one electron from the porphyrin ligand generating the radical Fe^{IV} intermediate **G**. This latter compound is able to insert an oxygen atom into a camphor C-H bond through a very regio- and stereoselective process. The exact nature of the species responsible for the oxygen insertion is a matter of debate but the formation of an iron oxo species such as complex **G** is mostly accepted[11]. The biological pathways can be "short-circuited" by using hydrogen peroxide instead of O_2 as the oxidizing agent (so-called "peroxide shunt" in *Scheme 5*).
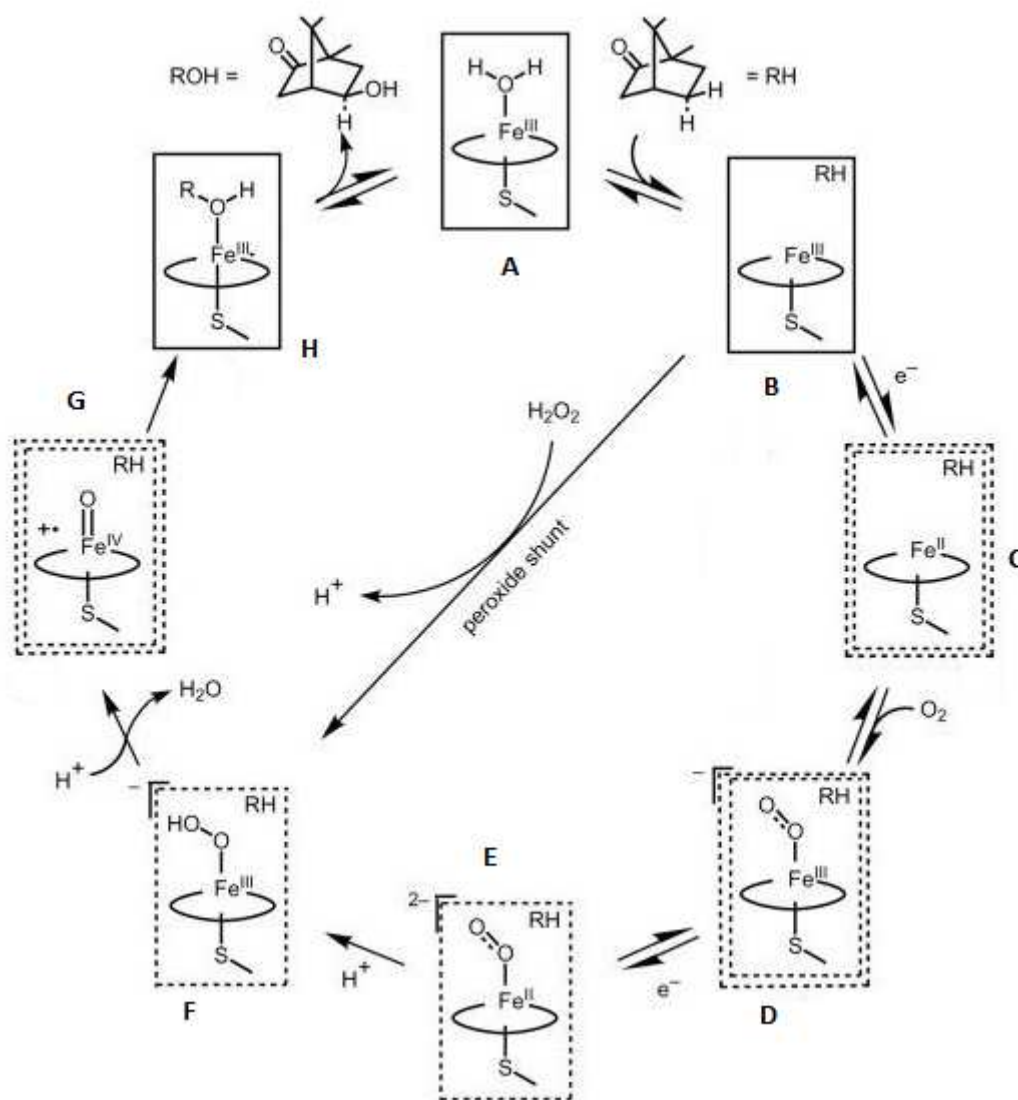
Scheme 5. *Catalytic cycle of P450cam for regioselective camphor oxidation.*

Many efforts have been made to synthesise iron porphyrins as artificial counterparts of the biological systems. The first reported biomimetic system for catalytic hydrocarbon oxidation by the "peroxide shunt pathway" was published by Groves *et al* in 1979.[12] They showed that alkene epoxidation and alkane hydroxylation could be performed by Fe(TPP)Cl using PhIO as the oxygen donor. The main problem of this system was the irreversible oxidation of the iron center, because, in absence of the biological superstructrure of heme-proteins, a significant amount of catalytically inactive μ-oxo iron(III) porphyrin dimers is produced. A number of hindered iron-porphyrins systems was developed in order to better mime the protein environment of heme-proteins and to prevent irreversible dimerization/oxidation.[13] Among this biomimetic systems the so-called "picket fence" porphyrins[14] are an important class of ligands, their corresponding iron(II)-complexes were studied as models of hemoglobin for oxygen binding (***Figure 4***).[15]
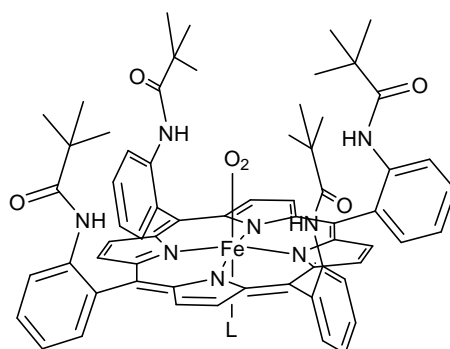

Figure 4. *Example of iron(II) picket fence porphyrin complex, L = N-methyl imidazole.*

1.2.3 Ruthenium Porphyrin Complexes

Ruthenium coordinates strongly to the porphyrin ligand, these complexes cannot be completely demetalated even in the presence of concentrated sulphuric acid. An interesting chemistry is related in these compounds because of the intriguing possibility to have species in an oxidation state ranging from -2 to +6.

Initially ruthenium porphyrins were studied to reproduce the behaviour of cytochrome P450 systems for oxygen activation because of their relationships to iron-porphyrins. These two metals lay on the same group of the periodic table and, therefore, share the same electronic structure in the outer shell. Indeed, in the 80's high-valent dioxo ruthenium(VI) porphyrins were found to be able to activate molecular oxygen and to perform catalytic olefin epoxidation.[16]

The first investigations concerning ruthenium porphyrin complexes were restricted to carbonyl complexes [Ru^{II}(porph)(CO)], common product of the insertion of ruthenium in the free-base porphyrin. These compounds are stable and do not undergo metal oxidation in air atmosphere, conversely to the related iron(II) porphyrin complexes, thanks to the π-acceptor CO ligand which is strongly bound to the metal centre.

Two routes are possible to remove the carbonyl ligand, the first is the photochemical ejection in a suitable coordinating solvent (e.g. pyridine) obtaining complexes of the general formula Ru^{II}(porph)(solvent)$_2$. The second method is the oxidative removal leading to high-valent ruthenium porphyrin complexes; for example, in 1984 Groves reported the first synthesis of a dioxo-ruthenium(VI) porphyrin complex by the reaction of Ru^{II}(TMP)CO (TMP = dianion of *meso*-tetramesitylporphyrin) with *meta*-chloroperbenzoic acid[17]. This complex has a truly biomimetic behaviour since it can transfer the oxygen moiety to an organic substrate[16], furthermore, because ruthenium porphyrin are more inert to substitution then the first-row congeners, Ru^{VI}(porph)(O)$_2$ are good systems for mechanistic investigations. Several dioxo-ruthenium(VI) porphyrin complexes were synthesised and found to be active species for oxygen transfer reactions[18], many systems based on ruthenium porphyrin were developed to perform catalytic olefin epoxidation and hydrocarbons oxidation mainly using *N*-oxide heterocycles as the oxygen donor (***Scheme 6***).[19, 20]
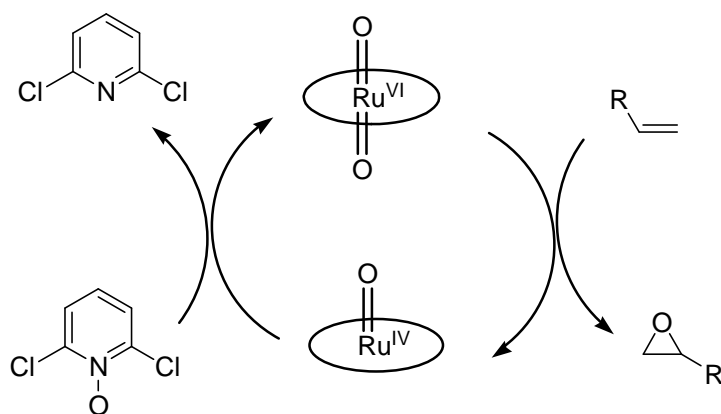
Scheme 6. *Proposed mechanism for alkene epoxidation using pyridine N-oxides as the terminal oxidants.*

Collman and co-workers proposed a mechanism for the Ru^{II}(porph) oxidation by reaction of the ruthenium complex with molecular oxygen (***Scheme 7***). At first the μ-peroxo dimer **A** should be formed, then the homolytic cleavage of the O-O bond gives the elusive species $[Ru^{IV}$(porph)(O)] **B**. Then, depending on the sterical properties of the porphyrin ligand, **B** undergoes a disproportionation reaction that leads to a ruthenium dioxo complex (**D**), otherwise a μ-oxo ruthenium porphyrin dimer (**C**) may be formed by formal addition of a water molecule. The oxidation of the sterically encumbered Ru^{II}(TMP)CO leads to a Ru^{VI}-dioxo species, conversely, if the porphyrin ligand carries less hindered *meso*-aryl groups, a μ-oxo-Ru^{IV} porphyrin dimer species is formed under the same reaction conditions. This was the case when Ru^{II}(TPP)CO or Ru^{II}(TTP)CO were used as starting reagents[17] (TPP = dianion of tetraphenylporphyrin, TTP = dianion of tetratolylporphyrin).
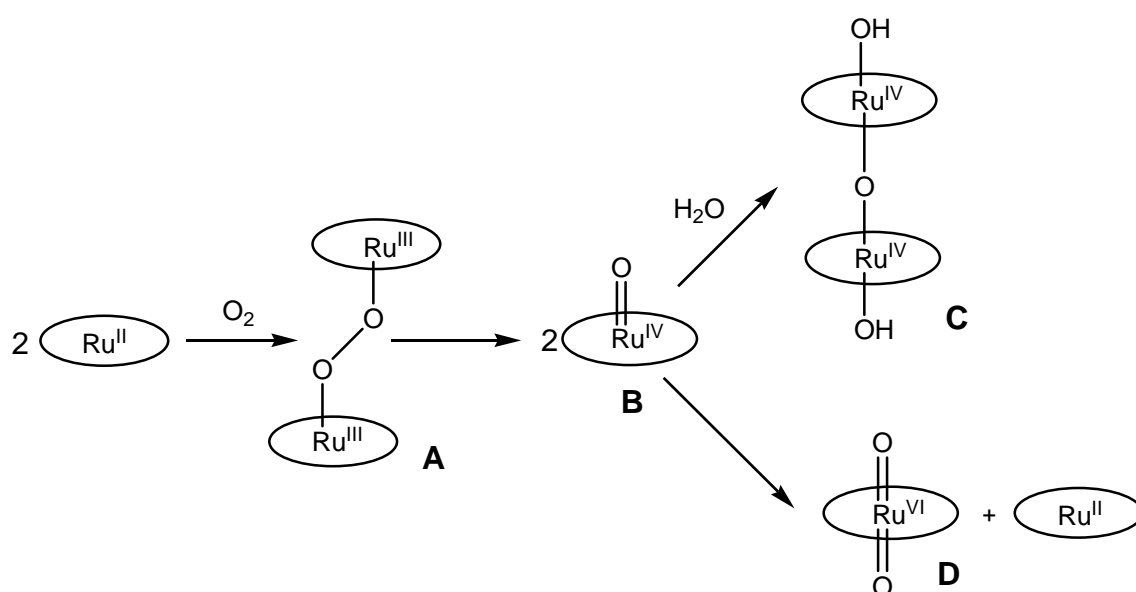
Scheme 7. *Mechanism of oxidation of Ru(II) porphyrin complexes by dioxygen.*

Also the solvent seems to play a key role to control the reaction outcome, it has been shown that $Ru^{VI}(TPP)(O)_2$ can be obtained even if the porphyrin ligand is sterically unhindered in the presence of a weak coordinating solvent such as an alcohol.[21]

The synthesis of oxo-bridged dimers was studied in the early 80's using as starting material ruthenium(II)-carbonyl complexes of unhindered porphyrin ligands, such as TPP and OEP (octaethylporphyrin dianion). The first report concerns the oxidation of Ru(OEP)CO by *tert*-butylhydroperoxide to give the dimer complex $[Ru^{IV}(OEP)(OH)]_2O$[22], which is highly stable and diamagnetic, generally unexpected for ruthenium(IV) complexes. μ-Oxo dimers easily exchange the axial ligand under acidic conditions and a number of compounds of the general formula $[Ru^{IV}(porph)(L)]_2O$ were produced.[23] However, these compounds did not find any particular application because the μ-oxo dimers are generally highly stable and do not transfer the oxygen moiety, therefore, $[Ru^{IV}(porph)(L)]_2O$ do not promote hydrocarbon oxidation reactions. Only recently Zhang and co-workers[24] created an efficient catalytic system in which ruthenium μ-oxo porphyrin dimers catalyse the oxidation of hydrocarbons upon photochemical activation (***Scheme 8***).

Under irradiation with visible light (λ = 350 nm) of $[Ru(TPP)(OH)]_2O$ underwent a photodispoportionation generating an elusive and highly reactive $Ru^V=O$ species[25] which was responsible for oxygen transfer to a double bond or for oxygen insertion in a C-H bond of many different hydrocarbon substrates. After the rapid hydrocarbon oxidation step the so-obtained $Ru^{III}(TPP)OH$ was oxidized by atmospheric oxygen to give the starting $[Ru(TPP)(OH)]_2O$ catalyst.
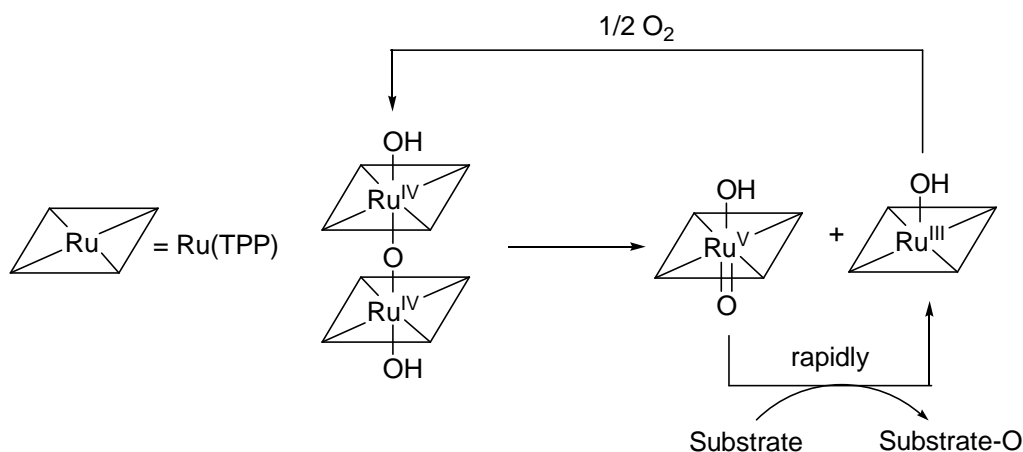
Scheme 8. *The catalytic system developed by Zhang.*

1.3. Metalloporphyrin-Catalysed Amination Reaction

The biological and pharmaceutical activities of organonitrogen compounds prompted the scientific community to develop new methods for the direct and selective C‑N bond formation in order to synthesise useful fine chemicals in an economical fashion and using environmentally benign technologies. Recently, the use of nitrene precursors for the introduction of a "NR" moiety into an organic molecule received special attention and many reviews have been published on this subject.[26, 27]

Nitrenes are the nitrogen analogues of carbenes and their reactivity is due to the presence of four non-bonding electrons. These species can exist in two different spin states: in a singlet state nitrene the electrons are arranged as two lone pairs, whereas, if the electrons are present in three orbitals, one filled and two semi-filled, the corresponding nitrene is in a triplet state and shows a diradical behaviour (*Figure 5*). In both cases, nitrenes are not stable as free molecules and react very easily with a great variety of organic substrates.
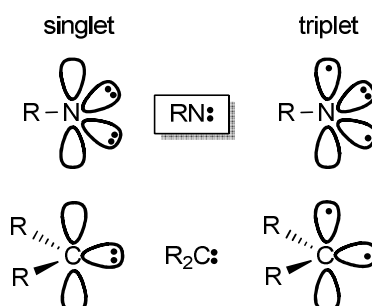
Figure 5. Singlet and triplet states for nitrenes and carbenes.

Typical nitrene sources used for the synthesis of nitrogen-containing molecules are reported in *Figure 6*. The "classical" nitrene source for amination reactions are iminophenyliodinanes (PhI=NR) that can be also formed *in situ* by the reaction of the corresponding amine (RNH_2) with an oxidant such as $PhI(OAc)_2$ or PhIO. As indicated below, iminophenyliodinanes suffer from several drawbacks, therefore alternative nitrogen sources such as chloramine-T (TsN(Cl)Na) (Ts=tosyl), bromamine-T (TsN(Br)Na) and especially organic azides (RN_3) were recently investigated.
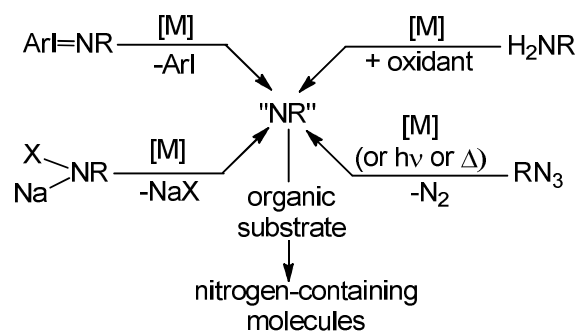
Figure 6. *General scheme for the nitrene formation and transfer.*

The formation of the "RN" moiety is promoted by transition metals that can also selectively drive the nitrene transfer towards organic molecules. Transition metal complexes of porphyrins were shown to be very efficient in both stoichiometric and catalytic nitrene transfer reactions.

The aim of this section is to examine a selection of papers concerning the activity of metalloporphyrins in several nitrene transfer reactions using different nitrene sources to give an overview of the potentiality and limits of these methodologies. A particular attention will be given to the ruthenium-porphyrin-catalysed amination using aryl azides as nitrene sources.

1.3.1. ArI=NR as nitrene sources

The synthesis of a new type of iodine-nitrogen ylide, *N*-tosylimino aryliodinane together with a study of its reactivity was reported by Yamada in 1975[28] but it was the group of Evans to develop the nitrene transfer to olefins by PhI=NTs into a synthetically useful method.[29] Breslow and Gellman[30] in 1982 demonstrated that PhI=NTs, the tosylimido analogue of iodosobenzene, is active in the M(TPP)Cl (M = Mn(III), Fe(III)) catalysed C‑H amidation of cyclohexane (*Scheme 9*). The fact that even cytochrome P-450 is catalytically active indicated that this reaction can be considered a "nitrogen version" of the hydroxylation of C‑H bonds performed in Nature.
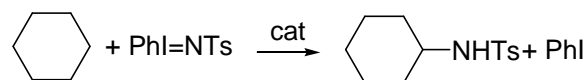
cat = Fe(TPP)Cl or Mn(TPP)Cl or cytochrome P-450
Ts = tosyl

Scheme 9. *C‑H amidation of cyclohexene.*

The recovered yield of the aminated product was very low (3–8%) but since the publication of the previously cited papers several efforts were devoted to improve the efficiency of the amination of alkanes, reagents that generally show low chemical reactivity. Nitrene insertion reactions occur more easily into activated C–H bonds such as allylic and benzylic ones.[31] In fact, the synthesis of allylic and benzylic amines was efficiently catalysed by manganese porphyrin complexes also when using natural products such as equilenin acetate[32] (**Scheme 10**) as starting materials.

TFPP = dianion of 5,10,15,20-tetrakis(pentafluorophenyl)porphyrin
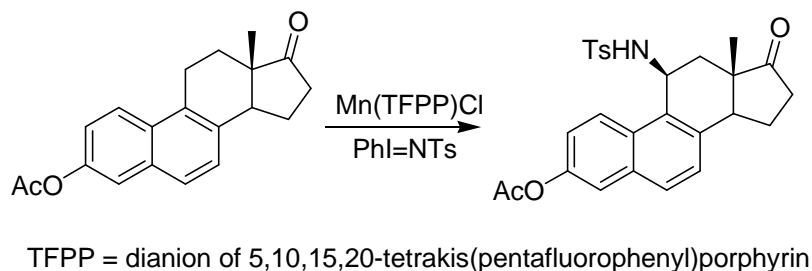
Scheme 10. *Selective amidation of a benzylic C-H bond of equilenin acetate.*

A mechanism for this reaction was initially proposed by Mansuy and co-workers.[33] As shown in **Scheme 11**, the insertion of the "NR" moiety into the C‑H bond should occur through a hydrogen atom abstraction by a metallo-nitrene intermediate complex. The formation of an active imido intermediate was suggested on the basis of the analogy with the C‑H hydroxylation, in which a high valent metal-oxo compound is responsible for the oxidation reaction.
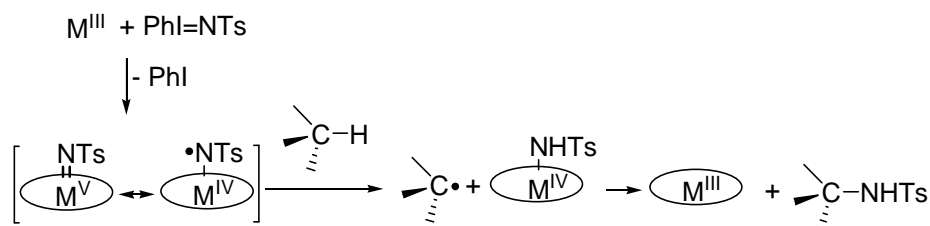
Scheme 11. *Proposed mechanism for the tosyl amidation of alkanes, catalysed by M(porphyrin)Cl (M = Mn^{III} or Fe^{III}) complexes.*

The possible existence of iron imido intermediates was supported by the isolation and characterization of complex **1** (**Scheme 12**) in which a nitrene functionality is bridging the metal centre and a nitrogen atom of the porphyrin ligand. Mansuy and co-workers proposed that **1** was formed by an insertion of the tosylimido moiety into the iron-pyrrolic nitrogen bond of the unstable terminal imido porphyrin complex.[34]
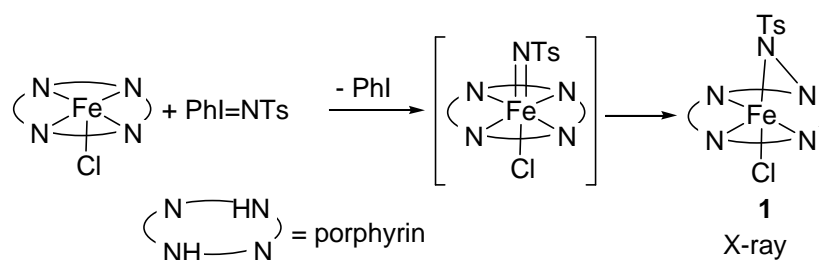
Scheme 12. Synthesis of the bridged iron nitrene porphyrin complex 1.

A significant progress in understanding the mechanism of the reaction was achieved by using ruthenium in place of iron because of the higher stability of the imido complexes, this substitution also allowed the improvement of the efficiency of the catalytic systems.[35]

To investigate the mechanism of the ruthenium-catalysed C–H amination, the reaction between ruthenium(II) porphyrin catalysts and the nitrene source $PhI=NSO_2R$ was investigated (*Scheme 13*). Notably, numerous *bis*-imido complexes of the general formula $Ru^{VI}(porphyrin)(NSO_2R)_2$ were isolated,[36-38] but unfortunately their poor stability prevented an X-ray characterization at that time and only very recently an X-ray single crystal structure of $[Ru^{VI}(TMP)(=NMs)]$ (**2**) (in which Ms = SO_2-*p*-MeO-C_6H_4) was obtained.[39] The general synthesis of ruthenium *bis*-tosylimido complexes is reported in *Scheme 13*.

2, $R_1 = 2,4,6\text{-}(Me)_3C_6H_3$, $R_2 = H$, $R_3 = 4\text{-}(MeO)C_6H_4$
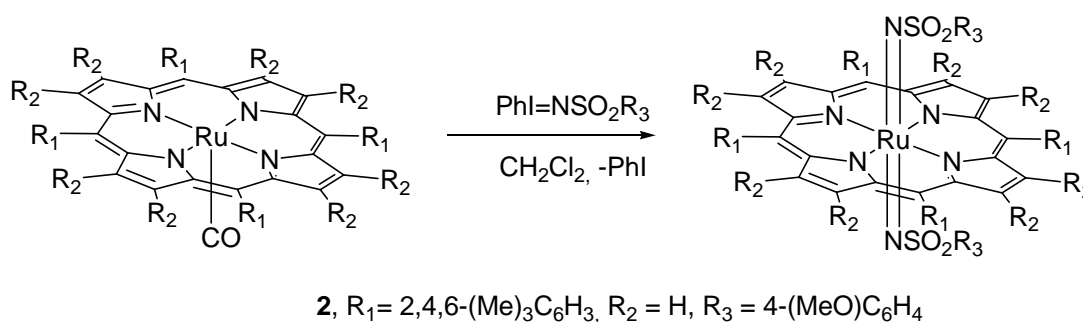
Scheme 13. Synthesis of ruthenium bis-tosylimido porphyrin complexes.

The nitrene functionalities of $Ru^{VI}(porphyrin)(NSO_2R)_2$ complexes are transferable to hydrocarbons affording the corresponding aminated species and uncharacterized ruthenium products. If the reaction was run in the presence of pyrazole, amido ruthenium porphyrin complexes were isolated and fully characterized (*Scheme 14*).
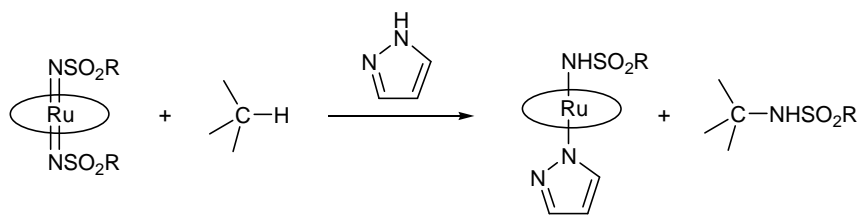
Scheme 14. *Nitrene transfer reaction from the bis-imido ruthenium complex to a hydrocarbon with the concomitant formation of a $Ru^{IV}(porphyrin)(NHSO_2R)(pz)$ complex.*

The nitrene transfer reaction was studied in detail by Che and co-workers and all collected data indicated the mechanism illustrated in **Scheme 15**.[37]
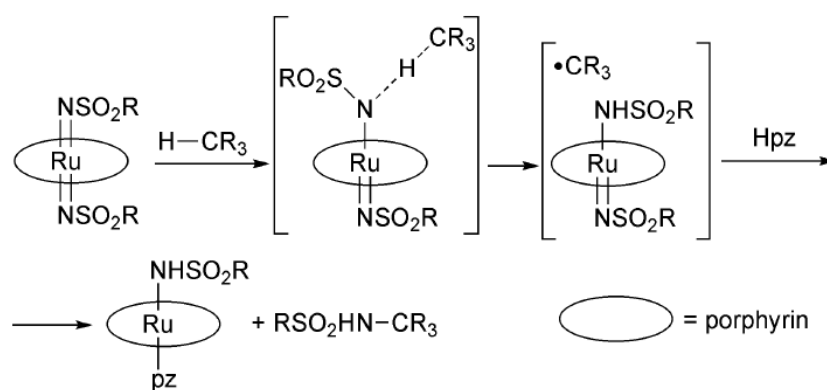
Scheme 15. *Proposed mechanism for the nitrene transfer reaction to hydrocarbons.*

The authors suggested that the amidation reaction proceeds *via* carboradical intermediates. A hydrogen atom abstraction by the ruthenium imido complex should occur on the periphery of the complex, since the imido moiety is bound to the coordinatively and electronically saturated ruthenium centre. Recently, the nitrene transfer reaction of **2** with ethylbenzene was investigated also from a theoretical point of view through DFT calculations.[39]

N-tosylimido compounds can be also employed to synthesise aziridines (**Scheme 16**). This class of molecules[40] show various biological properties and they represent useful building blocks in organic synthesis for the high reactivity of the three-membered ring. The first metalloporphyrin-catalysed synthesis of aziridines by a nitrene transfer reaction from iminoiodinanes was performed in the presence of iron and manganese complexes.[41]

cat = Fe(porph)Cl or Mn(porph)Cl
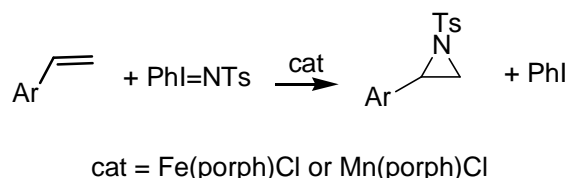
Scheme 16. *Aziridination reaction using N-tosylimidoiodinanes as nitrene sources.*

Stereospecific versions of this reaction were also developed using chiral porphyrin ligands obtaining the aziridine product in a moderate enantiomeric excess.[42] Ruthenium porphyrins also showed a very good catalytic activity in aziridination reaction with iminoiodinanes,[36] even in enantioselective reactions.[43] If the reaction is conducted using the $RNH_2/PhI(OAc)_2$ protocol, intramolecular aziridinations can also be performed.[44]

1.3.2. Chloramine-T and bromamine-T as nitrene sources

In spite of the extensive use of iminoiodinanes, there are some limitations for a practical application of this class of reagents. ArI=NR compounds are not commercially available and their synthesis is frequently not easy, they have poor solubility in common organic solvents and the process has not a good atom economy since the stoichiometric side product of the reaction is ArI. To overcome synthetic problems, other nitrene sources such as chloramine-T, the alkylammonium salt of chloramine-T, and bromamine-T have been explored (**Scheme 17**). In this case the stoichiometric byproduct is a sodium or alkylammonium salt.

chloramine-T	X=Cl Y=Na
alkylammonium salt of chloramine-T	X=Cl Y=NR_3R'
bromamine-T	X=Br Y=Na
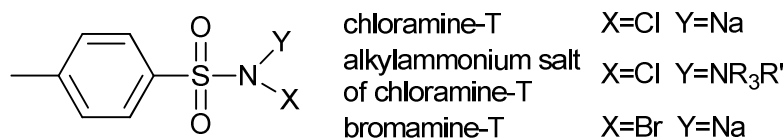
Scheme 17. *Chloramine-T, the alkylammonium salt of chloramine-T and bromamine-T.*

In 1983 Barton and co-workers[45] reported on the use of *in situ* generated ferrous chloride-chloramine-T complex for the amination and aziridination of several hydrocarbon substrates. Afterwards, chloramine-T has been employed in the presence of several catalytic systems.[46]

One inconvenience associated with the use of chloramine-T is its poor solubility in low polar solvents. To circumvent this problem Cenini and co-workers[47] reported on the use of the alkylammonium salt of chloramine-T as aminating agent of cyclic olefins in the presence of iron or

manganese porphyrin complexes in methylene chloride. The corresponding allylic amines were obtained. On the other hand, by using a more polar reaction solvent such as CH_3CN and bromamine-T as nitrene source, excellent results were achieved by Zhang's group[48] in the aziridination of a broad selection of olefins and the amination of benzylic sp^3 C-H bonds using iron and cobalt porphyrins as the catalyst.

1.3.3. Organic azides as nitrene sources

The chemistry of organic azides (RN_3) as nitrogen sources have been explored to a large extent due to the high synthetic versatility of this class of molecules.[49] The lability of the N_α–N_β bond of the N_3 group allows the generation of a nitrene unit ("RN"), with the eco-friendly molecular nitrogen as the only reaction side-product (*Scheme 18*). Therefore, organic azides can be considered as atom-efficient nitrene transfer reagents.
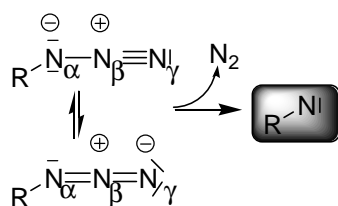
Scheme 18.

The nitrene transfer from RN_3 to an organic substrate can be performed by thermal or photochemical activation,[50] but drastic experimental conditions are required and very often the chemoselectivity of the reaction is not easily controlled. The best results have been achieved in intramolecular reactions[51] that represent an useful methodology to produce aza-heterocycles such as carbazoles. To improve the selectivity of intermolecular nitrene transfer reactions and to use milder reaction conditions, the presence of transition metal catalyst is required. The first metal-catalysed nitrogen atom-transfer from organic azides was reported by Kwart and Kahn, who demonstrated that copper powder promoted the decomposition of benzenesulfonyl azide when heated in cyclohexene.[52]

The first example of a stoichiometric nitrene transfer reaction from an imido porphyrin complex to olefins to give aziridines was due to Groves and Takahashi.[53] They produced the nitride complex $Mn^{III}(TMP)(N)$ (**3**) by photochemical decomposition of the corresponding azido complex and reacted it with trifluoroacetic anhydride (TFAA) to give the imido complex (**4**). The addition of

cyclooctene gave $Mn^I(TMP)(TFA)$ (**5**) (TFA = trifluoroacetate) and the (trifluoroacetyl)aziridine of cyclooctene (*Scheme 19*).
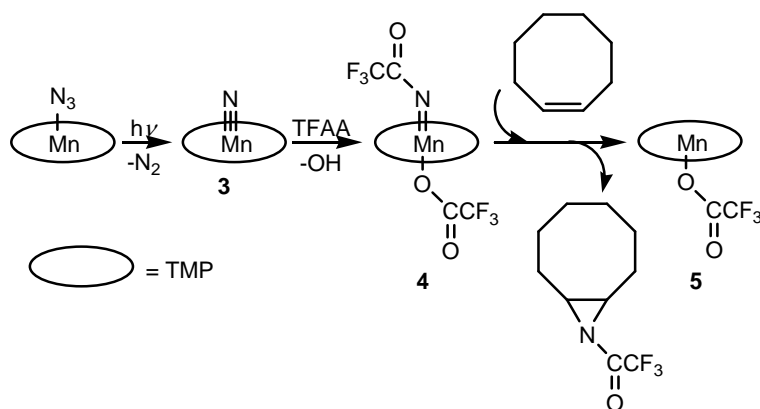
Scheme 19. The stoichiometric formation of (trifluoroacetyl)aziridine of cyclooctene.

The use of cobalt porphyrin complexes allowed the catalytic aziridination of olefins by using organic azides. Zhang and co-workers[54] reported on the use of diphenylphosphoryl azide (DPPA) as the nitrene source in the aziridination of styrenes by Co(TPP). The methodology allowed the synthesis of *N*-phosphorylated aziridines in good yields (*Scheme 20*).
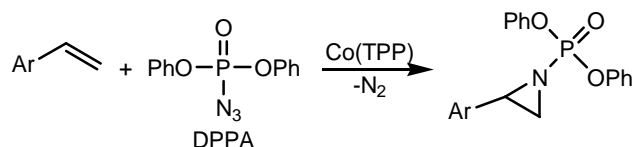
Scheme 20. Synthesis of N-phosphoryl aziridines.

It should be noted that *N*-phosphorylated aziridines offer advantages as synthetic building blocks because the protecting group can be easily displaced to yield non *N*-substituted aziridines. Very recently, Che and co-workers[55] demonstrated that the amination of benzylic and allylic substrates by phosphoryl azides is also efficiently catalysed by ruthenium(IV) complexes. Among tested catalysts, $Ru^{VI}(F_{20}\text{-}TPP)Cl_2$ performed the best (F_{20}-TPP = dianion of *meso*-tetra(pentafluorophenyl)porphyrin).

Sulphonyl azides can also be employed as nitrene source. Zhang and co-workers reported that simple cobalt porphyrins, such as $Co^{II}(TPP)$, could not promote the aziridination reaction of olefin

using arylsulphonyl azides. However, a different cobalt complex (**6**) functionalised with NH-acyl moieties at the *meso*-aryl groups of the porphyrin ligand was an effective catalyst because of hydrogen bonding interactions between the sulphone group of the organic azide and N-H bond of the ligand (*Scheme 21*).[56]
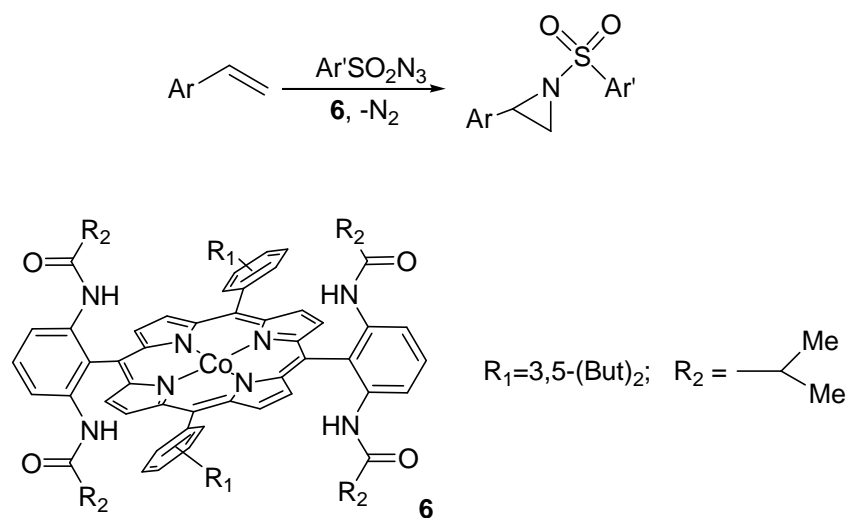
Scheme 21. Cobalt catalysed aziridination of olefins by arylsulphonyl azides.

A significant contribution to this topic was provided by Che *et al.* with the investigation of the catalytic activity of Fe^{III}(F$_{20}$-TPP)Cl[57]. The aziridine product was obtained in good yields by using styrene derivatives as substrates and, surprisingly, when α-methyl styrene derivatives were employed the allylic C-H bond amination occurred without the simultaneous formation of corresponding aziridines (*Scheme 22*), thus giving an excellent chemoselectivity to this methodology.
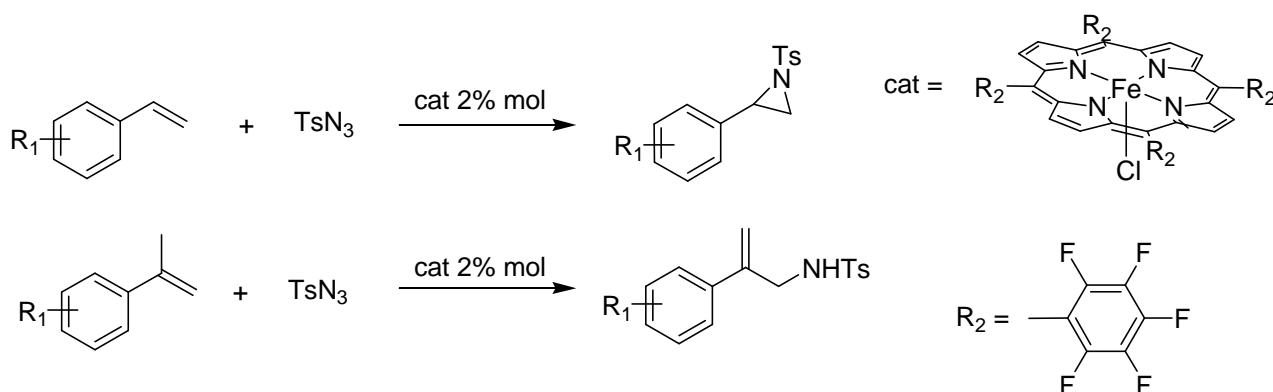
Scheme 22. Chemoselectivity of the Fe^{III}(F$_{20}$-TPP)Cl-catalysed amination using TsN3 as nitrene source.

Our research group intensively studied aryl azides as nitrene sources, these compounds can be prepared through the well-known Sandmeyer reaction by the reacting the diazonium salts of the corresponding anilines with sodium azide (**Scheme 23**, path A). This methodology, which will be adopted for the preparation of aryl azides used for this work, is easily carried out on multi-gram scales. A plethora of diversely functionalised aryl azides can be synthesised, since, depending on the feature of the functional group present in the starting aniline, also neutral (**Scheme 23**, path B) and basic (**Scheme 23**, path C) conditions are available for their synthesis.
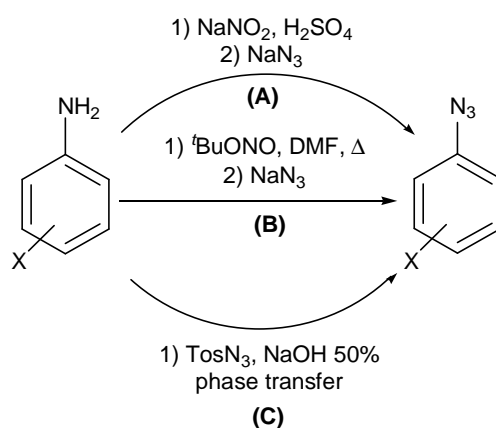
Scheme 23. Main synthetic routes for the preparation of aryl azides.

Organic azides are active aminating agents in the presence of ruthenium porphyrin complexes (**Scheme 24**). Our research group intensively studied the reaction between aryl azides and olefins to give aziridine in the presence of Ru(porphyrin)CO complexes.[58] Quantitative yields and short reaction times have been achieved using terminal olefins and aryl azides bearing electron withdrawing groups on the aryl moiety. The effect of the substituents on the porphyrin ligand was also investigated, it was found that the functionalisation of the *meso* position with aryl groups bearing an EDG or bulky substituents hampers the reaction.
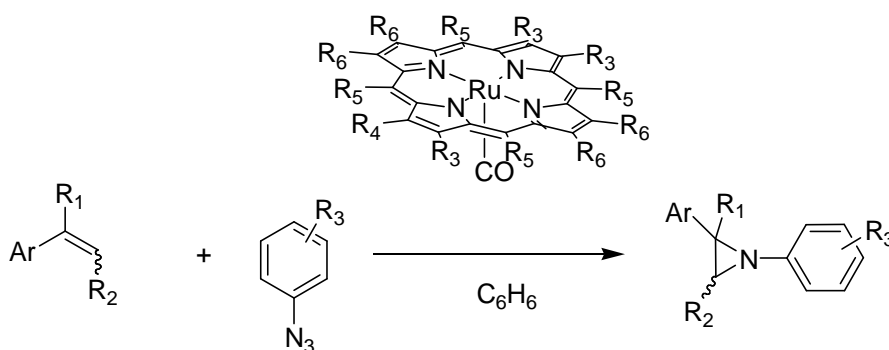
Scheme 24. General route for the synthesis of N-aryl aziridines.

It is worth to report that using the commercially available catalyst Ru(TPP)CO a very high TON (2300) for the amination of α-methylstyrene by 4-nitrophenyl azide was obtained.

Since the uncatalysed reaction between olefins and aryl azides leads to triazolines, these compounds were often detected in the crude of aziridination reactions especially by running the reaction at high olefin concentration, it was found that triazolines compete with the azide for the coordination to the metal centre inhibiting the catalytic process.[59] In a precedent thesis work, the catalytically inactive ruthenium complex **6** (*Scheme 25*) was isolated and characterized by crystal diffraction analysis and it was shown that the axial triazoline ligand is never transformed into the corresponding aziridine even under forcing conditions. A detailed mechanistic study in which the inhibitor role of the triazoline species was demonstrated from an experimental and theoretical point of view is reported in **Section 2.3**.
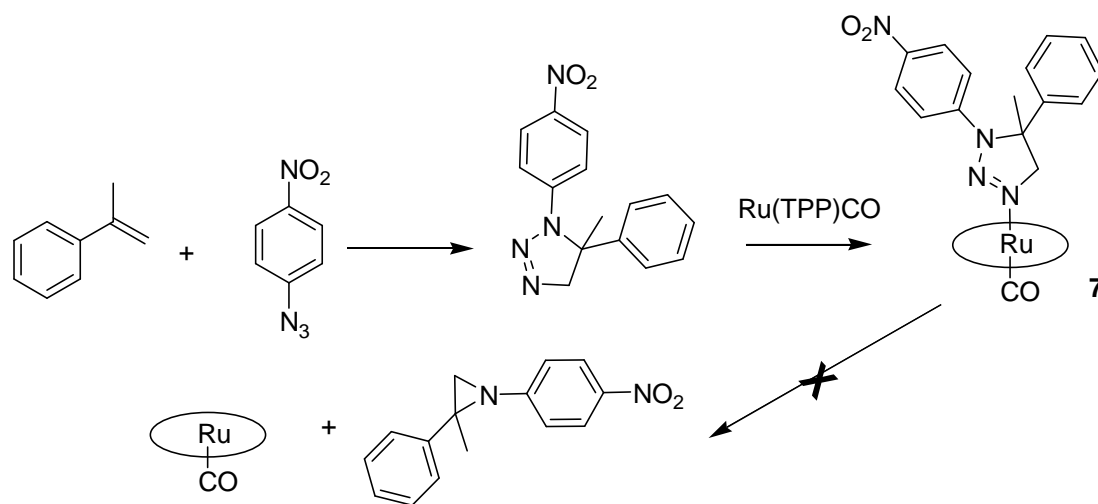
Scheme 25. Synthesis of complex 7.

Organic azides can be largely employed as reagent for C-H aminations. A few years ago, our reasearch group published the first synthesis of benzylic amines and imines from hydrocarbons carrying a benzylic group catalysed by cobalt porphyrin complexes (*Scheme 26*).[60]
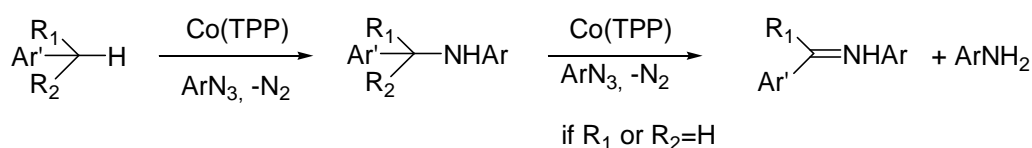
Scheme 26. Cobalt porphyrins-catalysed synthesis of benzylic amines and imines.

As illustrated in *Scheme 26*, aryl azides reacted with hydrocarbons to form the corresponding benzylic amines and, if R_1 or R_2 was a hydrogen group, the reaction proceeded further to give the imine with the consumption of one aryl azide equivalent. The study of the reaction scope revealed that a wide range of aminated products can be achieved also because of the synthetic availability of aryl azides. The reaction proceeds in good yields when the aromatic azide bears electron-withdrawing substituents and the hydrocarbons are not sterically encumbered.

The cobalt(II) porphyrin-catalysed amination of benzylic substrates was then performed by Zhang using 2,2,2-trichloroethoxycarbonyl azide (TrocN$_3$) as the nitrene source (*Scheme 27*).[61] The benzylic amines were obtained without the contemporary formation of the corresponding imines. Noteworthy, the α-amino ester product **8** was obtained, although in a low yield, from the benzylic amination of ethyl phenylacetate.

8, Ar = Ph, R = COOMe
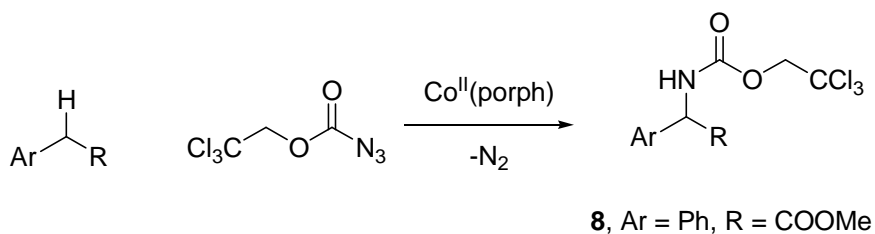
Scheme 27. Co-catalysed benzylic amination using TrocN$_3$ as nitrene source.

The mechanism of Co-catalysed benzylic amination was proposed on the basis of a DFT and EPR study[62] (*Scheme 28*). In this case the active species is the Co^{III} nitrene radical complex **C** which performs a hydrogen abstraction at the benzylic position of ethylbenzene (model substrate for this study) to give the close catalyst-radical pair **D**. Then a facile radical substitution occurs restoring the Co^{II} catalyst **A** and the benzylic amine **E**. The imine side-product should be formed by a hydrogen abstraction from the benzylic position of **E** by complex **C**. The same nitrene radical complex **C** was also proposed as active species in Co(porph)-mediated aziridination of olefins.[63]
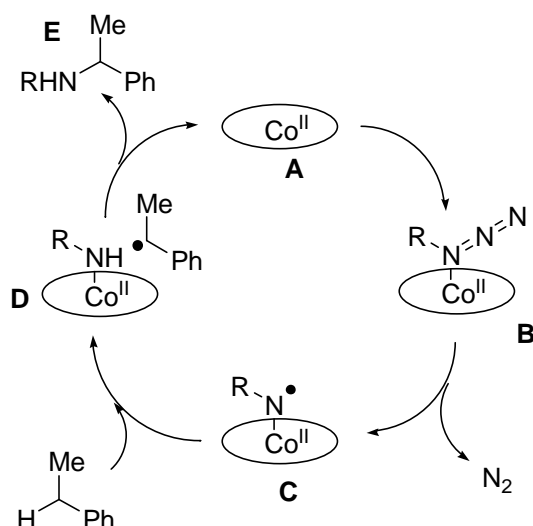
Scheme 28. Proposed mechanism for Co-catalysed benzylic amination.

Cobalt porphyrin complexes were also effective in aminating allylic C–H bonds (*Scheme 29*) in moderate yields.[64] It should be noted that the double C=C bond of endocyclic olefins, such as cyclohexene, did not react with the aryl azide to give the corresponding aziridine therefore indicating a good chemoselectivity towards the allylic amine formation.
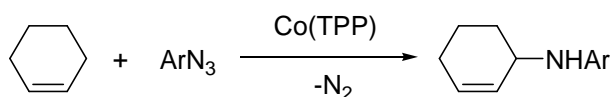
Scheme 29. Co-catalysed allylic amination of cyclohexene.

Better synthetic results have been obtained by using ruthenium porphyrin complexes as catalytic species which are active in the amination of both benzylic[65] and allylic[66] C–H bonds (*Scheme 30*). The commercially available Ru(II)(TPP)CO was found to be a good catalyst and the best catalytic results were obtained by using aryl azides bearing EWG substituents on the aryl moiety and a high hydrocarbon excess with yields up to 90% using a 2% mol catalyst loading.

A very recent advance in this field was reported by Che and Lo[67] who used *bis*(NHC)ruthenium(II) porphyrin complexes for the nitrene insertion reactions into saturated C-H bonds (NHC = *N*-heterocyclic carbene ligands). [Ru(T(*p*-F)PP)(BIMe)$_2$] (**9**) (BIMe = 1,3-di-methyl-2,3-dihydro-l*H*-benzimidazol-2-ylidene, T(*p*-F)PP = dianion of *meso*-tetra(*p*-fluoro)phenylporphyrin) allowed the smooth insertion of pentafluorophenyl azide into allylic and benzylic sp^3 C-H bonds affording the corresponding amines in 88-96% yields using a very low catalyst loading (0.5% mol). The nitrene insertion reaction proceeded well also with the unactivated C-H bond of cyclohexane (90% yield).

The authors proposed that the high catalytic activity is due to the axial NHC ligand which is a strong σ-donor and, therefore, it afford a better stabilization of the *trans* electrophilic M=NR moiety then the π-acceptor carbonyl, the axial ligand of Ru(TPP)CO. This is in accord with the employed mild conditions since the amination reaction was carried out at 40°C using **9** as the catalyst, whilst high temperature (80°C) is generally required for amination reactions using Ru(TPP)CO as the catalyst.
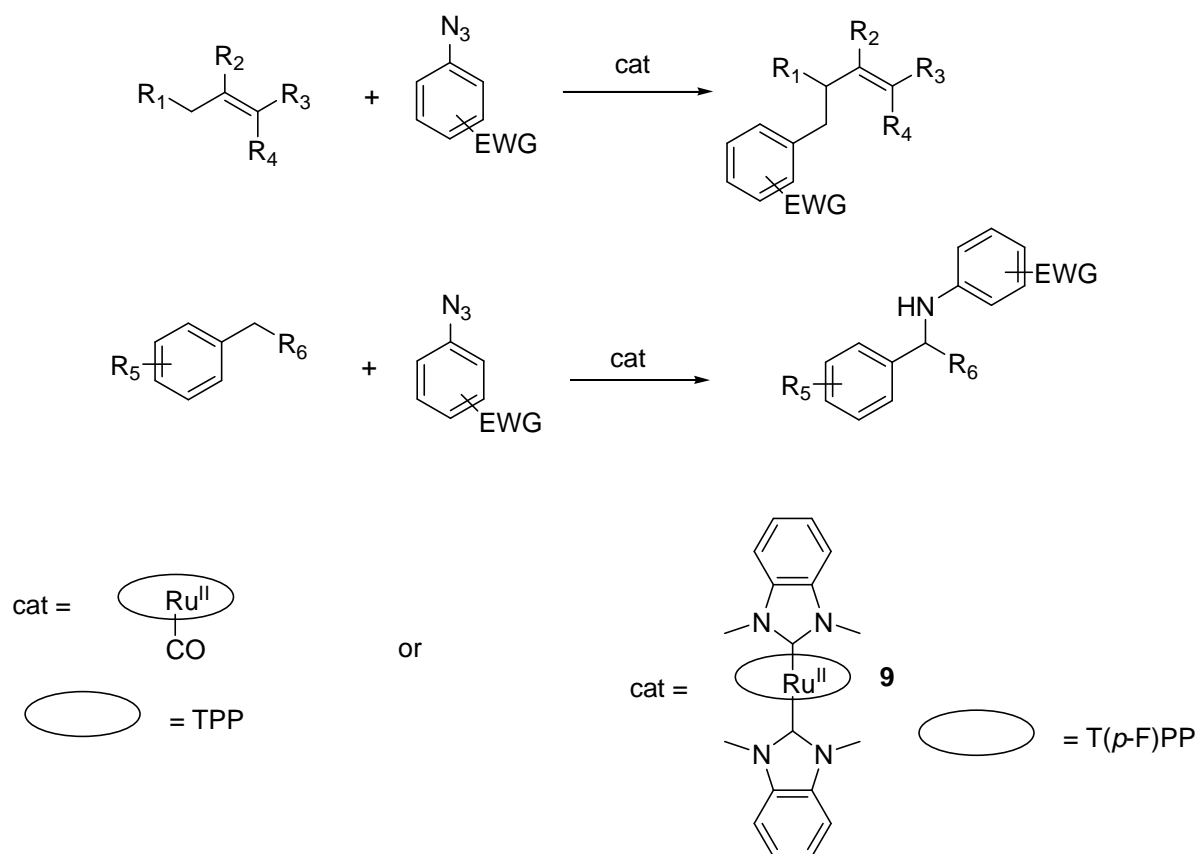
Scheme 30. *Ruthenium catalysed benzylic and allylic amination.*

1.3.4. Mechanistic insights of the ruthenium porphyrin-catalysed amination reaction of hydrocarbons by aryl azides.

Our research group devoted many efforts in mechanistic investigations of Ru(TPP)CO-catalysed amination. It is generally assumed that the active intermediate in metalloporphyrins-catalysed nitrene transfer reactions is an imido complex, which is formed after the aryl azide activation through the cleavage of the N_α–N_β bond. Many ruthenium *bis*-imido complexes were isolated using PhI=NR nitrene sources as described in **Section 1.3.1.** and X-ray crystal structure of complex **2** was recently published.[39]

A new class of *bis*-imido complexes was disclosed by our research group in 2009[68] by the stoichiometric reaction between ruthenium(II) porphyrins and aryl azides (*Scheme 31*). Complex Ru(TPP)(NAr)$_2$ (Ar = 3,5-*bis*(trifluoromethyl)phenyl) (**10**) was isolated in a 70% yield and fully characterized also by X-ray single crystal diffraction.
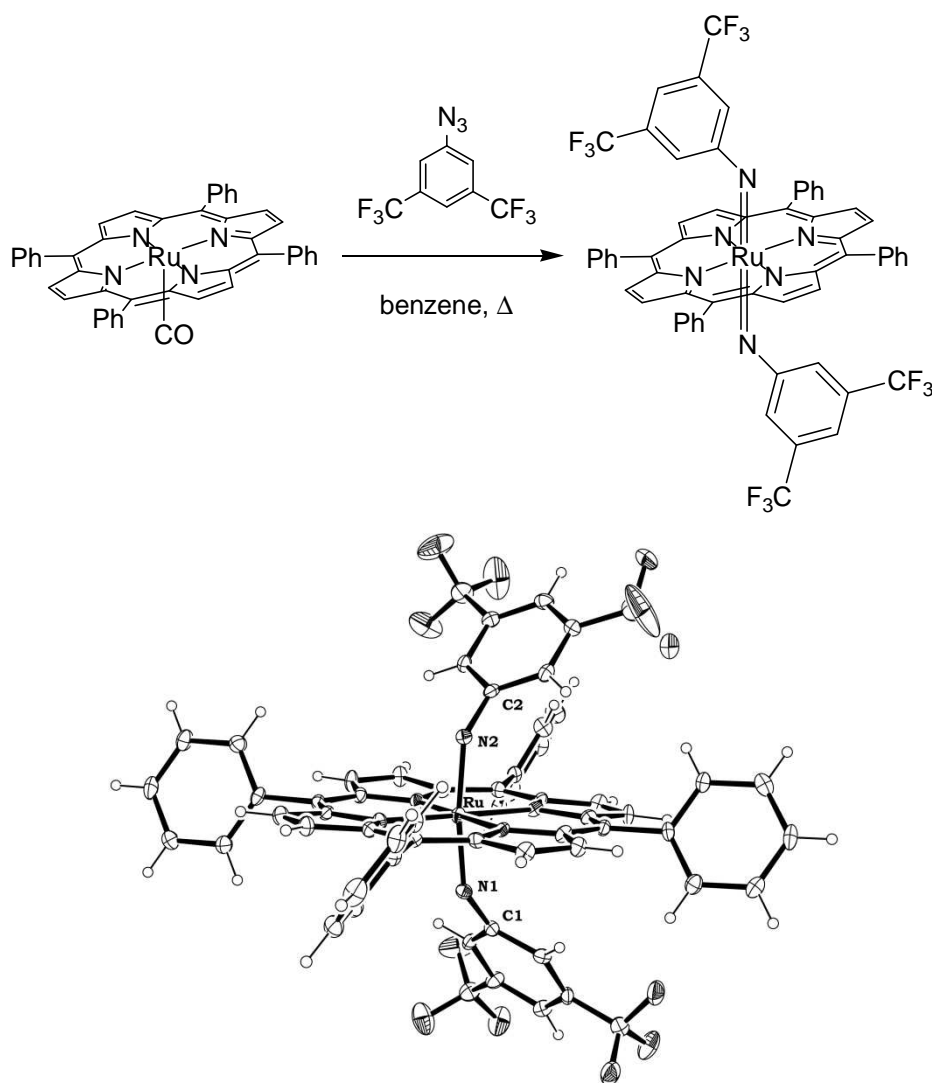
Scheme 31. *Synthesis and X-ray structure of **10**.*

The structures of complexes **10** and **2** share some common features (e.g. similar Ru=N bond distance) but different Ru-N-X imido angles were observed (X= S for complex **2,** X =C for complex **10**). The imido angle of 163° of **2** indicates almost a linearity of the imido moiety whilst the values around 140° for Ru–N–C of **10** indicate the existence of bent imido angles. This last feature is maybe responsible for the good stability/reactivity relationship observed for the latter complex. Complex **10** was stable in the solid state for days and, conversely to previously isolated ruthenium porphyrin *bis*-imido complexes, it is a very active catalyst for allylic and benzylic C-H aminations and also performs efficiently stoichiometric nitrene transfer reactions. These observations allowed us to truly consider complex **10** as a catalytic intermediate.

It is worth to report that only the reaction of 3,5-*bis*(trifluoromethyl)phenyl azide and Ru(TPP)CO afforded a stable *bis*-imido complex. If a different azide bearing EWGs, such as 4-(trifluoromethyl)phenyl azide or 4-nitrophenyl azide, was employed, spectroscopic evidences of the formation of a *bis*-imido species were obtained but the isolation of the complex was not always successful.[66] By using aryl azides bearing EDGs, such as *tert*-butylphenyl azide, the formation of a *bis*-imido complex was never observed.

To shed some light on the catalytic amination mechanism a kinetic[66] and theoretical[69] investigation were undertaken. For this purpose the allylic amination of cyclohexene by aryl azides promoted by Ru(TPP)CO was considered a model reaction.

The kinetic investigation indicated the coexistence of at least two independent catalytic cycles based on two different active species (*Scheme 32*). In the catalytic cycle **B** a ruthenium(VI) *bis*-imido complex (**14)** undergo nitrene transfer while the ruthenium(IV) *mono*-imido carbonyl complex **12** is the active species for cycle **A**. The latter complex was neither isolated nor spectroscopically observed.
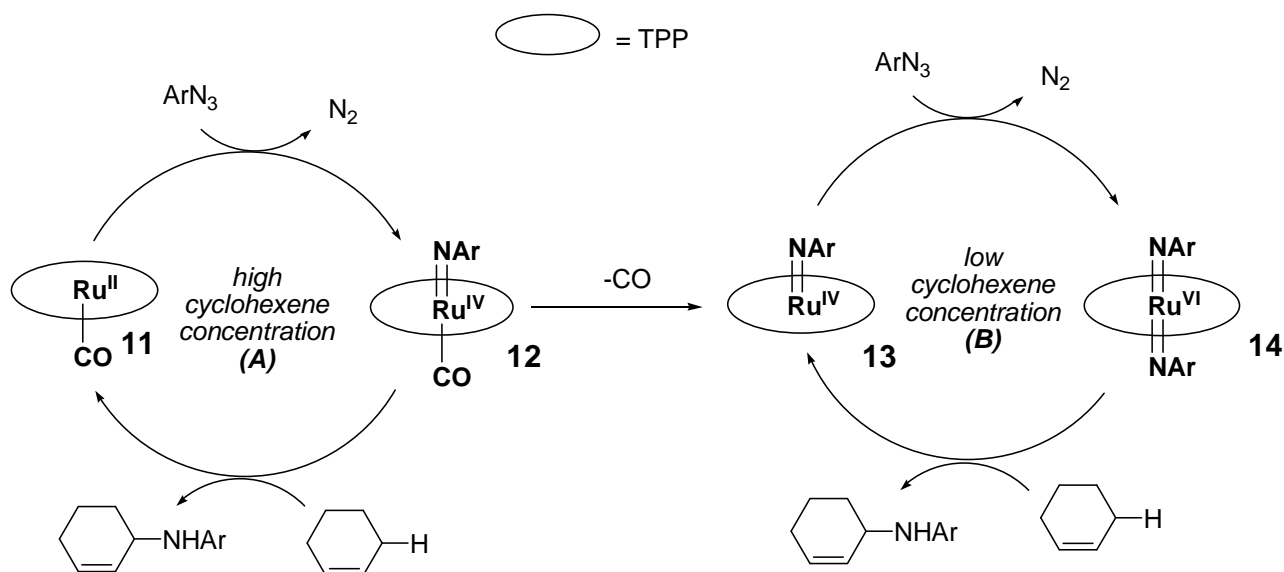
Scheme 32. Mechanism of Ru(TPP)CO-catalysed allylic amination of cyclohexene.

Kinetic experiments carried out at different cyclohexene concentrations pointed out that this parameter is crucial for the prevalence of catalytic cycle **A** or **B**. The latter cycle is likely to be the dominant one at low hydrocarbon concentration while the *mono*-imido complex **12** should be responsible for nitrene transfer at high hydrocarbon concentrations.

However, a clear distinction between the two catalytic cycles was observed only by using 3,5-*bis*(trifluoromethyl)phenyl azide as the nitrene source, the reaction mechanism with other aryl azides was likely restricted to catalytic cycle **A** (*Scheme 32*) because of the poor stability of the resulting imido derivatives.

Two other ruthenium complexes were identified by analyses of the reaction crude (*Scheme 33*). The aniline complex **15** was observed when the reaction is run at high cyclohexene concentration and 3,5-*bis*(trifluoromethyl)phenyl azide is employed as aryl azide. It should be the product of decomposition of the *mono*-imido complex **12** by formal hydrogen abstraction (*Scheme 33*, equation **a**). Similar aniline complexes of the general formula [Ru(TPP)CO(ArNH$_2$)] were the main product of the stoichiometric reaction between Ru(TPP)CO and aryl azide functionalised with EDGs.

The *bis*-amido complex **16** is a ruthenium (IV) diamagnetic species and the catalyst resting state in the occurrence of the catalytic cycle **B** (*Scheme 32*), it should be present in the reacting mixture when the *bis*-imido complex **10** is formed. An NMR experiment showed the reversible transformation of **10** into **16** and vice-versa depending on the [aryl azide]/[cyclohexene] ratio (*Scheme 33*, equation **b**).
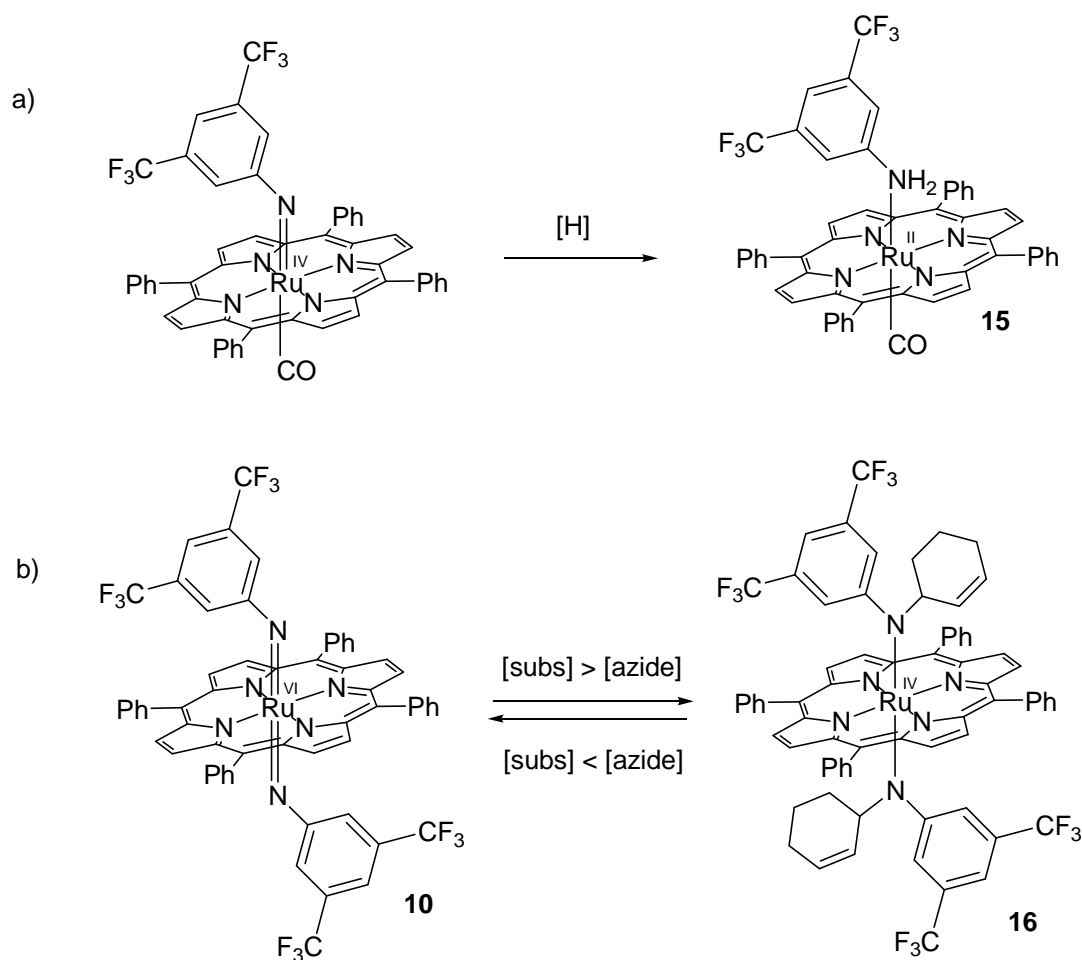
*Scheme 33. Proposed mechanism for formation of complexes **15** and **16**.*

A theoretical DFT investigation of the allylic amination of cyclohexene was performed and it supported the hypothesis of two independent and coexisting catalytic cycles. The reaction pathway for azide activation and nitrene transfer was calculated for both catalytic cycles.

The ruthenium porphine complex ([Ru]) and methyl azide were used instead of Ru(TPP) and aryl azides in order to facilitate the electronic interpretation and to speed up the calculation.

At first the mechanism for azide activation by [Ru]CO was calculated (***Figure 7***, part 1), the first step should be the azide coordination to give the complex [Ru](R-N$_3$)(CO) (**17**) through a slightly exoenergonic process(-3,5 Kcal/mol) in which the azide interacts with the ruthenium centre through the N$_\alpha$ atom. The calculated low stabilization is in agreement with the fact that a ruthenium-azide adduct was never isolated or detected. The second step is nitrogen elimination that goes through a transition state (**18**) in which the initially linear N$_\alpha$-N$_\beta$-N$_\gamma$ angle move to 136° and the N$_\beta$-N$_\gamma$

distance shorten to liberate molecular nitrogen. The ΔG cost of this step (26.8 Kcal/mol using methyl azide) is in accord with the need of high temperature (80°C) to run the reaction.

1) azide activation　　　　　　　　**2) C-H activation**
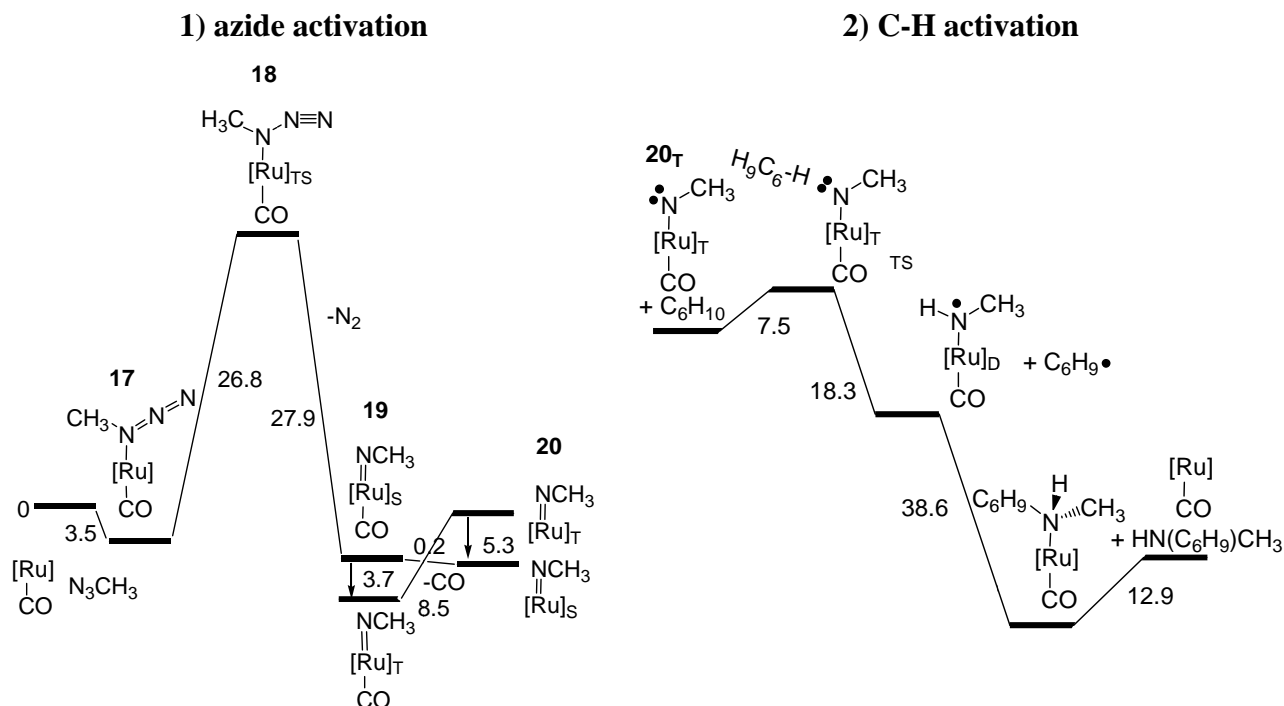
Figure 7. Calculated pathway for the "mono-imido catalytic cycle".

The so obtained complex (**19**) undergoes a singlet→triplet interconversion because somewhat the *mono*-imido carbonyl complex is more stable in the triplet state (**19$_T$**). Since a radical mechanism is involved, **19$_T$** should be active to nitrene transfer rather than **19$_S$**. A spin-density calculation (***Figure 8***) indicated a larger concentration at the N atom of **19$_T$** then at the ruthenium center. Therefore, a significant diradical character is attributed to the imido ligand, which is necessary to accomplish a C-H homolytic dissociation of the organic substrate.

a)　　　　　　　　　　　　　　　　b)
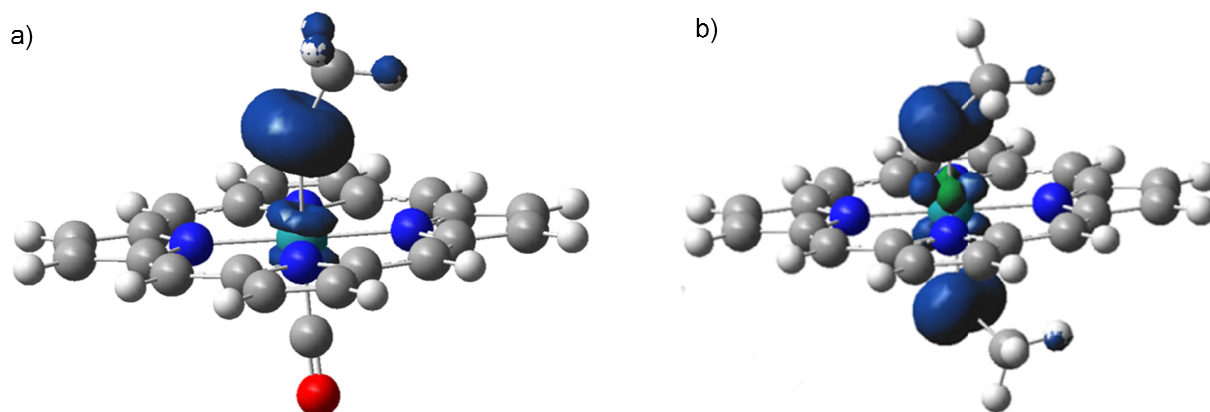
*Figure 8. Spin density plot for complexes **19$_T$** (a) and **22$_T$** (b).*

The *mono*-imido carbonyl complex bears a weaker ruthenium-carbonyl bond then the former catalyst one, especially in the singlet state (**19$_S$**). So, **19$_S$** is more prone to cleave the loose Ru-CO bond and yield the *mono*-imido complex [Ru](NR) (**20**) which is more stable in the singlet state, conversely to **19**, and is the starting point for the "*bis*-imido catalytic cycle" (**Scheme 32**, cycle B).

The azide-activation pathway by complex **20** was calculated. It was found that in this case the cost for azide activation is lower (14 Kcal/mol using methyl azide) and the *bis*-imido species (**22**) was formed with a -41 Kcal/mol energy gap, showing that **22** is a stable complex in its singlet state, in accord with experimental data. The empirical catalytic activity of complex **10** was explained since **21$_S$** can undergo a singlet→triplet interconversion to give the reactive species (**22$_T$**) which lies 16 Kcal/mol above and was considered an excited state of the *bis*-imido complex. Spin density plot of **22$_T$** (**Figure 8**) showed that the spin is localized on the two N atoms, therefore the two unpaired electrons are equally distributed on the imido ligands.

The activation of the allylic C-H bond of cyclohexene (C$_6$H$_{10}$) (part 2 of **Figure 7** and **Figure 9**) occurs by abstraction of the allylic hydrogen through a C-H•••N adduct detected as a transition state (**21**) concerning the *mono*-imido catalytic cycle (**Figure 7**). The formation of the desired allylic amine follows a "rebound" mechanism in which the nitrogen and carbon atoms radicals couple to yield the organic product and the starting catalyst. Alternative pathways are possible for the radical rebound of the "*bis*-imido catalytic cycle" (**Figure 9**, pathways a and b) depending on the occurrence of cyclohexenyl radical migration. This explains the observed side reaction to give the *bis*-amido species **16**.
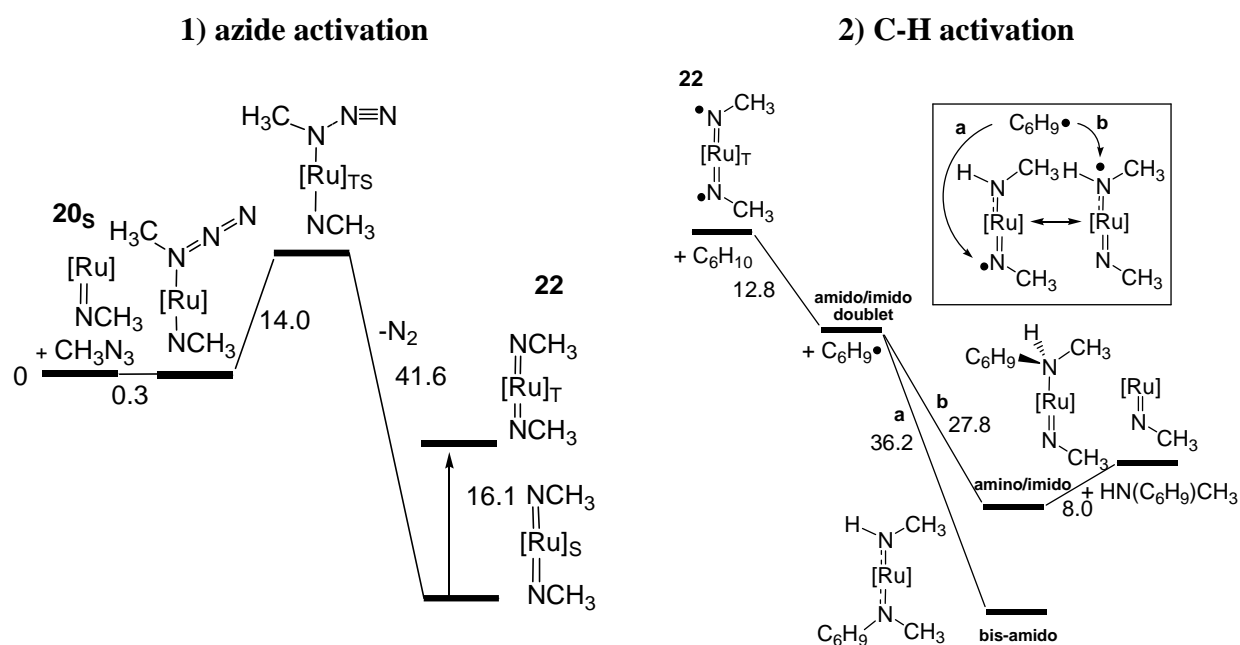
Figure 9. *Calculated pathway for the "bis-imido catalytic cycle".*

1.4. Synthesis of α- and β-Amino Esters: Recent Strategies for Transition Metal Catalysed C-N bond formation

α-Amino acids are essential molecules in many scientific areas, for example from a synthetic chemist point of view these compounds have an impressive number of applications for the development of organocatalysts[70], for their use as a chiral pool for ligands design[71] and in total syntheses[72].

Less naturally abundant β-amino acids are also an important class of molecules for their occurrence in products of biological and pharmaceutical interest, taxol and (R)-β-Dopa among the most famous examples (*Figure 10*), and as potential precursors for β-lactams, one of the most important classes of antibiotics.
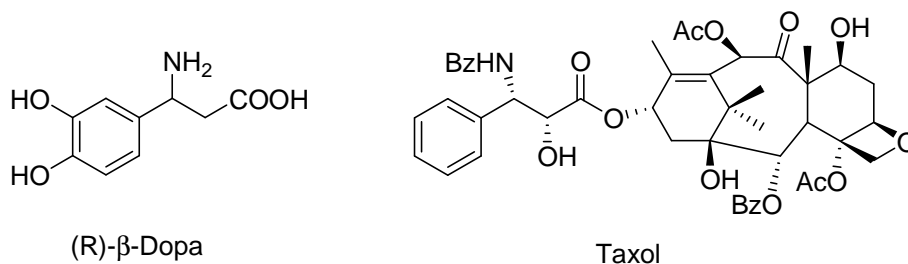
Figure 10. Examples of biologically important β-amino acids derivatives.

The increasing demand of these optically active compounds prompted the scientific community to develop new methodologies for the synthesis of α- and β-amino acids. Asymmetric catalysis is the most powerful way to achieve a wide variety of enantiomerically enriched compounds *versus* biotechnological processes and resolution of racemic mixtures.

A complete overview of the synthetic strategies for these compounds would be a nearly impossible task. Generally, asymmetric hydrogenation of enamine esters is one of the most important catalytic enantioselective methods. Since the pioneering work of Knowles[73], about the industrial manufacture of L-Dopa promoted by a rhodium complex with a chiral bidentate phosphine (*Scheme 34*), the use of transition metal catalysts, especially Rh and Ru complexes, with chiral ligands dominated the scene.[74]
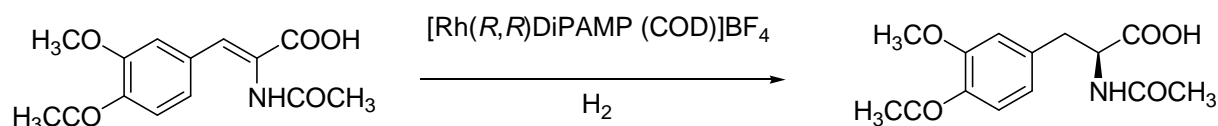
Scheme 34. L-Dopa asymmetric hydrogenation reported by Knowles.

This section will be focused on a particular approach for the amino acid derivatives synthesis, the introduction of an amino group in α position of a carboxylic acid derivative. The formation of a new C-N bond can provide a complementary route to new unnatural amino acids which are highly needed in the development of peptide drugs to replace natural amino acids in order to enhance the activity or discover new functionalities.

The synthesis of β –amino acid derivatives through a C-N bond formation will not be discussed since it mainly concerns the addition of an amine nucleophile to an α,β-unsaturated carboxylic acid derivative through the well-known aza-Michael reaction (*Scheme 35*).[75] These processes can be efficiently metal-catalyzed in the presence of chiral ligands (e.g. M/chiral *bis*-oxazoline, M = Sc^{3+}, Cu^{2+}, Mg^{2+} etc.) or promoted by chiral organocatalysts.
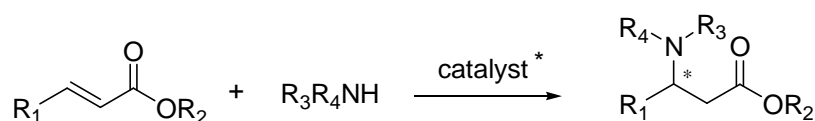
Scheme 35. General Aza-Michael approach to the asymmetric β-amino esters synthesis.

1.4.1. Aziridination of imines with diazocompounds

Synthesis of the aziridinecarboxylic acids and their derivatives can be afforded by the reaction of imines with α-diazoesters.[27] These compounds are useful in the search for new series of constrained α-amino acids or as valuable intermediates in the synthesis of natural products considering the importance of the aziridine ring as a building block.

In a relevant example, aziridine carboxylic esters were obtained in high yields and excellent enantio- and diastereomeric ratios by employing boron complexes derived from (*S*)-Vanol (**23**) (*Scheme 36*).[76] The complex gave good results in the generation and further stabilization of the reactive carbene. The *cis/trans* ratio (up to >50/1) was another interesting aspect of this catalytic enantioselective transformation.
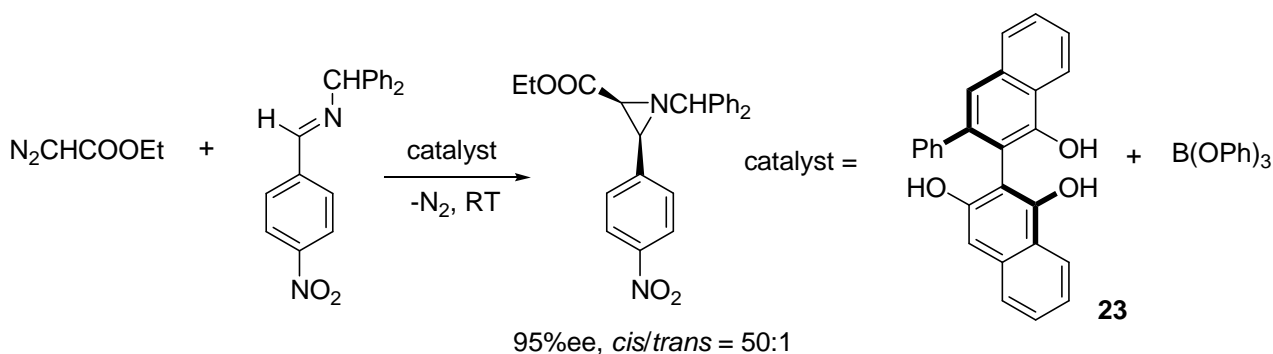
Scheme 36. *Aziridination of imines catalysed by borate complexes.*

1.4.2. Electrophilic amination of ester enolates

Electrophilic amination of enolates was firstly explored by reacting azodicarboxylate esters ($RO_2CN=NCO_2R$) with activated (coordinating) carboxylic species, such as β-keto ester or acyloxazolidinones (**Scheme 37**). Versatile metal-catalysed[77] and organocatalytic processes[78] have now become available. However, the resultant N-N bond in the aminated product should undergo cleavage under relatively harsh reductive conditions, which is often problematic.
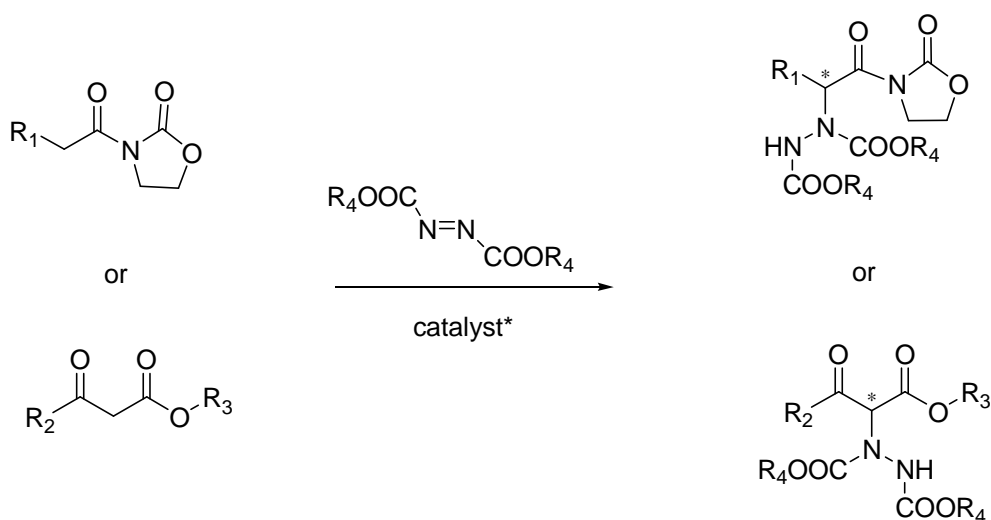
Scheme 37. *Amination of "activated" esters using azodicarboxylate species.*

Although other protocols were reported, for example involving the aziridination of silyl enol ethers with phenyl iodinane (TsN=IPh)[79] or amidation of aryl ketones and aldehydes with chloramine T[80], most of them are restricted to the aldehyde and ketone oxidation levels.

Miura and co-workers[81] reported an effective method for the amination of the α position of carboxylic esters derivatives by reacting ketene silyl acetals and hydroxyl amines as the electrophilic nitrogen source (**Scheme 38**). The reaction is promoted by a copper(II) salt in the presence of a bidentate posphine ligand, (Cu^{II}/dpppen, dpppen = 1,5-(diphenylposphino)pentane) and lead to the synthesis of unnatural α-amino esters with good yields and using mild experimental conditions.
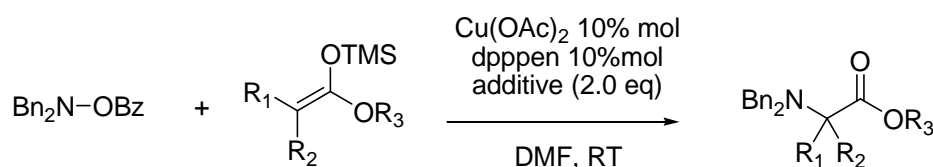
Scheme 38. Ketene silyl acetal electrophilic amination.

1.4.3. Carbene insertion into N-H bonds

The insertion of metal carbenes or carbenoids, generated in situ from α-diazoesters, into N-H bonds is an efficient approach to α-amino acid derivative; it benefits from mild reaction conditions and high efficiency. First investigations about N-H insertions employed copper catalysts[82], subsequently many efforts were devoted to the development of modern versions of this reaction, for example, employing continuous-flow systems[83] or metal-free reactions.[84]

A remarkable work by Zhou[85] showed that highly stereoselective reactions can be promoted by a copper(I) catalyst in the presence of a spiro-*bis*oxazolidine ligand **24** (**Scheme 39**). The use of a bulky and non-coordinating counteranion (BAr$_F^-$, tetrakis[3,5-*bis*(trifluoromethyl)phenyl]borate) improved the enantioselectivity up to 98%.
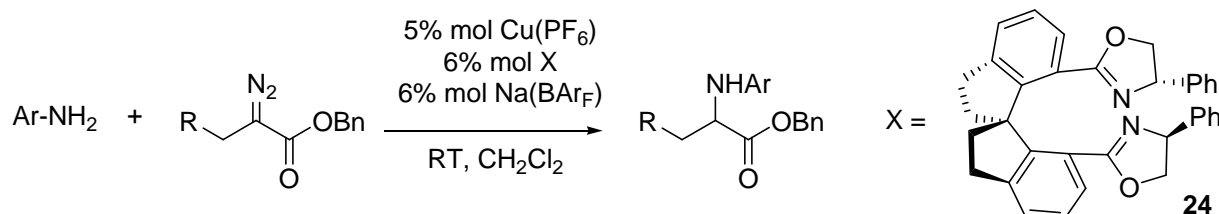
Scheme 39. Relevant example of enantioselective N-H insertion of α-diazoesters.

An example of a very active porphyrin catalyst was reported by Woo and co-workers[86], Fe(TPP)Cl (1% mol) promoted the N-H insertion of ethyl diazoacetate in short reaction times and yields ranging from 68% to 97%. Another interesting application of this reaction is the synthesis of proline

derivatives, published by Che's group,[87] through an intramolecular carbene N-H insertion catalysed by [RuCl$_2$(p-cymene)]$_2$ and affording the final product in a good diastereoselectivity.

1.4.4. C-H bond amination

As previously discussed in **Section 1.3.3.**, Zhang and co-workers firstly reported the synthesis of the α-amino ester **8** through the intermolecular benzylic amination of ethyl phenylacetate using TrocN$_3$ as the organic azide and cobalt porphyrin catalysts. Since a poor yield was obtained (18%) the authors proposed that the reaction was hampered by the electrondeficiency of C-H bond placed in α position of a carbonyl group towards radical activation.[61]

Recently the same group reported the synthesis of cyclic α-amino acid derivatives by the intramolecular amination of an electron-deficient C-H bond.[88] The starting reagents were a *N*-benzyl sulfamoyl azides species **25** functionalised with an EWG, the six-membered product **26** was obtained using the Co-complex **6** as the catalyst (*Scheme 40*). Probably the interaction between the porphyrin ligand N-H moiety and the sulphonyl group and the pre-organization given by the intramolecular reaction were pivotal to overcome the low reactivity of electron deficient C-H bond towards homolytic cleavage.
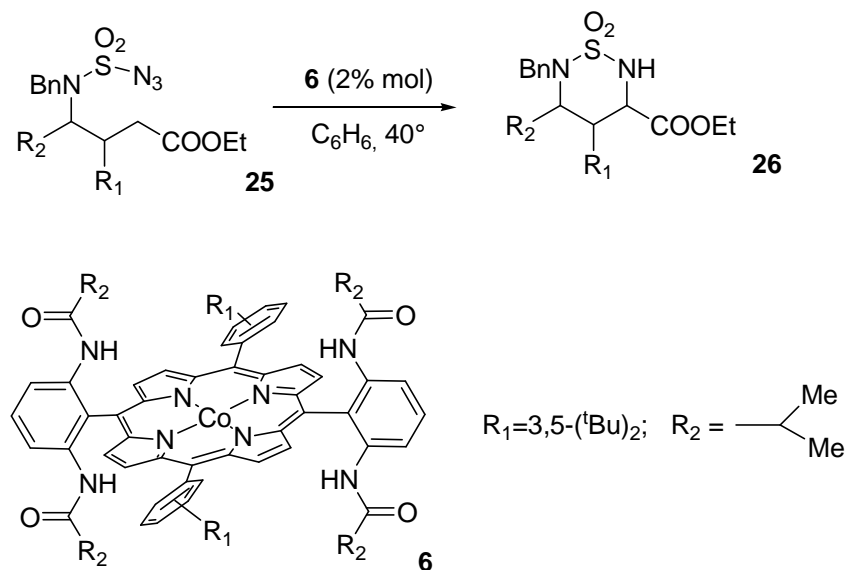
Scheme 40. Co-catalysed intramolecular C-H amination to give cyclic α-amino ester.

1.5. Catalytic Methods for Indoles Synthesis

Indole is unambiguously one the most important heterocycles. It is an electron rich heteroaromatic system with an enhanced reactivity in electrophilic aromatic substitution, especially at C3 position (enamine type reactivity) and it is the most widely distributed heterocycle in Nature. Many indoles show significant biological activities, thus is not surprising that this structural motif is a component in many of today's pharmaceuticals (*Figure 11*).[89]
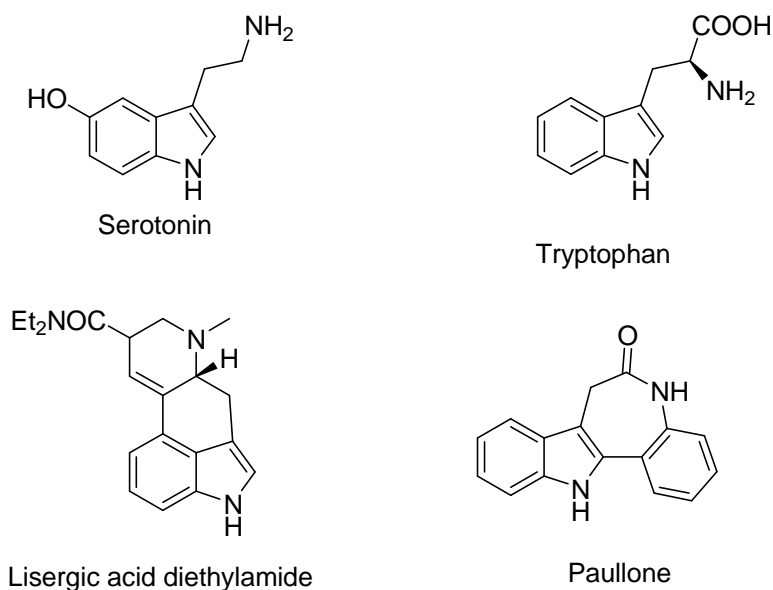
Figure 11. Examples of indole-based compounds with important biological activities.

A great number of practical synthetic method were developed beside the classical Fischer indole synthesis,[90] however the diversity of indoles as well as their great biological/pharmaceutical relevance still prompts academic and industrial researchers to look for new and improved synthesis for these compounds.

The aim of this section is to take an overview of the recent advances in indole synthesis focusing on metal catalysis, which has become a powerful tool for synthetic methodologies. Generally the electrophilic activation of a substrate (such as an alkyne or an organic azide) by a transition metal complex and the subsequent either intermolecular or intramolecular addition has become a popular strategy to prepare functionalised indoles.

1.5.1. Catalytic Hydroamination of alkynes with arylhydrazine:

Since 1883 the Fischer reaction has remained one of the essential methods for indoles synthesis, it consists of the condensation of an aromatic hydrazine with a ketone followed by a [3,3] sigmatropic rearrangement, ammonia elimination and rearomatisation. The development of the hydroamination

reaction permitted a new approach to indole synthesis by the reaction between alkynes and aryl hydrazines with a Fischer-related mechanism (*Figure 12*).

a) Fischer synthesis
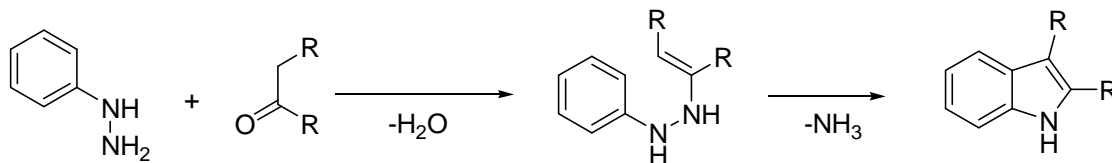
b) Indole synthesis via alkyne hydroamination
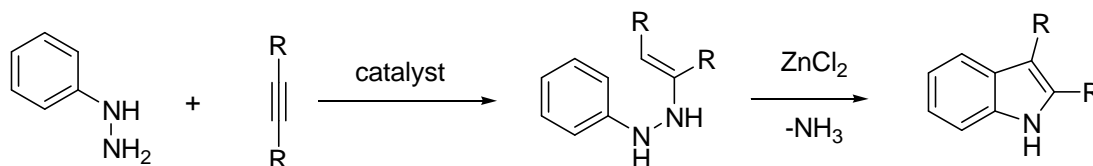
Figure 12.

Pioneering studies of this interesting approach were accomplished by Bergman in 1991[91], later catalytic procedures using titanium complexes as catalysts and zinc salts as additives were developed by Odom and co-workers.[92] These protocols unfortunately presented some drawbacks in terms of the sensitivity of functional groups towards titanium, the necessity to protect the hydrazine or low regioselectivities. Some of this disadvantages were overcome by Beller who was able to use this methodology to synthesis electron-rich functionalised indoles with high regioselectivity.[93] Subsequently, the use of a titanium catalyst was avoided by using only zinc salts in stoichiometric amounts both for the hydroamination and the cyclization step.[94]

Another interesting synthetic strategy was developed by Wakatsuki and co-workers[95] as a one-pot synthesis of 2-substituted 3-methylindoles using anilines and propargyl alcohol derivatives (*Figure 13*) in the presence of $Ru_3(CO)_{12}$ as the catalyst and aniline hydrochloride as additive. The same methodology was improved by Liu and co-workers by using $Zn(OTf)_2$ as the catalyst.[96]
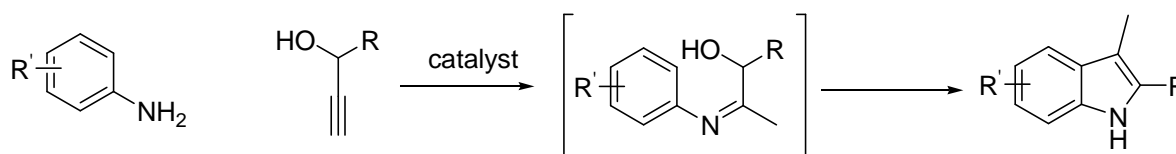
Figure 13. Synthesis of 2-substituted 3-methylindoles by hydroamination/cyclization.

1.5.2. The reaction between *o*-haloanilines and alkynes: Larock indole synthesis

The so-called Larock synthesis was reported firstly in 1991[97] and has become one of the most attractive and practical method for the synthesis of 2,3-substituted indoles. It consists in a palladium-catalysed heteroannulation of internal alkynes with *N*-protected *o*-aloanilines (generally *o*-iodo anilines). The reaction mechanism is reported in ***Figure 14*** and shows the reason for the observed regioselectivity when unsymmetrical alkynes are employed. The more hindered group (R_L) of the alkyne is inserted away from the sterically encumbered aryl group of intermediate **C** and it is recovered in C2 position of the final indole product. Nevertheless, with similarly substituted alkynes, mixtures of regioisomers are obtained.
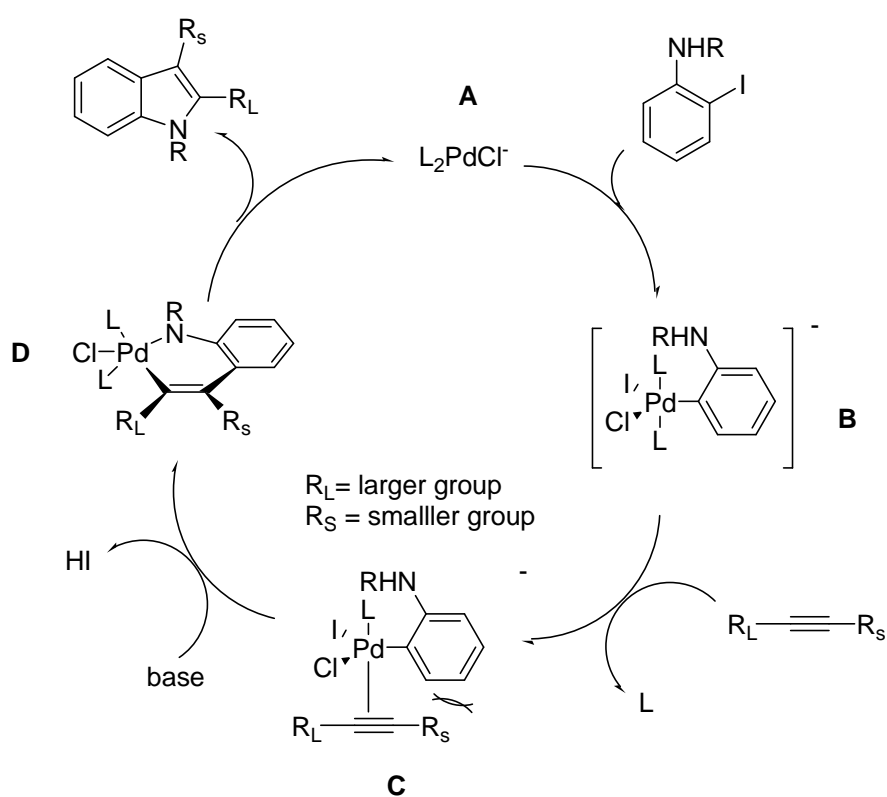
Figure 14. *Mechanism for the Larock heteroannulation.*

Two more regioselective pathways to obtain 2,3-substitued indoles starting from *o*-aloanilines were investigated by Ackermann[98] and Barluenga[99]. The first one consists in a one-pot titanium-catalysed hydroamination of asymmetrical alkynes followed by a palladium-catalysed intramolecular Heck coupling. The Barluenga strategy makes use of alkenyl bromides as coupling partner of o-aloanilines, noteworthy, by using the same catalyst a Buchawald-Hartwig type C–N-bond formation was performed giving rise to an enamine intermediate which underwent an intramolecular Heck-coupling.

1.5.3. Cyclization of *o*-alkynylaniline derivatives

The transition metal-catalysed hydroamination of *o*-alkynylaniline derivatives has become an established approach for the preparation of 2-substituted indoles. This method usually requires two steps: 1) introduction of the alkynyl moiety through Sonogashira reactions and 2) subsequent cyclization reaction (*Scheme 41*).
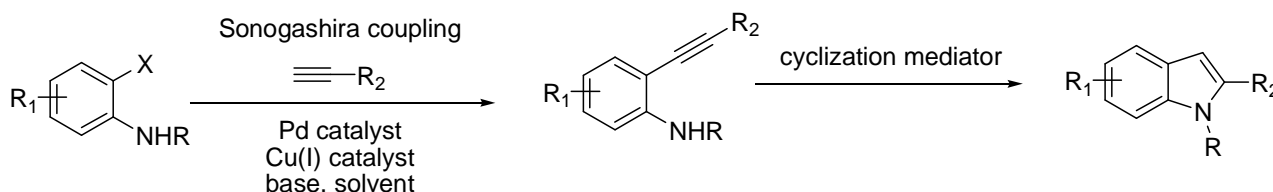
Scheme 41.

The second step is feasible by using a wide variety of metal catalyst,[100] more interesting examples are the ones that include further functionalisation, for example, at C3 position like the methods developed by Cacchi[101] and Lu[102]. An impressive one-pot three-component domino reaction including Sonogashira coupling, cyclization and functionalisation at C3 position was reported by Lu and co-workers[103] starting from *o*-iodoanilines and using a Pd(OAc)$_2$ as the catalyst. This methodology circumvents the time-consuming preparation of o-alkynylanilines and afford the 2,3-disubstituted indoles in excellent yields (*Scheme 42*).
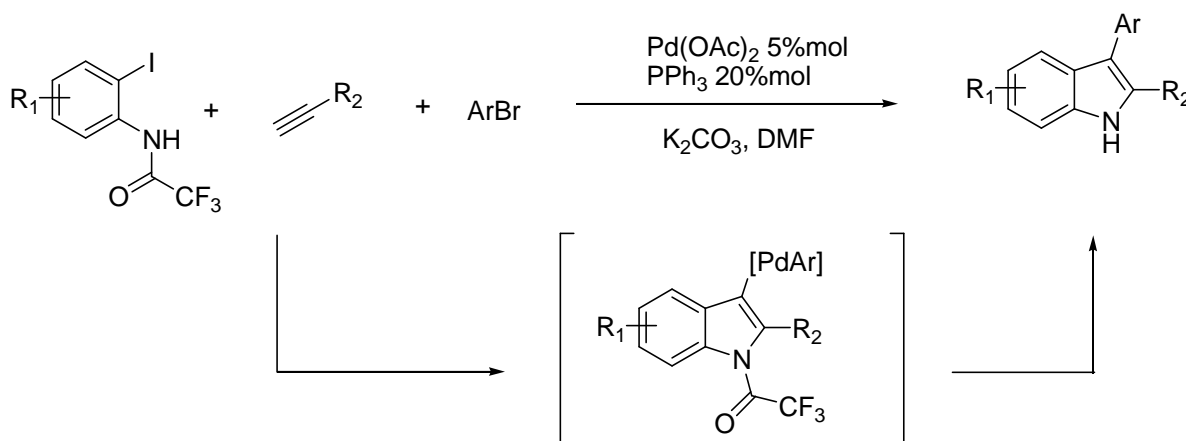
Scheme 42. One-pot multicomponent reaction developed by Lu.

Another example is quite interesting for what concerns the present thesis. It consist, to the best of our knowledge, of the only case of intramolecular annulations between an alkynyl moiety and an azide group to give 2,3-substituted indoles.[104] The reaction is gold-catalysed and includes elegant

functionalisation at C3 position by a nucleophilic attack of a C-H bond of an electronrich arene species (*Scheme 43*).
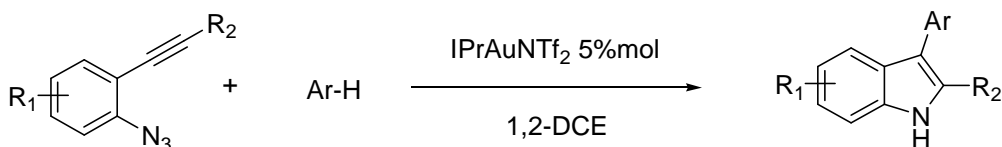
Scheme 43. Intramolecular reaction between azide and alkyne to give indoles.

1.5.4. Synthesis of Indoles *via* metal-catalysed nitrene insertions

Modern methods for the synthesis of indoles usually use the well-established protocols of cross-coupling reaction to form C-N bond. Nevertheless, less conventional nitrogen sources of nitrogen, such as nitrenes, have been successfully employed in indole synthesis.

Nitrenes can be generated *in situ* by rearrangement of 2*H*-azirine that, when bearing an aryl substituent at C2 position, could undergo an intramolecular C-H insertion yielding the corresponding indole. This transformation can be either thermally[105, 106] or catalytically induced[107], recently Zheng described the preparation of 2,3-disubstituted indole by reacting 2*H*-azirine in the presence of FeCl$_2$[108], the reaction took place through a ring opening of a 2*H*-azirine and the subsequent formation of iron–nitrene species, then the indole was obtained through intramolecular amination (*Scheme 44*).
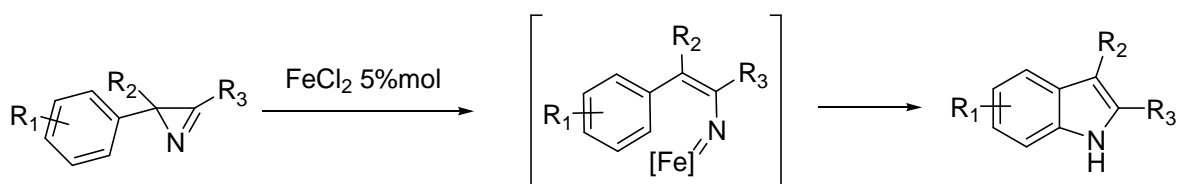
Scheme 44. Synthesis of indole through rearrangement of 2H-azirines.

Readily available azides proved to be convenient precursors of nitrenes as well. In a series of studies, Driver developed complementary routes to indoles through regioselective intramolecular amination, which made use of β-styrylazides[109] or *o*-vinylarylazides[110] as substrates.

These rhodium-catalysed processes could be performed under mild reaction conditions, avoiding undesired by-product formation. For instance, 2-indole carboxylate was obtained almost quantitatively using vinylazides (*Scheme 45*, **a**), while the preparation of 2-aryl substituted indoles was accomplished using aryl azides (*Scheme 45*, **b**). The reaction can be considered a classical

insertion of a nitrene into a C-H bond; however detailed mechanistic studies were performed and disclosed a more complicated mechanism.
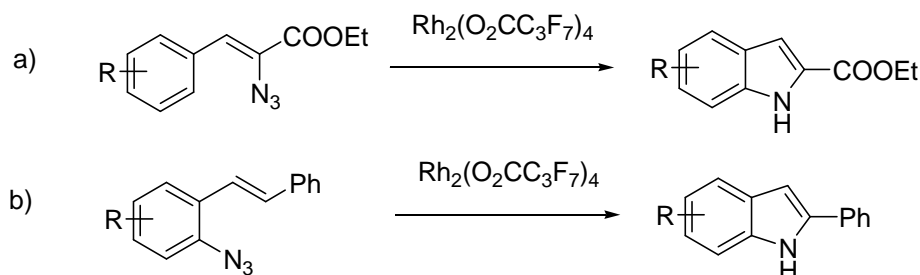
Scheme 45. Driver's synthesis of indoles through intramolecular amination.

1.5.5. C-H functionalisation by Oxidative Coupling

The catalytic methods present in section **1.5.2.**, **1.5.3.** and **1.5.4.** require *ortho*-disubstituted arenes, which are prefunctionalised substrate that must be synthesised thereby lengthening the overall process. An approach starting from *mono*-functionalised arenes, which should involve a C-H-bond functionalization, would be highly desirable. In this way, a wider collection of starting materials would be accessible and synthetic routes would be shortened. Generally, the use of an oxidant as additive was necessary for the catalyst regeneration.

Among the first indole synthesis through oxidative C-H bond functionalisation there is the cyclization of *N*-aryl enamines reported by Glorius.[111] This palladium-catalysed transformation made use of easy-to-prepare enamines as starting material, however a large excess of a copper salt was required as terminal oxidant (**Scheme 46**, **a**). Hartwig and co-workers reported a synthetic strategy making use of β-aryloximes ester derivatives[112] and consisting of a C-N bond formation via palladium-catalysed intramolecular amination of an aromatic C–H-bond with no need for terminal oxidants (**Scheme 46**, **b**).
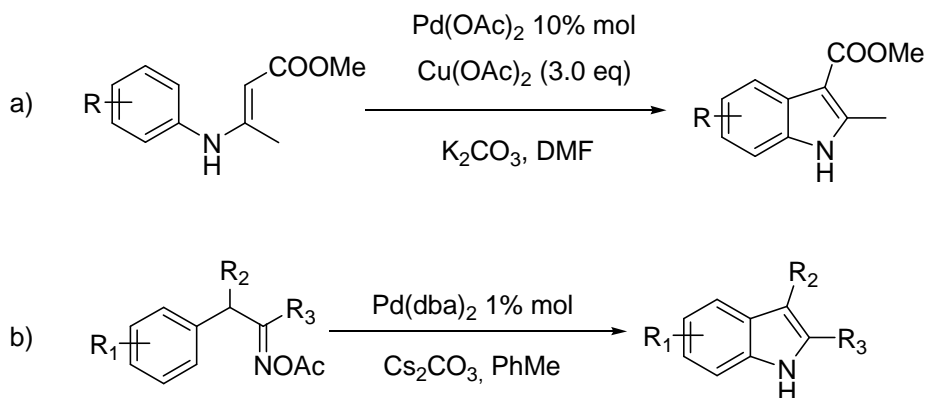
Scheme 46. Indole synthesis developed by a)Glorius and b)Hartwig.

In terms of accessibility of the starting reagents, intermolecular oxidative couplings would be more convenient approaches to the indole core, as was cleverly devised by Fagnou.[113]

Hence, in an evocation of the Larock indole synthesis, Fagnou developed a rhodium-catalysed cyclization of protected anilines with alkynes. Extensive optimization studies allowed for the development of mild reaction conditions, which turned out in a remarkably ample scope and made possible the use of simple O_2 as terminal oxidant (**Scheme 47**). Indoles were obtained with a high Larock-type regioselectivity (> 40:1) when alkynes functionalised with an aryl moiety were used, while, employing aliphatic alkynes, a poor selectivity was observed. Later, the use of aliphatic alkynes bearing an alkenyl group lead to the formation of 2-alkenyl indoles as single regioisomers.[114]
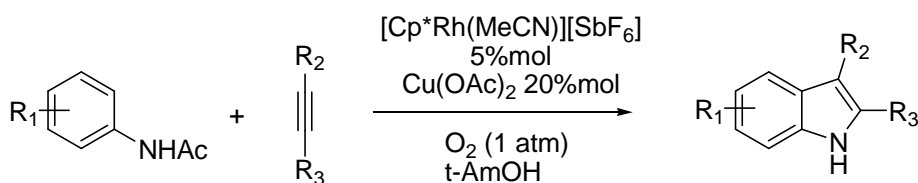
Scheme 47. *Fagnou's catalytic system, R_3 = larger group, R_2 = smaller group.*

1.5.6. Cycloaddition of nitro and nitrosoarenes with alkynes

In 2002, Nicholas and Penoni reported a [RuCp*(CO)$_2$]$_2$-catalysed reaction of nitroarenes with aryl alkynes to give indoles at high temperature[115]. Although the reaction proceeded with excellent regioselectivity in the 3-aryl indole, the yields of the corresponding indoles were only moderate. A more active palladium catalyst for this reaction was published by Ragaini and co-workers[116]. The reaction consist in the generation of a nitroso arene species by reductive carbonylation of the nitroarene, this species interacts reversibly with the alkyne and gives the *N*-hydroxyl indoles by cyclization (**Scheme 48**). The presence of an aryl substituent on the alkyne should be required in order to stabilize charges or a radical at the α position. Finally the *N*-hydroxyl indole is reduced to indole.
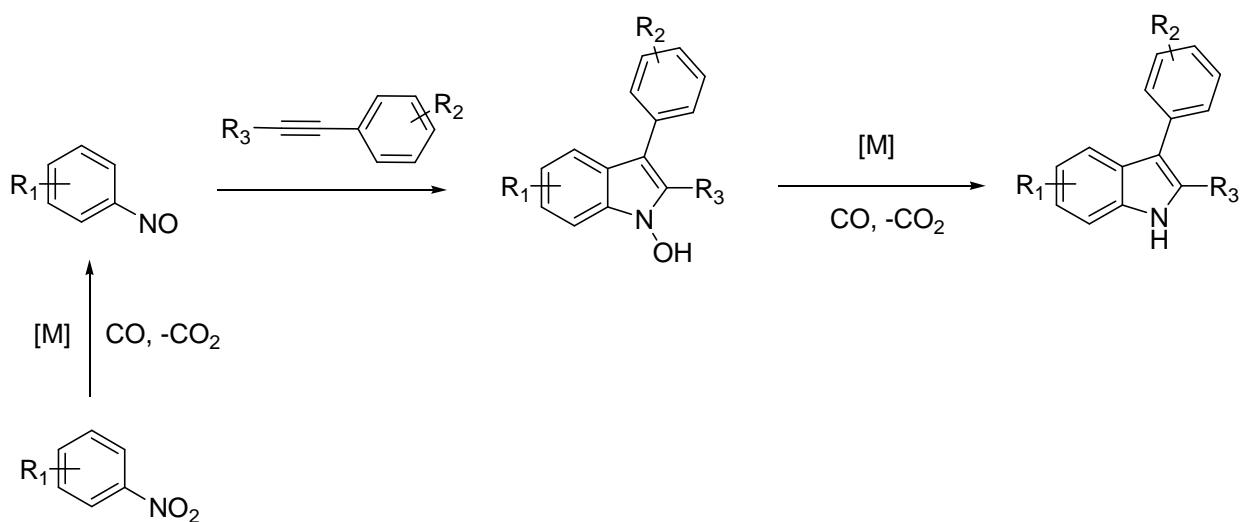
Scheme 48. *Indole synthesis via reductive carbonylation of nitroarenes.*

A similar reaction was reported by Nicholas[117], in this case the nitroso species was generated from phenylhydroxylamines in the presence of iron (III) phthalocyanine complex and underwent cycloaddition with aryl alkynes to give the corresponding indole.

2. Discussion

2.1. 1,2-Dihydronaphthalene amination catalysed by Co-porphyrins

The reaction between hydrocarbons and aryl azides catalysed by metalloporphyrins has been widely studied by our research group in the last decades.

Depending on the functional groups of the hydrocarbon substrate different reactions were observed. If ruthenium porphyrins were used as catalysts, the reaction between styrenes and aryl azides gave aziridines,[58] while in the presence of a substrate carrying an activated allylic[66] or benzylic[65] C-H bond, the nitrene insertion was observed and the organic product was an allyl amine or a benzyl amine.

The chemoselectivity is also determined by the nature of the metal coordinated to the porphyrin skeleton. In fact, the amination of a benzylic substrate yields diverse aza-compounds by running the reaction in the presence of a Co(TPP) or Ru(TPP)CO as the catalyst, obtaining an imine[60] or an amine [65] respectively (see **Introduction**, **Section 1.33**). This different behaviour derives from the mechanisms of the nitrene transfer reaction that involves different intermediates depending on the employed metal.

The stoichiometric reaction between ruthenium-carbonyl porphyrin complexes and aryl azides yields *bis*-imido complexes, which are active species in C-H amination (***Scheme 49***).[68] On the other hand, Zhang, De Bruin and co-authors proposed, on the basis of theoretical and EPR data, the formation of an active cobalt(III) nitrene radical intermediate during the cobalt(II) porphyrin catalysed amination of both saturated and unsaturated hydrocarbons (***Scheme 49***).[62],[63]
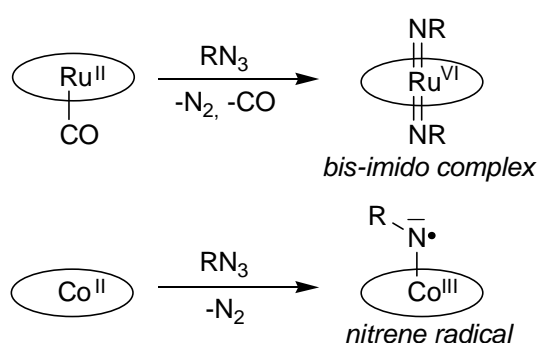
Scheme 49*. Reaction between an organic azide and a ruthenium or cobalt porphyrin.*

If the substrate carries more than one functional group that is reactive towards aryl azides, the chemoselectivity of the reaction may be affected. In the case of cyclohexene, which has an

endocyclic double bond and four allylic positions available, the reaction selectivity was totally driven towards the allyl amine using both Co(TPP)[64] and Ru(TPP)CO[66] as catalysts.

However, the amination of *β*-substituted styrenes with an endocyclic double bond, such as 1,2-dihydronaphthalene, showed a low chemoselectivity for the ruthenium porphyrin-catalysed reactions.[66] This is probably due to the simultaneous presence of an activated double bond, allylic and a benzylic C-H bonds in the same molecule (*Scheme 50*). A mixture of **28** and **29** was obtained using Ru(TPP)CO as the catalyst.
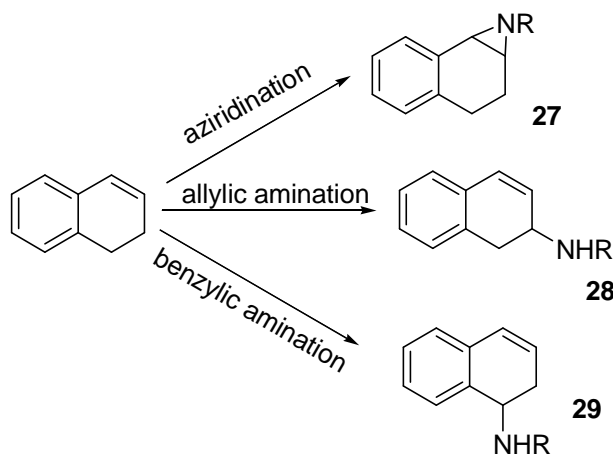
Scheme 50. Amination pathways for 1,2-dihydronaphthalene amination.

In order to improve the chemoselectivity of the reaction, we studied the efficiency of cobalt porphyrins in the catalytic amination reaction discussed above. Experimental data reported herein show an unusual reactivity of the C-C double bond due to the peculiarity of dihydronaphthalene being a very active hydrogen donor.

The reaction between dihydronaphthalene and 4-nitrophenyl azide in the presence of Co(TPP) yielded three different and unexpected products (*Scheme 51*). Interestingly, compound **30** is the organic product usually obtained from the benzylic amination of tetrahydronaphthalene, **31** is the corresponding imine of **30** and the ketone **32** should be formed by hydrolysis of **31** during the purification process. It is worth noting that naphthalene was detected in the reaction crude by GC-MS analysis.
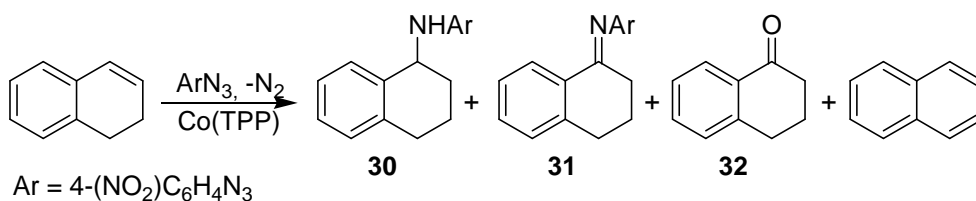
Scheme 51. Co(TPP)-catalysed amination of 1,2-dihydronaphthalene.

To rationalise this experimental result we repeated the reaction in absence of the catalyst and the azide completely converted into a mixture of **31** and **32**. Since it is known that the reaction between olefins and organic azides[50],[59] can afford imines by thermal decomposition of 1,2,3-triazolines we proposed the blank reaction mechanism illustrated in *Scheme 52*.
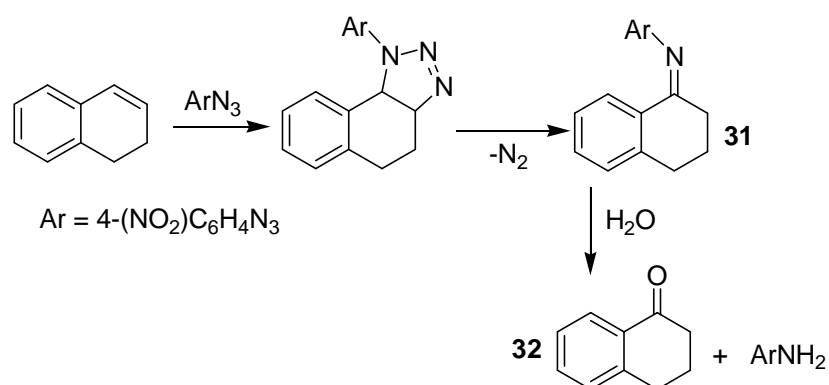
Scheme 52. Blank reaction mechanism.

The reaction conditions were optimised and the reaction between 1,2-dihydronaphthalene and 4-nitrophenylazide was chosen as a model reaction. The results of the optimisation are listed in ***Table 1***, the best solvent/catalyst combination was Co(TMOP)/1,2-dichloroethane (entry 3, ***Table 1***), although the electronic properties of the catalyst seem to have just a little influence on the catalysis outcome.

Table 1. *Catalyst/solvent screening for the Co-catalysed amination of dihydronaphthalene by 4-nitrophenyl azide.*[a]
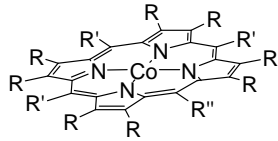
Entry		time(h)[b]	30 (%)[c]	31 + 32 (%)[c]
1[d]	Co(TPP); R=H; R'=R''=C_6H_5	10	23	22
2	Co(TPP); R=H; R'=R''=C_6H_5	3	27	25
3	Co(TMOP); R=H; R'=R''= 4-$CH_3OC_6H_4$	1.5	40	34
4	Co(4-^{n}BuTPP); R=H; R'=R''= 4-^{n}BuC_6H_4	3	32	20
5	Co(4-CF_3TPP); R=H; R'=R''= 4-$CF_3C_6H_4$	4.5	23	41
6	Co(OEP); R=Et; R'=R''= H	1.5	22	21
7	Co(4'MPyP); R=H; R'= C_6H_5; R''=Py	2.5	19	56

[a]Experimental conditions: Co/4-nitrophenylazide = 4:50, [Co] = 2 x 10^{-5} M, solvent = 1,2-dihydronaphthalene/1,2-dichloroethane 1:1 (5.0 ml). [b]Time required to reach complete aryl azide conversion. [c]Isolated yield. [d]Reaction run in benzene.

In order to assess the generality of the process we repeated the reaction using different aryl/sulphonylazides. As reported in **Table 2**, the yields in the amine (**A**) were comparable in every case, longer reaction times were observed using aryl azides bearing EDGs. The best results in terms of product **A** were obtained using sulphonylazides (NsN_3, TsN_3; entry 6-7, **Table 2**).

Table 2. *Co(TMOP) catalysed reaction between dihydronaphthalene and organic azides.*[a]
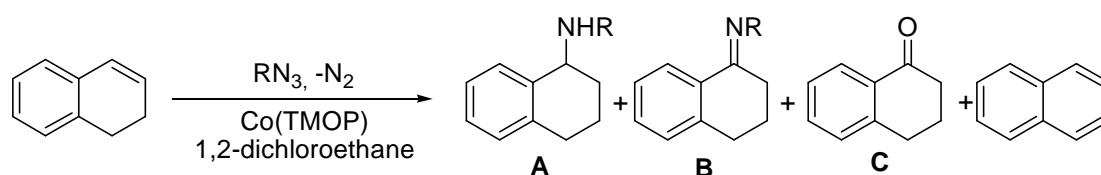
entry	azide	time(h)[b]	A (%)[c]	B+C (%)[c]
1	$4\text{-}(NO_2)C_4H_3N_3$	1.5	40	34
2	$4\text{-}(CH_3O)C_4H_3N_3$	11	32	29
3	$4\text{-}(CN)C_6H_4N_3$	3.5	34	36
4	$4\text{-}(^tBu)C_6H_4N_3$	18	37	19[d]
5	$3,5\text{-}(CF_3)_2C_6H_3N_3$	1.5	21	20
6	$4\text{-}(NO_2)C_6H_4SO_2N_3$	2	41	18
7	$4\text{-}(CH_3)C_6H_4SO_2N_3$	5	44	11

[a]Experimental conditions: Co(TMOP)/azide = 4:50, [Co] = 2 x 10^{-5} M, solvent = 1,2-dihydronaphthalene/1,2-dichloroethane 1:1 (5.0 ml). [b]Time required to reach complete aryl azide conversion. [c]Isolated yield. [d]Only **C** was isolated, the imine was detected by GC-MS analysis of the reaction mixture.

To investigate the reaction mechanism we took into account that 1,2-dihydronaphthalene can be easily involved in hydrogen transfer reactions[118],[119] as supported by the presence of naphthalene in the reaction crude. Considering the model reaction, we thought that the formation of **30** could be due either to a hydrogenation process of **31** (*path a*, ***Scheme 53***), or to an amination of tetrahydronaphthalene formed by a cobalt-mediated disproportionation of dihydronaphthalene (*path b*, ***Scheme 53***). Both proposals were not supported by experimental data.
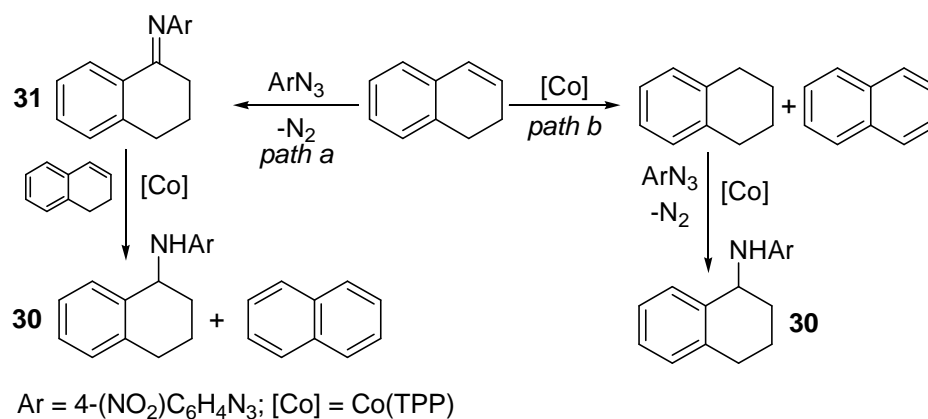
Scheme 53. *Potential pathways for the synthesis of **30**.*

Taking into account the aziridination mechanism proposed by Zhang and De Bruin[63], we proposed the following catalytic cycle (**Scheme 54**). We first suggest the formation of the nitrene radical **B** that reacts with dihydronaphthalene to form the carboradical **C** which could evolve through different pathways. We propose that the good hydrogen donor capacity of dihydronaphthalene favoured a hydrogen transfer reaction (*path a*) forming benzylic amine **E** and avoiding the olefin aziridination to **D** (*path b*). The absence of compounds deriving from benzylic or allylic amination of dihydronaphthalene (see **Scheme 50**) is probably due to the high reactivity of the endocyclic C-C double bond.
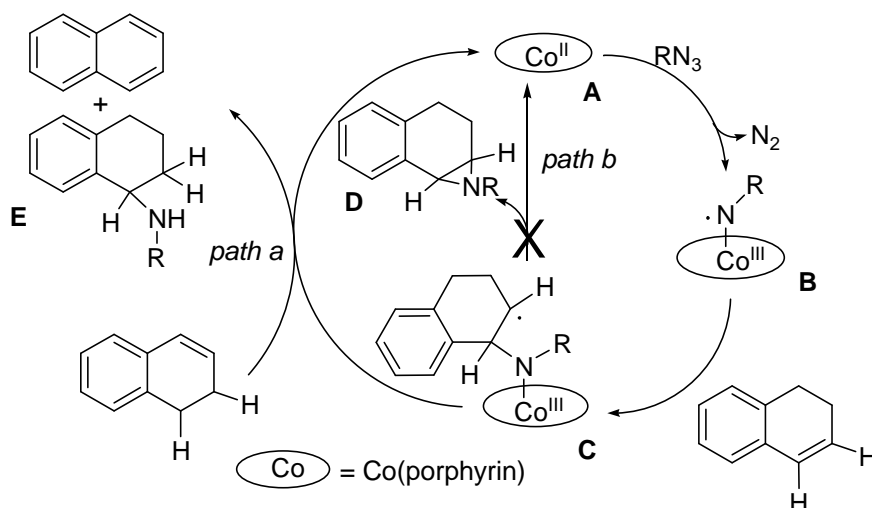
Scheme 54. *Mechanistic proposal for dihydronaphthalene amination.*

To confirm the direct amination of the double bond and to rule out the possibility of C-H benzylic amination, we studied the reactivity of 4-nitrophenyl azide towards 1-phenyl-1,2-dihydronapthalene.

The exclusive formation of amine **34** in 54% yield (*Scheme 55*) definitely pointed out the amination of the unsaturated position to sustain mechanisms illustrated in *Scheme 54*. The GC-MS analysis of the crude revealed the presence of 1-phenylnaphthalene.
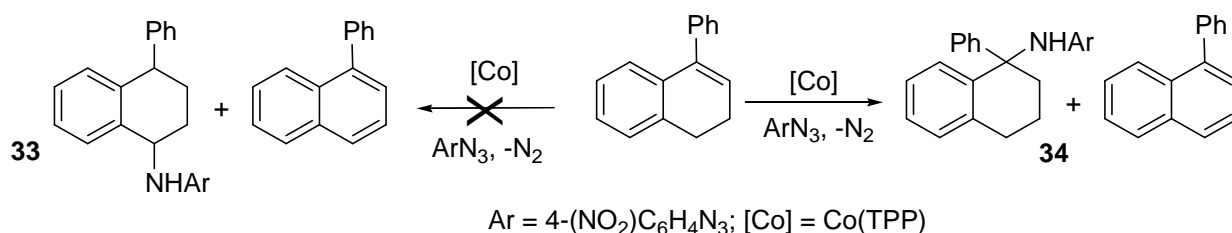
Scheme 55. 1-phenyl-1,2-dihydronaphthalene amination.

In order to confirm the hydrocarbon involvement in a hydrogen transfer process, we performed the reaction using an endocyclic olefin that cannot convert in the corresponding aromatic compound such as indene (*Scheme 56*). When indene was allowed to react with 4-nitrophenylazide in the presence of Co(TMOP) the only detected aminated product was the imine **36**, beside indene polymerization products. The absence of amine **35** confirmed again that cobalt porphyrins are not competent catalysts for benzylic C-H amination of endocyclic styrenes, conversely, using Ru(TPP)CO as the catalyst for the same reaction, **36** was obtained in moderate yield.[66]
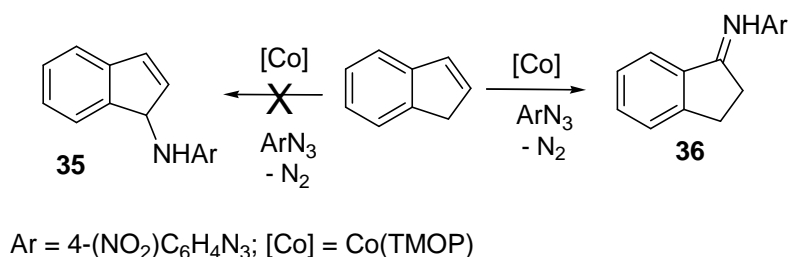
Scheme 56. Reaction between indene and 4-nitrophenyl azide in the presence of Co(TMOP).

2.2 Resonance Raman Mechanistic Study of Allylic Amination Catalysed by Ruthenium Porphyrins

As reported in **Section 1.3.4.**, the mechanism of the allylic amination of cyclohexene catalysed by Ru(TPP)CO was deeply investigated.[66],[69] It was found that two different catalytic cycles take place depending on the aryl azide/substrate ratio (*Scheme 57*). At high cyclohexene concentration the active species is likely to be the *mono*-imido species **C** which is very reactive and it is immediately trapped by a substrate molecule giving the aminated product and the starting catalyst Ru(TPP)CO. If the azide/substrate ratio is low, the *mono*-imido **C** species undergoes a further reaction with the aryl azide giving the *bis*-imido complex **E**, formally a Ru^{VI} complex, which is an active species in allylic amination.[68]
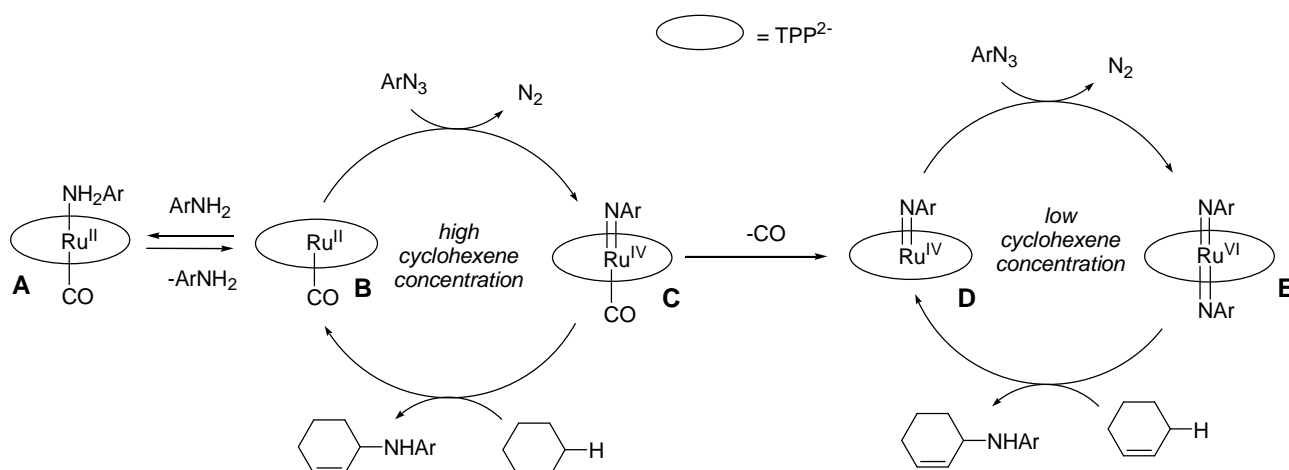
Scheme 57. Catalytic cycle proposed for allylic amination catalysed by Ru(TPP)CO.

This mechanistic hypothesis was supported by a DFT study,[69] however, none of the Ru^{IV} active species was ever isolated or detected with common techniques (IR, NMR). For this reason, we tried to investigate this reaction from a different point of view, using Resonance Raman Spectroscopy (RRS). This technique requires a tunable laser source whose frequency has to be close to the absorption wavelength of a chromophore of the analyte. In this way the radiation act as a probe exciting selectively the analyte molecules and the Raman signals are greatly enhanced. Using RRS we could follow the catalyst behaviour by recording the signals corresponding to the vibrational modes of the porphyrin skeleton even in the complex catalytic mixture. These experiments were carried out in the laboratories of Leicester University with the collaboration of Dr. A.Hudson and Dr. G.Solan thanks to an Erasmus grant.

Since the catalytic intermediates reported in **Scheme 57** have different oxidation state at the ruthenium atom, we recorded the RR spectra of a ruthenium (II), a ruthenium (IV) and a ruthenium (VI) porphyrin species: [Ru^{II}(TPP)CO], a μ-oxo dimer species [Ru^{IV}(TPP)(OCH$_3$)]$_2$O (**92**), and the *bis*-imido complex **10** [Ru^{VI}(TPP)(N=Ar)$_2$] (Ar = 3,5-*bis*(trifluoromethyl)phenyl) (**Figure 15**). We obtained spectra with intense signals even in diluted benzene solutions (10^{-4} M), the signal pattern for the porphyrin skeleton vibrations in the 1200-1600 cm^{-1} region was consistent with a previous RR study performed on Ru(TPP) complexes by Spiro et al.[120] We identified a weak signal around 1020 cm^{-1} in complex **10** spectrum (**Figure 15**, right spectrum) that was assigned to the aromatic ring stretching of the nitrene moiety. This signal was also observed in the Raman spectrum of the aniline-complex **15** [Ru^{II}(TPP)CO(3,5-*bis*(trifluoromethyl)aniline)], hence, it can be considered as an evidence of coordination of an axial ligand containing an aryl moiety.
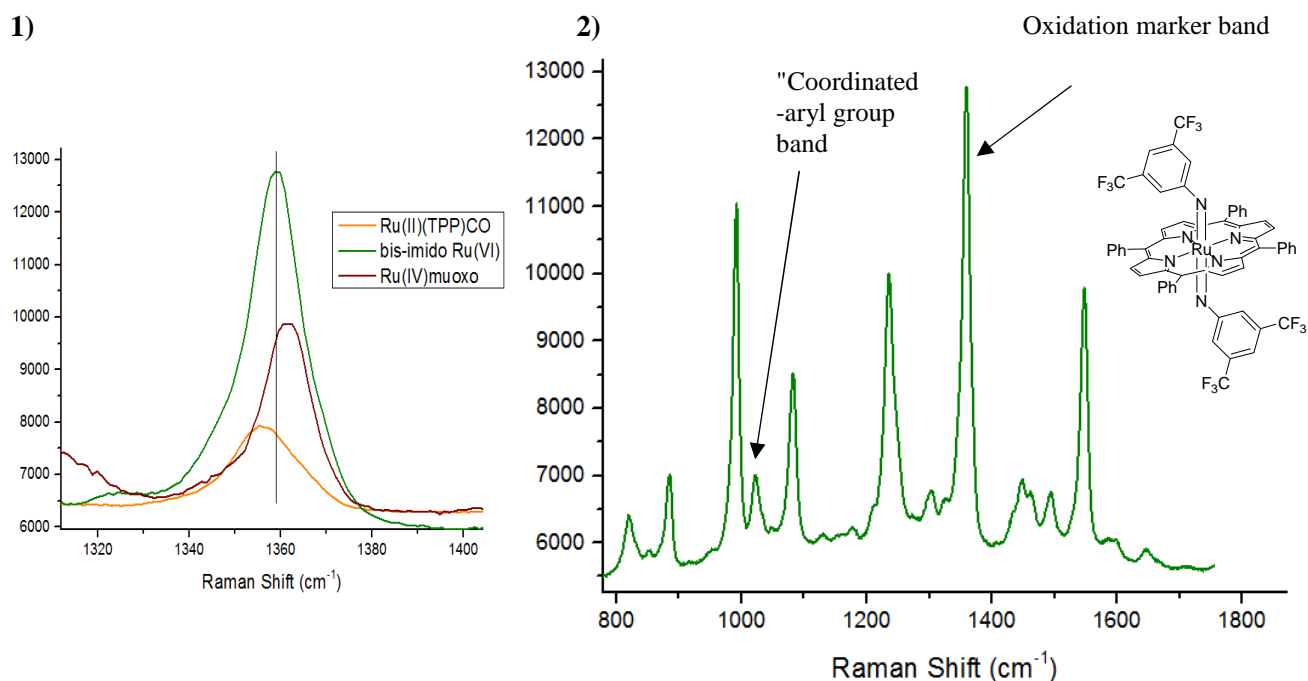
Figure 15. 1) *Oxidation marker band of the three Ru(porph) complexes.* 2) *RR spectrum of complex* ***10****(right spectrum).*

We also identified an oxidation marker band in the RR spectra of ruthenium-porphyrin complexes around 1360 cm^{-1}. Generally, a right-shift of this peak is an evidence of ruthenium oxidation (**Figure 15**, left spectra) while a left-shift of the oxidation marker band is a sign of electron enrichment at the metal centre. For example a left shift was observed when 3,5-*bis*(trifluoromethyl)aniline (**37**), a coordinating species, was added to a Ru(TPP)CO solution at room temperature. Upon this addition complex **15** should be formed in solution.[66]

Keeping in mind this information, we recorded the RR spectrum of Ru(TPP)CO in the presence of 3,5-*bis*(trifluoromethyl)phenyl azide (**38**) in benzene. We obtained a clear evidence of a coordinative interaction between Ru(TPP)CO and the aryl azide through, which is believed to be the very first step of the catalytic cycle.[69] The coordinative bond between the ruthenium atom and the aryl azide is very weak, and because of this no evidences of the interaction were found using other techniques (such as NMR, IR spectroscopy).

The changes in the RR spectrum of Ru(TPP)CO in the presence of aniline **37** or aryl azide **38** are similar: a better resolved spectrum, probably due to an increased solubility at RT in benzene and a left-shift of the oxidation marker band (**Figure 16**, left spectra). The growth of a weak "coordinated-aryl group band" in the 1000-1050 cm^{-1} region was observed upon the addition of aryl azide **38** but the peak had a lower intensity with respect to the one observed for complex **15** (**Figure 16**, right spectra).

1)   **2)**
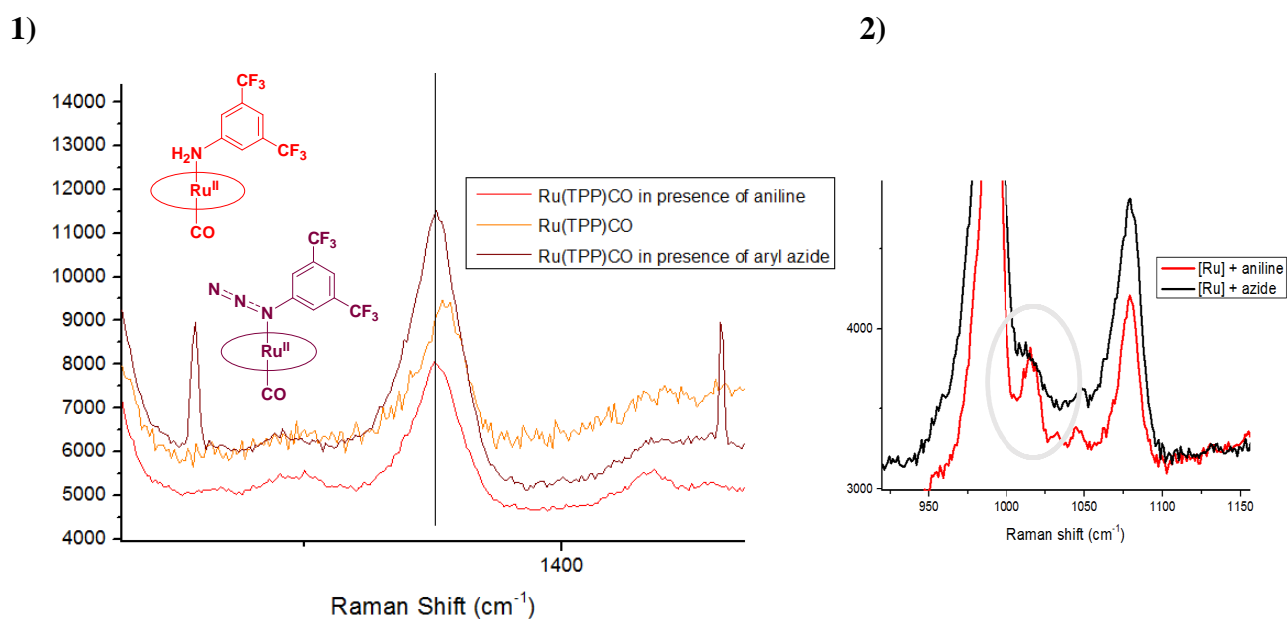
Figure 16. 1) *Ru(TPP)CO oxidation marker band shifts upon coordination of an axial ligand.* **2)** *Coordinated aryl group band in the spectra of complex* **15** *(red line) and of Ru(TPP)CO in the presence of* **38***(black line).*

In order to get additional mechanistic information on the Ru(TPP)CO-catalysed amination of cyclohexene, we had to record the time-resolved RR spectrum of the catalytic mixture as close as possible at the original reaction conditions (T = 80°C, nitrogen atmosphere). A new experimental set up was developed, the spectra of the catalytic mixture were recorded using a hermetically closed

aluminium cell which was loaded with the solution of the reagents in a dry box and heated to 70°C with a heating plate while kept in optical contact with the instrument lens.

The catalytic experiment were performed at different cyclohexene concentrations, using Ru(TPP)CO as the catalyst and 3,5-*bis*(trifluoromethyl)phenyl azide as the aryl azide.

The conversion of the aryl azide in the organic product of the allylic amination reaction was witnessed by the rise of the spectrum baseline during the reaction as usually happens when a fluorescent product is formed. In fact, when we recorded the RR spectra of a benzene solution of the organic product in the presence of Ru(TPP)CO we obtained a spectrum with the typical ruthenium porphyrin signals along with a very broad peak around 440 nm.

In the experiment at high cyclohexene concentration (cyclohexene as reaction solvent) we observed a very slight right-shift of the oxidation marker band and the growth of the "coordinated-aryl group band" (*Figure 17*). In the last acquisitions the oxidation marker band shifted left to a suitable frequency for the anilino complex **15**. It is worth reporting that the aryl azide conversion was complete in this experiment as observed by TLC analysis. This can be the evidence of a catalytic cycle involving Ru^{II}-Ru^{IV} as active species and the ruthenium(II) anilino complex as the catalyst resting state.

1)   **2)**
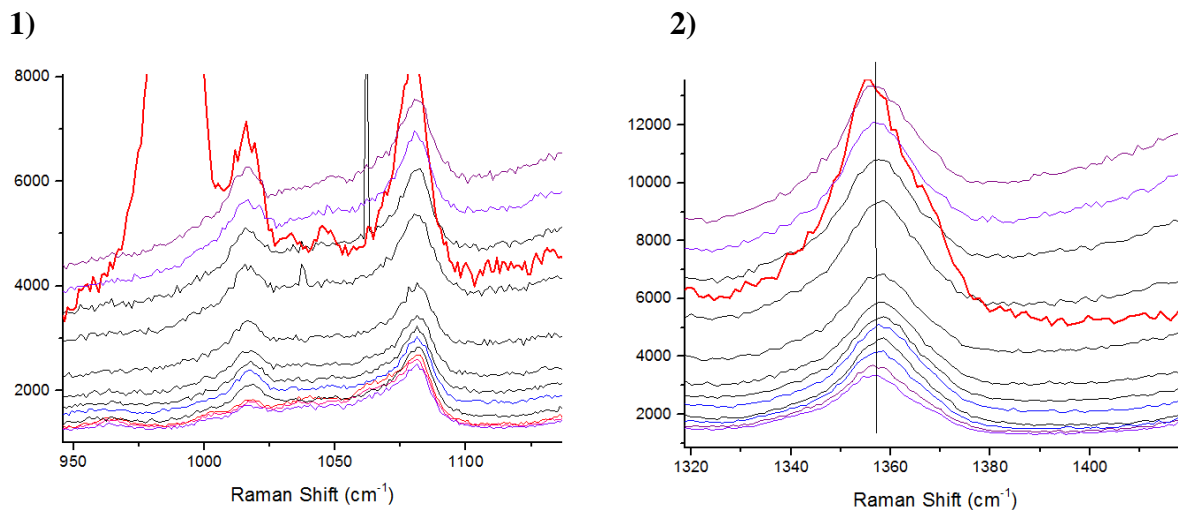
Figure 17. Time resolved spectra of the catalytic mixture in the region of the "coordinated aryl group band" (1) and the oxidation marker band region (2), the red line and corresponds to the anilino complex 15 spectrum and was added for comparison.

At low hydrocarbon concentration, only an initial right-shift of the oxidation marker band was observed without any further change in the spectrum (*Figure 18*). This is consistent with an oxidation of the ruthenium (II) catalyst to the Ru^{IV}/Ru^{VI} intermediates of the second catalytic cycle

reported in *Scheme 57*. Unfortunately at these reaction conditions a low conversion of the aryl azide occurred, as observed by TLC analysis and no catalyst final state was observed.
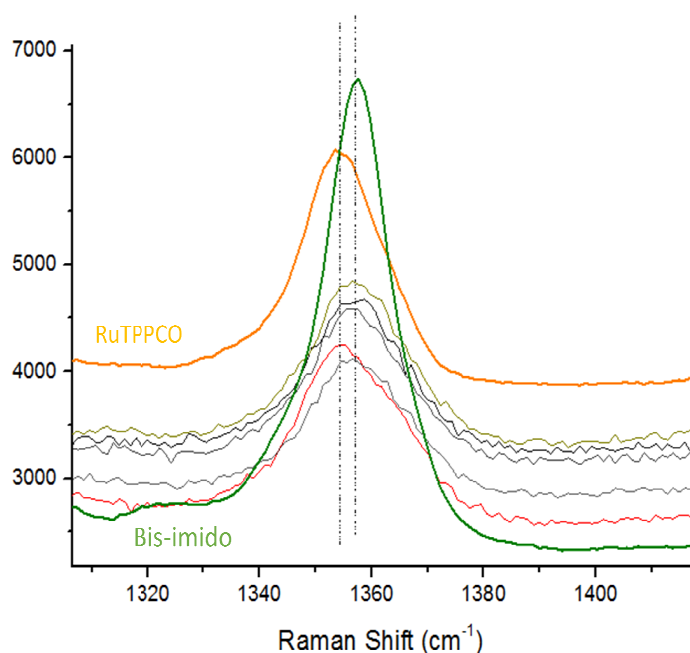
Figure 18. Time resolved spectra of the catalytic mixture in the oxidation marker band region, the pale red line is the first spectrum acquired, the pale green is the last acquisition. The bold lines are the reference spectra of Ru(TPP)CO and the bis-imido complex 10.

In conclusion, a preliminary study of the ruthenium porphyrin-catalysed allylic amination was done, we demonstrated that RRS is a useful tool to get information about the porphyrin complexes state in the catalytic mixture during the reaction. An optimisation of the experimental set up and a complete assignment of the porphyrin signals in the Raman spectrum may lead to a better understanding of the reaction mechanism.

2.3 Mechanistic Insights of the Ru(Porph)-Catalysed Aziridination of α-Methyl Styrene by Aryl Azides

The reaction between aryl azides and styrenes catalysed by ruthenium porphyrins to give aziridines was already mentioned in **Section 1.3.3.** and was deeply investigated in the past years by our research group. The first example in which aryl azides were used as nitrogen source was reported in 1999 by Cenini and co-workers[121] and the scope of the reaction was well studied in a subsequent paper[58].

A particular deactivation pathway was discovered while studying the effect of the substrate concentration on the catalytic outcomes: a linear dependence between the kinetic constants and the styrene concentration was observed increasing the olefin amount up to 30% (v/v), at higher concentrations the observed relationship disappeared and the reaction rate strongly decreased by increasing the styrene concentration.
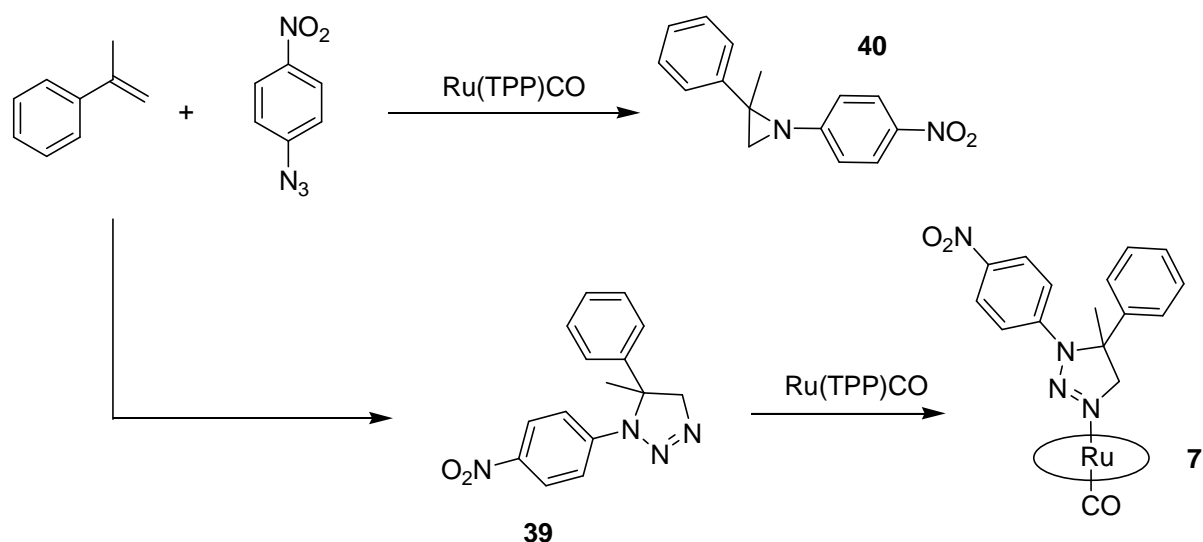
Scheme 58. *Ru-catalysed and uncatalysed reaction between α-methyl styrene and 4-nitrophenyl azide.*

This discrepancy was explained by the competition between the catalytic reaction and the uncatalysed reaction between styrenes and aryl azides to give triazolines (***Scheme 58***). [59] This last reaction is relevant at high substrate concentrations and the triazoline **39** was observed in the reaction crude beside the aziridine **40**. Triazoline **39** is a coordinating species and in the presence of Ru(TPP)CO yields the hexa-coordinated complex **7**. This latter compound is not a catalytic intermediate since both using complex **7** or Ru(TPP)CO in the presence of the triazoline **39** the reaction rate decreased drastically (k(Ru(TPP)CO)/k(**7**) = 10:1). The logical explanation of this

lower activity is that the triazoline act as an inhibitor and competes with the aryl azide for the coordination at the axial site of Ru(TPP)CO.

To confirm this hypothesis we performed a mechanistic investigation and we implemented the information obtained from previous works[58, 59] with the data obtained by kinetic and DFT studies.

2.3.1 Kinetic Study

At first, the reaction between 4-nitrophenyl azide and α-methyl styrene was taken as a model reaction for the kinetic experiments. It was known from a precedent study[59] that using Ru(TPP)CO as the catalyst a first-order both in the aryl azide and α-methyl styrene was observed but the linear dependence of the kinetic constant with the substrate concentration was lost at high α-methylstyrene concentrations and a progressive inhibition was observed by increasing the substrate concentration. A first-order was observed with respect to the catalyst concentration.

Interestingly, we found that the functionalisation at the *para* position of the *meso* aryl of the porphyrin ligand may cause a modification of the kinetic order in the aryl azide (***Table 3***). Generally, a first-order in the aryl azide was obtained with ligands bearing EDGs (entries 1-3, ***Table 3***) and a zero-order was obtained by functionalisation with EWGs (entries 4-6, ***Table 3***).

Table 3. *Dependence of the kinetic order of the aziridination reaction on the employed porphyrin ligand[a].*
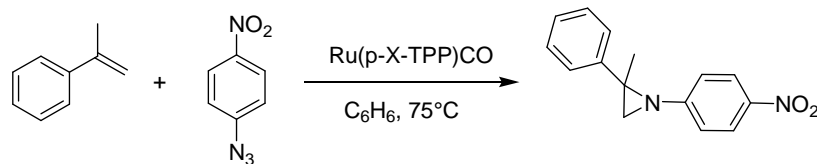
Entry	Employed Catalyst	t (h)	Conv. %	Kinetic Order[b]
1	Ru(p-MeO-TPP)(CO)	6	95 %	1
2	Ru(p-Cl-TPP)(CO)	8	85 %	1
3	Ru(p-^{t}Bu-TPP)(CO)	2	77 %	1
4	Ru(p-CF$_3$-TPP)(CO)	1.5	100%	0
5	Ru(p-COOMe-TPP)(CO)	1.5	100%	0
6	Ru(p-F-TPP)(CO)	2	100%	0
7	Ru(p-nBu-TPP)(CO)	2	100%	0/1

[a]Experimental Conditions: Ru/4-nitrophenyl azide/ α-methyl styrene = 1:50: 250, nitrogen atmosphere, 75°C. [b]Kinetic order with respect to the aryl azide.

This marked change in the kinetics of the reaction depending on the porphyrin *meso* substituents is very hard to explain. Probably the more electronwithdrawing is the ligand the faster is the coordination of a sixth axial ligand (such as the aryl azide) on the ruthenium centre. Therefore the aryl azide concentrations should not affect the speed of the whole process by using catalysts of the type Ru(p-EWG-TPP)(CO).

A second kinetic study was performed using another model reaction (**Scheme 59**): Ru(T(p-CF$_3$)PP)(CO) (**41**) and 3,5-*bis*(trifluoromethyl)phenyl azide (**38**) where chosen because their use ensures the best catalytic performances, as illustrated in the previously performed[58] catalysts and aryl azides screening. α-Methyl styrene was chosen as model substrate.
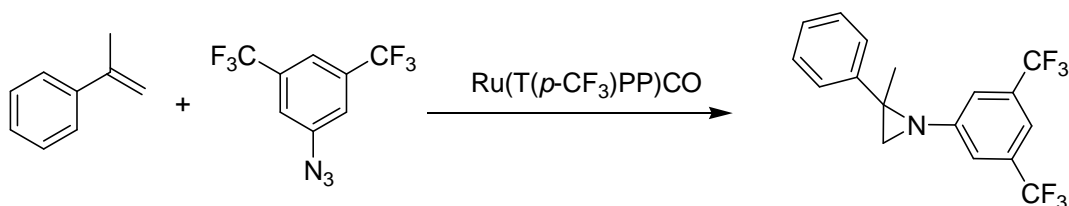
Scheme 59. *Second model reaction for the kinetic study.*

An ambiguous behaviour was observed for the kinetic order with respect to the aryl azide at different substrate concentrations: in the typical catalytic conditions (catalyst/azide/substrate = 1:50:250) the kinetic order was zero (*Figure 19*, graph a), at higher substrate concentration (more than 1.5 M, 20% v/v) the reaction started with a zero-order relationship and gradually converted in a first-order in the aryl azide (*Figure 19*, graph b), then at 40% v/v (3.0 M) of α-methylstyrene a clean first order dependence in the aryl azide was observed (*Figure 19*, graph c).
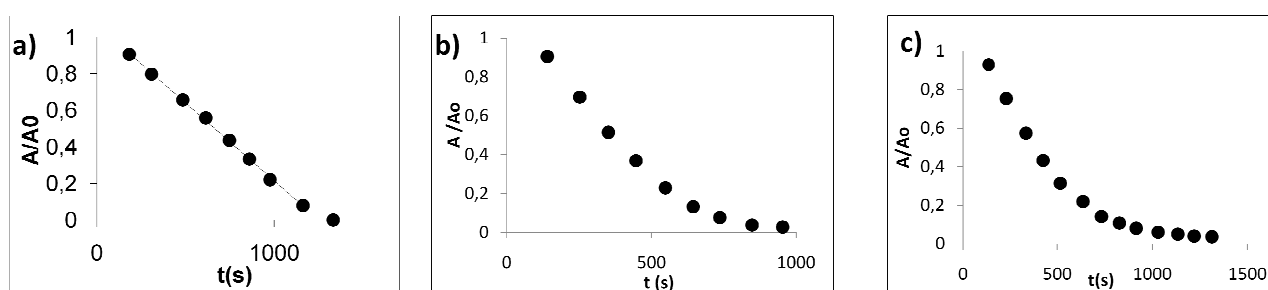
*Figure 19. Aryl azide consumption monitored by IR spectroscopy at [styrene] = 0.1 M (**a**), 2.1 M (**b**), 3.0 M (**c**).*

A plot of the reaction rate (ΔM/Δt) *versus* the olefin concentration revealed a dependence very similar to the one found for the first model reaction (*Scheme 60*).[59] A first order in α-methyl styrene at low concentration (up to 0.77 M) followed by a drop in the reaction rate at high concentrations. The loss of linearity in the reaction speed *vs.* olefin concentration dependence and the observation of a change in the aryl azide kinetic order from zero to mixed zero-first were coincident.
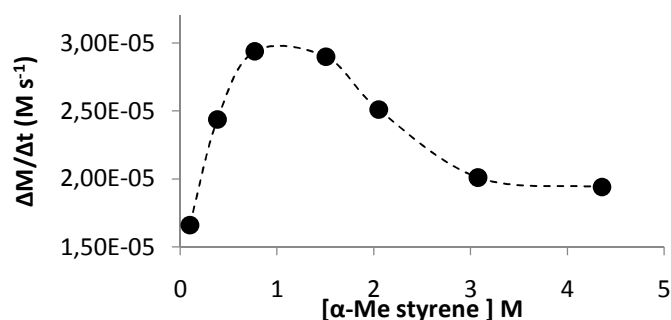
Scheme 60. Plot of the reaction rate versus α-methyl styrene concentration.

As stated above, the uncatalysed reaction becomes relevant at high olefin concentrations. The inactive triazoline-complex **42** (*Figure 20*), which is analogous to **7**, is formed in the reacting mixture, as confirmed by NMR analysis of the reaction crude. The drop in the reaction speed is due

to the competition between the aryl azide and the triazoline for coordination at the ruthenium centre, thus this substitution becomes rate-determining. Moreover, the change in the kinetic order of the aryl azide is justified since a fist order in the incoming coordinative species (the aryl azide) is suitable for a ligand exchange reaction.[122]
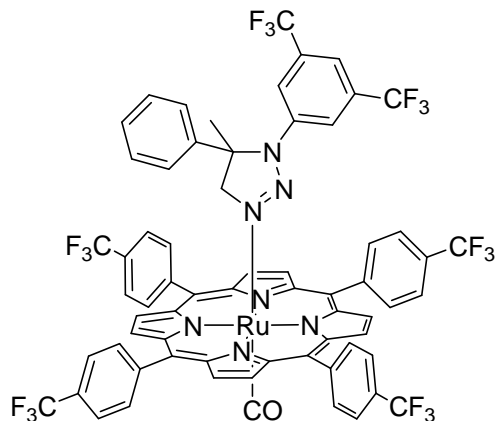
Figure 20. *Triazoline complex* ***42***

To confirm the hypothesis stated above we synthesised complex **42** and we employed it as the catalyst for the kinetic experiments, using aryl azide **38** and α-methyl styrene as reagents. We observed a much slower reaction and a clean first order in the aryl azide at any substrate concentration, thus confirming that the kinetics of the entire process are strongly conditioned by the presence of the triazoline.

2.3.2. DFT Study

In collaboration with Prof. Carlo Mealli and Dr. Gabriele Manca of ICCOM-CNR (Florence) we performed a computational investigation of the mechanism of Ru(porph)-catalysed aziridination of olefins. A mechanism analogous to the one represented in *Scheme 57* (**Section 2.2**) was initially proposed but, since the ruthenium-carbonyl species were always detected in the aziridination reaction crudes by IR analysis, we excluded the possibility that the *bis*-imido species (second catalytic cycle in *Scheme 57*) may be involved in the aziridination reaction.

Therefore, the starting point of the study was the ruthenium-porphine *mono*-imido species [Ru](NCH_3)(CO)_T (**43_T**) in the triplet state, whose formation by the reaction between Ru(porphine)CO and methyl azide was already discussed from a computational point of view[69] As pointed out in the Introduction (**Section 1.3.3**), the singlet-triplet interconversion of the ruthenium

mono-imido species allows the possibility of spin localization over the nitrogen atom and is necessary to reproduce the observed radical reactivity.[69]

The reaction of complex **43$_T$** with isobutene to give the corresponding aziridine was studied, isobutene was chosen as the olefin instead of α-methyl styrene in order to speed up the calculations. The transition state of the reaction (**44** in *Scheme 61*) was reached with a relatively small energy barrier of +9.3 kcal mol^{-1}. The TS nature of **44** was confirmed by its unique imaginary frequency at -267.0 cm^{-1} associated to formation of the N-C linkage. Any effort to obtain a similar transition state starting from complex **43** the singlet spin state failed.
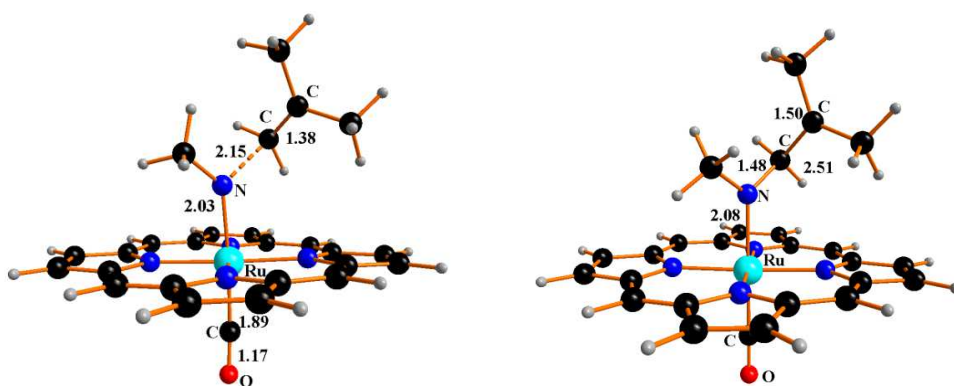
Figure 21. *Optimised structures of the transition state **44***(left structure) and complex **45** (right structure).*

The complete formation of the C-N bond leads to complex **45**, in the triplet state, through an exoergonic step (-14.4 kcal mol^{-1}). The optimized structure of **45** shows a quite large distance of 2.51 Å between the nitrogen and the distal carbon atom. Since the final aziridine product is obtained through a ring closure, the two unpaired electrons of complex **45** should be paired, thus a triplet-singlet interconversion must occur. The energy cost of the spin crossing was calculated to be close to zero since the intersystem crossing occurs near to the energy minimum of **45** (C-N distance of 2.56 Å vs. 2.51 Å). After the crossing point, the complex [Ru](aziridine)(CO)$_S$ (**46**) was obtained with a free energy gain of -30.4 kcal mol^{-1}. The Ru-N(aziridine) bond in complex **46** is very elongated (ca. 2.38 Å), suggesting that the aziridine moiety is ready to depart and restore the precursor [Ru](CO) with a slightly endoergonic (ΔG = +8.7 kcal mol^{-1}) de-coordination step.
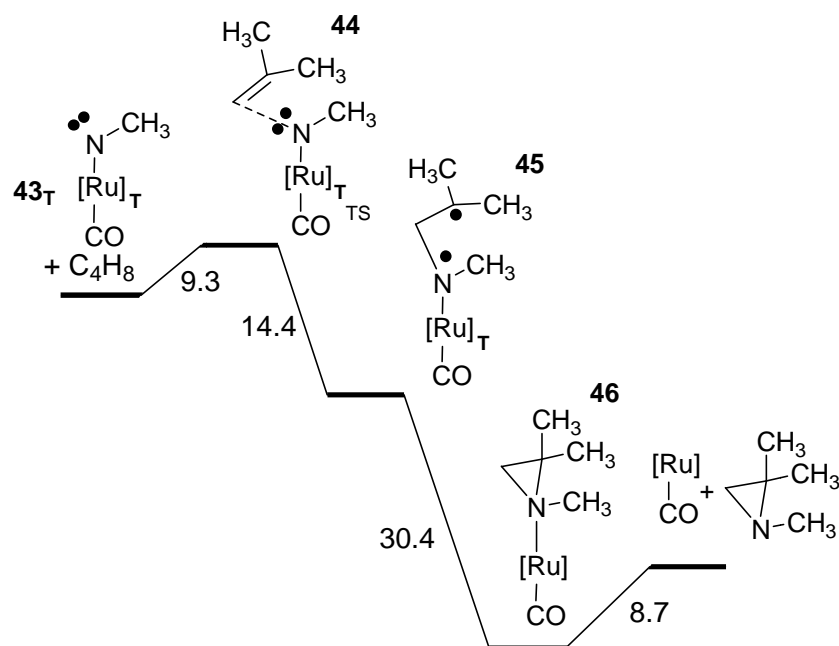
Scheme 61. *Energy profile for the aziridination starting from [Ru](NCH₃)(CO)ₜ.*

The stability of Ru(porphine)CO-triazoline adducts was investigated by the optimization of the structure of complex [Ru](1-*N*-methyl-5,5-dimethyltriazoline)CO (**47**) (***Figure 22***). The free energy gain in the coordination of the triazoline species to Ru(porphine)CO was -12.7 kcal mol^{-1}, while the same transformation in the presence of methyl azide gives only a -3.5 kcal mol^{-1} stabilization. This last data demonstrates that the triazoline is a stronger coordinative species then the organic azide, this is in accord with the observation discussed above concerning the inhibition of the aziridination reaction by the triazoline complexes **7** and **42**.
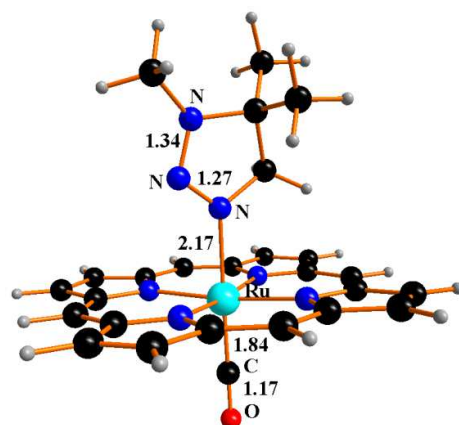
Figure 22. *Optimized structure of compound [Ru](triazoline)(CO)* **47.**

The catalytic cycle represented in *Scheme 62* was proposed on the basis of the studies discussed above. Considering the precedent mechanistic studies (see **Introduction**, **Section 1.3.4.**), the mechanistic hypothesis was restricted to the "*mono*-imido catalytic cycle" and a pre-equilibrium between complexes **A** and **C** (*Scheme 62*) was added to represent the competition between the aryl azide and the triazoline.
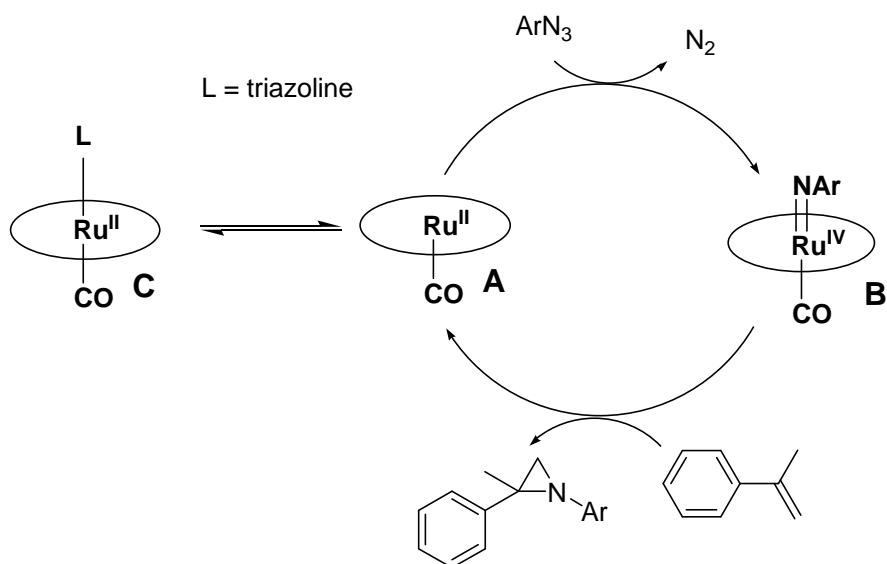
Scheme 62. Mechanistic hypothesis for Ru(porph)CO-catalysed aziridination.

2.4 Synthesis of Amino esters by Ruthenium Porphyrin-Catalysed Amination of C-H Bonds

The C-H amination of hydrocarbons catalysed by metal complexes is an efficient tool to synthesise high value nitrogen-containing compounds employing cheap starting materials. The importance of amino acid derivatives as well as the wide variety of catalytic methods developed for their synthesis was already discussed in **Section 1.4.** An appealing strategy affording α- or β-amino ester is the nitrene insertion into a benzylic C-H bond placed in α or β position to an ester group respectively (*Scheme 63*). As described in **Section 1.3.**, the metalloporphyrin-catalysed nitrene insertion into C-H bonds was well studied, however, only a few applications of this methodology for α-amino esters synthesis were reported.[61],[88]
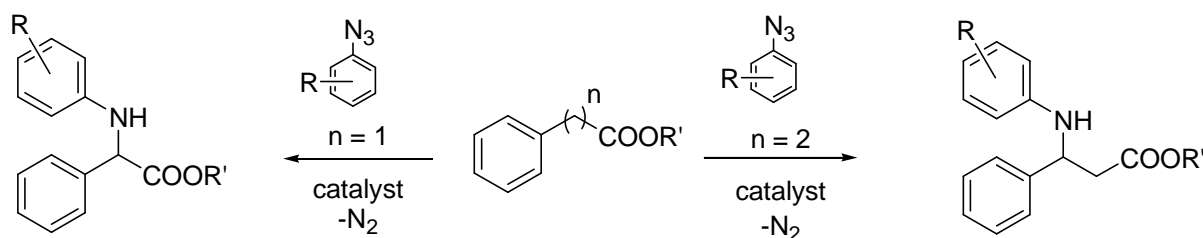
Scheme 63. *Synthesis of α- or β-amino esters by the benzylic amination reaction.*

This is due to the electron deficiency of the benzylic C-H bonds placed near an EWG, such as a carboxyl group, which hampers the C-H bond homolytic cleavage performed by the electrophilic metallo-nitrene intermediates.

Herein we discuss our results in the ruthenium porphyrin-catalysed benzylic amination of these challenging substrates.[123]

We started studying the reaction between methyl phenylacetate and 3,5-*bis*(trifluoromethyl)phenyl azide (**38**) in the presence of different catalysts and solvents (***Table 4***).

Table 4. *Amination of methyl phenylacetate by aryl azide 38.*[a]
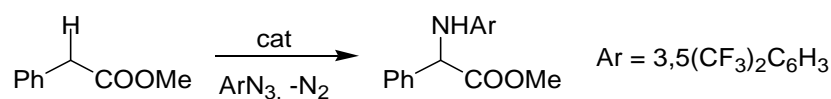
Entry	Catalyst	conv. %[b]	t (h)	yield %[c]
1	Ru(TPP)CO	100	8	64
2	Ru(TPP)CO	100	21[d]	30
3	Ru(TPP)CO	100	31[e]	40
4	Ru(TPP)CO	100	3[f]	70
5	Ru(p-CF$_3$TPP)CO	100	10	60
6	Co(TPP)	100	3	51
7	Mn(TPP)Cl	0	-	-
8	Fe(TPP)Cl	0	-	-

[a]Experimental Conditions: T = 80°C, under nitrogen, catalyst/ArN$_3$/substrate = 1:10:50. [b]IR monitoring. [c]NMR yield. [d]Run in 1,2-dichloroethane. [e]Run in acetonitrile. [f]Run in methyl phenylacetate.

As reported in **Table 4** ruthenium porphyrins (entry 1,5) showed a better catalytic efficiency in terms of yield in the desired product. Shorter reaction times were achieved by using methyl phenylacetate as the solvent (**Table 4**, entry 4). If the temperature of the reaction run in methyl phenylacetate was increased from 80°C to 100°C, Methyl (3,5-*bis*(trifluoromethyl)phenylamino)-phenylacetate (**48**) was obtained in only 1.5 hours at a 72% yield.

The azide/substrate ratio is a crucial parameter in order to have a good catalytic performance because it has a strong influence on the transformation of the ruthenium-catalyst, as explained below.
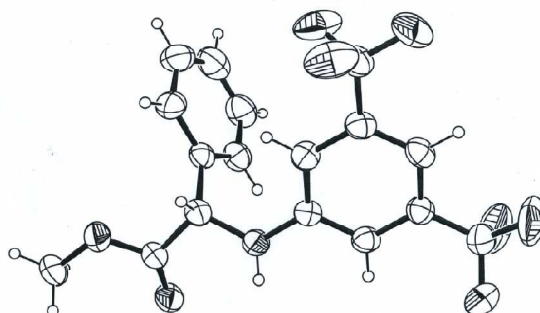
Figure 23. *ORTEP plot of the molecular structures of **48**.*

The TLC analyses of the crude of the reactions catalysed by Ru(TPP)CO (***Table 4***, entry 1,4) revealed the presence of different ruthenium species according to the employed solvent. Ru(TPP)CO is the only ruthenium complex observed when methyl phenylacetate is the reaction solvent, whilst a new purple ruthenium species was formed besides Ru(TPP)CO by running the reaction in benzene. If in the latter case the catalytic azide concentration was doubled (the Ru(TPP)CO/azide/methyl phenylacetate ratio of 1:10:50 was replaced by 1:20:50), the aryl azide conversion was not complete (80%), organic compound **48** was obtained in a low yield (29%) and the new purple complex was the only ruthenium species detectable by TLC of the catalytic mixture. Conversely, when the reaction was performed in methyl phenylacetate as the reaction solvent, a complete conversion of the aryl azide was reached even by using a Ru(TPP)CO/azide catalytic ratio of 1:50 (***Table 5***, entry 1).

Any attempt to recover this new complex in a pure form failed due to the constant presence of **48** traces. By using Ru^{II}(p-CF$_3$TPP)CO (**41**) as the catalyst the purification of the crude by flash chromatography allowed the isolation of the *bis*-amido complex Ru^{IV}(p-CF$_3$TPP)(N(R)Ar)$_2$(R = CH(Ph)COOMe, Ar = 3,5(CF$_3$)$_2$C$_6$H$_3$) **49** as purple crystals. Complex **49** was fully characterised and its molecular structure was determined by single crystal X-ray diffraction as reported in ***Figure 24***.
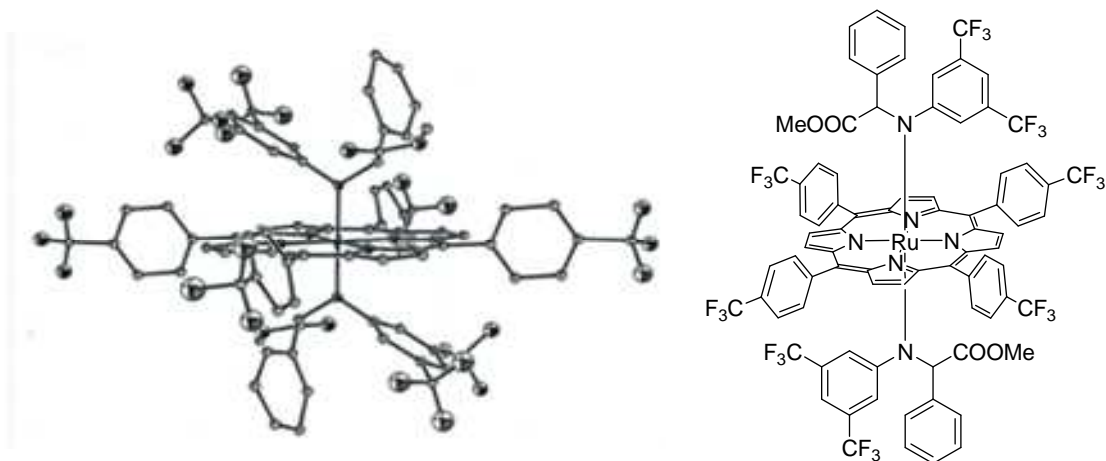
*Figure 24. ORTEP plot (left) and molecular structure (right) of complex **49**.*

The average Ru-N$_{porphyrin}$ bond distance is 2.049(4) Å. The coordination of the axial ligand is also quite similar to that of other *bis*-amido porphyrin complexes: Ru-N(Ar) is 1.944(5) Å, comparable to that of Ru^{IV}(*p*-CH$_3$TPP)(*p*-ClC$_6$H$_4$NH)$_2$[124] or Ru^{IV}(TPP)(3,5-(CF$_3$)$_2$C$_6$H$_3$N(C$_6$H$_9$)).[68] The most important change between **48** and **49** structures occurs for the N-C$_{aryl}$ bond which is much longer in **49** (1.462(7) or 1.470(6) Å) than in **48** (1.375(3) or 1.376(3) Å).

Complex **49** is a very stable compound and it does not show any catalytic activity in the reaction between azide and methyl phenylacetate. We hypothesised that complex **49** is a deactivated catalyst which can be obtained by the *bis*-imido complex Ru(*p*-CF$_3$TPP)(NAr)$_2$(**50**) formed during the catalysis run at low substrate concentrations (***Scheme 57*** of **Section 2.2**). We observed that the formation of **49** from **50** occurs only in the presence of both the substrate and the aryl azide probably through an a homolytic cleavage of the substrate benzylic C-H bond similarly to what already described for the synthesis of the analogous *bis*-amido ruthenium(IV) complex **16**.[66] When we employed the *bis*-imido complex **50** as the catalyst for the model reaction the *α*-amino ester **48** was obtained in 22 hours at a 51% yield indicating that ruthenium(VI) *bis*-imido complex **50** is a less efficient catalyst than the corresponding ruthenium(II) carbonyl complex **41** (***Table 4***, entry 5). The analysis of the reaction crude revealed the presence of the inactive complex **49**.

We propose the following mechanism (***Scheme 64***) taking into account the DFT mechanistic study concerning Ru(TPP)CO-catalysed allylic amination.[69] A central role in the catalytic cycle is played by the *mono*-imido ruthenium (IV) complex **C**. We suggest that complex **B** reacts with the aryl azide forming the *mono*-imido species Ru(TPP)(NAr)CO (**C**) that can either be trapped by methyl phenylacetate to yield the desired amino ester or be transformed into the *bis*-imido derivative Ru(TPP)(NAr)$_2$ (**E**) depending on the benzylic substrate concentration.

Scheme 64. labels: ArN₃, N₂, = TPP²⁻, Ar = (CF₃)₂C₆H₃, R = -CH(Ph)COOMe, RH, Ru^II, CO, A, B, (1), NAr, Ru^IV, CO, C, -CO, NAr, Ru^IV, D, (2), NAr, Ru^VI, NAr, E, Ru^VI, F, NHAr, COOMe, H COOMe

Scheme 64 content:

$$\text{Ar} = (CF_3)_2C_6H_3$$
$$R = -CH(Ph)COOMe$$
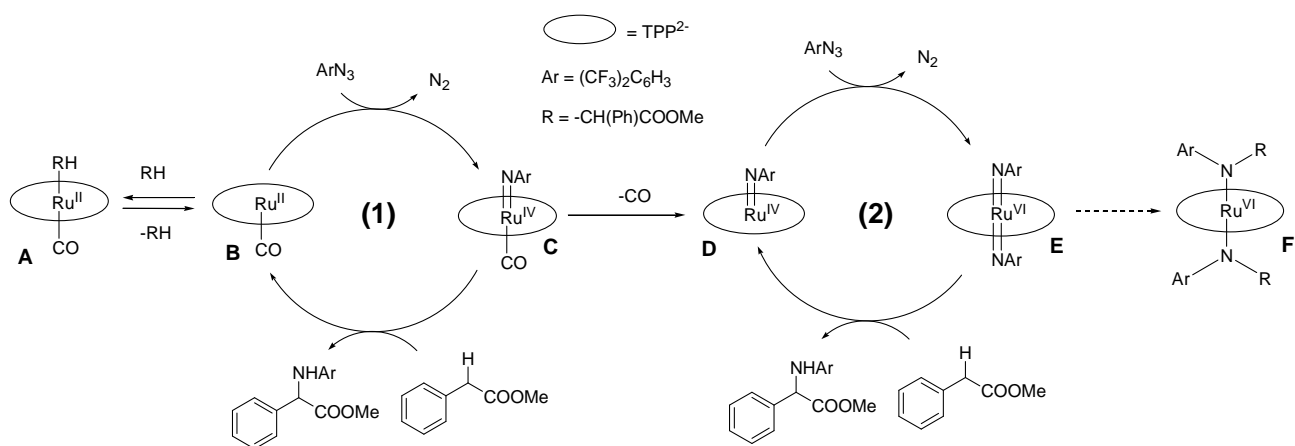
Scheme 64. *Mechanistic proposal*

This proposal is in accord with our experimental results that indicate that better catalytic performances are achieved by working at high substrate concentrations, at these conditions the first catalytic cycle is prominent, therefore, the formation of the *bis*-imido complex **E** and its consequent decomposition to give the deactivated catalyst **F** are limited (***Scheme 64***).

We investigated the influence of the substrate concentration by measuring the reaction rate at different methyl phenylacetate concentrations using a catalyst/azide ratio = 1:5. The employed azide amount was chosen in order to limit the formation of the *bis*-imido derivative (**E**) and the occurrence of the *cycle 2* of ***Scheme 64***.

The reaction rate increased by increasing the methyl phenylacetate concentration from 0.1 mol L^{-1} to 0.6 mol L^{-1}, then a substrate inhibition was evident (***Figure 25*a**). As clearly reported in ***Figure 25*b**, the reaction rate was inversely proportional to the methyl phenylacetate concentration in the 1.0-7.0 mol x L^{-1} range.
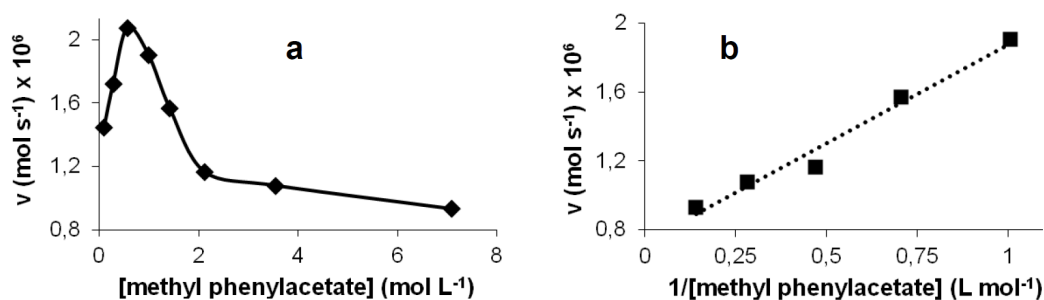
Figure 25. *Dependence of the reaction rate with respect to the methyl phenylacetate concentration.*

The observed inhibition process can be due to a reversible coordination of the ester substrate to the metal centre. This hypothesis was supported by the IR analysis of the reaction between Ru(TPP)CO and a methyl phenylacetate excess. A shift of the CO absorbance was observed after the addition of methyl phenylacetate to a dichloromethane suspension of Ru(TPP)CO (**Figure 26**). We propose that the competition among the benzylic substrate and the aryl azide for the coordination at the metal centre generates an equilibrium that is the first step of the catalytic cycle, as reported in **Scheme 64**. Clearly, the entire process depends also on the substitution reaction rate, which is determined by the substrate concentration.
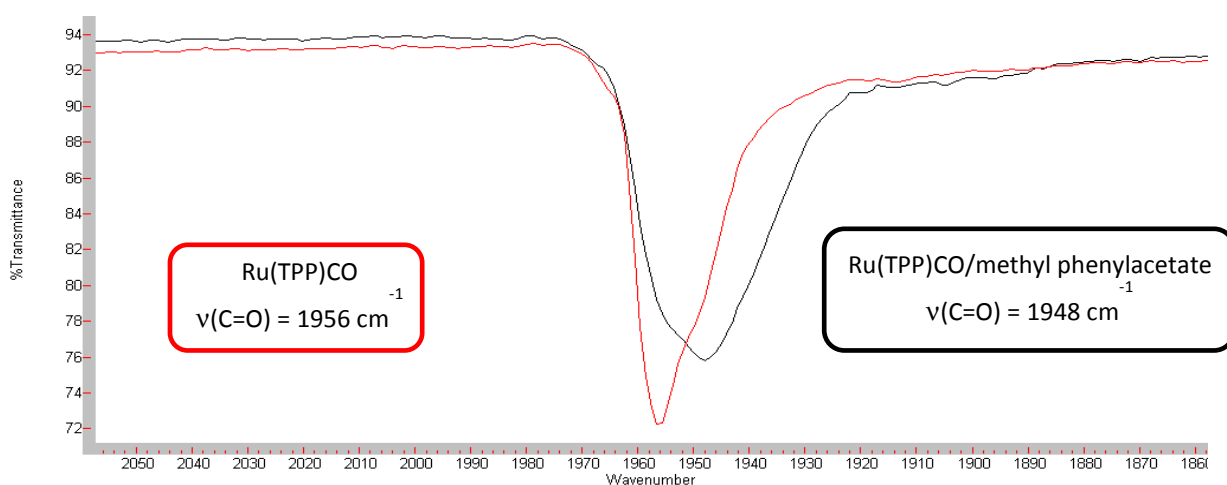
Figure 26. IR spectra of Ru(TPP)CO (red line) and Ru(TPP)CO in the presence of methyl phenylacetate (black line)

The benzylic substrate plays a double role in the reaction mechanism: a high methyl phenylacetate concentration is necessary to avoid the formation of the inert *bis*-amido complex **F** and to maintain active the catalytic cycle 1 reported in **Scheme 64**; however, the benzylic substrate is also responsible for a sort of competitive inhibition by the generation of complex **A**.

Taking into account all this mechanistic information, we studied the scope of the reaction by reacting methyl phenylacetate with other aryl azides and by investigating the reactivity of methyl dihydrocinnamate as substrate (**Table 5**).

Table 5. *Synthesis of α- and β-amino esters catalysed by Ru(TPP)CO (2).*[a]

entry	substrate	product	Ar	t^b (h)	yield[c] %
1[d]	(benzyl COOMe)	(NHAr, COOMe)	**48**, 3,5(CF$_3$)$_2$C$_6$H$_3$	6	80
			51, 4(CF$_3$)C$_6$H$_4$	5	26
			52, 4(NO$_2$)C$_6$H$_4$	8	32
			53, 4(^{t}Bu)C$_6$H$_4$	5	20
2	(COOMe)	(NHAr, COOMe)	**54a**, 3,5(CF$_3$)$_2$C$_6$H$_3$	10	77
3[e]	(OTMS, OMe)	(NHAr, COOMe)	**54a**, 3,5(CF$_3$)$_2$C$_6$H$_3$	0.25	65
			55a, 4(CF$_3$)C$_6$H$_4$	2	38
			56a, 4(NO$_2$)C$_6$H$_4$	0.75	55
			57a, 3,5(Cl)$_2$C$_6$H$_3$	1.2	65
		(COOMe, NHAr)	**54b**, 3,5(CF$_3$)$_2$C$_6$H$_3$	0.25	12
			55b, 4(CF$_3$)C$_6$H$_4$	2	14
			56b, 4(NO$_2$)C$_6$H$_4$	0.75	21
			57b, 3,5(Cl)$_2$C$_6$H$_3$	1.2	8
4	(COOMe, OAc)	(NHAr, COOMe, OAc)	**58**, 3,5(CF$_3$)$_2$C$_6$H$_3$	23	35,*syn/anti =* 20/80
5	(COOMe, OMe)	(NHAr, COOMe, OMe)	**59**, 3,5(CF$_3$)$_2$C$_6$H$_3$	6.5	53,*syn/anti =* 45/55
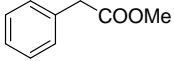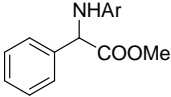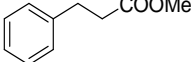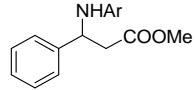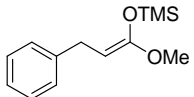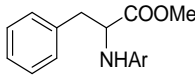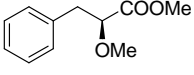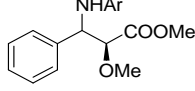
[a]Reactions were run under nitrogen in benzene at 80°C with **2**/ArN$_3$/ester = 1:50:1000. [b]Time required to complete the ArN$_3$ conversion. [c]Isolated yields. [d]Run in methyl phenylacetate at 100°C; [e]**2**/ArN$_3$/substrate = 1:50:250.

Experimental results indicate that aryl azide **38** is the most effective azide for the amination of both methyl phenylacetate (***Table 5***, entry 1) and methyl dihydrocinnamate (***Table 5***, entry 2). In fact, the amination of methyl phenylacetate by other aryl azides afforded the corresponding aminated compounds in a low yield and the reaction of the same azides with methyl dihydrocinnamate afforded only traces of the corresponding *β*-amino esters. It should be noted that the reaction reported in *entry 2* allowed the synthesis of methyl 3-(3,5-*bis*(trifluoromethyl)phenylamino)-3-phenyl-propanoate (**54a**) in good yields but long reaction time (10 h). If the reaction was carried out

with a lower azide loading (catalytic ratio Ru/azide/methyl dihydrocinnamate = 1:15:1000) the reaction time was reduced to 2 hours with an 81% yield of **54a**, suggesting that a deactivation process similar to the one observed in the methyl phenylacetate case is occurring. In fact, the TLC analysis of the reaction crude revealed the presence of another porphyrin species as a purple spot. This new ruthenium complex (**60**) was isolated by performing the synthesis of **54a** using complex **50** as the catalyst, the analytic data for complex **60** are very similar to those reported for **49** to indicate an analogous *bis*-amido molecular structure (***Figure 27***).
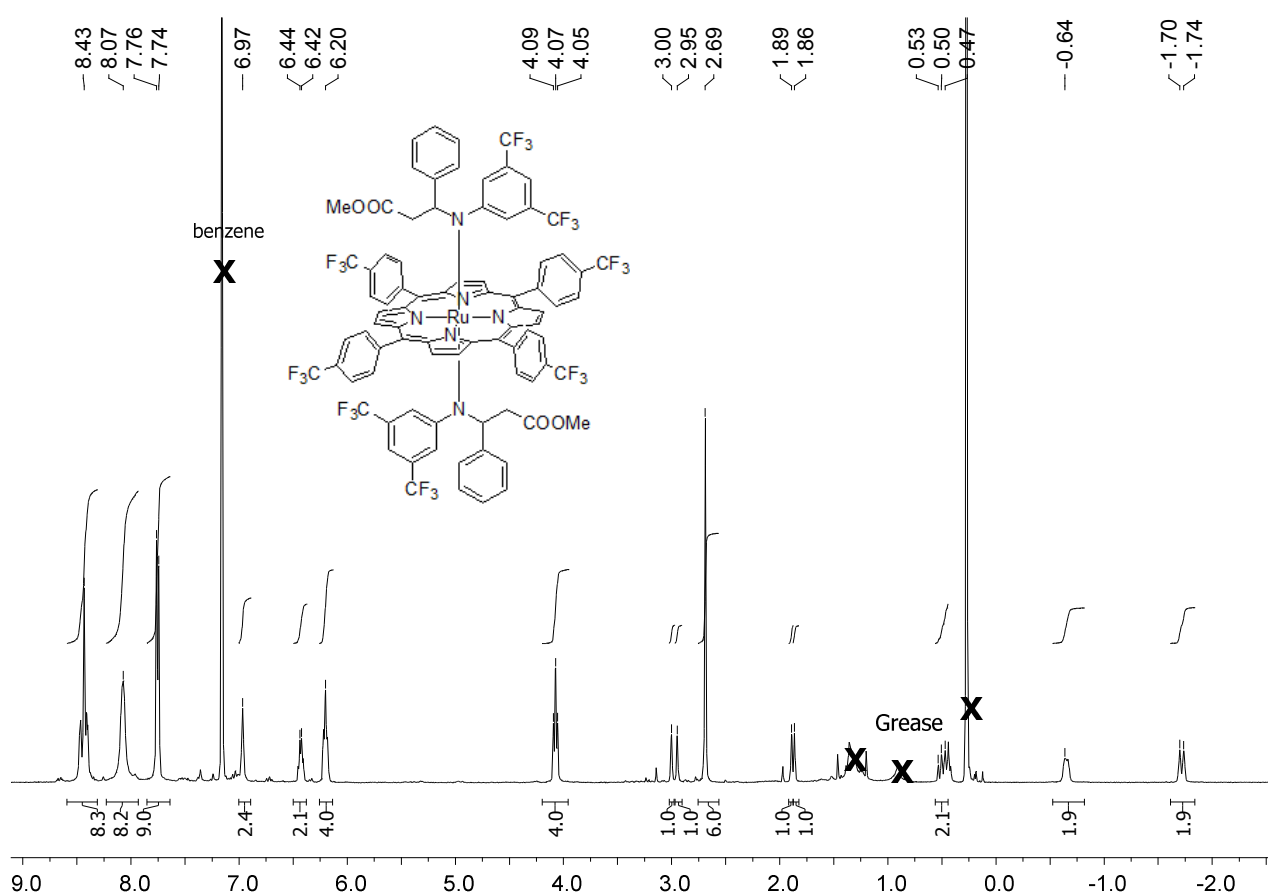
Figure 27. *NMR spectra of complex **60**.*

To optimise the synthesis of **54a**, we used the ketene trimethylsilyl acetal of methyl dihydrocinnamate (**61**) as the substrate (***Scheme 65***), this compound is a rather strong nucleophile and carries C-H bond that are both benzylic and allylic, therefore, it should be very reactive towards the electrophilic metallo-nitrene species generated during the catalysis.

Ar = 3,5-(CF₃)-C₆H₃
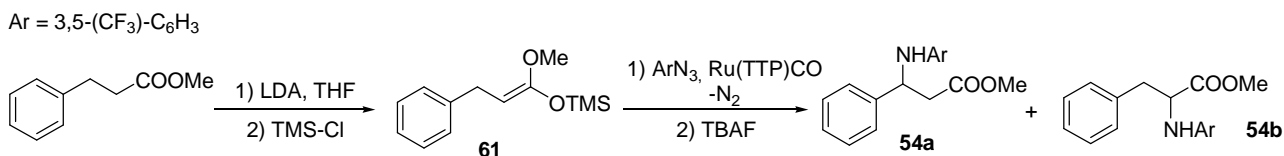
Scheme 65. *Synthesis of ketene silyl acetal **61** and its employment as substrate in catalytic amination.*

The reaction time decreased from 10 hours to 15 minutes but in the meantime a decrease of the reaction selectivity was observed. The *β*-amino ester **54a** was formed along with the α-amino regioisomer **54b** in a ratio **54a**/**54b** = 85/15. The formation of compound **54b** can be due to the reaction of ketene silyl acetal and an electrophilic nitrogen source (see electrophilic amination of enolates discussed in **Section 1.4.2**), also it could be due to the uncatalysed reaction between ketene silyl acetal **61** and the aryl azide, since a similar compound was obtained by the reaction between tosyl azide and **61**.[125] We repeated the reaction in the absence of the ruthenium catalyst but after 2 hours the IR analysis did not reveal any consumption of the aryl azide. The use of ketene silyl acetal enlarged the scope of the reaction, this experimental procedure allowed the synthesis of *β*-amino esters derived from different aryl azides bearing EWG groups in short reaction times and with a lower excess of the substrate (***Table 5***, entry 3). Even if the employment of the ketene silyl acetal decreased the reaction selectivity, it is important to underline that the two obtained isomers can be separated by flash chromatography. We tried to isolate the product of the benzylic amination of the ketene silyl acetal **61** and aryl azide **38** before the desilylation with TBAF. We obtained good evidences of his presence in the reaction crude by ¹H-NMR analysis, unfortunately any attempt to purify this product lead to its decomposition.

We performed the synthesis of α-oxy-β-amino esters using L-3-phenyllactate derivatives as substrates (***Table 5***, entry 4-5), these products are interesting because they are precursors of biological relevant compounds such as β-lactams[126] and 2-oxazolidinones.[127] The reaction requires a protective group on the α-hydroxyl moiety of methyl L-3-phenyllactate (***Scheme 66***), and compounds **62** and **63** were obtained in moderate yields using acetoxy or methoxy moieties as protective groups and a large substrate excess. We performed the reaction using unprotected methyl L-3-phenyllactate a substrate, but no complete azide conversion occurred over 20 h in refluxing benzene and only traces of product were detected by GC-MS analysis.
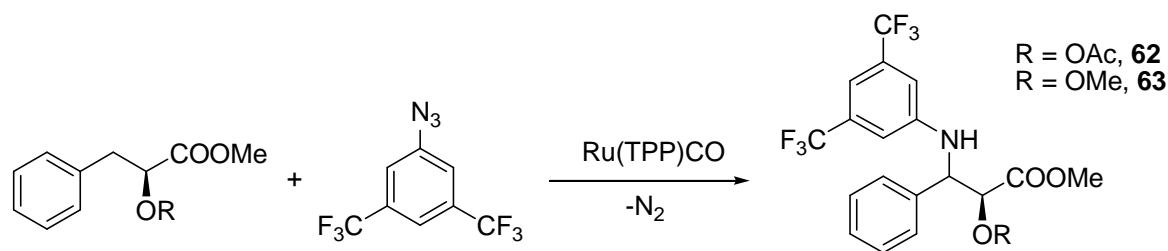
Scheme 66. Synthesis of α-oxy-β-amino esters

A moderate *syn/anti* diastereoselection was obtained in the synthesis of compound **62** but it was almost negligible using the methoxy-protected phenyllactate derivative as substrate (***Table 5***).

The purification of the reaction crude during the synthesis of **62** allowed the isolation of a new "purple spot" ruthenium complex, the ESI-MS analysis was compatible with a *bis*-amido complex similar to **49** and **52**.

We studied the conversion of the diastereoisomeric mixture of compound **63** into the corresponding *β*-lactam, which was obtained as a single *trans* diastereoisomer (**64**) in 30% yield. The stereochemistry of compound **64** was assigned by comparing its NMR data with those reported in literature for a similar compound.[128] It is worth noting that compound **64** was obtained in a few steps starting from L-phenyl alanine (***Scheme 67***).
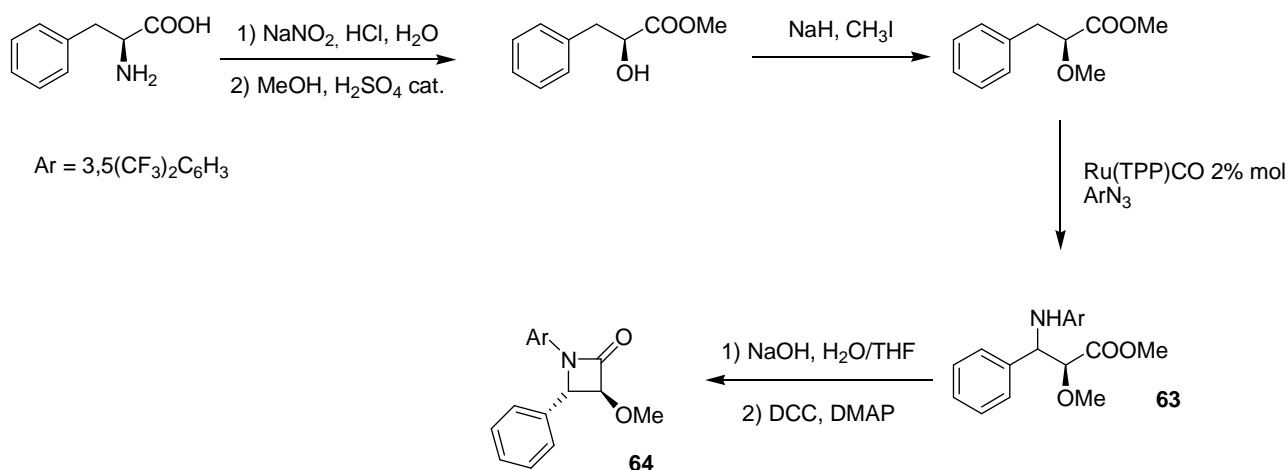
Scheme 67. Synthetic pathway for β-lactam 64 starting from L-phenylalanine.

2.5 Ruthenium Porphyrin-Catalysed Synthesis of Indoles by the Reaction between Aryl Azides and Alkynes

Indole-containing molecules represent a very important class of compounds from a biological/pharmaceutical point of view. The scientific community developed a massive number of methods for indoles synthesis, an overview of the recent advances in this area was given in the **Introduction** (**Section 1.5.**).

Herein we reported the first synthetic strategy to obtain indoles involving an intermolecular reaction between aryl azides and aryl alkynes.[129]

At first, we discovered that the reaction between 3,5-*bis*(trifluoromethyl)phenyl azide (**38**) and phenylacetylene afforded selectively the indole **65** in the presence of a ruthenium porphyrin catalyst. This was surprising because generally when organic azides and alkynes are allowed to react the well-known [3+2] Huisgen cycloaddition occurs giving the corresponding triazoles; moreover, ruthenium-based catalysts for this reaction are very well-known.[130]

The catalyst and solvent screening for the synthesis of **65** is reported in ***Table 6***.

Table 6. *Synthesis of 65.*
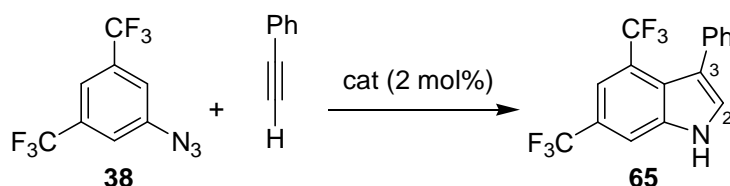
entry	Cat	conv. (%)	t (h)	**65** yield (%)[b]
1	None	15	6	-
2	$Ru^{II}(TPP)CO$	100	6	65
3	$[Ru^{IV}(TPP)(OMe)_2]_2O$ (**92**)	90	14.5	60
4	$Ru^{VI}(TPP)(NAr)_2$ (**10**)	100	1	86
5	$Ru^{VI}(TPP)(NAr)_2$ (**10**)	100[c]	2.5	73
6	$Ru^{VI}(TPP)(NAr)_2$ (**10**)	29[d]	12.5	19
7	$Ru^{VI}(TPP)(NAr)_2$ (**10**)	96[e]	12	36

[a]Nitrogen atmosphere, benzene, T = 80 °C cat/azide/alkyne = 1:50:250. [b]NMR yield. [c]Run in refluxing 1,2-dichloroethane. [d]Run in refluxing *n*-hexane (T = 69°C). [e]Run in decalin.

The reaction optimisation enabled the synthesis of the C3-substituted indole **65** in a high yield and short reaction time, the C2-substituted regioisomer was never observed. We tested three ruthenium catalyst with different oxidation state (**Table 6**, entries 2-4), the best catalytic performance was obtained by using the ruthenium(VI) *bis*-imido complex **10**, Ru(TPP)CO and [Ru(TPP)(OMe)]$_2$O promoted the formation of the desired product in moderate yields but in longer reaction time than **10**.

Co(TPP) and Fe(TPP)Cl were also tested as catalysts for the model reaction, in both cases a poor azide conversion was observed and the indole was not detected by NMR analysis.

As reported in entry 1 of **Table 6**, the catalyst-free reaction of aryl azide **38** with phenylacetylene in refluxing benzene (80 C) occurred without a significant azide conversion (12%) and with the formation of a mixture of triazoles **66a** and **66b** (**Scheme 68**).
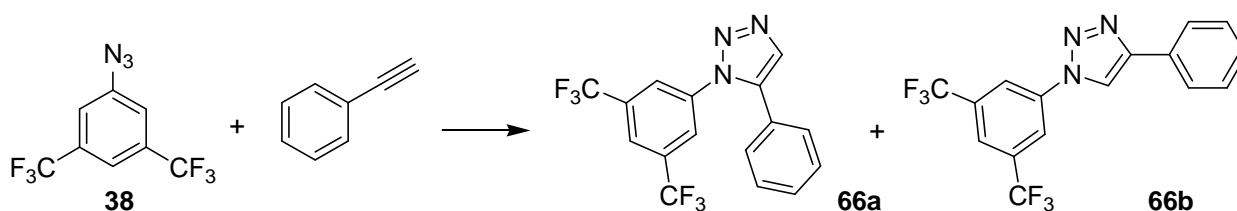
Scheme 68. *Uncatalysed reaction between phenylacetylene and 3,5-bis-(trifluoromethyl)phenyl azide*

The triazoles yield was quantitative when the reaction was executed in decalin at 120 C; in both cases the formation of indole **65** was not observed. No reaction occurred when the mixture of so-formed triazoles was treated with Ru(TPP)CO, thus excluding that **65** was obtained by a metal-catalysed rearrangement of triazoles formed by the azide-alkyne cycloaddition.[131]

Our first concern was to propose a plausible reaction mechanism to highlight the synthetic potentiality of the present procedure, therefore we performed a series of experiment to gain some mechanistic information:

- **Nitrene-Transfer Experiment**: the stoichiometric reaction between **10** and phenylacetylene yielded the indole **65** in a 25% yield (**Scheme 69**). Aniline **37** was also detected along with unidentified ruthenium porphyrin species. Thus, the metallo-nitrene species is truly an intermediate of the catalytic reaction.
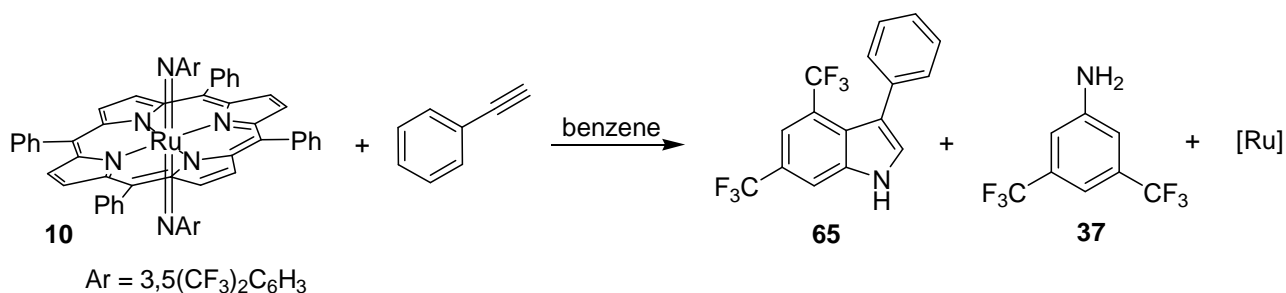
Scheme 69. Nitrene transfer experiment.

- **Isotope Tracing Experiment:** the terminal C-H bond of phenylacetylene is not involved in the reaction. When phenylacetylene-d_1 was reacted with aryl azide **38** in the presence of **10**, the indole **65**-d_1 bearing a deuterium atom in the C2 position was exclusively formed. The catalytic performance was almost identical to the one obtained using regular phenylacetylene, thus the thermodynamics and the kinetics of the reaction are unaffected by this isotope change.
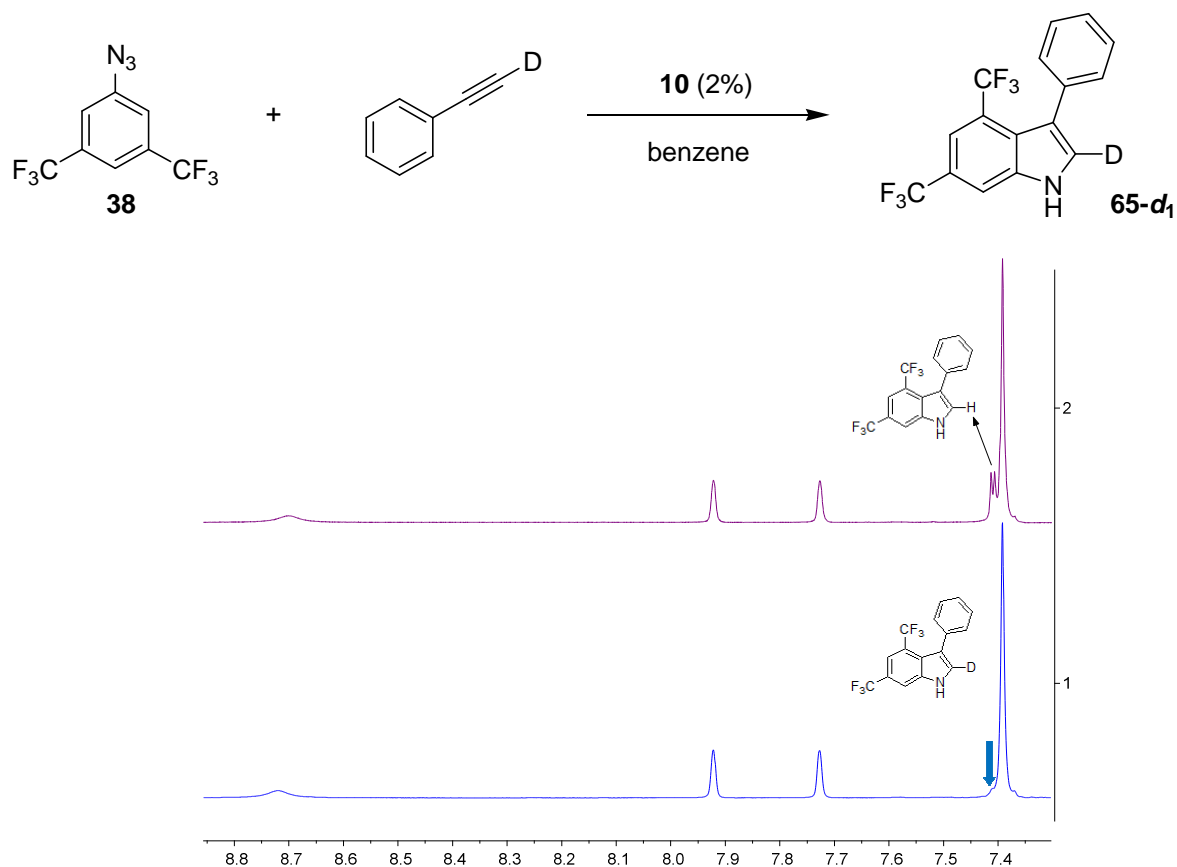
Scheme 70. Isotope tracing experiment and comparison between the ^1H NMR spectrum of 65 (purple line) and the ^1H NMR spectrum of 65-d_1 (blue line).

- **Kinetic Isotope Effect (KIE):** The aryl azide C-H bond activation is not the rate-determining step of the entire process. This was proved by performing a KIE experiment by two different methods.

  In the first experiment, the reaction between phenylacetylene and an equimolar amount of **38** and fully deuterated **38-d_3** (see **Experimental Section**, **Section 3.4.5.** for the synthesis of **38-d_3**) was performed. A k_H/k_D value of 1.1 was calculated by ^{1}H NMR analysis.

  In the second experiment k_H and k_D were measured separately by performing the reaction in two different batches, one using **38-d_3** and the other using **38**. The first order kinetic constant was evaluated by quantifying the azide consumption by IR spectroscopy. The resulting k_H/k_D = 1.6 was quite in agreement with the previous experiment and confirmed that the C-H bond cleavage in not involved in the rate-determining step of the reaction.

- **Synthesis of 65 in presence of TEMPO:** A lack of inhibition of the catalytic reaction was observed when the radical trap TEMPO (2,2,6,6-tetramethyl-1-piperidinyloxy) was added to the reaction mixture. Thus, a mechanism involving long-lived radical intermediates is excluded.

The reaction between a nitrene species and alkynes should afford an unstable and antiaromatic 1*H*-azirine[132], although this species were never truly isolated[133] because of the easy rearrangement to the more stable 2*H*-azirine[134] or other transformations.[131] Interestingly, 1-aryl-2*H*-azirine can afford 2,3-disubstituted indoles through a ring opening rearrangement that can be either thermally[105] or catalytically[108] induced (see **Introduction, Section 1.5.4.**).

Tai-Chu Lau and co-workers recently reported a particular reactivity of a ruthenium(VI) nitride complex towards alkynes.[135] As illustrated in *Scheme 71*, the reaction of 1-hexyne with complex **67** affords a ruthenium(IV) aziro (deprotonated azirine) complex **68** that undergoes rapidly a nucleophilic attack by pyridine and rearrange to the more stable 2*H*-aziridine complex **69**, which gives the final product by hydrogen atom transfer (HAT). This mechanism was the result of a theoretical DFT study.
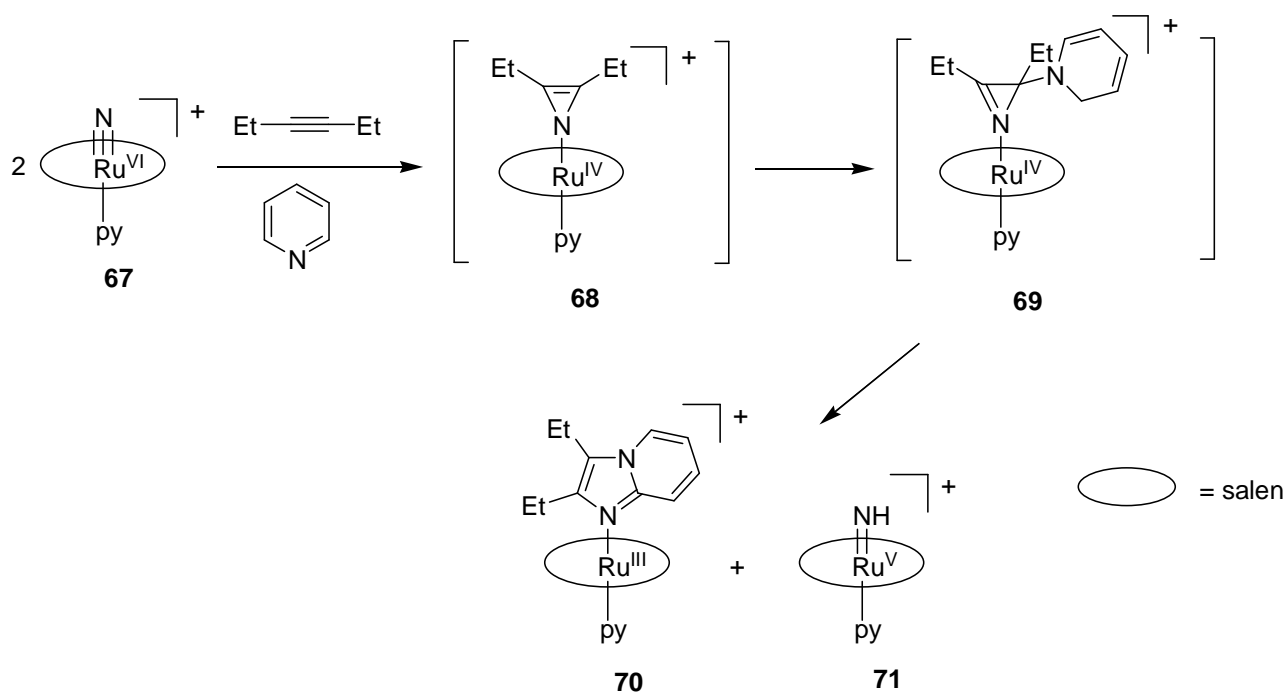
Scheme 71.

We proposed that a similar reaction may occur also between a ruthenium(VI) *bis*-imido complex and phenylacetylene affording a *N*-substituted-1*H*-azirine complex (intermediate **A** in *Scheme 72*) in accord with the general reaction between a nitrene species and alkynes. Intermediate **A** cannot rearrange to a more stable 2*H*-azirine because a transposition of the aryl moiety from position 1 to position 2 would be required, therefore the azirine undergoes ring opening and activate the C-H bond in *ortho* position of the aryl moiety (*Scheme 72*) obtaining the observed indole product.
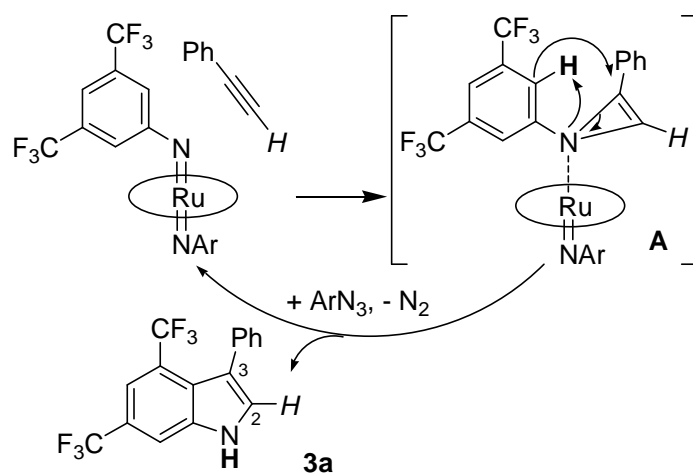
*Scheme 72. Proposed mechanism for the reaction of **10** with phenylacetylene to give 3-phenyl indole.*

The formation of an "elusive" 1*H*-azirine intermediate can explain the experimental observations, especially the almost negligible KIE, since the fast rearrangement of **A** is very unlikely to be the rate-determining step. The regioselective formation of the C3-functionalised indole should derive by the stabilisation of the positive charge formed during the ring opening reaction on the phenyl-substituted carbon atom of the alkyne. Any attempt to detect intermediate **A** failed, a theoretical calculation should be performed in order to confirm this mechanistic hypothesis.

Table 7. *Synthesis of 3-arylindoles using **10** as the catalyst*[a].

65, 86% yield 1.0 h time	**72**, 75% yield 0.75 h time

65, 86% yield
1.0 h time

72, 75% yield
0.75 h time

73, 69% yield[b]
14 h time

74, 95% yield
0.5 h time

75, 90% yield
1.25 h time

76, 65% yield
4.5 h time

77, 95% yield
1 h time

78, 30% yield[c,e]
16 h time

79, 37% yield[c,d]
15 h time

80, 82%(80%)[f] yield
0.5 h(0.5 h)[f] time

81, 70% yield
0.5 h time

82 87% yield
0.25 h time

83, 68% yield
2.5 h time

84, 83% yield
0.5 h time

85, 60% yield[c]
1.5 h time

86a, 82% yield[c,g] **86b**, 5% yield[c,g]
6.0 h time

87a, 45% yield[g] **87b**, 15%yield[g]
4.5 h time

88a, 35% yield[g] **88b**, 6% yield[g]
6.0 h time

[a]Nitrogen atmosphere, benzene, T = 80°C, **10** as the catalyst, Ru/azide/alkyne = 1:50:250, 100% azide conversion, NMR yield. [b]83% azide conversion. [c]**10**/aryl azide/alkyne = 1:50:1000. [d]89% azide conversion. [e]81% azide conversion. [f]Complex (**89**) was used as the catalyst. [g]NMR selectivity calculated in the **86a/86b** isolated mixture.

In all the cases reported in *Table 7* the missing mass balance was the aniline and the diazene derived from a partial decomposition of the employed azide. Initially the reactivity of aryl azide **38** towards differently substituted alkynes (*Table 7*, compounds **72**-**79**) was tested. The reaction of **38** with aromatic terminal alkynes afforded the 3-phenylindoles in high yields and with full regioselectivity. The catalytic efficiency of the reaction depends on the electronic characteristic of the *para* substituent of the alkyne (R^4) and best yields and shortest reaction times were achieved when R^4 was an electron-donating group. Internal alkynes were converted in the desired indoles in moderate yields, but the azide conversion was incomplete over 15 hours. The steric hindrance between the *di*-substituted alkyne and the porphyrin ligand may be the cause of the longer reaction times and modest yields. It is important to underline that when 1-phenylpropyne was used only the regioisomer **78** was observed, supporting the already stated hypothesis that the regioselectivity is given by a better stabilization of a transient positive charge by the phenyl group. The procedure was ineffective towards aliphatic alkynes, no indole product was observed using trimethylsilyl acetylene and 1-heptyne as substrate, while ethyl propiolate gave the corresponding 3-carboxyethyl indole in a low yield (13%).

The synthetic versatility of the reported methodology was then investigated by reacting phenyl acetylene with different aryl azides. It should be underlined that we employed complex **10** as the catalyst instead of using the *bis*-imido complex corresponding to the employed azide for each reaction. This is due to stability problems of the *bis*-imido complexes derived from different aryl azides. Only the *bis*-imido complex Ru(TPP)(NAr') (Ar' = 3,5-(NO$_2$)$_2$C$_6$H$_3$) (**89**) was stable enough to be prepared in high yields and employed as the catalyst for the synthesis of **80**, as shown in *Table 7*, a similar catalytic performance was obtained by using **89** instead of **10**. It is worth noting that the use of **10** as the catalyst implied a sacrificial role of his nitrene "ArN" moieties which were transferred to alkyne forming the corresponding undesired indole **65**. This collateral reaction can be tolerated due to the small quantity of **65** derived from the nitrene moieties of **10** (2% catalyst

loading) and because it can be separated from the desired indole during chromatographic purification.

The high reactivity of 3,5-dinitrophenyl azide allowed us to perform another alkyne screening using this aryl azide. We obtained five different derivatives (compounds **80**-**84**, *Table 7*) with high yields and short reaction times. It is worth to report that the latter indoles were recovered by simple filtration since 3-aryl-4,6-dinitroindoles are insoluble in benzene, even at refluxing temperature, and in chlorinated solvents. Yields and reaction times were similar using aryl alkynes with different electronic properties, maybe because of the driving force given by the insolubility of the organic products in the reaction media.

We further investigated the regioselectivity of the reaction using aryl azides bearing only one substituent in the *meta* position. In this case two different C-H bonds may be involved in the HAT process yielding two different indoles, as reported in ***Scheme 73***.

$R_3 = CF_3, NO_2$
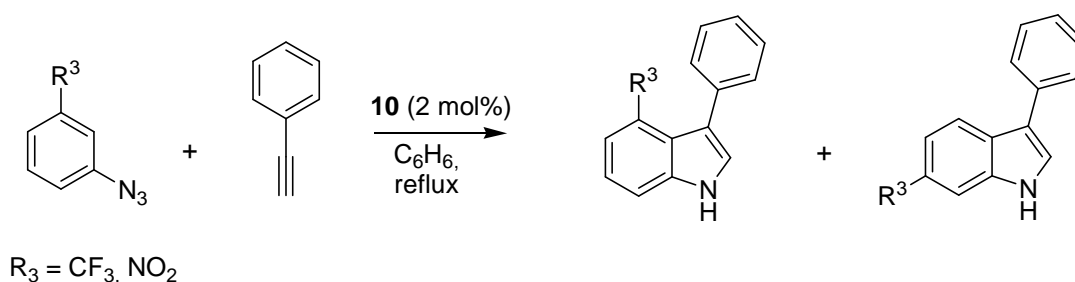
Scheme 73. *Reaction between phenylacetylene and mono-substituted aryl azides catalysed by **10**.*

When 3-trifluoromethylphenyl azide was employed, the regioisomer **86a** was the strongly favoured reaction product (***Table 7***) indicating that a trifluoromethyl group activated the cleavage of a C-H bond placed in an *ortho* position better than in *para* position. The replacement of CF_3 by a NO_2, a stronger electronwithdrawing group, provoked a decrease in the reaction selectivity, isomer **87b** was formed in higher yields (15%) than **86b**. The indole formation was not observed using both aryl azide bearing EDGs, such as 3,4,5-methoxyphenyl azide, and aryl azides bearing EWGs in the *para* position, such as 4-nitrophenyl azide and 4-tert-butylphenyl azide. 4-trifluoromethylphenyl azide gave only traces of the desired product, as detected by GC-MS analysis. This pointed out the relevance of the EWGs on the *meta* positions of the aryl azide in order to obtain the desired product. Finally, it should be noted that indoles **72**, **78**, **81** and **88** were obtained without the contemporary amination of the benzylic methyl group, although the good catalytic activity of the ruthenium(VI) *bis*-imido **10** in benzylic aminations by aryl azides was well-established.[68]

Generally, *mono*-substituted azides were much less effective for the indole synthesis then the corresponding *di*-substituted derivatives. For example, if *m*-nitro- or *m*-(trifluoromethyl)phenyl azide were employed in the same conditions used for the corresponding *di*-substituted azides (Ru/azide/alkyne = 1:50:250) the yield in the desired indole product was less than 25%. To overcome this problem a consistent alkyne excess must be used. The large amount of substrate can be fully recovered either by distillation as a benzene solution in the case of phenylacetylene or by chromatographic purification for high boiling alkynes. However, the alkyne substrate may be very expensive and using a large excess in order to increase the indole yield is not the best solution from an economical point of view.

We tried many possible additives in order to facilitate the HAT step and avoid the need of a substrate excess, the reaction between 3-trifluoromethylphenyl azide and phenylacetylene with a catalytic ratio Ru/azide/alkyne = 1:50:250 was chosen as a model reaction for these studies. Unfortunately the high yields observed using a large alkyne amount were never replicated: the employment of an H-donor compound, such as cyclohexene, or of a base, such as triethylamine, led to the inhibition of the reaction. The use of proton donors like methanol or benzoic acid led to a consistent reduction of the reaction times but only a slight improvement in the indole yield was observed.

2.6. New Porphyrin Catalysts for Amination Reaction

2.6.1. μ-Oxo Ruthenium Porphyrin Dimers

The catalytic cycle of ruthenium-catalysed amination reactions was deeply discussed in the previous sections. A general observation is that the active species are generally Ru^{IV} or Ru^{VI} complexes, usually derived from the oxidation reaction between the organic azide and the starting catalyst, a ruthenium(II) porphyrin carbonyl species. Nevertheless, the *bis*-imido complex **10**, a ruthenium(VI) species, is a better catalyst then Ru(TPP)CO in both benzylic[65, 68] and allylic amination,[66, 68] unless particular deactivation pathways are involved in the catalytic cycle[123] (see **Section 2.3**).

Hence, we focused our attention on the synthesis of ruthenium porphyrin complexes with a high oxidation state; we investigated their reactivity towards organic azides and their catalytic activity in the amination reactions.

In the past years, the synthesis and characterization of high-valent metalloporphyrins attracted the attention of the scientific community due to their relations with the structure of many heme-proteins in their redox processes. For example, an iron(IV)-oxo-porphyrin moiety is involved in the catalytic cycle of peroxidases and cytochrome P450 and high-valent ruthenium porphyrin are considered to be a good model of iron porphyrins. The oxidation of ruthenium(II) porphyrin complexes can lead to two different products: a ruthenium(VI)-dioxo species or a ruthenium(IV)-μ-oxo dimer, as shown in *Scheme 7*.[136] Generally, a sterically demanding porphyrin ligand prevents the formation of the dimer species and affords selectively the dioxo complex.[17]

Ruthenium(VI) dioxo complexes were largely studied and their catalytic activity in oxidation reactions of hydrocarbons was well established[20, 137]. We focused on the synthesis of μ-oxo ruthenium(IV) porphyrin dimers using as starting reagent the complex [Ru^{II}(TPP)(CO)(MeOH)] (**90**), whose porphyrin ligand is not sterically hindered. We chose *m*CPBA (*meta*-chloroperbenzoic acid) as oxidizing agent.

The reaction of **90** with 7.5 equivalents of *m*CPBA in a CH$_2$Cl$_2$ solution afforded the complex [Ru^{IV}(TPP)(*m*CB)]$_2$O (**91**), a dimer species with *meta*-chlorobenzoate (*m*CB) anions at the axial positions (*Scheme 74*). Complex **91** was unequivocally identified by mass spectroscopy and by NMR spectroscopy, which detected strongly shifted signals for the aromatic protons of the *m*CB moiety as usually happens for axial ligands in porphyrin complexes (*Figure 28*). We clearly observed also the typical signal pattern of a μ-oxo tetraphenylporphyrin complex, in which the aromatic protons of the *meso* substituent are split in five different signals.
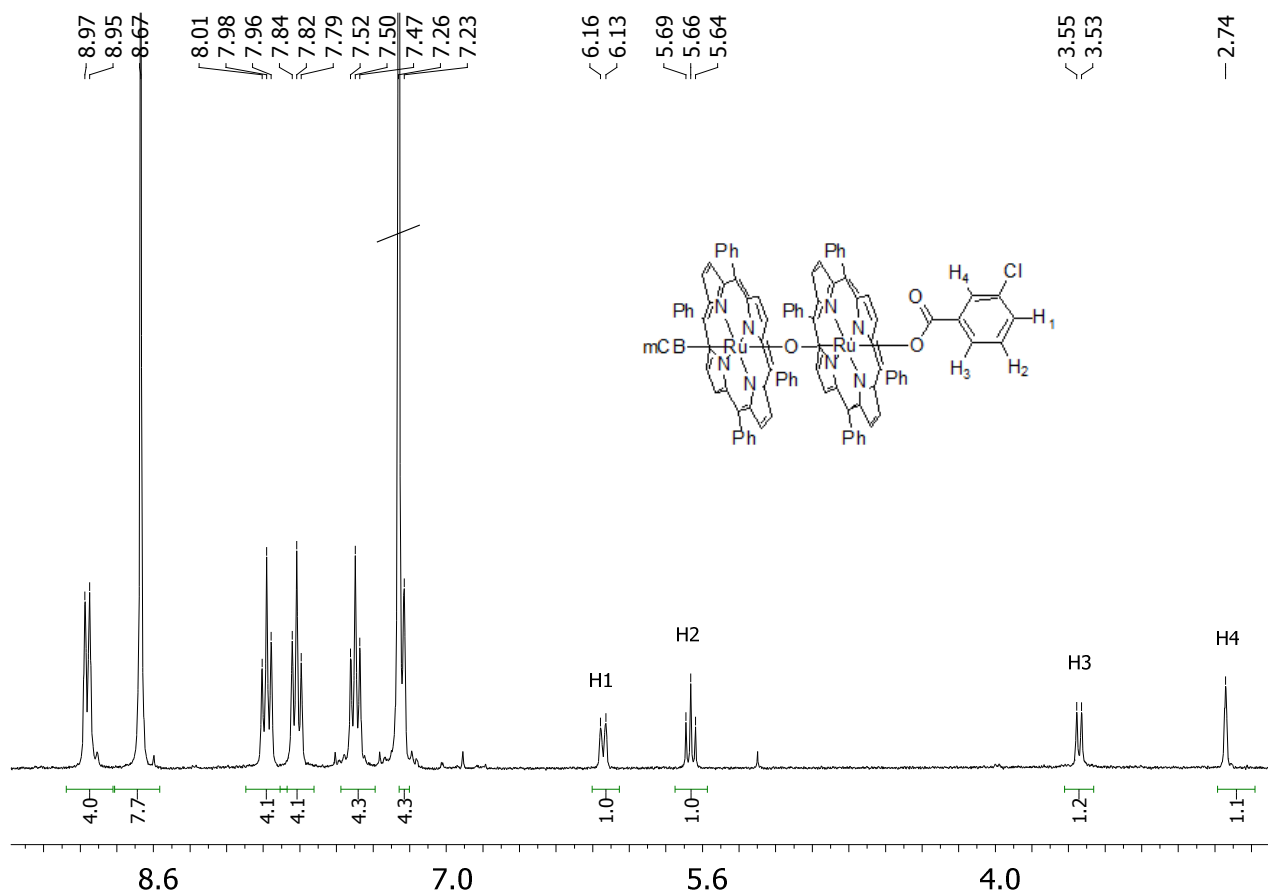
Figure 28. *^{1}H NMR spectrum of complex **91**, typical pattern for Ru(TPP) μ-oxo complexes is observed in the aromatic region, highly shielded protons of the benzoate moiety were detected between 6.5-2.5 ppm.*

Complex **91** was obtained in a 39% yield after a filtration over neutral Al_2O_3 using CH_2Cl_2 as eluent. The missing mass balance is due to the partial decomposition of **91** over the stationary fase during the purification. The "decomposed product" was recovered by eluition with CH_2Cl_2/MeOH 10:0.2 as the μ-oxo dimer complex [Ru^{IV}(TPP)(OCH$_3$)]$_2$O (**92**) in a 40% yield (***Scheme 74***). The complex was unambiguously identified by mass spectroscopy and by ^{1}H-NMR analysis in C_6D_6 that revealed again the typical signal pattern of a μ-oxo dimer ruthenium-tetraphenylporphyrin complex[23] and the signal at negative chemical shift suitable with a methoxy moiety coordinated to the metal centre. The methoxy group seems to be quite labile in chlorinated solvents since if the spectrum of pure **92** was recorded in chloroform complex multiplets were observed, however, if an excess of methanol was added to the sample a spectrum similar to the one recorded on the benzene solution was observed. This behaviour was not observed with complex **91**.
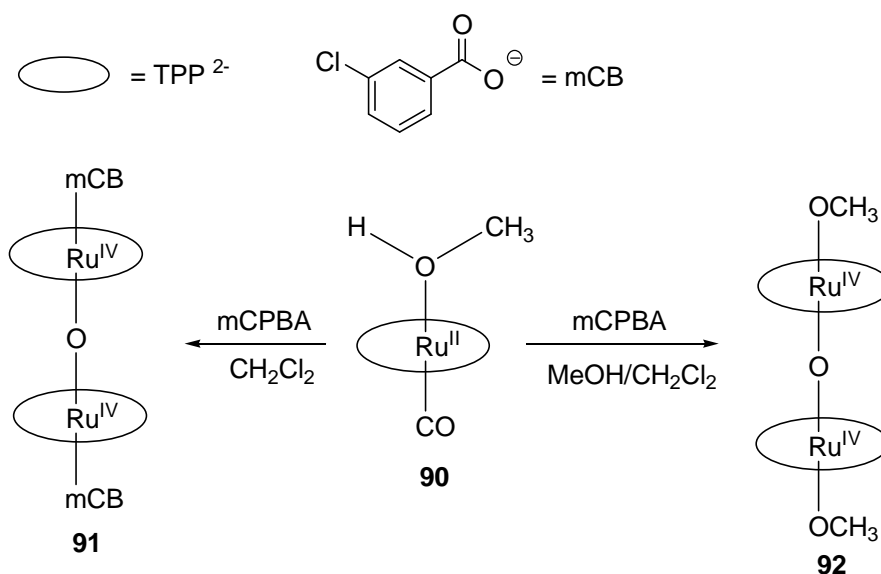
Scheme 74. *Synthesis of **91** and **92**.*

We synthesised **92** in high yields by running the reaction in the presence of methanol. The synthetic procedure was optimised in terms of oxidant amount and reaction solvent. The crucial parameter was the MeOH/CH$_2$Cl$_2$ ratio to use as reaction solvent, because methanol is required to prevent the irreversible formation of complex **91**, but an excessive amount of alcohol caused the incomplete conversion of the starting complex **90** even if a large oxidant excess was added. An 81% yield in the μ-oxo complex **92** was obtained by suspending complex **90** in CH$_2$Cl$_2$ and adding dropwise a MeOH/CH$_2$Cl$_2$ (10 :1) solution containing 8 equivalents of *m*CPBA.

We studied the reactivity the μ-oxo dimer complexes towards organic azides. Aryl azide **38** did not react with complex **91** even under light irradiation, while **92** readily converted in the *bis*-imido complex **10** (***Scheme 75***).
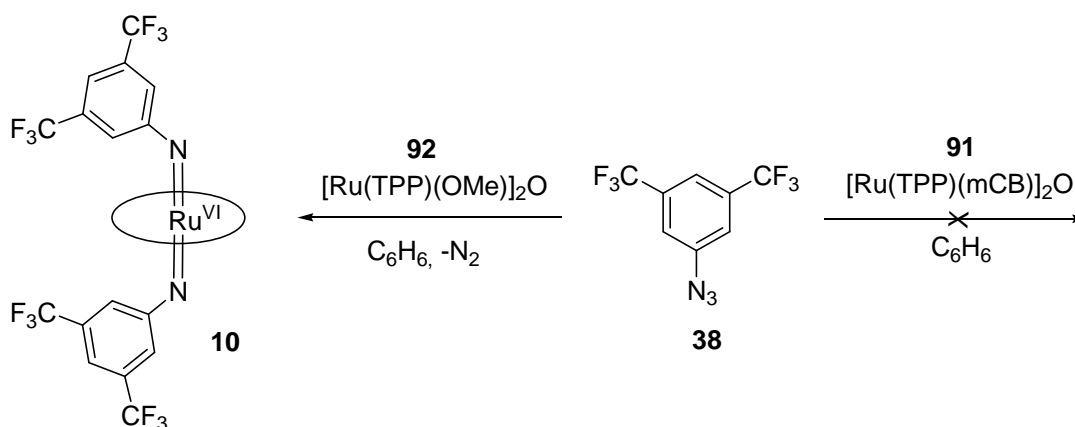
Scheme 75. *Reaction between the μ-oxo dimer complexes and aryl azide **38**.*

The reaction between 4-*tert*-butylphenyl azide and **92** gave the new *bis*-imido complex **93**. This latter complex cannot be synthesised by the conventional reaction between [Ru(TPP)CO] and an organic azide, the only product obtained when 4-*tert*-butylphenyl azide is used is the complex [Ru^{II}(TPP)CO(4-^{t}Bu-aniline)] (**94**). Probably this is due to the poor stability of the *mono*-imido intermediate (*Scheme 76*) in which the negative charge on the nitrogen atom[69] is not stabilized by an EWG on the aryl group and it reacts by an hydrogen atom abstraction instead of reacting with another azide molecule. On the other hand, the use of ruthenium(IV) complex **92** allowed the synthesis of a *bis*-imido complex which bears an EDG on the nitrene aryl moiety.
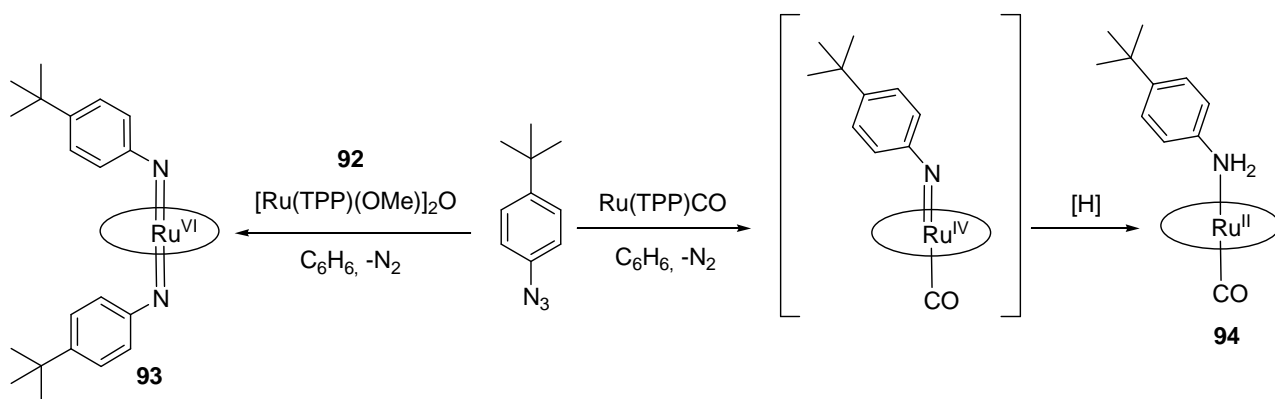
Scheme 76. *Reaction between 4-tert-butylphenyl azide and ruthenium complexes with different oxidation state.*

We allowed to react **92** with tosyl azide and adamantyl azide but no product was observed in both cases, the reaction with benzyl azide lead to unidentified products. When we reacted **92** with organic azides (RN$_3$), whose R is a good leaving group (trityl, trimethylsilyl) for electrophilic substitution, the new μ-oxo dimer complex [Ru^{IV}(TPP)(N$_3$)]$_2$O (**95**) was obtained (*Scheme 77*). It is worth to report that the reaction between **92** and trimethylsilyl azide occurred at room temperature in a few minutes. Compound **95** was completely characterized and its molecular structure was determined by single crystal X-ray diffraction.
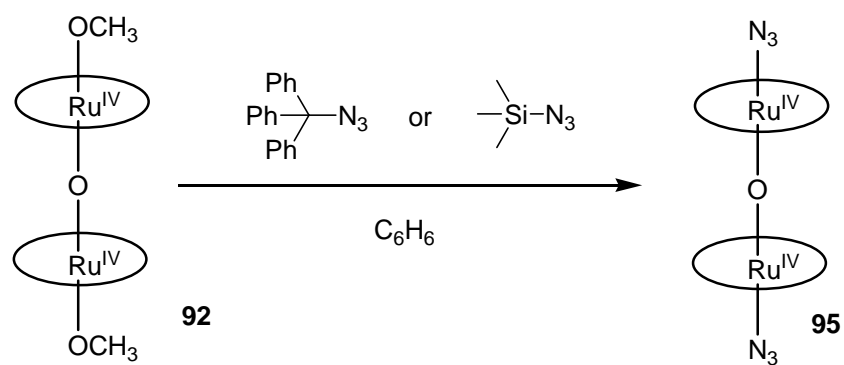
Scheme 77. *Synthesis of complex 95*
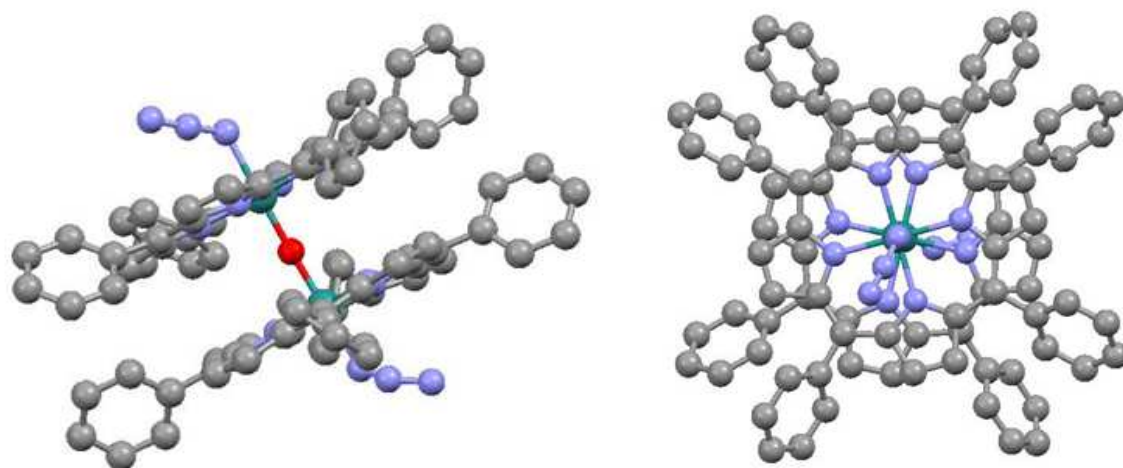
Figure 29. *Structure of complex 95 as determined by X-ray diffraction.*

We studied the catalytic activity of complex **92** in the amination reaction of hydrocarbons by aryl azides. The experimental results are summarised in **Table 8**.

Table 8. *Catalytic performances of complex **92** as the catalyst for the amination of hydrocarbons.*

Substrate	Product	Yield (%)[a]	Time (h)
ᵇ	—NHAr	65	0.75
ᶜ	NHAr	58	0.1
ᵈ		99	1
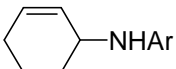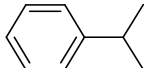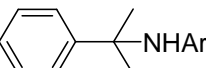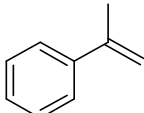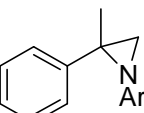
3,5-*bis*(trifluoromethyl)phenyl azide was used as aryl azide. [a]NMR yield (2,4 dinitrotoluene as internal standard). [b]Ru/azide = 1:25, solvent: refluxing cyclohexene as solvent. [c]Ru/azide = 1:50, solvent: refluxing cumene as solvent. [d]Ru/azide/α-methyl styrene = 1:50:250, 4-nitrophenyl azide was used as aryl azide, solvent: benzene.

Complex **92** is an active catalyst in allylic amination, benzylic aminations and aziridination reaction. The catalytic performance in the amination of cumene is particularly interesting for its very short reaction time. The catalytic activity of **92** was investigated in the allylic amination of cyclohexene using aryl azides bearing EDGs (e.g. 4-*tert*-butylphenyl azide and 4-anisyl azide, see Experimental Section) because of the particular reactivity observed in the formation of the new *bis*-imido species **93** using this kind of nitrene sources. Unfortunately, the yields in the desired product are lower than those obtained with the commercially available Ru(TPP)CO[65, 123] almost in every case, thus complex **92** is not a competitive catalyst.

2.6.2. Glycoporphyrin Complexes

Glycoporphyrins are generated by the conjugation of saccharide units with a porphyrin molecule.[138] These compounds have several biological applications due to the good activity of carbohydrates in ligand-acceptor interaction and recognition and because the porphyrin ligand is a biocompatible scaffold and photosensitizer.[139] Glycoporphyrin complexes of transition metal could be active catalysts in reactions commonly catalysed by simple metallo-porphyrins but only a few papers have been published concerning this possible application.[140] Taking advantage of the chiral and hydrophilic nature of saccharide units, this class of compounds can be potentially used either for asymmetric synthesis or to develop new sustainable water-soluble catalysts.

The glycoporphyrins synthesis was carried out in collaboration with Prof. Luigi Lay of Milan University. We followed two strategies to conjugate the porphyrin and saccharide units:

- **Aromatic Nucleophilic Substitution (S$_N$Ar)**: *meso*-tetrakis(pentafluorophenyl)porphyrin (F$_{20}$-TPPH$_2$) (**96**) was reacted with a monosaccharide carrying an unprotected hydroxyl moiety (**97**) in the presence of sodium hydride (*Scheme78*) following a reported procedure for *mono*-substituted glycoporphyrins.[141] The substitution of the fluoride atom at the *para* position of the *meso*-aryl group of F$_{20}$-TPPH$_2$ with the saccharide unit was achieved, we obtained the tetra-substituted glycoporphyrin **98** in good yields.
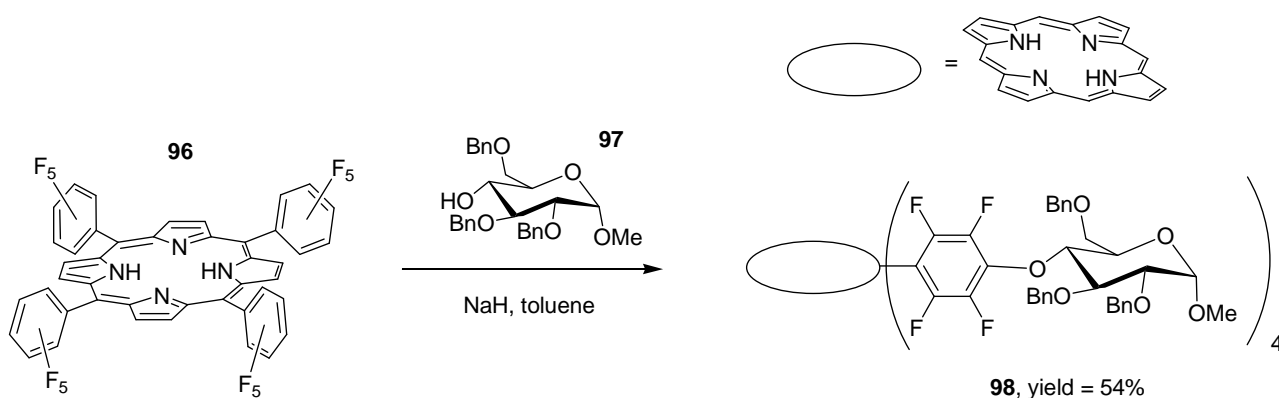
***Scheme78.** Glycoporphyrin synthesis via S$_N$Ar*

- **Copper-catalysed azide-alkyne cycloaddition (CuAAC):** we synthesised the zinc-porphyrins **99** starting from *meso*-tetrakis(4-aminophenyl)porphyrin (TAPPH$_2$). The glycosylation step was performed by forming a triazole linkage by the copper-catalysed

[3+2] cycloaddition between the azido groups of **99** and a monosaccharide functionalised with a propargyl moiety (**100**) (*Scheme 79*). The protection of the porphyrin core as zinc complex was necessary to avoid the complexation of copper to the porphyrin ligand in the CuAAC step. The tetra-glycosylated porphyrin **101** were easily obtained adopting the reaction conditions employed for a similar reaction.[142]
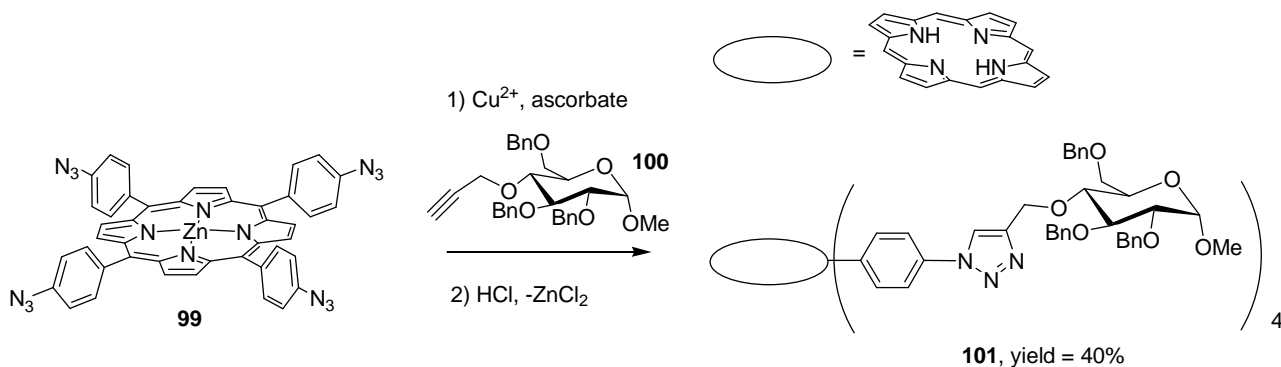
Scheme 79 .Glycoporphyrin synthesis via CuAAC

The corresponding cobalt(II) and iron(III)-methoxy complexes of the glycoporphyrins derivatives were obtained by direct metalation using either $CoCl_2 \cdot 6(H_2O)$ or $FeBr_2$ as metal source following reported procedures (*Scheme 80*).[143],[144] The axial ligand of the iron (III) complexes was considered a methoxide anion. The complexes were paramagnetic as expected for iron (III) and cobalt (II) porphyrin species, therefore, the characterisation by NMR spectroscopy of these compounds is very difficult, therefore the glycoporphyrin complexes were characterised by mass spectroscopy and UV-Vis analysis. The latter technique allowed us to observe the decrease in number and intensity of the Q bands with respect to the free-base UV spectrum which is typically observed in iron(III) porphyrin complexes.[145] The synthesis of the ruthenium(II) carbonyl complex **Ru-98** was performed by glycosylation of the complex $Ru(F_{20}\text{-}TPP)CO$ using the S_NAr protocol described above. The direct metalation of glycoporphyrin **98** with $Ru_3(CO)_{12}$ was ineffective under many conditions, maybe because of the steric hindrance of the saccharide units of the porphyrin ligand. The glycosylation step afforded the desired product in higher yields and shorter reaction time if $Ru(F_{20}\text{-}TPP)CO$ was used instead of the free-base $F_{20}TPPH_2$, the so-obtained ruthenium(II)-carbonyl glycoporphyrin complex was characterised by NMR and IR spectroscopy.
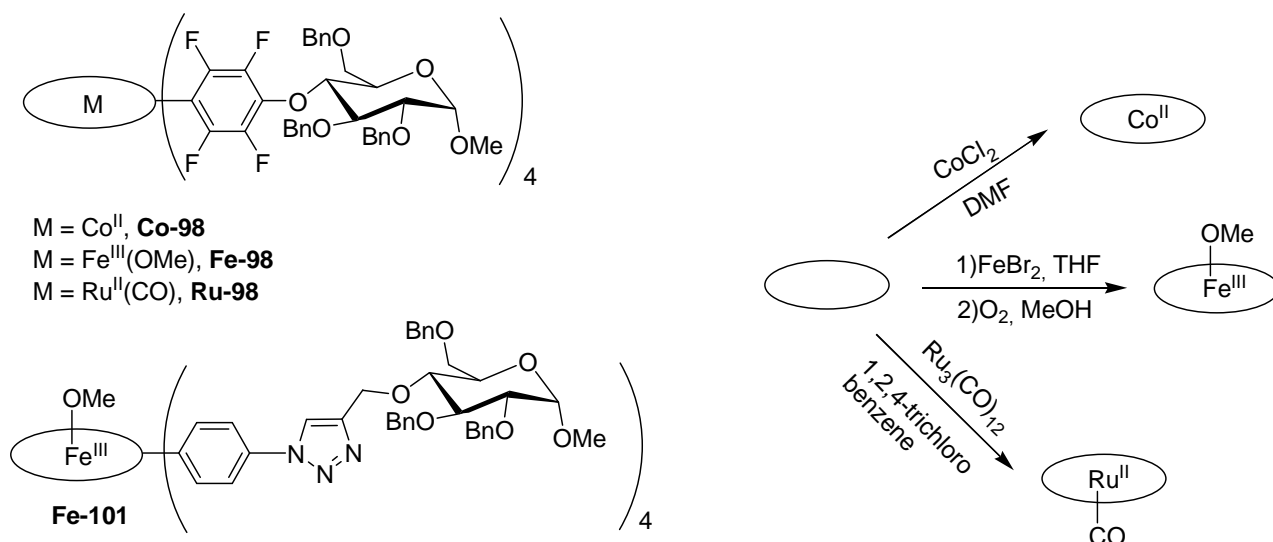
Scheme 80. *Representation of the synthesised glycoporphyrin complexes and the adopted methodologies.*

The catalytic activity of glycoporphyrin complexes was tested in carbene/nitrene transfer reactions, such as cyclopropanation of α-methylstyrene with ethyl diazoacetate (EDA) and benzylic amination of ethyl benzene with 3,5-*bis*(trifluoromethyl)phenyl azide.

Table 9. *Cyclopropanation of α-methyl styrene with EDA using glycoporphyrin complexes as catalysts.*
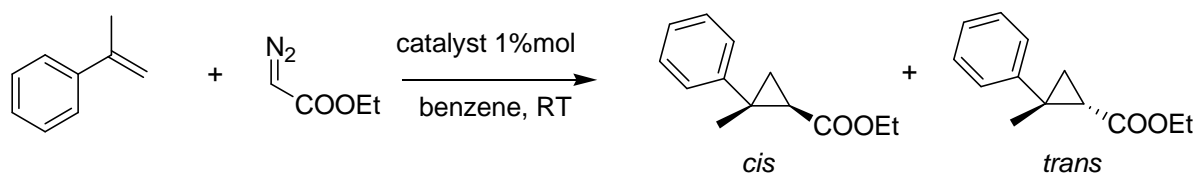
Catalyst	Yield (%)	Reaction Time (h)	*cis/trans* ratio
[a]**Co-98**	14	3.5	1:1
[b]**Fe-98**	76	1.5	1:1
[c]**Ru-98**	69	1	2:1

Experimental conditions: [a]catalyst/EDA/α-methyl styrene = 1:100:1000, EDA was added with a syringe pump over 100 minutes. [b,d]Catalyst/EDA/α-methyl styrene = 1:110:250. [c]Ru/EDA/α-methyl styrene = 1:1000:2000, EDA was added with a syringe pump over 100 minutes.

Table 10. *Benzylic amination of ethylbenzene with 3,5-bis(trifluoromethyl)phenyl azide using glycoporphyrin complexes as catalysts.*
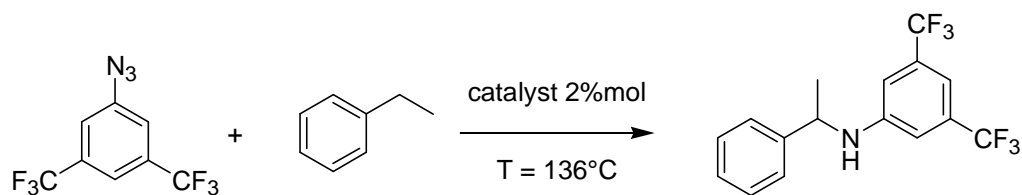
Catalyst	Yield (%)	Reaction Time (h)
[a]Co-98	60	4
[b]Fe-98	88	0.66
[c]Ru-98	92	1
[d]Fe-101	14	30

Experimental conditions: catalyst/azide/ethylbenzene = 1:50:neat, solvent: refluxing ethylbenzene.

The complexes of ligand **98** showed good catalytic activity allowing the formation of the desired product in reasonable yields and reaction times. A very poor catalytic activity was observed concerning the iron complex of ligand **101** obtained from the CuAAC protocol, maybe the presence of a coordinative group such as the triazole moiety hampers the catalytic reaction.

Unfortunately, no enantioselection was observed and only racemic mixtures were obtained in any case. The ruthenium complex **Ru-98** showed a marked diastereoselectivity towards the *cis* isomer in the cyclopropanation reactions, as expected when the catalyst is a porphyrin complex carrying bulky *meso*-aryl groups.[146]

In order to synthesise a water-soluble catalyst we performed the deprotection of the saccharide unit of complex **Ru-98** removing the benzyl ethers groups by Pd-catalysed hydrogenation. We obtained the deprotected ruthenium glycoporphyrin complex **Ru-102** (*Scheme 81*) this complex was insoluble in both water and chlorinated solvents, a moderate solubility in methanol was observed.
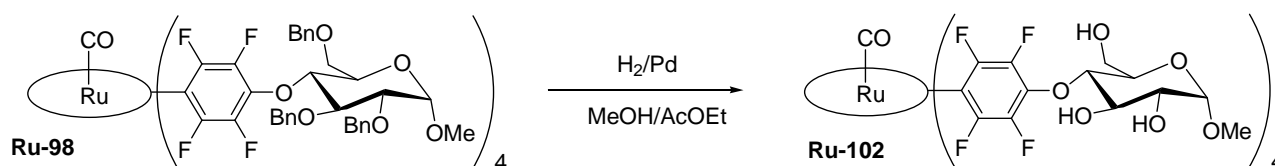
Scheme 81. Synthesis of complex Ru-102.

A particular behaviour was observed when **Ru-102** was suspended in a hydrocarbon solvent such as ethyl benzene; when the mixture was heated to reflux the complex was completely dissolved but when the solution was cooled at RT the complex precipitated. The complex could be recovered by filtration and UV analysis of the filtered hydrocarbon solution detected only traces of **Ru-102**.

We performed the benzylic amination of ethylbenzene using **Ru-102** as the catalyst, at the end of the reaction the catalyst was recovered in 78% yield in a pure form, as revealed by NMR analysis. The yield in the benzylic amine was 80%.

2.7. Conclusion

In this Ph.D. thesis several aspects around the topic of metal porphyrins-catalysed nitrene transfer reactions were investigated. It is worth to remark the importance of this sustainable synthetic methodology, it affords valuable nitrogen-containing compounds using cheap starting materials and, if organic azides are employed as nitrene source, molecular nitrogen is the only by-product of the reaction.

The scope of ruthenium porphyrin-catalysed amination reaction was extended to the synthesis of important compounds from a biological and pharmaceutical point of view. New strategies to obtain amino acid derivatives and indoles by C-N bond formation were developed. In particular, the reported synthesis of the latter compounds was the first example of intermolecular reaction between an alkyne species and an organic azide affording the indole motif instead of triazoles; thus, it was demonstrated that a great control on the reaction selectivity can be achieved using metal porphyrin catalysts.

The optimisation of these transformations was carried out also by studying the mechanism of the catalytic reaction. The generality of a previously performed mechanistic investigation concerning ruthenium porphyrin catalysed allylic amination was assessed. The point of view of Resonance Raman allowed the study of the catalytic system from a different perspective, whilst kinetic and theoretical studies shed some light into the mechanism of ruthenium-porphyrin catalysed aziridination of olefins and benzylic amination to give α- and β-aminoesters.

The development of new catalysts to improve the catalytic performances and the process sustainability was also considered. Glycoporphyrin complexes, being potentially active compounds in promoting asymmetric synthesis or reactions in aqueous media, seem suitable for the accomplishment of this target. A preliminary study revealed the good catalytic activity in nitrene and carbene transfer reaction of this biocompatible substances, moreover the basis for a catalyst recovery/reuse system were laid.

3. Experimental Section

General Conditions. Unless otherwise specified, all the reactions were carried out under nitrogen atmosphere employing standard Schlenk techniques and magnetic stirring. Toluene, n-hexane and benzene were dried by M. Braun SPS-800 solvent purification system. THF, α-methylstyrene, cyclohexene, cumene and decalin were distilled over sodium and stored under nitrogen. 1,2-Dichloroethane and CH_2Cl_2 were distilled over CaH_2 and immediately used. Methyl phenylacetate was distilled over Na_2SO_4 and stored under nitrogen. Phenylacetylene was filtered through activated alumina, distilled under vacuum and stored under nitrogen, phenylacetylene-d_1 was synthesised by using a reported procedure.[147] Commercial mCPBA(77%) was purified using a reported procedure[148] and stored at -20°C. All the other starting materials were commercial products used as received. NMR spectra were recorded at room temperature, unless otherwise specified, on a Bruker avance 300-DRX, operating at 300 MHz for ^{1}H, at 75 MHz for ^{13}C and at 282 MHz for ^{19}F, or on a Bruker Avance 400-DRX spectrometers, operating at 400 MHz for ^{1}H , at 100 MHz for ^{13}C and at 376 MHz for ^{19}F. Chemical shifts (ppm) are reported relative to TMS. The ^{1}H NMR signals of the compounds described in the following have been attributed by COSY and NOESY techniques. Assignments of the resonance in ^{13}C NMR were made using the APT pulse sequence and HSQC and HMBC techniques. GC-MS analyses were performed on a Shimadzu QP5050A equipped with Supelco SLB -5 ms capillary column (L 30m × I.D. 0.25 mm × 0.25 μm film thickness). GC analyses were performed on a Shimadzu GC - 2010 equipped with a Supelco SLB - 5ms capillary column (L 10m × I.D. 0.1 mm × 0.1 μm film thickness). Infrared spectra were recorded on a Varian Scimitar FTS 1000 spectrophotometer. UV/Vis spectra were recorded on an Agilent 8453E instrument. Elemental analyses and mass spectra were recorded in the analytical laboratories of Milan University.

3.1. Porphyrin synthesis

Porphyrin syntheses were carried out in the air.

3.1.1 Synthesis of *meso*-tetraphenylporphyrin (TPPH$_2$).
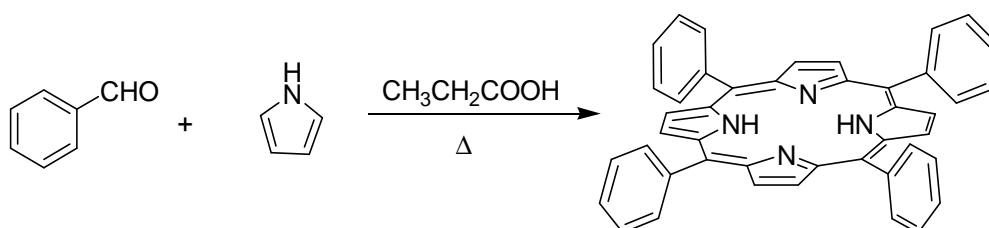
Reagent grade benzaldehyde (36.5 mL, 360 mmol) was dissolved in propionic acid (500 mL). The colourless mixture was heated to 50°C, then a solution of distilled pyrrole (25.0 mL, 360 mmol) in propionic acid (30 mL) was added dropwise in about 10 minutes. The resulting mixture was refluxed in air for 30 minutes. During this period the mixture turned to red at first and then to deep black. The reaction mixture was allowed to cool at RT and the formation of a crystalline violet precipitate was observed. The dark suspension was filtered, washed with methanol (50 mL), water (50 mL) and finally again with methanol until the filtrate was clear. The crystalline purple solid was dried *in vacuo* (10.6 g, 8.2 %).

^{1}H NMR (300 MHz, CDCl$_3$): δ 8.86 (8H, s, H$_\beta$), 8.22 (8H, m, H$_o$), 7.78 (12H, m, H$_m$ and H$_p$), -2.74 (s, NH).

UV-Vis (CH$_2$Cl$_2$): λ$_{max}$ (log ε) 417 (5.66), 514 (4.30), 549 (3.91), 590 (3.73), 647 (3.74).

3.1.2 Synthesis of *meso*-tetra(4-(trifluoromethyl)-phenyl)porphyrin (T(*p*-CF$_3$)PPH$_2$).
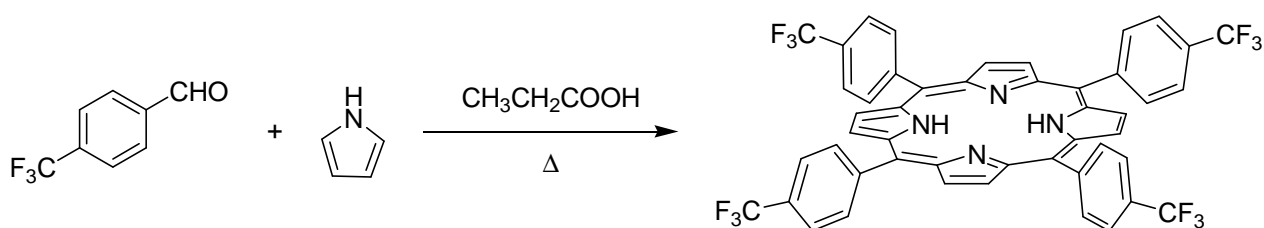
4-(Trifluoromethyl)benzaldehyde (4.50 mL, 33 mmol) was dissolved in propionic acid (100 mL). The colourless mixture was heated to 50°C, then a solution of distilled pyrrole (2.50 mL, 36 mmol)

in propionic acid (30 mL) was then added dropwise in about 10 minutes. The resulting mixture was refluxed in air for 30 minutes during which the mixture turned to deep black. The reaction mixture was allowed to cool at RT and the formation of a crystalline violet precipitate was observed. The dark suspension was filtered, washed with water (10 mL) and with methanol until the filtrate was clear. The crystalline purple solid was dried *in vacuo* (1.56 g, 21.4 %).

^{1}H NMR (300 MHz, CDCl$_3$): δ 8.82 (s, 8H, H$_\beta$), 8.34 (d, 8H, J = 8.1 Hz, H$_o$), 8.05 (s, 8H, J = 8.1 Hz, H$_m$), -2.83 (2H, s, NH).

^{19}F NMR (282 MHz, CDCl$_3$): δ -62.39 (CF$_3$).

3.1.3. Synthesis of *meso*-tetra(pentafluorophenyl)porphyrin (F$_{20}$-TPPH$_2$).
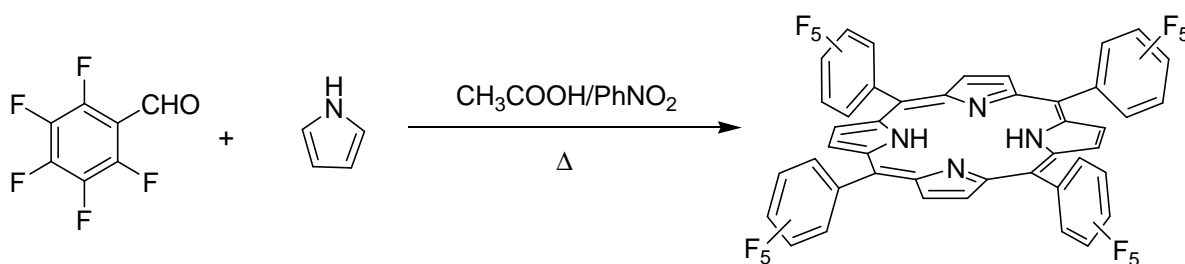
Pentafluorobenzaldehyde (1.81 g, 9.2 mmol) was dissolved in a mixture of glacial acetic acid (60 mL) and nitrobenzene (50 mL). The solution was heated to 50°C then a solution of pyrrole (700 µL, 11 mmol) in acetic acid was added dropwise and the obtained mixture was heated to reflux for 2 hours. The solvent was evaporated to dryness giving a black tar which was purified by filtration over a short alumina column using *n*-hexane and *n*-hexane/CH$_2$Cl$_2$ 100:2 as eluent. The porphyrin fraction was evaporated to dryness and dried *in vacuo* (249 mg, 10%).

^{1}H NMR (300 MHz, CDCl$_3$): δ 8.92 (8H, s, Hβ), -2.90 (2H, s, NH)

^{19}F NMR (282 MHz, CDCl$_3$): δ -136.8 (8F, dd, J = 23.6 Hz, J = 6.6 Hz, F$_o$), -151.53 (8F, t, J = 21.0 Hz, F$_p$), -161.71 (8F, td, J = 23.6 Hz, J = 8.3 Hz, F$_m$).

UV-Vis (CH$_2$Cl$_2$): λ$_{max}$ (log ε) 411 nm (7.43), 506 nm (6.32), 582 nm (5.83), 637 nm, 658 nm.

3.1.4. Synthesis of *meso*-tetra(4-aminophenyl)porphyrin (TAPPH$_2$).
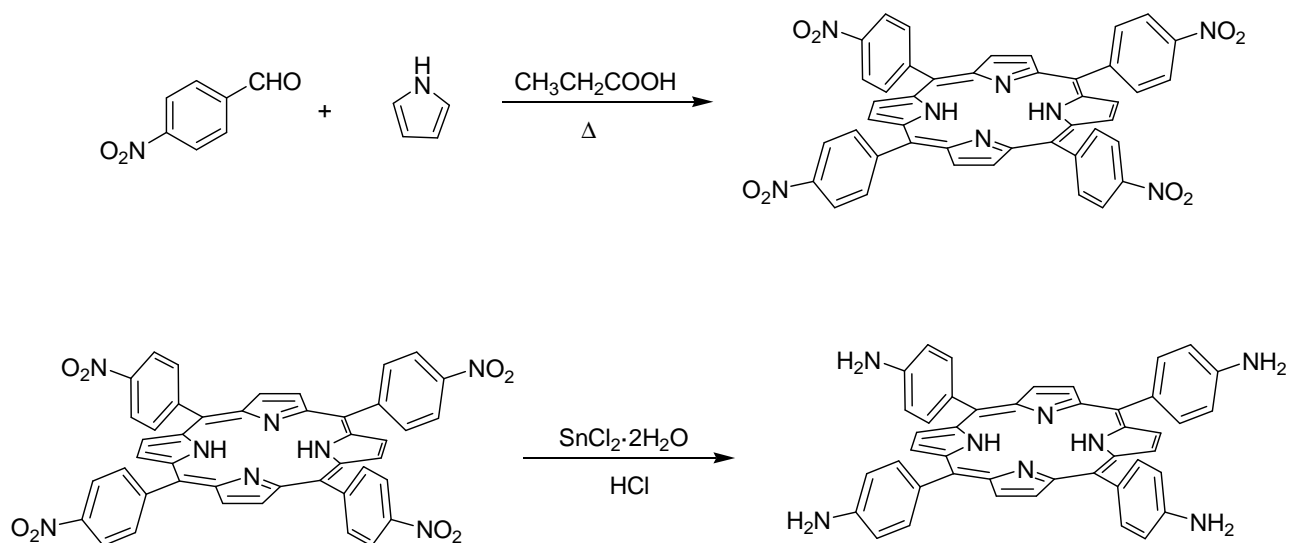
1) Synthesis of *meso*-tetra(*p*-nitrophenyl)porphyrin (T(*p*-NO$_2$)PPH$_2$).

4-Nitrobenzaldehyde (3.86 g, 26 mmol) was dissolved in a mixture of propionic acid (80 mL) and acetic anhydride (4.0 mL). The resulting solution was heated to reflux then a solution of distilled pyrrole (1.80 mL, 26 mmol) in propionic acid (20 mL) was added dropwise in about 15 minutes. The mixture was refluxed for 30 minutes and allowed to cool at RT. The dark suspension was filtered and washed with water (50 mL × 2). The filtered tar was re-crystallised from refluxing pyridine (25 mL) and washed with acetone. The filtered solid was insoluble in common laboratory solvents, therefore, NMR analysis was not performed.

2)Reduction of T(*p*-NO$_2$)PPH$_2$ to give TAPPH$_2$.

Under a nitrogen atmosphere, the previously obtained solid (640 mg, cca 0.81 mmol) was suspended in HCl 37% (70 mL) and a solution of SnCl$_2$·2H$_2$O (3.92 g, 17 mmol) in HCl 37% (15 mL) was added. The mixture was heated up to 75°C for 30 minutes then cooled using an ice bath. A 30% ammonia solution (65 mL) was added and the resulting suspension was stirred for 1 hour observing the precipitation of a dark green solid, which was filtered, suspended in NaOH 2% (100 mL) filtered again and washed with H$_2$O. The product was recovered by continuous Soxhlet extraction in acetone (314 mg, total yield = 2%).

^{1}H NMR (300 MHz, CDCl$_3$): δ 8.90 (s, 8H), 7.99 (d, *J* = 7.6 Hz, 8H), 7.06 (d, *J* = 7.7 Hz, 8H), -2.70 (s, 2H).

3.1.4. Synthesis of *meso*-tetra(4-azidophenyl)porphyrin T(*p*-N$_3$)PPH$_2$.
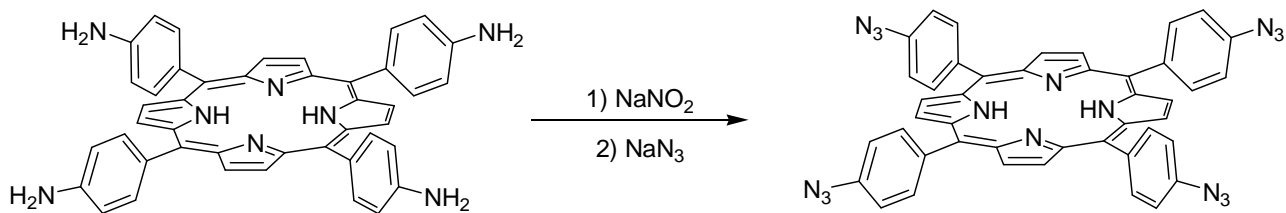
Under nitrogen atmosphere TAPPH$_2$ (163 mg, 2.4×10^{-1} mmol) was dissolved in trifluoroacetic acid (5.0 mL) and the dark green solution was cooled using an ice bath. A solution of NaNO$_2$ (134 mg, 1.9 mmol) in H$_2$O (1 mL) was added and the mixture was stirred at 0°C for 15 minutes. A solution of NaN$_3$ (222 mg, 2.0 mmol) in H$_2$O (1 mL) was added and the mixture was stirred for 1 hour at RT observing a colour change of the solution form dark green to dark blue. H$_2$O (20 mL) was added and the mixture was extracted with CH$_2$Cl$_2$ (50 mL × 3). The organic phases were collected and washed with H$_2$O (3 ×50 mL) until the solution colour turned to purple. The solution was dried over Na$_2$SO$_4$ and the solvent was evaporated to dryness. A dark violet solid was obtained (131 mg, 69%).

^{1}H NMR (300 MHz, CDCl$_3$): δ 8.84 (s, 8H), 8.19 (d, *J* = 8.0 Hz, 8H), 7.44 (d, *J* = 7.8 Hz, 8H), -2.80 (s, 2H).
IR(ATR): 2123 cm^{-1} ($\nu_{N=N}$), 2085 cm^{-1} ($\nu_{N=N}$).

3.1.5. Synthesis of Glycoporphyrin 98.
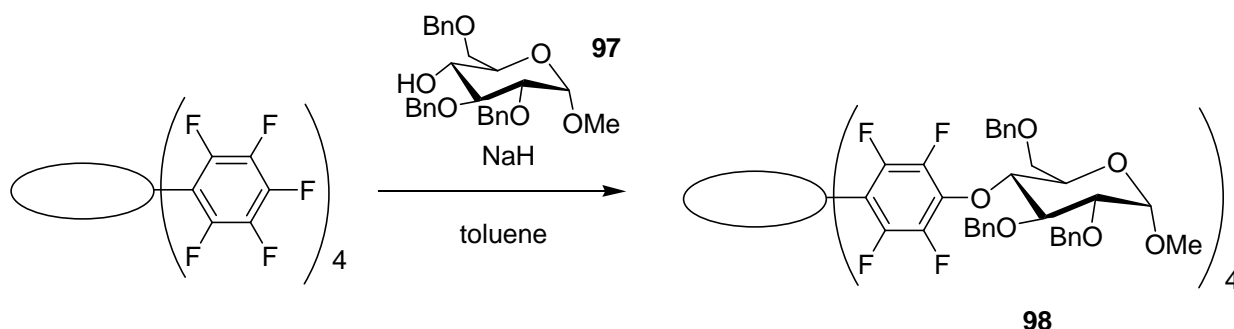
$F_{20}TPPH_2$ (72 mg, 7.4×10^{-2} mmol) and monosaccharide **97** (207 mg, 4.6×10^{-1} mmol) were dissolved in toluene (10 mL), then NaH 60% (120 mg, 3.0 mmol) was added and the resulting mixture was heated to reflux in absence of light (by wrapping the Schlenk flask with an aluminum foil) for 24 hours monitoring the reaction by TLC (SiO_2, *n*-hexane/AcOEt 5:5). 20 mL of HCl 0.5 M were added dropwise to quench the sodium hydride excess, $CHCl_3$ (40 mL) was added and the organic phase was washed with water (50 mL $\times$ 2) until the aqueous phase was neutral. The organic phase was dried over Na_2SO_4 and the solvent was evaporated to dryness. The crude was purified by flash chromatography (silica gel, *n*-hexane/AcOEt 7:3). Compound **98** was obtained as a dark violet solid (103 mg, 50%).

^{1}H NMR (300 MHz, $CDCl_3$) δ 8.48 (8H, s, H_β), 7.50 – 7.01 (60H, m, H_{Ar}), 5.28 (4H, d, $J = 10.9$ Hz, C(*H*)H-OBn), 4.95 – 4.67 (28H, m, $H_{saccharide}$), 4.45 (4H, dd, $J = 16.1, 7.1$ Hz, $CH_{saccharide}$), 4.31 (d, $J = 8.5$ Hz, $CH_{saccharide}$), 4.06 (8H, m, CH_2-Ph), 3.83 (dd, $J = 9.2, 2.3$ Hz, $CH_{saccharide}$), 3.56 (12H, s, OCH_3), -3.01 (2H, s, NH).

^{19}F NMR (282 MHz, $CDCl_3$): δ -139.23 (8F, d, $J = 17.2$ Hz), -156.36 (8F, d, $J = 18.5$ Hz).

UV-Vis (CH_2Cl_2): λ_{max} (log ε) 416 nm (5,54), 509 nm (4,36), 585 nm (3,90), 656 nm (3.08).

Synthesis of glycoporphyrin 101.

1) Synthesis of zinc complex 99.
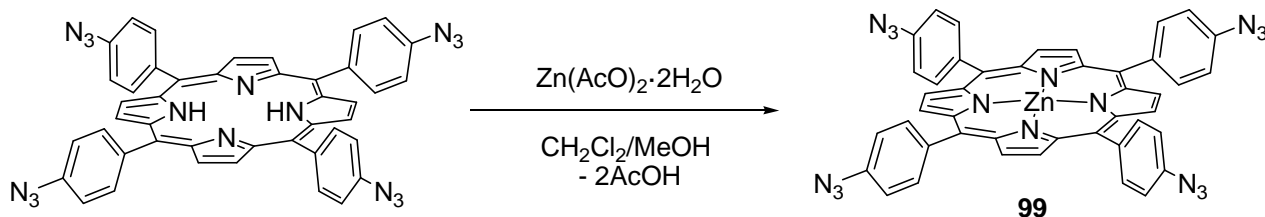
T(p-N$_3$)PPH$_2$ (75 mg, 9.6×10^{-1} mmol) was dissolved in CH$_2$Cl$_2$ (10 mL) and a solution of Zn(AcO)$_2 \cdot$2H$_2$O (350 mg, 1.6 mmol) in MeOH (1.5 mL) was added. The mixture was stirred for 4.5 hours at room temperature, until a complete conversion of the free-base porphyrin into the zinc complex was observed by TLC monitoring (SiO$_2$, n-hexane/ CH$_2$Cl$_2$ 7:3). The solution was washed with H$_2$O (50 mL × 3), dried over Na$_2$SO$_4$ and the solvent was evaporated to dryness obtaining a dark violet solid (**99**) (70 mg, 87%).

2) Synthesis of zinc glycoporphyrin complex Zn-101.
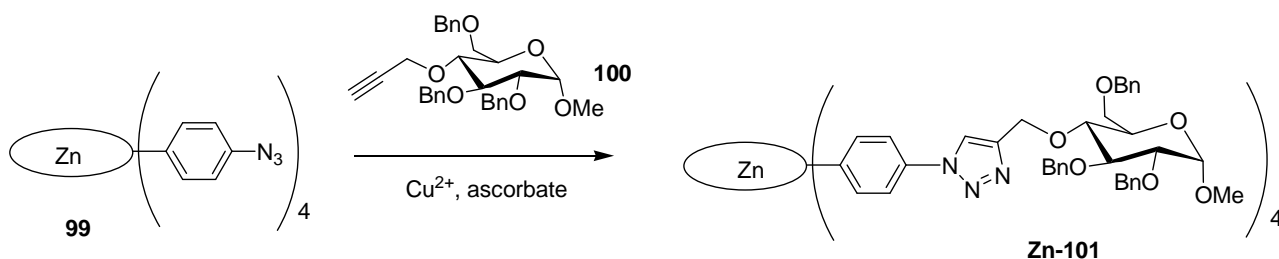
Zinc complex **99** (30 mg, 3.6×10^{-2} mmol) was suspended in THF/H$_2$O 1:1 (8.0 mL), then monosaccharide **100** (90 mg, 0.18 mmol), CuSO$_4 \cdot$5H$_2$O (45 mg, 0.18 mmol) and sodium ascorbate (35 mg, 0.18 mmol) were added. The so-obtained mixture was heated up to 50°C for 3 hours till the starting zinc complex was no longer detected by TLC analysis (SiO$_2$, CH$_2$Cl$_2$ /MeOH 100:2). The reaction mixture was cooled, H$_2$O (10 mL) was added and the mixture was extracted with CH$_2$Cl$_2$ (15 mL × 3), the organic phase was dried over Na$_2$SO$_4$ and the solvent was evaporated to dryness. The crude was purified by flash chromatography (silica gel, gradient elution from CH$_2$Cl$_2$ /MeOH 99:1 to CH$_2$Cl$_2$ /MeOH 98:2). Complex **Zn-101** obtained as a dark violet solid (40 mg, 40%).

^{1}H NMR (400 MHz, CDCl$_3$) δ 9.00 (8H, s, H$_\beta$), 8.34 (8H, d, J = 8.2 Hz, H$_{ortho\ meso\text{-}phenyl}$), 7.87 (8H, d, J = 7.9 Hz, H$_{meta\ meso\text{-}phenyl}$), 7.73 (s, 4H, H$_{triazole}$), 7.42-7.17 (60H, m, H$_{Ar}$), 4.99 (1H, d, J = 11.0

Hz, C5$_{saccharide}$–C(H)H), 4.87 – 4.41 (36H, m, 5H, H$_{saccharide}$), 3.94 (4H, t, J = 9.0 Hz, CH$_{saccharide}$ in position 4), 3.72 – 3.54 (20H, m, H$_{saccharide}$), 3.38 (3H, s, anomeric OMe).

3) Synthesis of the free-base glycoporphyrin 101.
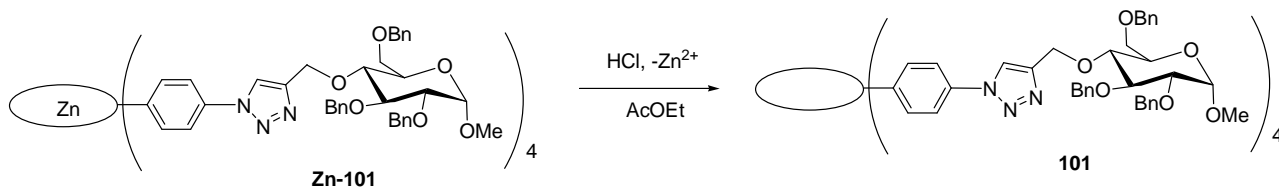
Zn-101 (52 mg, 1.8×10^{-2} mmol) was dissolved in AcOEt (10 mL), then HCl 37% (2.5 mL) was added. The mixture was stirred for 3 hours, then was washed with water (50 mL × 2) until the aqueous phase was neutral. The organic phase was dried over Na$_2$SO$_4$ and the solvent was evaporated to dryness obtaining a dark solid (48 mg, 94%).

^{1}H NMR (300 MHz, CDCl$_3$) δ 8.96 (8H, s, H$_\beta$), 8.38 (8H, d, J = 8.3 Hz, H$_{ortho\ meso\text{-}phenyl}$), 8.04 (8H, d, J = 8.3 Hz, H$_{meta\ meso\text{-}phenyl}$), 7.95 (4H, s, H$_{triazole}$), 7.54 – 7.16 (60H, m, H$_{Ar}$), 5.24 – 4.50 (28H, m, H$_{saccharide}$), 4.39 (4H, dd, J = 15.2, 2.2 Hz, C(H)H-OBn), 4.22 (4H, dd, J = 15.3, 2.2 Hz, C(H)H-OBn), 4.13 – 3.47 (24H, m, H$_{saccharide}$), 3.43 (3H, s, anomeric OMe), -2.71 (2H, s, NH).

3.2. Ruthenium complexes synthesis.

3.2.1. Synthesis of $Ru_3(CO)_{12}$.

$$RuCl_3 \cdot 6H_2O \xrightarrow[\text{MeOH, } \Delta]{\text{CO(60 bar)}} Ru_3(CO)_{12}$$
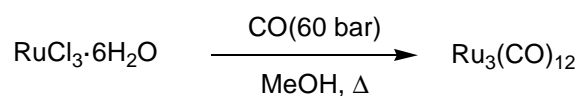
Method A (using $RuCl_3 \cdot 3H_2O$ as starting material): Trihydrated ruthenium trichloride (1.24 g, 4.8×10^{-3} mol) was dissolved in methanol (30 mL) inside a 100 mL glass liner equipped with a screw cap and a glass wool. The dark mixture was cooled with liquid nitrogen and degassed performing three vacuum-nitrogen cycles. The flask was transferred into a stainless steel autoclave, three vacuum-nitrogen cycles were performed and CO (60 bar) was charged at room temperature. The autoclave was placed in a preheated oil bath at 120°C and stirred for about 8 hours, then it was cooled at room temperature and slowly vented. The obtained orange suspension was filtered, the solid was dissolved in THF and purified by filtration in continuous on a celite pad. The solvent was evaporated to dryness and an orange crystalline solid was obtained (736 mg, 73 %). The mother liquors of the filtration were collected and stored at 4°C to be used as solvent for the subsequent $Ru_3(CO)_{12}$ synthesis (the same methanol solution was re-used maximum twice).

IR(nujol): 2059.7 cm^{-1}, 2015.4 cm^{-1}, 1996.6 cm^{-1}.

Elemental Analysis calc. for $C_{12}O_{12}Ru_3$: C, 22.54; O, 30.03; Ru, 47.43; found: C, 23.01;

Method B (ruthenium recovery): The following procedure was performed in the air. Any solid or any solution of a low-boiling solvent containing a reasonable fraction of ruthenium porphyrin complexes were reunited and evaporated to dryness. In a typical experiment, 10 mL of a 7:3 mixture of HNO_3 (65%) and H_2O_2 (30%) were added dropwise to the residue (1.25 g) observing the generation of brown fumes and heat. The mixture was stirred for 1 hour then other 10 mL of the same mixture were added dropwise. After one hour 45 mL of concentrated HCl (37%) were added and the solution was stirred overnight. The acidic solution was distilled and the obtained dark red tar was dried under vacuum at 100°C for a couple of hours. The crude was suspended in 30 mL of MeOH and filtered. The methanol solution was directly used for the $Ru_3(CO)_{12}$ synthesis described above. Sometimes the final product was a brown crystalline solid, in that case re-crystallization from acetone gave pure $Ru_3(CO)_{12}$.

The yield of the entire process was calculated by evaluating the ruthenium content of a dichloromethane solution of the initial crude by ICP analysis. Since the ruthenium weight percentage in 1.25 g of crude was 4.66% and we obtained 38 mg of Ru_3CO_{12}, the total recovery yield was 31%.

Elemental Analysis calc. for $C_{12}O_{12}Ru_3$: C, 22.54; O, 30.03; Ru, 47.43; found: C, 22.57; H, 0.19.

3.2.2. Synthesis of Ru(TPP)CO.
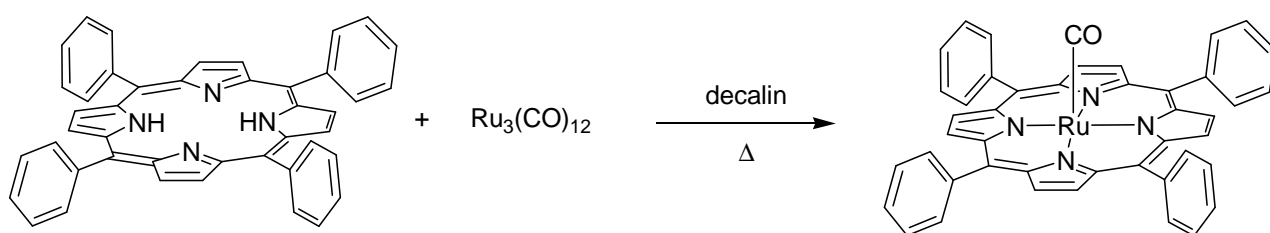
$Ru_3(CO)_{12}$ (626 mg, 9.8×10^{-1} mmol) and $TPPH_2$ (1.23 g, 2.0 mmol) were suspended in dry decalin (60 mL). The reaction mixture was refluxed for 7 hours, cooled at room temperature and the precipitate was collected and washed with *n*-hexane (3×10 mL). The violet solid was then purified by flash-chromatography (silica gel, starting from CH_2Cl_2/*n*-hexane 8:2, then using CH_2Cl_2/*n*-hexane 8:2 with 2% AcOEt to elute unreacted $TPPH_2$ and finally using pure CH_2Cl_2 to elute the product). The Ru(TPP)CO fraction was evaporated to dryness and dried *in vacuo* at 120°C. The product was obtained as a purple crystalline solid (1.09 g, 73%).

^{1}H NMR (300 MHz, $CDCl_3$): δ 8.68 (8H, s, H_β), 8.22 (4H, m, H_{ortho}), 8.11 (4H, m, $H_{ortho'}$)7.73 (m, 12H, $H_{meta +para}$).
UV-Vis (CH_2Cl_2): λ_{max} (log ε) 412 (5.38), 528 (4.29), 588 (3.51).
IR (ATR): 1956 cm^{-1} (v_{CO}), 1008 cm^{-1} (oxidation marker band).

ATR-IR spectrum of Ru(TPP)CO in the presence of methyl phenylacetate.

Experiment Conditions: Ru(TPP)CO (50 mg, 6.7×10^{-2} mmol) was suspended in a mixture of dichloromethane (4.0 mL) and methyl phenylacetate (1.0 mL). The resulting suspension was refluxed until Ru(TPP)CO was completely dissolved obtaining a dark red solution, then

dichloromethane was evaporated and *n*-hexane (10 mL) was added. The so obtained red solid was filtered and analysed by IR spectroscopy. $\nu(CO) = 1948 \text{ cm}^{-1}$.

3.2.3. Synthesis of Ru(T(*p*-CF₃)PP)CO (41).
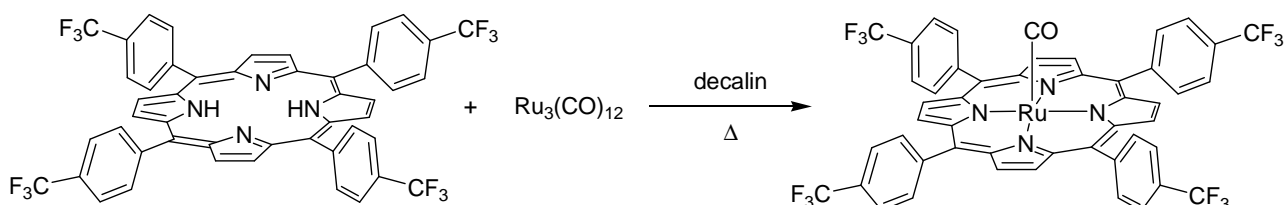
Ru₃(CO)₁₂ (187 mg, 2.9×10^{-1} mmol) and T(*p*-CF₃)PPH₂ (491 mg, 5.5×10^{-1} mmol) were suspended in dry decalin (60 mL). The reaction mixture was refluxed for 4 hours, when the TLC control showed the absence of the free-base porphyrin, cooled at room temperature and the precipitate was collected and washed with *n*-hexane (3×3 mL). The purple solid was dried *in vacuo* at 120°C (466 mg, 83%).

^{1}H NMR (300 MHz, CDCl₃): δ 8.67 (8H, s, H$_\beta$), 8.16 (8H, d, *J* = 7.4 Hz, H$_{ortho}$), 7.73 (8H, d, *J* = 8.0 Hz, H$_{meta}$).
^{19}F NMR (282 MHz, CDCl₃): δ -62.36 (CF₃).
IR (ATR): 1981 cm^{-1} (ν_{CO}), 1008 cm^{-1} (oxidation marker band).

3.2.4. Synthesis of Ru(F₂₀-TPP)CO.
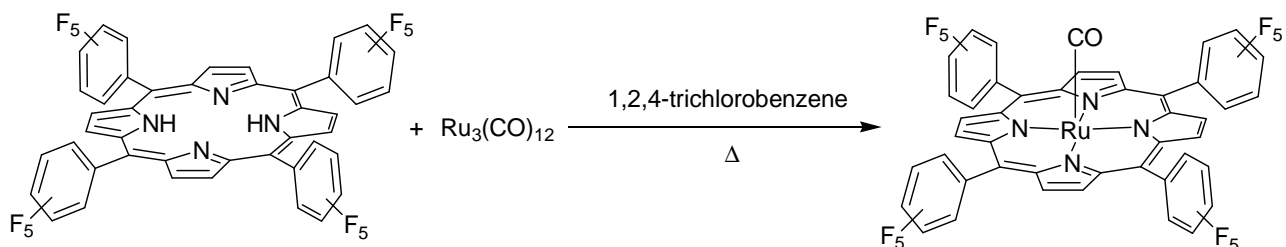
F₂₀-TPPH₂ (130 mg, 1.3×10^{-1} mmol) and Ru₃(CO)₁₂ (85 mg, 1.3×10^{-1} mmol) were dissolved in degassed 1,2,4-trichlorobenzene (20 mL). The mixture was refluxed for 6 hours, then the solvent

was evaporated to dryness. The crude was purified by chromatographic column (Al$_2$O$_3$, *n*-hexane/CH$_2$Cl$_2$ 1:1 to elute residual free-base porphyrin and CH$_2$Cl$_2$/acetone 1:1 to elute the ruthenium complex). The product fraction was evaporated to dryness and dried *in vacuo* to give a red solid (115 mg, 78%).

^{1}H NMR (300 MHz, CDCl$_3$): δ 8.71 (8H, s, H$_β$)

^{19}F NMR (282 MHz, CDCl$_3$): δ -136.0 (2F, d, *J* = 23.4 Hz), -137.6 (2F, d, *J* = 20.3 Hz), 152.0 (1F, t, *J* = 20.0 Hz), -161.4 (2F, m), -162.0 (2F,m).

IR(ATR):

3.2.5. Synthesis of Ru(TPP)CO(MeOH) (90).
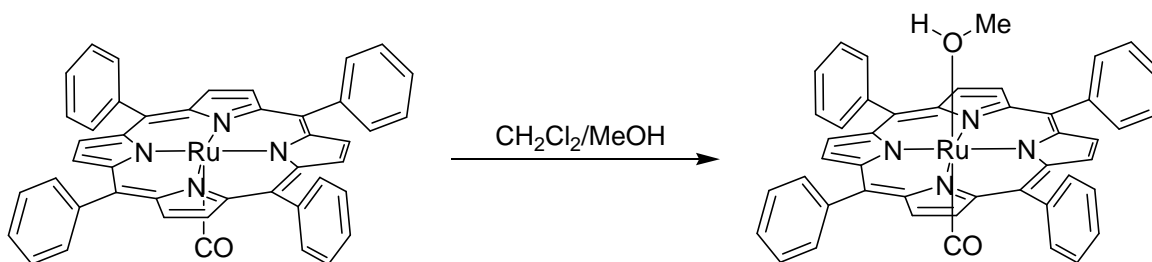
Ru(TPP)CO (767 mg, 1.0 mmol) was suspended in 33 mL of mixture CH$_2$Cl$_2$/MeOH 1:2 and refluxed for 3 h. The reaction was followed by IR(nujol) spectroscopy. The orange precipitate was filtered and dried *in vacuo* at RT (751 mg, 94%).

^{1}H NMR (300 MHz, CDCl$_3$): δ 8.71 (8H, s, H$_β$), 8.21 (8H, m, H$_{ortho}$), 7.74 (8H, m, H$_{meta\ and\ para}$)

IR (nujol): 1939 cm^{-1} (ν$_{CO}$), 1008 cm^{-1} (oxidation marker band)

Elemental Analysis calc. for C$_{46}$H$_{32}$N$_4$O$_2$Ru: C C, 71.40; H, 4.17; N, 7.24; O, 4.14; Ru, 13.06.

Found: C, 70.47; H, 4.11; N, 7.24.

3.2.6. Synthesis of complex 42.

3.2.6.1. Synthesis of 1-(3,5-*bis*(trifluoromethyl)phenyl)-5-methyl-5-phenyl-1H-1,2,3-triazoline.
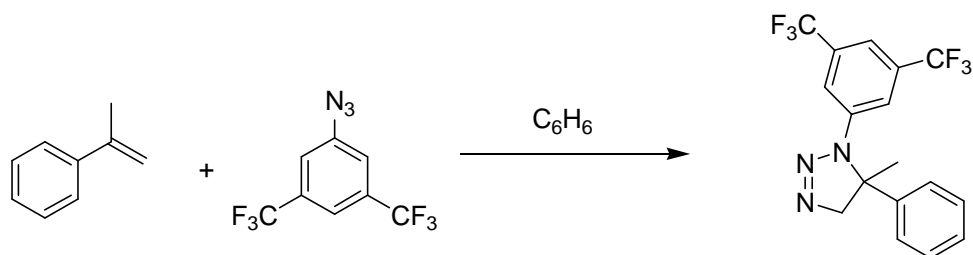
3,5-*bis*(trifluoromethyl)phenyl azide (100 µL, 0.58 mmol) was dissolved into a 1:1 mixture of α-methyl styrene and benzene (14 mL) and heated to 85°C for 16 hours (azide conversion = 98%, measured by IR spectroscopy, $v_{N=N}$ = 2116 cm^{-1}). The solution was evaporated to dryness to give an orange oil (220 mg, 99%).

^{1}H NMR (300 MHz, CDCl$_3$): δ 7.50-7.20 (8H, m, H$_{Ar}$), 4.71 (1H, d, J = 17.4 Hz, CHH), 4.50 (1H, d, J = 17.4 Hz, CHH), 1.77 (3H, s, CH$_3$).
^{19}F NMR (282 MHz, CDCl$_3$): δ -63.66 (CF$_3$).

3.2.6.2. Synthesis of complex 42.
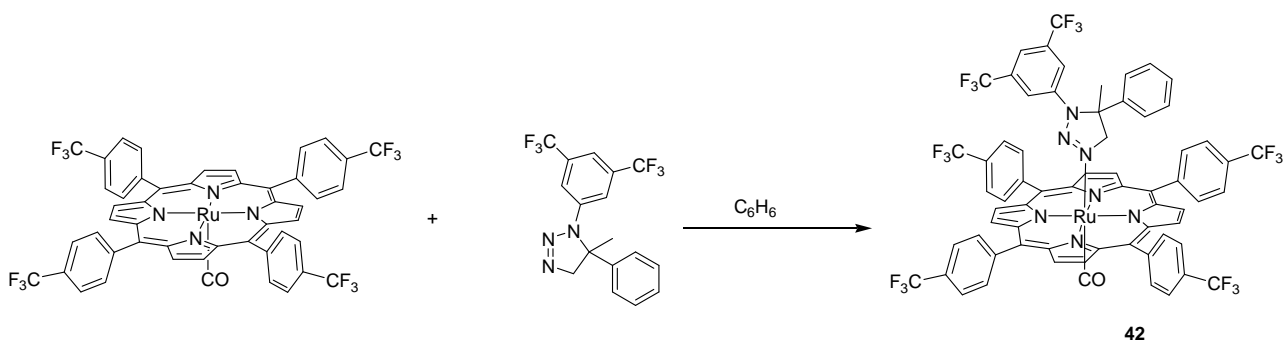
The previously obtained triazoline (55 mg, 1.5×10^{-1} mmol) and Ru(T(*p*-CF$_3$)PP)CO (**41**) (100 mg, 9.8×10^{-2} mmol) were dissolved in benzene (25 mL) and the solution was heated to reflux for 1 hour, when the TLC control showed a complete conversion of Ru(T(*p*-CF$_3$)PP)CO. The solution was concentrated to about 2 mL and *n*-hexane (15 mL) was added. A purple crystalline solid was collected by filtration and dried *in vacuo* (92 mg, 68%).

^{1}H NMR (300 MHz, CDCl$_3$): δ 8.60 (8H, s, H$_β$), 8.38 (4H, d, J = 8.0 Hz, H$_{Ar-meso}$), 8.01 (8H, pst, H$_{Ar-meso}$), 7.91 (4H, d, J = 7.9 Hz, H$_{Ar-meso}$), 7.13 (1H, s, H$_{Ar-triazo}$), 7.04 (2H, t, J = 7.3 Hz, H$_{Ph}$), 6.89

(2H, t, J = 7.7 Hz, H_{Ph}), 5.69 (2H, s, $H_{Ar\text{-}triazo}$), 5.24 (2H, d, J = 7.7 Hz, H_{Ph}), -0.04 (3H, s, CH_3), -1.19 (1H, d, J = 17.1 Hz, CHH), -1.31 (1H, d, J = 17.1 Hz, CHH).

^{19}F NMR (300 MHz, $CDCl_3$): -62.33 (CF_3 porph), -63.82 (CF_3 triazo).

IR (ATR): 1968 cm^{-1} (v_{CO}).

Elemental Analysis calc. for $C_{66}H_{37}N_7F_{18}ORu$: C, 57.15; H, 2.69; F, 24.65; N, 7.07; O, 1.15; Ru, 7.29. Found: C, 55.98; H, 2.24; N, 6.64.

3.2.7. Synthesis of [Ru(TPP)(*m*CB)]₂O (91).
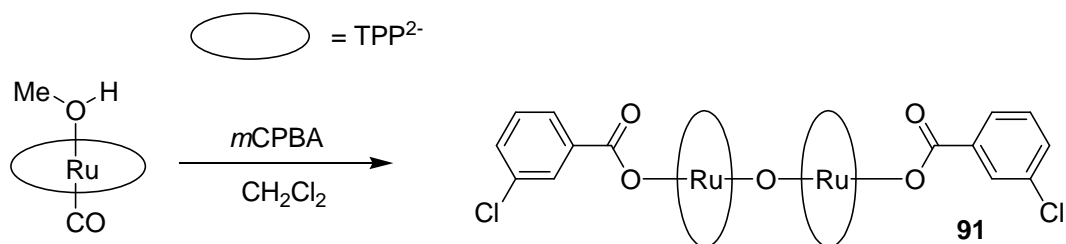
The synthesis was performed in the air. Ru(TPP)CO(MeOH) (**90**) (102 mg, 1.4×10^{-1} mmol) was suspended in CH_2Cl_2 (20 mL) and a solution of *m*CPBA (123 mg, 7.2×10^{-1} mmol) in CH_2Cl_2 (25 mL) was added dropwise in 30 minutes. The initial red suspension turned into a dark red solution. The reaction was stirred for 1.5 hours, TLC control (Al_2O_3, CH_2Cl_2) revealed the presence of unreacted **90**. An additional amount of *m*CPBA (52 mg, 3.0×10^{-1} mmol) was added and the solution was stirred for 3 hours. TLC and IR controls (nujol, $\nu_{C=O}$ of **90** at 1939 cm^{-1}) showed the absence of the starting reagent . The solution was concentrated to about 20 mL and filtered through a short (5 cm) alumina column. The product fraction was evaporated to dryness, the resulting dark solid was dried *in vacuo* (47 mg, 39%).
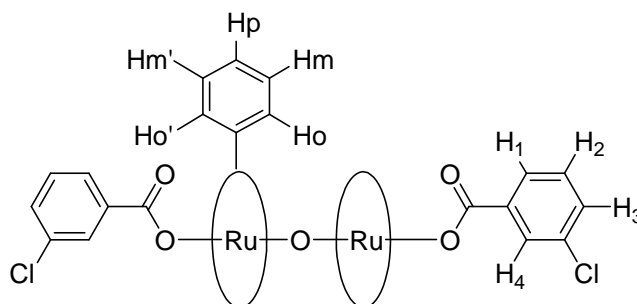
^{1}H NMR (300 MHz, CDCl₃): δ 8.96 (8H, d, J = 7.6 Hz, H$_o$), 8.67 (16H, s, H$_\beta$), 7.98 (8H, t, J = 7.2 Hz, H$_m$), 7.82 (8H, t, J = 7.5 Hz, H$_p$), 7.50 (8H, t, J = 7.6 Hz. H$_{m'}$), 7.25 (8H, overlaid with chloroform signal, H$_{o'}$), 6.14 (2H, d, J = 7.9 Hz, H$_3$), 5.66 (2H, t, J = 7.8 Hz, H$_2$), 3.54 (2H, d, J = 7.8 Hz, H$_1$), 2.74 (2H, s, H$_4$).

^{13}C NMR (75 MHz, CDCl₃): δ 142.1 (C$_\alpha$), 141.3 (*C*-C$_{meso}$), 136.2 (CH$_{o'}$), 135.0 (CH$_o$), 131.6 (CH$_\beta$), 128.9 (C-H$_3$), 127.9 (CH$_p$), 126.9 (CH$_{m'}$), 126.8 (C-H$_2$), 126.6 (CH$_m$), 126.1 (C-H$_4$), 124.2 (C-H$_1$), 121.1 (C$_{meso}$), the carbonyl signal and the *C*-COO-Ru signal were not detected.

IR (ATR): 1735 cm^{-1} ($\nu_{C=O}$), 1014 cm^{-1} (oxidation marker band).

MS (ESI+): *m/z* 1599 [M – 155(*m*CB)]$^+$.

3.2.8. Synthesis of [Ru(TPP)(OMe)]$_2$O (92).
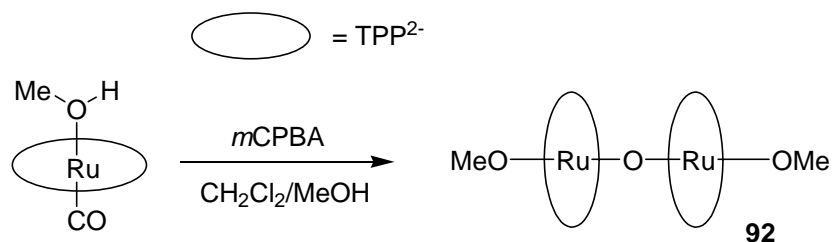
The synthesis was performed in the air. Ru(TPP)CO(MeOH) (**90**) (103 mg, 1.3×10^{-1} mmol) was suspended in CH$_2$Cl$_2$ (20 mL) and a solution of *m*CPBA (137 mg, 8.0×10^{-1} mmol) in CH$_2$Cl$_2$ (30 mL) and MeOH (3 mL) was added dropwise in 40 minutes. The initial red suspension turned into a dark red solution. The reaction was monitored by TLC and IR controls (nujol, $\nu_{C=O}$ of **90** at 1939 cm^{-1}), which revealed the presence of unreacted Ru(TPP)CO(MeOH) after 5 hours at RT. An additional amount of *m*CPBA (45 mg, 2.6×10^{-1} mmol) was added and the solution was stirred overnight. TLC and IR analysis showed the absence of the starting reagent, so the solution was washed with a sat. NaHCO$_3$ solution (50 mL×4) and purified by filtration over basic Al$_2$O$_3$ (eluent: at first CH$_2$Cl$_2$ then CH$_2$Cl$_2$/MeOH 100:4). The violet solid was re-crystallised by dissolution in 3.0 mL of CH$_2$Cl$_2$ and stratification of 20 mL of MeOH. The slow mixing (overnight) of the two solvents afforded the product as dark violet crystalline solid which was collected by filtration and dried *in vacuo* (80.5 mg, 81%).

^{1}H NMR (400 MHz, C$_6$D$_6$): δ 9.18 (8H, d, *J* = 7.5 Hz, H$_o$), 8.70 (16H, s, H$_\beta$), 7.86 (8H, t, *J* = 7.5 Hz, H$_m$), 7.60 (8H, t, *J* = 6.9 Hz, H$_p$), 7.26 (16H, m, H$_{m'}$ and H$_{o'}$), -3.22 (6H, s, CH$_3$O).

^{13}C NMR (75 MHz, C$_6$D$_6$): δ 162.6 (C), 142.4 (*C*-C$_{meso}$), 142.1 (C$_\alpha$), 136.5 (CH$_{o'}$), 136.1 (CH$_o$), 131.3 (CH$_\beta$), 127.8 (CH$_p$, overlaid with solvent signal), 126.9 (CH$_{m'}$), 126.6 (CH$_m$), 120.9 (C$_{meso}$), a signal suitable for O*C*H$_3$ moiety was not observed, however, a good correlation was detected by HSQC analysis of a CDCl$_3$ solution of [Ru(TPP)(OMe)]$_2$O between the methoxy protons signal (-3.8/-3.9 ppm in CDCl$_3$) and a spot around 49 ppm.

UV-Vis (CH$_2$Cl$_2$): λ_{max} (log ε) 408 nm (5.37), 524 nm (sh), 550 nm (4.56).

IR (ATR): 1012 cm^{-1} (oxidation marker band).

Elemental Analysis calc. for C$_{90}$H$_{62}$N$_8$O$_3$Ru$_2$: C, 71.79; H, 4.15; N, 7.44; O, 3.19; Ru, 13.43. Found: C, 70.28; H, 4.25; N, 7.18.

3.2.9. Synthesis of [Ru(TPP)(N₃)]₂O (95).
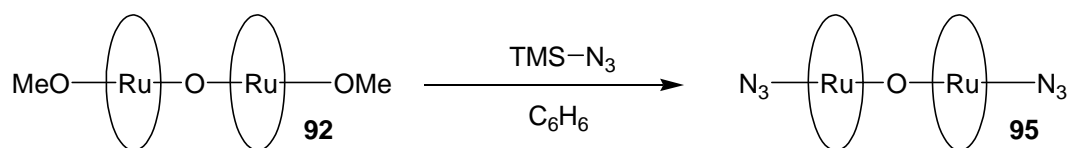
Method A: [Ru(TPP)(OMe)]₂O (**92**)(102 mg, 6.8×10^{-2} mmol) was dissolved in benzene (20 mL) and trimethylsilyl azide was added (36 µl, 2.7×10^{-1} mmol). Immediately the solution turned form dark red to dark green, the mixture was stirred for 1 hour at RT monitoring the reaction by TLC and IR analysis. The solution was evaporated to dryness then, in the air, *n*-hexane (10 mL) was added and the dark violet solid was collected by filtration and washed with *n*-hexane (10 mL) (90 mg, 87%).
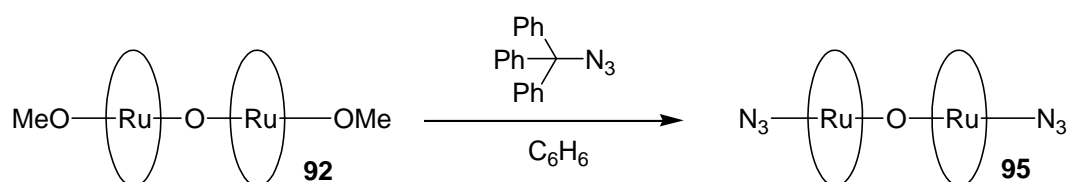
Method B: [Ru(TPP)(OMe)]₂O (**92**) (108 mg, 7.1×10^{-2} mmol) was dissolved in benzene (30 mL) and trityl azide was added (217 mg, 7.6×10^{-1} mmol). The solution was heated to reflux for 29 h and the reaction was monitored by TLC and IR analysis (a poor azide consumption was observed, $\nu_{N=N}$ = 2101 cm^{-1}). The solution was evaporated to dryness, the crude was washed with *n*-hexane (30 mL ×2) and purified by chromatography (Al₂O₃, *n*-hexane/CH₂Cl₂ 6:4). A dark violet solid was obtained (46 mg, 41%).

^{1}H NMR (300 MHz, CDCl₃): δ 8.87 (8H, d, *J* = 7.6 Hz, H$_o$), 8.65 (16H, s, H$_β$), 7.97 (8H, t, *J* = 7.6 Hz, H$_m$), 7.84 (8H, t, *J* = 7.5 Hz, H$_p$), 7.56 (8H, t, *J* = 7.5 Hz, H$_{m'}$), 7.43 (8H, d, *J* = 7.6 Hz, H$_{o'}$).

^{13}C NMR (75 MHz, CDCl₃): δ 141.69 (C$_α$), 141.22 (*C*-C$_{meso}$), 136.27 (CH$_{o'}$), 135.41 (CH$_o$), 131.78 (CH$_β$), 127.97 (CH$_p$), 127.00 (CH$_{m'}$), 126.62 (CH$_m$), 120.83 (C$_{meso}$).

UV-Vis (CH₂Cl₂): λ$_{max}$ (log ε) 280 nm (4.43), 393 nm (5.46), 554 nm (4.18), 592 nm (4.21).

IR (ATR): 2023 cm^{-1} ($\nu_{N=N}$), 1012 cm^{-1} (oxidation marker band)

Elemental Analysis calc. for C₈₈H₅₆N₁₄ORu₂: C, 69.19; H, 3.69; N, 12.84; O, 1.05; Ru, 13.23. Found: C, 69.31; H, 3.55; N, 12.47.

X-ray quality crystals were obtained by slow diffusion of a CDCl₃ solution of **95** into *n*-hexane.

3.2.10. Synthesis of [Ru(TPP)(NAr)$_2$] Ar = (CF$_3$)$_2$C$_6$H$_3$ (10).
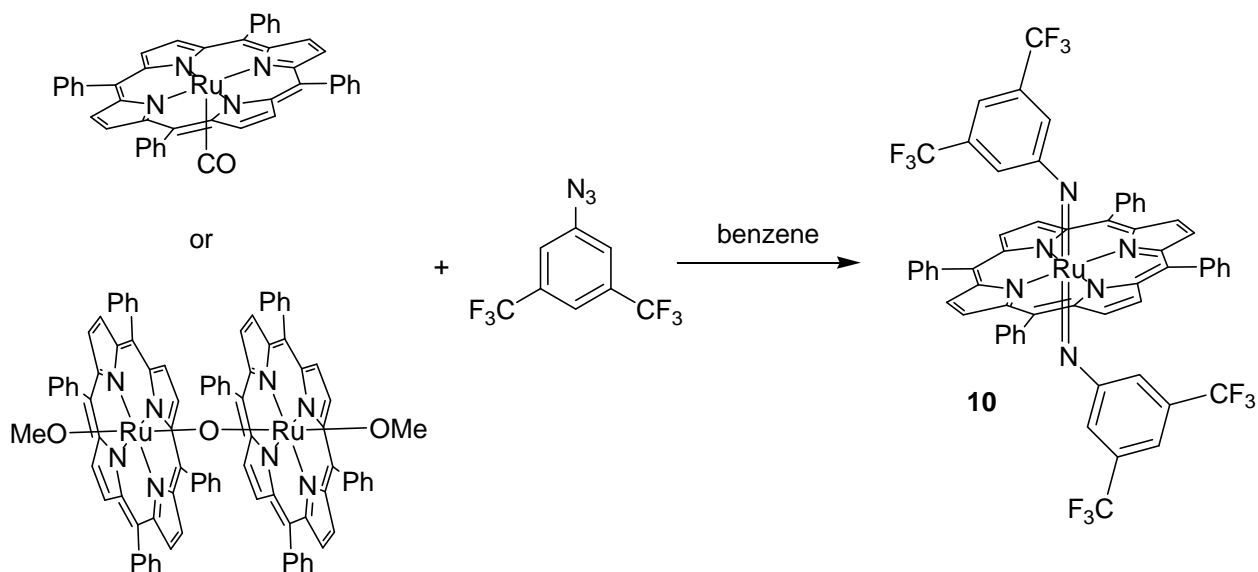
Method A: 3,5-*Bis*(trifluoromethyl)phenyl azide (368 mg, 1.4 mmol) was added to a benzene (30 mL) suspension of Ru(TPP)CO (346 mg, 4.7×10^{-1} mmol). The resulting dark mixture was refluxed for 2.5 hours observing the complete consumption of Ru(TPP)CO (TLC, *n*-hexane/CH$_2$Cl$_2$ = 7:3). The solution was concentrated to cca 5 mL and *n*-hexane (20 mL) was added. A crystalline violet solid was collected by filtration and dried *in vacuo* (381 mg, 70%).

Method B: 3,5-*Bis*(trifluoromethyl)phenyl azide (52 mg, 2.0×10^{-1} mmol) was added to a benzene (40 mL) solution of [Ru(TPP)(OCH$_3$)]$_2$O (**92**) (50 mg, 3.3×10^{-2} mmol). The red mixture was refluxed for 5.5 hours monitoring the reaction by IR ($\nu_{N=N}$ = 2116 cm^{-1}) and TLC analysis (Al$_2$O$_3$, *n*-hexane/CH$_2$Cl$_2$ 7:3), which revealed the formation of a ruthenium porphyrin species as a green spot. The dark greenish solution was evaporated and the crude was purified by chromatography (Al$_2$O$_3$, *n*-hexane/CH$_2$Cl$_2$ 9:1). A dark violet solid was obtained (50 mg, 65%).

^{1}H NMR (300 MHz, CDCl$_3$) δ 8.87 (8 H, s, H$_\beta$), 8.08 (8 H, d, *J* = 6.9 Hz, H$_o$), 7.83-7.76 (12 H, m, H$_{m-p}$), 6.60 (2 H, s, H$_{Ar}$), 2.66 (4H, s, H$_{Ar}$).

^{13}C NMR (75 MHz, CDCl$_3$) δ 151.9 (C), 142.5 (C), 141.9 (C), 134.6 (CH), 131.9 (CH), 129.7 (q, *J* = 33.2 Hz, *C*-CF$_3$), 128.4 (CH), 127.2 (CH), 123.6 (C), 122.3 (q, *J* = 271.7 Hz, *C*F$_3$), 118.1 (CH), 117.8 (CH). ^{19}F NMR (282 MHz, CDCl$_3$) δ -64.06 (CF$_3$).

IR (ATR): 1014 cm^{-1} (oxidation marker), 877 cm^{-1} (imido band).

UV-Vis (CH$_2$Cl$_2$): λ_{max} (log ε) 419 nm (5.03), 526 nm (4.00).

3.2.11. Synthesis of [Ru(T(*p*-CF₃)PP)(NAr)₂] Ar = 3,5-(CF₃)₂C₆H₃.(50).

Ar = —⟨ ⟩—CF₃
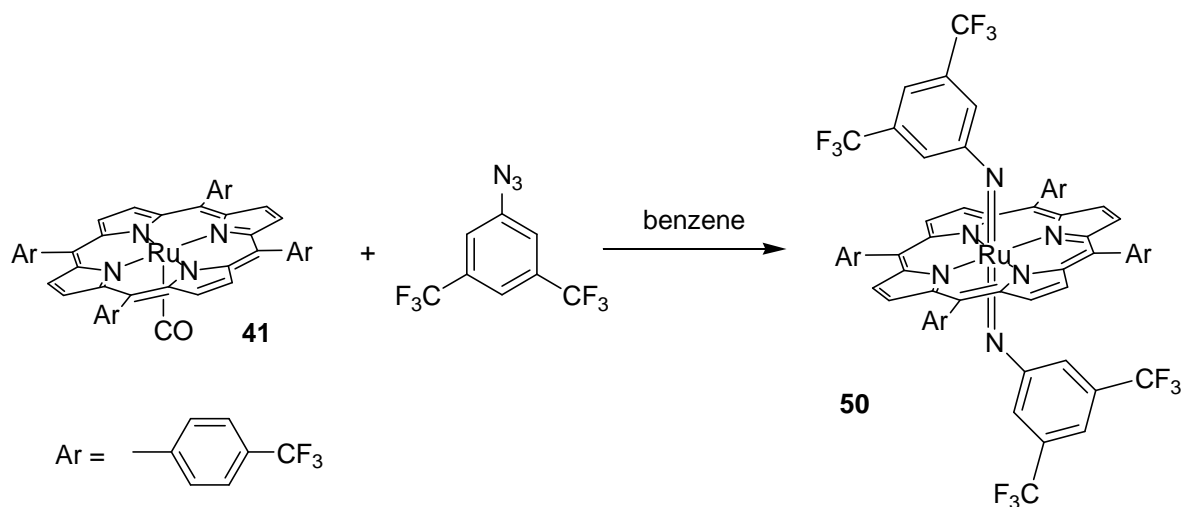
Method A: 3,5-*Bis*(trifluoromethyl)phenyl azide (42 mg, 1.7×10^{-1} mmol) was added to a benzene (30 mL) suspension of Ru(*p*-CF₃TPP)CO (**41**) (41 mg, 4.0×10^{-2} mmol). The resulting dark mixture was refluxed for 5 hours until the complete consumption of **41** (TLC, *n*-hexane/CH₂Cl₂ = 7:3). The solvent was evaporated to dryness and *n*-hexane (20 mL) was added. The precipitated dark violet solid was collected by filtration and dried in vacuum (29 mg, 50%).

^{1}H NMR (300 MHz, C₆D₆): δ 8.70 (8H, s, H$_{\beta}$), 7.98 (8H, d, J = 7.8 Hz, H$_{\text{Ar porphyrin}}$), 7.76 (8H, d, J = 8.0 Hz, H$_{\text{Ar porphyrin}}$), 6.50 (2H, s, H$_{\text{Ar}}$), 2.76 (4H, s, H$_{\text{Ar}}$).

^{13}C NMR (75 MHz, C₆D₆) 151.6 (C), 144.9 (C), 142.4 (C), 134.4 (CH$_{\text{Ar}}$), 132.2 (CH$_{\beta}$), 131.7 (CF₃), 129.9 (CF₃), 124.4 (C), 122.6 (C), 118.3 (CH), 117.8 (CH).

^{19}F NMR (282 MHz, C₆D₆) -61.67 (12F, s, CF$_{3 \text{ porphyrin}}$), -63.46 (12F, s, CF$_{3 \text{ Ar}}$).

UV-Vis (CH₂Cl₂): λ$_{\text{max}}$ (log ε) = 359 nm (4.63), 419 nm (5.24), 524 nm (3.97), 590 (3.75).

IR (ATR): 1014 cm^{-1} (oxidation marker band), 884 cm^{-1} (imido band).

MS (FAB^{+}): *m/z* 1440 [M]$^{+}$.

3.2.12. Synthesis of [Ru(TPP)(NAr)$_2$] Ar = 3,5-(NO$_2$)$_2$C$_6$H$_4$ (89).
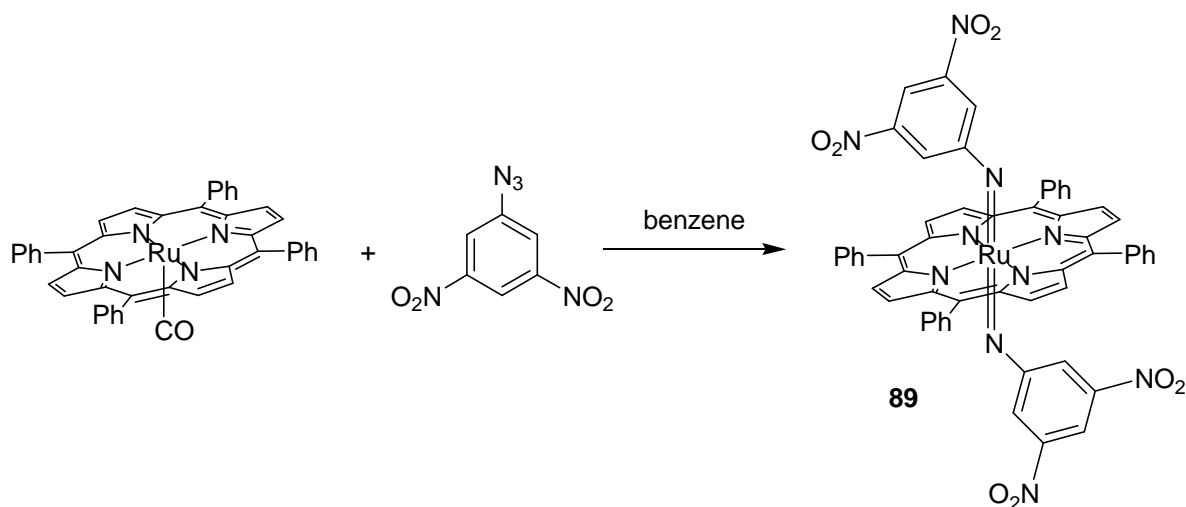
3,5-dinitrophenyl azide (70 mg, 3.3×10^{-1} mmol) was added to a benzene (25.0 mL) suspension of Ru(TPP)CO (100 mg, 1.3×10^{-1} mmol). The resulting red suspension was refluxed for 20 minutes obtaining a dark solution. The solvent was concentrated to 4.0 mL and *n*-hexane (10 mL) was added. The dark purple precipitate was collected by filtration and dried *in vacuo* (97 mg, 69%).

^{1}H NMR (300 MHz, C$_6$D$_6$) δ 8.90 (8H, s, H$_\beta$), 8.16 (8H, m, H$_{ortho\text{-phenyl}}$), 7.48 (12H, m, H$_{meta/para\text{-phenyl}}$), 7.16 (2H, overlaid with the solvent signal, H$_{Ar}$), 3.36 (4H, d, J = 1.9 Hz, H$_{Ar}$).

^{13}C NMR (75 MHz, C$_6$D$_6$): δ 152.1 (C-NO$_2$), 142.8 (C$_\alpha$), 141.5 (C), 134.7 (CH$_{ortho\text{-phenyl}}$), 132.3 (CH$_\beta$), 128.6 (CH$_{meta\text{-phenyl}}$) 127.5 (CH$_{para\text{-phenyl}}$), 124.5 (C), 117.1 (CH$_{Ar}$), 113.7 (CH$_{Ar}$).

IR (ATR): 1012 cm^{-1} (oxidation marker band) 889 cm^{-1} (imido band).

UV/Vis (benzene): λ_{max} (*log ε*) = 421 nm (5.23), 527 nm (4.16), 643 nm (3.77).

3.2.13. Synthesis of Ru(TPP)(NAr)$_2$ Ar = 4-(^{t}Bu)C$_6$H$_4$ (93).
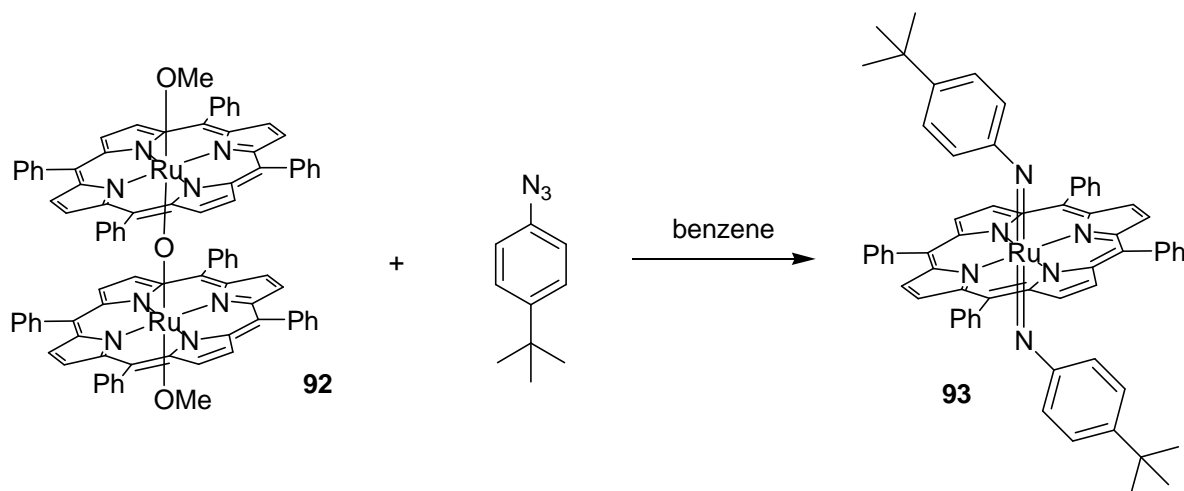
4-*Tert*-butylphenyl azide (32 mg, 1.8×10^{-1} mmol) was added to a benzene (35 mL) solution of [Ru(TPP)(OMe)]$_2$O (**92**) (42.0 mg, 2.8×10^{-2} mmol). The resulting dark mixture was refluxed for 8 hours till the complete consumption of the organic azide (IR monitoring $\nu_{N=N}$ = 2124, 2092 cm^{-1}). The solution was concentrated to 5 mL and *n*-hexane (15 mL) was added. By cooling the solution in an ice bath the formation of a violet precipitate was observed. The dark violet solid was collected by filtration and dried in vacuum.

^{1}H NMR (300 MHz, C$_6$D$_6$): δ 8.93 (8H, s, H$_\beta$), 8.12 (8H, m, H$_{ph-ortho}$), 7.47 (12H, m, H$_{ph-meta \text{ and } -para}$), 5.78 (4H, d, *J* = 8.7 Hz, H$_{Ar-meta}$), 2.77 (4H, d, *J* = 8.7 Hz, H$_{Ar-ortho}$), 0.64 (9H, s, H$_{tBu}$).

^{13}C NMR (100MHz, C$_6$D$_6$): δ 143.0 (C$_\alpha$), 134.7 (CH$_{ph-ortho}$), 131.6 (CH$_\beta$), 126.7 (CH$_{ph-meta \text{ and } -para}$), 123.1 (CH H$_{Ar-meta}$), 119.1 (CH$_{Ar-ortho}$), 30.75 (CH$_{tBu}$). A little amount of the complex decomposed during the carbon spectrum acquisition, five quaternary carbons were not detected.

IR (ATR): 2954 cm^{-1} (ν_{C-H}), 1012 cm^{-1} (oxidation marker band).

3.2.14. .Synthesis of Ru(p-CF$_3$TPP)(N(R)Ar)$_2$ (R = CH(Ph)COOMe, Ar = 3,5(CF$_3$)$_2$C$_6$H$_3$) (49).
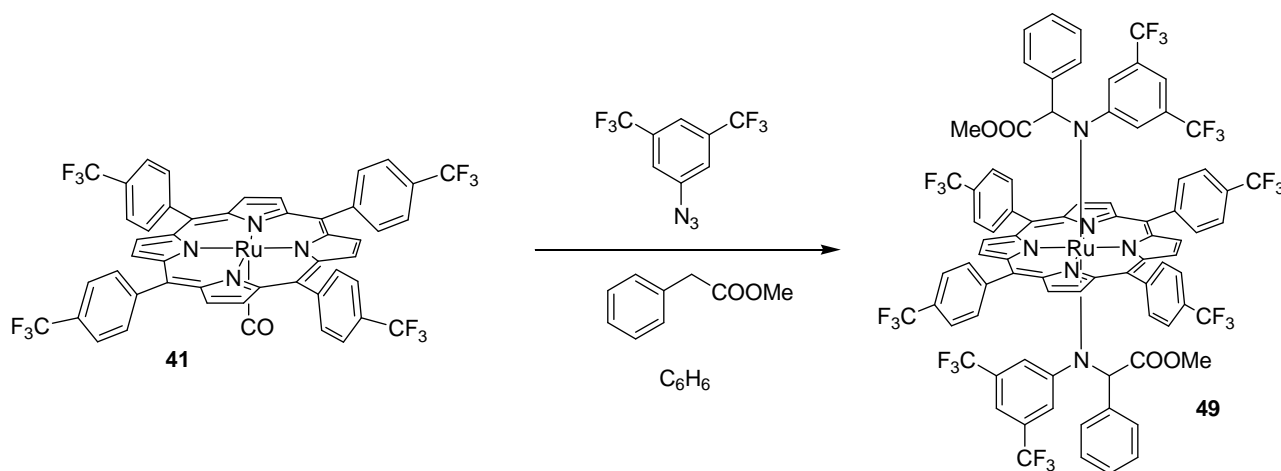
A benzene (30 mL) solution of Ru(p-CF$_3$TPP)CO (**41**) (46 mg, 5.2×10^{-2} mmol), 3,5-*bis*(trifluoromethyl)phenyl azide (141 mg, 5.5×10^{-1} mmol) and methyl phenylacetate (384 mg, 2.6 mmol) was refluxed until the complete aryl azide consumption (the reaction was monitored by IR spectroscopy, $\nu_{N=N} = 2116$ cm^{-1}). The solvent was evaporated to dryness and the residue purified by flash chromatography (silica gel, n-hexane/dichloromethane = 7:3) in 75% yield. The solid was dissolved in pentane and the solution was allowed to slowly concentrate at room temperature to give X-ray quality crystals.

^{1}H NMR (300 MHz, C$_6$D$_6$, 338 K): δ 8.40 (8H, s, H$_\beta$), 8.04 (8H, br, H$_1$), 7.75 (8H, d, J = 7.7 Hz, H$_2$), 6.93 (2H, s, H$_3$), 6.30 (2H, m, H$_4$), 6.11 (4H, m, H$_5$), 4.18 (4H, m, H$_6$), 4.11 (2H, s, H$_7$), 2.58 (3H, s, OCH$_3$), 2.52 (3H, s, OCH$_3$), 1.88 (2H, m, H$_8$), -0.88 (s, 2H, H$_9$). Proton labels reported in *Figure 30*.

^{13}C NMR (75 MHz, C$_6$D$_6$, 338 K): δ 162.9 (C=O), 158.6 (C), 145.5 (C), 144.0 (C), 134.1 (CH$_{Ar}$), 132.9 (CH$_\beta$), 131.9 (C), 131.1 (CF$_{3\ porphyrin}$), 127.4 (CH$_{Ar}$), 124.1 (CH$_{Ar}$), 121.9 (CH$_{Ar}$), 117.3 (CH$_{Ar}$), 80.2 (CH), 51.07 (OCH$_3$), 51.98 (OCH$_3$), the aryl CF$_3$ signals and three quaternary carbon sigals were not detected.

^{19}F NMR (282 MHz, C$_6$D$_6$, 338 K) -62.01 (12F, CF$_{3\ porphyrin.}$), -62.49 (6F, CF$_{3\ Ar}$), -63.07 (6F, CF$_{3\ Ar}$).

UV-Vis(CH$_2$Cl$_2$): λ_{max} (log ε) = 419 nm (5.20), 524 nm (4.53), 553 nm (4.36) sh.

IR (ATR): 1744 cm^{-1} ($\nu_{C=O}$), 1014 cm^{-1} (oxidation marker band).

MS (FAB$^+$): m/z 1362 [M – 376(R-N-Ar)]$^+$.

3.2.15. Synthesis of of Ru(*p*-CF₃TPP)(N(R)Ar)₂ (R = CH(Ph)CH₂COOMe, Ar = 3,5(CF₃)₂C₆H₃) (60).
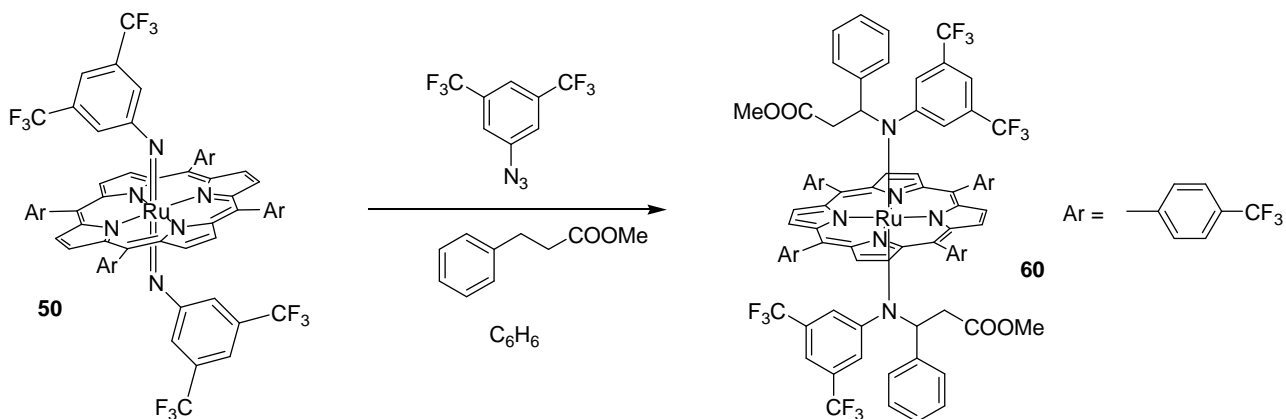
3,5-*Bis*(trifluoromethyl)phenyl azide (814.0 mg, 3.2 mmol) was added to a benzene (30 mL) solution of **50** (91 mg, 6.3×10^{-2} mmol) and methyl dihydrocinnamate (2.12 g, 13 mmol). The resulting solution was refluxed until the complete aryl azide consumption (the reaction was monitored by IR spectroscopy, $\nu_{N=N}$ = 2116 cm^{-1}). The mixture was concentrated and methyl dihydrocinnamate was removed by high vacuum distillation. The residue was purified by flash chromatography (silica gel, *n*-hexane/AcOEt = 50:1) to give a purple solid (46 mg, 30% yield).

^{1}H NMR (400 MHz, C₆D₆, 343 K): δ 8.43 (8H, m, H$_\beta$), 8.07 (8H, m, H₁), 7.75 (8H, d, *J* = 7.8 Hz, H₂), 6.97 (2H, s, H₃), 6.43 (2H, m, H₄), 6.20 (4H, m, H₅), 4.07 (4H, t, *J* = 7.6 Hz, H₆), 3.00 (1H, s, H₇), 2.95 (1H, s, H₇), 2.69 (1H, s, OCH₃), 1.89 (1H, s, H₈), 1.86 (1H, s, H₈), 0.49 (2H, m, H₉), -0.64 (2H, m, H₁₀), -1.72 (2H, d, *J* = 15.0 Hz, H₁₁). Proton labels reported in ***Figure 31***.

^{13}C NMR (75 MHz, C₆D₆, 343 K): δ 167.7 (C=O), 157.5 (C$_{Ar}$), 157.3 (C$_{Ar}$), 145.1 (C$_{Ar}$), 144.0 (C$_{Ar}$), 134.4 (CH$_{Ar}$), 133.3 (CH$_{Ar}$), 133.0 (C$_{Ar}$), 131.1 (CF₃), 127.3 (CH$_{Ar}$), 126.8 (CH$_{Ar}$), 124.2 (CH$_{Ar}$), 122.1 (CH$_{Ar}$), 119.2 (CH$_{Ar}$), 117.6 (CH$_{Ar}$), 75.2 (CH), 50.8 (OCH₃), 31.7 (CH₂), one CF₃ signal and three quaternary carbon signals were not detected.

^{19}F NMR (282 MHz, C₆D₆, 343 K): δ -62.31 (12F, s, CF$_{3\ porphyrin}$), -62.81 (12F, s, CF$_{3\ Ar}$), -63.53 (12F, s, CF$_{3\ Ar}$).

UV-Vis(CH₂Cl₂): λ_{max} (log ε) = 419 nm (5.11), 521 nm (4.32), 551 nm (4.20) sh.

IR (ATR): 1740 cm^{-1} ($\nu_{C=O}$), 1012 cm^{-1} (oxidation marker band).

MS (FAB^{+}): *m/z* 1376 [M – 390 (R-N-Ar)]$^{+}$.

Figure 30. ^{1}*H NMR spectrum of 49.*
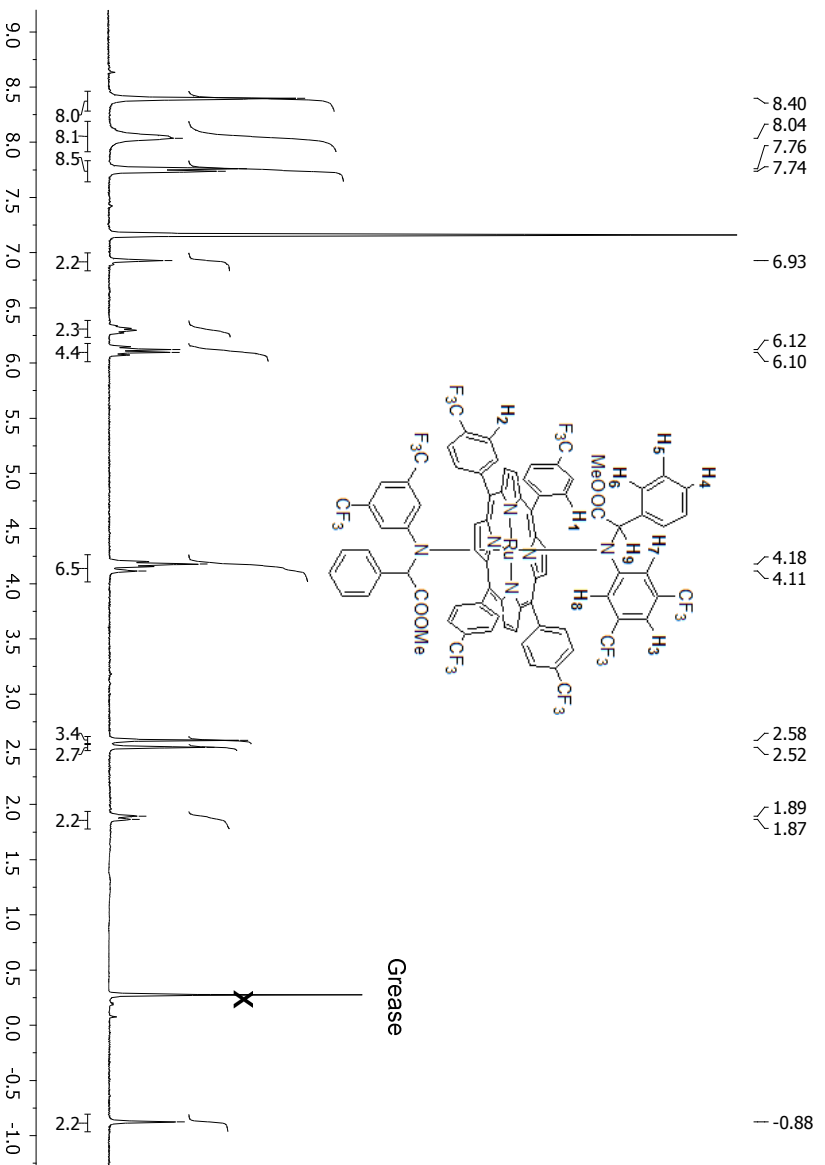
Figure 31. ^{1}*H NMR spectrum of 60.*
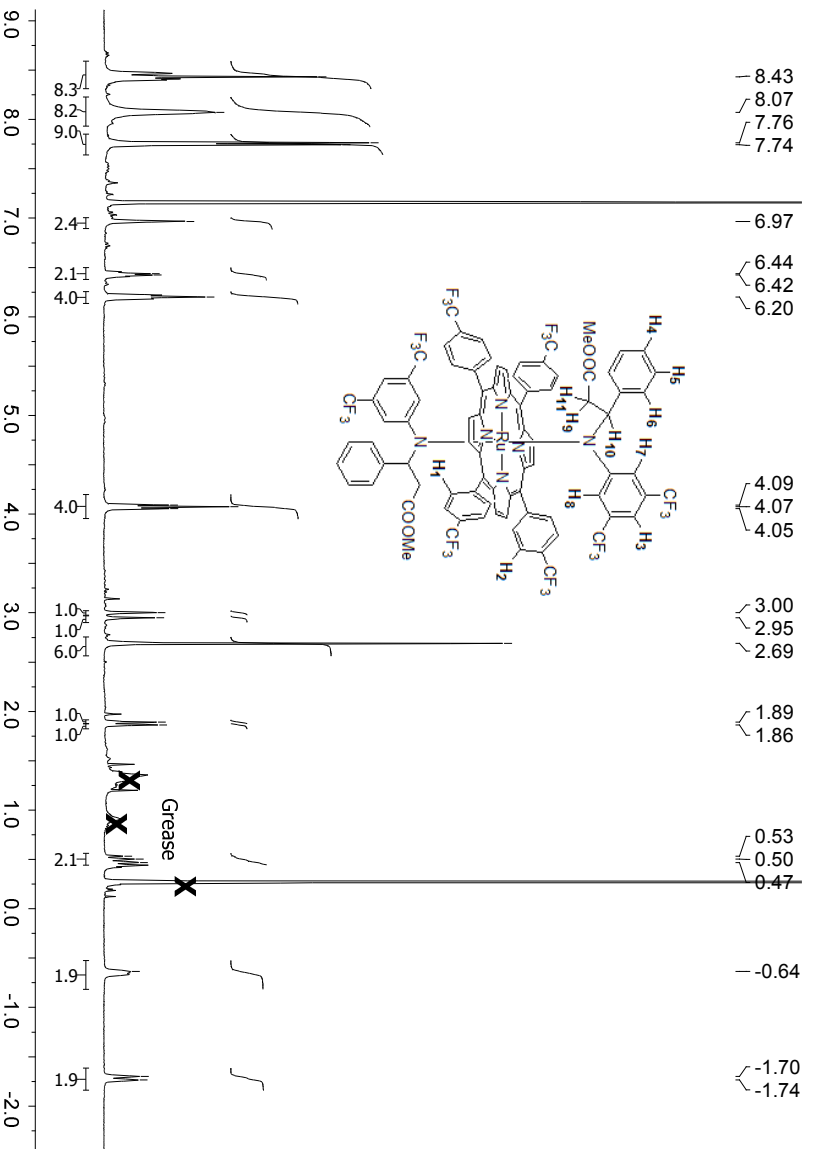
3.2.16. Synthesis of Ru-98.
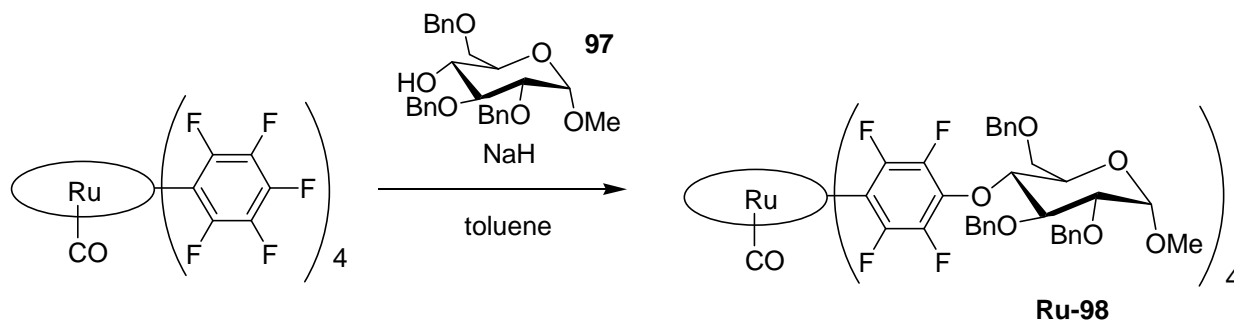
Ru(F$_{20}$TPP)CO (115 mg, 1.0×10^{-1} mmol) and monosaccharide **97** (290 mg, 6.2×10^{-1} mmol) were dissolved in toluene (14 mL), then NaH 60% (166 mg, 4.16 mmol) was added and the resulting mixture was heated to reflux in absence of light (by wrapping the Schlenk flask with an aluminum foil) for 10 hours, when the starting complex was completely consumed (TLC monitoring, SiO$_2$, *n*-hexane/AcOEt 7:3). 20 mL of HCl 0.5 M were added dropwise to quench the sodium hydride excess, CHCl$_3$ (40 mL) was added and the organic phase was washed with water (50 mL × 2) until the aqueous phase was neutral. The organic phase was dried over Na$_2$SO$_4$ and the solvent was evaporated to dryness. The crude was purified by flash chromatography (silica gel, *n*-hexane/AcOEt 7:3). The product was obtained as a dark violet solid (197 mg, 65%).

^{1}H NMR (300 MHz, CDCl$_3$): δ 8.31 (8H, br, H$_\beta$), 7.35 (60H, br, H$_{Ar}$), 5.23 (4H, d, *J* = 10.7 Hz, C(H)*H*-OBn), 4.94-4.59 (28H, m, 2C*H*$_2$-Ph, C(*H*)H-OBn, CH in position 1 and 4 of the saccharide unit), 4.42 (4H, br, CH in position 3 of the saccharide unit), 4.26 (4H, br, CH in position 5 of the saccharide unit), 4.03 (8H, br, C*H*$_2$-Ph), 3.76 (4H, br, CH in position 2 of the saccharide unit), 3.52 (12H, s, OC*H*$_3$).

^{19}F NMR (282 MHz, CDCl$_3$): δ -138.61 (4F, d, *J* = 18.3 Hz), -140.41 (4F, br), -156.65 (8F, m).

IR (ATR): 1954 cm^{-1} (ν$_{CO}$).

3.2.17. Synthesis of Ru-102.
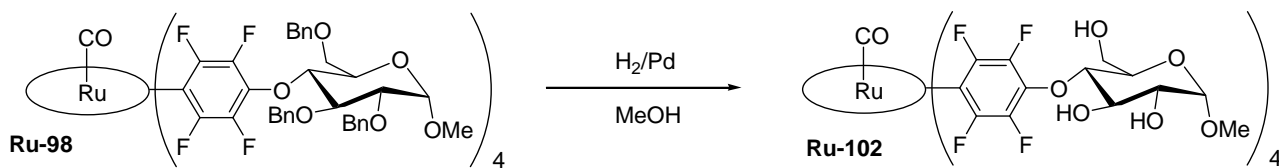
Ru-98 (90 mg, 3.1×10^{-2} mmol) was suspended in MeOH/AcOEt 1:1 (14 mL). Palladium supported over activated carbon was added and the mixture was stirred overnight under H_2 atmosphere. The resulting dark mixture was filtrated over a celite pad and the solvent was evaporated to dryness. The resulting solid was washed with chloroform (2 ml ×3) to give a violet crystalline solid (43 mg, 76%).

^{1}H NMR (400 MHz, DMSO) δ 8.86 (8H, s, H$_\beta$), 5.48 (4H, d, J = 6.4 Hz, H$_{saccharide}$), 5.16 (4H, d, J = 6.6 Hz, H$_{saccharide}$), 4.94 (4H, t, J = 5.5 Hz, H$_{saccharide}$), 4.71 (4H, d, J = 3.1 Hz, H$_{saccharide}$), 4.54 (4H, m, H$_{saccharide}$), 4.08-3.70 (20H, m, H$_{saccharide}$), 3.42 (12H, s, anomeric OCH$_3$).
^{19}F NMR (376 MHz, DMSO) δ -141.99 (s), -156.04 (s).

3.3. Iron complexes synthesis

3.3.1. Synthesis of Fe-98.

Fe-98
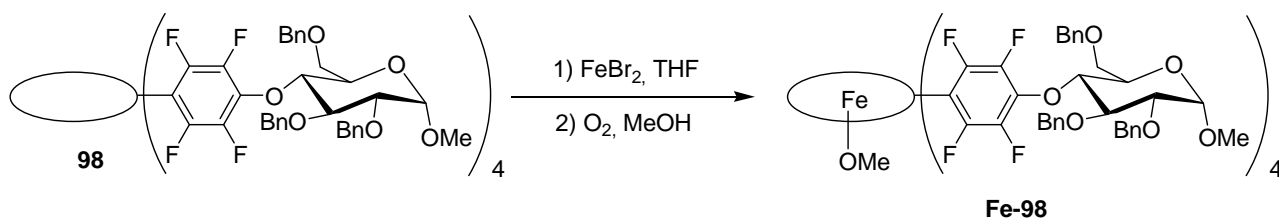
Free-base glycoporphyrin **98** (50 mg, 1.8×10^{-2} mmol) was dissolved in THF (15 mL), FeBr$_2$ (100 mg, 4.6×10^{-1} mmol) was added and the solution was refluxed for 24 hours observing the complete conversion of the starting reagent by TLC controls (SiO$_2$, CH$_2$Cl$_2$/MeOH 100:2). The solvent was evaporated, MeOH (5.0 mL) was added and the mixture was refluxed for 1 hour in the air, then the mixture was evaporated to dryness and filtered through a short alumina column using CH$_2$Cl$_2$/MeOH 100:2 as eluent. The complex fraction was evaporated to dryness giving a dark greenish solid (76%).

UV-Vis(CH$_2$Cl$_2$): λ_{max} (log ε) = 415 nm (5.03), 564 nm (4.05), 635 nm (3.40).
MS (FAB$^+$) *m/z*: 2856, 2811.

3.3.2. Synthesis of Fe 101

Fe-101
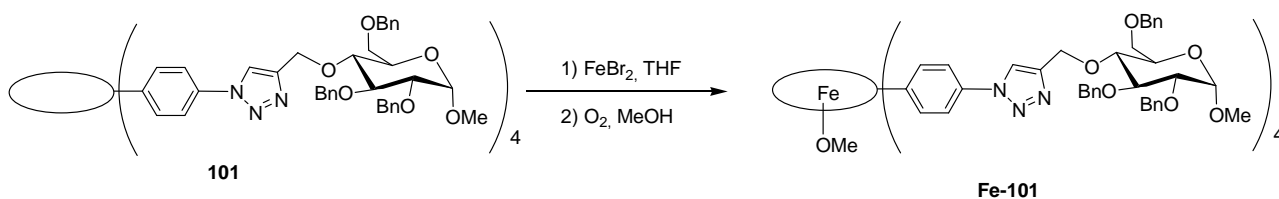
Free-base glycoporphyrin **101** (45.0 mg, 1.6×10^{-2} mmol) was dissolved in THF (10 mL), FeBr$_2$ (100 mg, 4.6×10^{-1} mmol) was added and the solution was refluxed for 24 hours observing the complete conversion of the starting reagent by TLC controls (SiO$_2$, CH$_2$Cl$_2$/MeOH 100:2). The solvent was evaporated to dryness, MeOH (5.0 mL) was added and the mixture was refluxed for 1 hour in the air, then the mixture was evaporated to dryness and filtered through a short alumina column using CH$_2$Cl$_2$/MeOH 100:2 as eluent. The complex fraction was evaporated to dryness giving a dark greenish solid (48 mg, 99%).

UV-Vis(CH$_2$Cl$_2$): λ_{max} (log ε) = 413 nm (5.46), 571 nm (3.92), 609 nm (3.68).

3.4. Organic Azide Synthesis

The azide syntheses were carried out in the air.

3.3.1. Synthesis of 4-nitrophenyl azide.
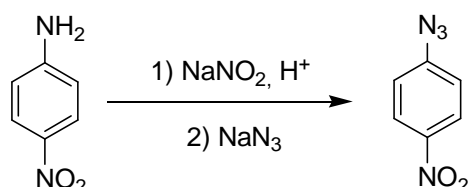
4-Nitroaniline (5.2 g, 38 mmol) was dissolved in aqueous solution of H_2SO_4 30% (75 mL). The yellow solution was placed in an ice bath and a solution of $NaNO_2$ (2.75 g, 40 mmol) in 25 mL of water was added. After 30 minutes urea (1.3 g, 22 mmol) was added in one portion to the pale yellow solution. Under vigorous magnetic stirring a solution of sodium azide (3.5 g, 54 mmol) in water (20 mL) was added to the cold mixture in about 15 minutes. The resulting yellow framing mixture was then allowed to reach room temperature and further stirred for 30 minutes. Dichloromethane (100 mL) was then added under vigorous stirring. The organic layer was collected, dried over Na_2SO_4, concentrated under reduced pressure to about 10 mL and n-hexane (150 mL) was slowly added under vigorous magnetic stirring. The so formed yellow solid was collected and dried under reduced pressure (4.3 g, 70%).

IR(nujol): 2125 cm^{-1} ($\nu_{N=N}$).
^{1}H NMR (300 MHz, C_6D_6): δ 7.62 (2H, $J = 9.1$ Hz, d), 6.15 (2H, $J = 9.1$ Hz, d).

3.4.2 Synthesis of 3,5-dinitrophenyl azide
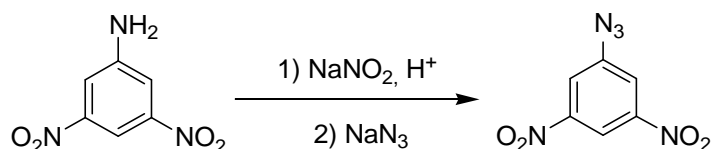
3,5-Dinitroaniline (1.58 g, 8.6 mmol) was suspended in a solution of 20 mL of H_2O and 5 mL of H_2SO_4 conc. The suspension was placed in an ice bath and a solution of $NaNO_2$ (640 mg, 9.3 mmol) in 8.0 mL of water was added dropwise. After 30 minutes urea (150 mg, 2.5 mmol) was added in

one portion. Under vigorous magnetic stirring a solution of sodium azide (688 g, 11 mmol) in water (8.0 mL) was added dropwise to the cold mixture. The resulting mixture was then allowed to reach room temperature and further stirred for 45 minutes. Dichloromethane (55 mL) was then added, the phases were separated and the inorganic layer was washed twice times with 30 mL of dichloromethane. By TLC control, an incomplete conversion of the starting 3,5-dinitroaniline was revealed, therefore, purification by chromatographic column was performed (SiO$_2$, n-hexane /AcOEt = 8:2). The product was obtained as a yellow solid (1.55 g, 86%).

IR(CH$_2$C$_2$): 2130 cm^{-1} ($\nu_{N=N}$).

^{1}H NMR (300 MHz, CDCl$_3$): δ 8.80 (1H, J = 1.9 Hz, t), 8.19 (2H, J = 1.9 Hz, d).

3.4.3 Synthesis of 3-nitrophenyl azide
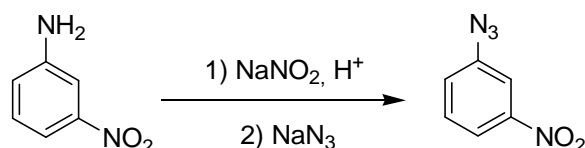
3-Nitroaniline (3.0 g, 22 mmol) was suspended in a solution of 33 mL of H$_2$O and 9.0 mL of H$_2$SO$_4$ conc. The yellow suspension was placed in an ice bath and a solution of NaNO$_2$ (2.28 g, 33 mmol) in 14 mL of water was added dropwise. After 30 minutes urea (820 mg, 14 mmol) was added in one portion. Under vigorous magnetic stirring a solution of sodium azide (2.0 g, 31 mmol) in water (8.0 mL) was added dropwise to the cold mixture. The resulting mixture was then allowed to reach room temperature and further stirred for 45 minutes. Dichloromethane (55 mL) was then added under vigorous stirring, the phases were separated and the inorganic layer was washed twice times with 30 mL of dichloromethane. The organic layers were collected, dried over Na$_2$SO$_4$, concentrated under reduced pressure to about 10 mL and n-hexane (150 mL) was slowly added. The so formed yellow solid was collected and dried under reduced pressure (2.9 g, 81%).

IR(CH$_2$C$_2$): 2122 cm^{-1} ($\nu_{N=N}$).

^{1}H NMR (300 MHz, CDCl$_3$): δ 8.00 (1H, d, J = 8.2 Hz), 7.89 (1H, t, J = 2.1 Hz), 7.54 (1H, t, J = 8.1 Hz) 7.34 (1H, J = 8.1 Hz, d).

### 3.4.4 Synthesis of 3-nitro-*p*-tolyl azide
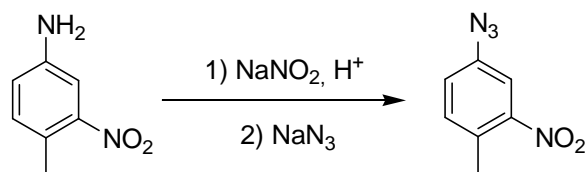
4-Methyl-3-nitroaniline (3.5 g, 23 mmol) was suspended in a solution of 35 mL of H_2O and 10 mL of H_2SO_4 conc. The yellow suspension was placed in an ice bath and a solution of $NaNO_2$ (2.42 g, 35 mmol) in 14 mL of water was added dropwise. After 30 minutes urea (870 mg, 15 mmol) was added in one portion. Under vigorous magnetic stirring a solution of sodium azide (2.1 g, 33 mmol) in water (9.0 mL) was added dropwise to the cold mixture. The resulting mixture was then allowed to reach room temperature and further stirred for 1 hour. Dichloromethane (60 mL) was then added under vigorous stirring, the phases were separated and the inorganic layer was washed twice times with 30 mL of dichloromethane. The organic layers were collected, dried over Na_2SO_4, concentrated under reduced pressure to about 10 mL and *n*-hexane (150 mL) was slowly added. The so formed yellow solid was collected and dried under reduced pressure (2.9 g, 81%).

IR(CH_2C_2): 2128 cm^{-1}, 2115 cm^{-1} ($v_{N=N}$).
^{1}H NMR (300 MHz, $CDCl_3$): δ 7.63 (1H, $J = 2.4$ Hz, d), 7.33 (1H, $J = 8.3$ Hz, d), 7.16 (1H, $J = 8.3$, 2.4 Hz, dd), 2.57 (3H, s).

3.4.5.1. Synthesis of 3,5-*bis*(trifluoromethyl)phenyl azide (38).
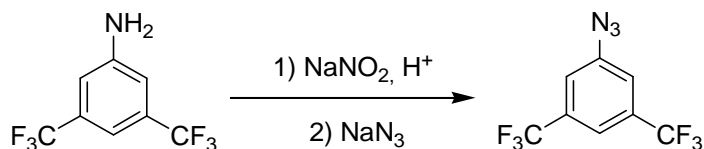
3,5-*bis*(trifluoromethyl)-aniline (3.75 mL, 24 mmol) was dissolved in a solution of 30 mL of HCl 37% and 42 mL of H_2O. The mixture was placed in an ice bath. To the white suspension was added dropwise a solution of $NaNO_2$ (2.23 g, 33 mmol) in 30 mL of water. The mixture was stirred for 30 minutes then urea (63 mg, 11 mmol) was added in one portion. Under vigorous magnetic stirring a solution of sodium azide (3.2 g, 49 mmol) in water (45 mL) was added to the cold mixture in about 15 minutes. The resulting mixture was then allowed to reach room temperature and further stirred

for 30 minutes. Diisopropyl ether (50 mL) was then added, the phases were separated and the inorganic layer was washed three times with 50 mL of diisopropyl ether. The organic phases were collected and dried over Na_2SO_4. The solvent was evaporated under reduced pressure to give a yellow oil (3.86 g, 70%).

IR(nujol): 2116 cm^{-1} ($\nu_{N=N}$).
^{1}H NMR (300 MHz, C_6D_6): δ 7.65 (1H, s), 7.14 (2H, s).

3.4.5.2. Synthesis of 3,5-*bis*(trifluoromethyl)phenyl azide-*d₃* (38-*d₃*).
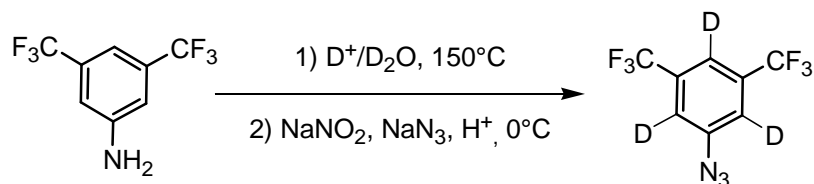
Under nitrogen atmosphere, oxalyl chloride (0.70 mL, 8.0 mmol) was added dropwise to D_2O (3.0 mL) in a pressure tube. The solution was stirred for 5 minutes and then 3,5-*bis*(trifluoromethyl)aniline (1.0 g, 4.4 mmol) was added to the mixture. The solution was heated to 150°C for 15 hours then cooled, diluted with CH_2Cl_2 (75.0 mL) and neutralised with an aqueous solution of Na_2CO_3. The organic phase was washed with brine (3×50 mL), dried with Na_2SO_4 and the solvent was removed to give a colourless oil that was directly used for the azide synthesis (*vide supra*) with two minor modifications: the acidic aqueous solution was kept at 0°C for all the reaction time and chromatographic purification (silica gel, petroleum ether) was required. The final product was obtained as a yellow oil (910 mg, 81%).

^{2}H-NMR (300 MHz, CHCl$_3$): δ 7.68 (1D, s, D$_{para}$), 7.48 (2D, s, D$_{ortho}$).

The isotopic purity was evaluated by measuring the protiated residue by ^{1}H-NMR spectroscopy using 2,4-dinitrotoluene as an internal standard (94 atom % D).

3.4.6. Synthesis of 4-(trifluoromethyl)phenyl azide
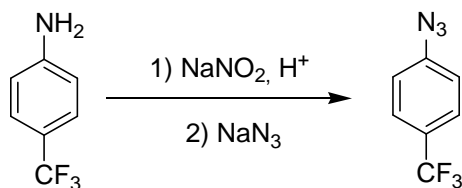
4-(trifluoromethyl)aniline (3.0 mL, 25 mmol) was dissolved in a solution of 30 mL of HCl 37% and 42 mL of H_2O. The mixture was placed in an ice bath. To the white suspension was added a solution of $NaNO_2$ (2.28 g, 33 mmol) in 30 mL of water. The mixture was stirred for 30 minutes then urea (66 mg, 11 mmol) was added in one portion. Under vigorous magnetic stirring a solution of sodium azide (3.2 g, 49 mmol) in water (45 mL) was added to the cold mixture in about 15 minutes. The resulting mixture was then allowed to reach room temperature and further stirred for 30 minutes. Diisopropyl ether (50 mL) was then added, the phases were separated and the inorganic layer was washed three times with 50 mL of diisopropyl ether. The organic phases were collected and dried over Na_2SO_4. The solvent was evaporated under reduced pressure to give a yellow oil (3.18 g, 68%).

IR(nujol): 2129 cm^{-1} ($\nu_{N=N}$).
^{1}H NMR (300 MHz, C_6D_6): δ 7.63 (2H, $J = 8.4$ Hz, d), 7.14 (2H, $J = 8.4$ Hz, d).

3.4.7 Synthesis of 3-(trifluoromethyl)phenyl azide
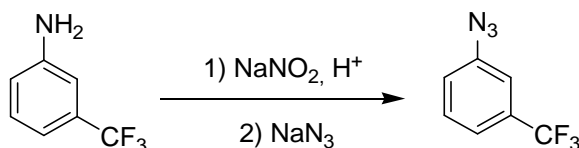
3-(trifluoromethyl)aniline (1.55 mL, 12 mmol) was dissolved in a solution of 15 mL of HCl 37% and 21 mL of H_2O. The mixture was placed in an ice bath. To the white suspension was added dropwise a solution of $NaNO_2$ (1.16 g, 17 mmol) in 15 mL of water. The mixture was stirred for 30 minutes then urea (32 mg, 5.3 mmol) was added in one portion. Under vigorous magnetic stirring a solution of sodium azide (3.2 g, 25 mmol) in water (23 mL) was added dropwise to the cold mixture. The resulting mixture was then allowed to reach room temperature and further stirred for 1

hour. Diisopropyl ether (50 mL) was then added, the phases were separated and the inorganic layer was washed twice with 25 mL of diisopropyl ether. The organic phases were collected and dried over Na_2SO_4. The solvent was evaporated under reduced pressure to give a yellow oil (2.10 g, 90%).

IR(CH_2C_2): 2112 cm^{-1} ($v_{N=N}$).
^{1}H NMR (300 MHz, CDCl$_3$): δ 7.48 (1H, J = 7.8 Hz, t), 7.40 (1H, J = 7.8 Hz, d), 7.29-7.17 (2H, m, overlaid with the solvent signal).

3.4.8. Synthesis of 4-*tert*-butyl-phenyl azide

$$Tf_2O + NaN_3 \longrightarrow TfN_3 + TfONa$$
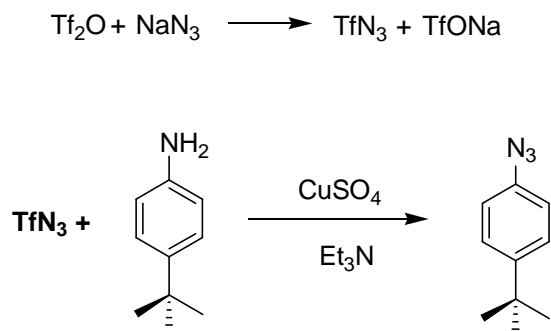
A solution of NaN$_3$ (15 g, 220 mmol), water (32 mL) and CH$_2$Cl$_2$ was cooled at 0°C. Under vigorous magnetic stirring trifluoromethanesulfonic anhydride (Tf$_2$O) (10 g, 35 mmol) was added and the mixture was further stirred for 2 hours at 0°C. Then the inorganic layer was extracted with CH$_2$Cl$_2$ (25 mL×2), washed with an aqueous solution of sat. NaHCO$_3$ (20 mL×2) and dried over Na$_2$SO$_4$.

Subsequently, to a solution of 4-tert-butylaniline (1.9 mL, 12 mmol) in CH$_2$Cl$_2$ were added 5.0 mL of Et$_3$N and a solution of CuSO$_4$ (96 mg, 3.8×10^{-1} mmol) in 2.0 mL of water. Then the solution of TfN$_3$ in CH$_2$Cl$_2$ previously prepared and 8.0 mL of MeOH were added to the reaction mixture.

The resulting mixture was stirred at room temperature for other 2 hours, aqueous sat. NaHCO$_3$ (30 mL) was added to the mixture and the inorganic layer was extracted with CH$_2$Cl$_2$ (3×30 mL). The organic phase was washed with brine and dried over NaSO$_4$. The crude was purified by flash chromatography (silica gel, petroleum ether) (1.35 g, 65%).

IR(nujol): 2123 cm^{-1}, 2092 cm^{-1} ($v_{N=N}$).
^{1}H NMR (300 MHz, C$_6$D$_6$) δ 7.39 (2H, J = 8.7 Hz, d), 6.99 (2H, J = 8.7 Hz, d), 1.34 (9H, s).

3.4.5 Synthesis of *p*-toluenesulfonyl azide
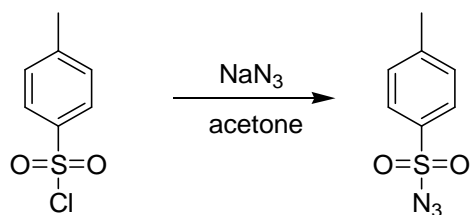
Tosyl chloride (18 g, 84 mmol) was dissolved in acetone (40 mL). The solution was placed in an ice bath and 10 mL of an aqueous solution of NaN$_3$ (6.5 g, 110 mmol) were added dropwise. The mixture was stirred for 2 hours. Ethyl ether (20 mL) was added to the reaction mixture and the inorganic layer was washed with ethyl ether (2×20 mL). The organic phases were collected and dried over Na$_2$SO$_4$. The solvent was evaporated under reduced pressure to give a white oil (16 g, 86%).

IR(CH$_2$Cl$_2$): 2123 cm^{-1} ($\nu_{N=N}$).

^{1}H NMR (300 MHz, C$_6$D$_6$): δ 7.72 (2H, J = 8.0 Hz, d), 6.67 (2H, J = 8.0 Hz, d), 2.32 (3H, s).

3.4.6 Synthesis of 4-nitrobenzenesulfonyl azide
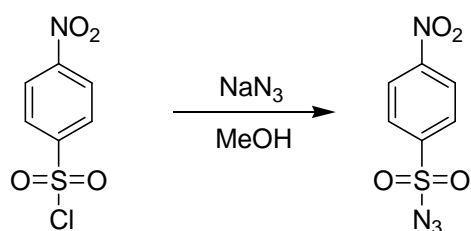
4-Nosyl chloride was dissolved in MeOH (50 mL) and 20 mL of an aqueous solution of NaN$_3$ (1.9 g, 29 mmol) were added dropwise. The resulting mixture was stirred for 90 minutes. Ethyl ether (30 mL) was added to the reaction mixture and the inorganic layer was washed with ethyl ether (2×30 mL). The organic phases were collected, dried over Na$_2$SO$_4$ and concentrated until a precipitation was observed, then 20 mL of n-hexane were added. The mixture was cooled at 4°C and the yellow solid was filtered and dried under vacuum (4.5 g, 88%).

^{1}H NMR (300 MHz, CDCl$_3$): δ 8.49 (2H, J = 8.8 Hz, d), 8.19 (2H, J = 8.8 Hz, d).

3.5. Synthesis of the Ester Substrates.

3.5.1. Synthesis of methyl dihydrocinnamate
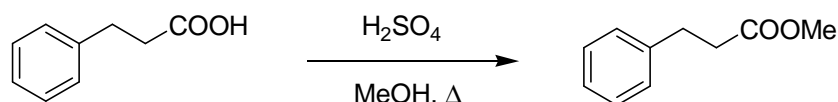
The reaction was performed in the air. Dihydrocinnamic acid (12.3 g, 82 mmol) was dissolved in methanol (125 mL) and sulfuric acid (5.0 mL, 94 mmol) was added. The resulting solution was refluxed for 15 hours then Na_2CO_3 (10.0 g, 94 mmol) was added in order to neutralise the sulfuric acid excess. The solvent was evaporated, then ethyl acetate (100 mL) was added. The so-obtained suspension was filtered, the solution was washed with an aqueous solution of $NaHCO_3$ 2.5% (3×50 mL), dried over Na_2SO_4 and evaporated to dryness to give a pale-yellow oil (12.6 g, 93%).

^{1}H NMR (400 MHz, CDCl$_3$): δ 7.33-7.18 (5H, m), 3.68 (3H, s), 2.97 (2H, J = 7.8 Hz, t), 2.65 (2H, J = 7.8 Hz, t).

3.5.2. Synthesis of silyl ketene acetal 61.
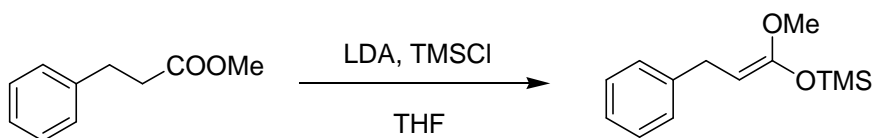
The reaction was performed following a reported procedure.[149] Diisopropylamine (5.0 mL, 36 mmol) was dissolved in anhydrous THF and cooled to 0°C. 18.0 mL of a butyllithium solution (1.84 M in *n*-hexane) were added drowise, the solution was stirred at 0°C for 10 minutes then it was cooled to -80°C using a liquid nitrogen/acetone bath. An anhydrous THF solution of dihydrocinnammate (4.50 g, 27 mmol) and trimethylsilyl chloride (5.0 mL, 39 mmol) was added dropwise in 40 minutes.

The solution was allowed to reach room temperature and stirred for 3 hours during which the precipitation of a white solid (LiCl) was observed. The solvent was evaporated and *n*-hexane (100 mL) was added, the suspension was filtered and evaporated to dryness to give a pale yellow oil (6.5 g, 99%).

^{1}H NMR (400 MHz, CDCl$_3$): δ 7.32-7.13 (5H, m), 3.89 (1H, J = 7.4 Hz, t), 3.57 (3H, s), 3.35 (2H, J = 7.5 Hz, d), 0.26 (9H, s). Traces of the E stereoisomer were observed (methoxy signal at 3.54 ppm).
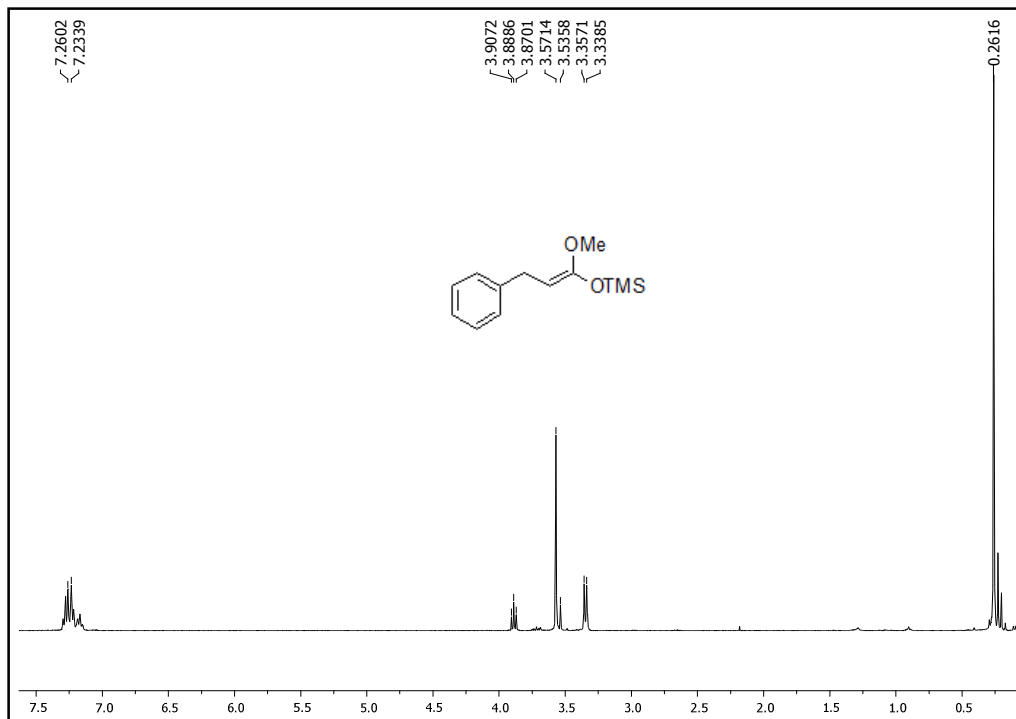
Figure 32. ^{1}H NMR spectrum of silyl ketene acetal **61**.

3.5.3. Synthesis of methyl L-3-phenyllactate from L-phenylalanine.
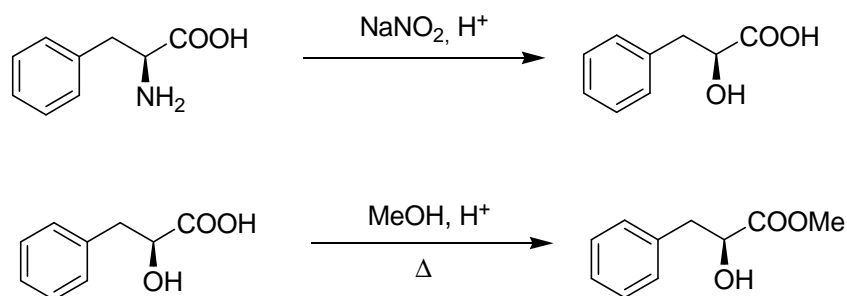
1) Synthesis of L-3-phenyllactic acid

The reaction was performed in the air following a reported procedure.[150] Phenylalanine (10.3 g, 62 mmol) was dissolved in H$_2$SO$_4$ 0.5 M (125 mL) and placed in an ice bath. An aqueous solution (25 mL) of NaNO$_2$ (7.14 g, 64 mmol) was added dropwise then the mixture was allowed to reach room temperature and stirred for 3 hours. The so-obtained suspension was extracted with ethyl acetate

137

(3×100 mL) and washed with brine (3×100 mL). The organic phase was dried over Na_2SO_4 and evaporated to dryness to give a white solid (7.91 g, 76%).

^{1}H NMR (300 MHz, $CDCl_3$): δ 7.37-7.23 (5H, m), 4.53 (1H, J = 7.2 Hz, J = 4.3 Hz, dd), 3.22 (1H, J = 14.0 Hz, J = 4.3 Hz, dd), 3.01 (1H, J = 14.0 Hz, J = 7.2 Hz, dd). OH and COOH signals were not detected.

1) Synthesis of Methyl L-3-phenyllactate

The reaction was performed in the air. 3-L-phenyllactic acid (7.91 g, 48 mmol) was dissolved in methanol (120 mL) and sulfuric acid (3.0 mL, 54 mmol) was added. The resulting solution was refluxed for 4 hours then Na_2CO_3 (5.67 g, 54 mmol) was added in order to neutralise the sulfuric acid excess. The solvent was evaporated, then ethyl acetate (100 mL) was added. The so-obtained suspension was filtered, the solution was washed with brine (3×50 mL), dried over Na_2SO_4 and evaporated to dryness to a yellow oil that became a whitish solid after drying in vacuum (6.87 g, 80%).

^{1}H NMR (300 MHz, $CDCl_3$): δ 7.34-7.18 (5H, m), 4.46 (1H, J = 6.6 Hz, J = 4.5 Hz, dd), 3.78 (3H, s), 3.13 (1H, J = 13.9 Hz, J = 4.4 Hz, dd), 2.97 (1H, J = 13.9 Hz, J = 6.8 Hz, dd), 2.68 (1H, br).

3.5.4. Synthesis of (2*S*)-methyl 3-phenyl-2-acetoxy-propanoate
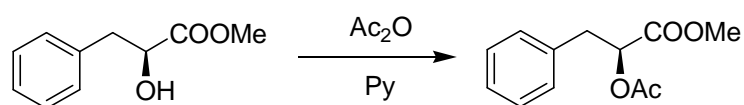
The reaction was performed in the air. Methyl 3-L-phenyllactate (2.78 g, 15 mmol) was dissolved in pyridine (30 mL) then acetic anhydride (1.9 mL, 20 mmol) was added. The solution was stirred at room temperature for 24 hours. 300 mL of a HCl 1M aqueous solution were added and the resulting mixture was extracted with diisopropyl ether (3×150 mL). The organic phases were collected, washed with brine (3×150 mL), dried over Na_2SO_4 and evaporated to dryness. The crude was purified by flash chromatography (silica gel, *n*-hexane/AcOEt 8:2) obtaining a colourless oil (3.04 g, 89%).

^{1}H NMR (300 MHz, CDCl$_3$): δ 7.34-7.18 (5H, m), 5.22 (1H, J = 8.6 Hz, J = 4.6 Hz, dd), 3.72 (3H, s), 3.18 (1H, J = 14.2 Hz, J = 4.6 Hz, dd), 3.08 (1H, J = 14.2 Hz, J = 8.6 Hz, dd), 2.08 (3H, s).

3.5.5. Synthesis of (2*S*)-methyl 3-phenyl-2-methoxy-propanoate
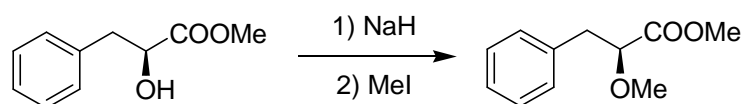
The reaction was performed following a reported procedure[150]. Methyl 3-L-phenyllactate (1.99 g, 11 mmol) was dissolved in anhydrous THF (30 mL) and sodium hydride 60% (0.498 g, 12 mmol) was added. The resulting mixture was heated to 50°C, then methyl iodide (1.1 mL, 18 mmol) was added dropwise and the mixture was stirred for 3 hours, observing the precipitation of a white solid. The reaction was quenched by addition of a small amount of water, ethyl acetate (100 mL) was added and the organic phase was washed with water (2×50 mL) and brine (2×50 mL), dried over Na$_2$SO$_4$ and evaporated to dryness. The crude was purified by flash chromatography (silica gel, *n*-hexane /AcOEt 9:1) obtaining a colourless oil (1.92 g, 90%).

^{1}H NMR (300 MHz, CDCl$_3$): δ 7.34-7.18 (5H, m), 3.98 (1H, J = 7.5 Hz, J = 5.4 Hz, dd), 3.72 (3H, s), 3.35 (3H, s), 3.02 (2H, m).

3.6. General procedure for catalytic amination reaction

Here the standard procedure for catalytic amination reactions is described, the nature and the amount of catalysts and reagents along with the experimental conditions are reported in each section.

All the catalytic reactions were monitored by IR spectroscopy by measuring the characteristic ν(N=N) signal absorbance in the range 2095–2130 cm^{-1}. Unless otherwise specified, a full conversion of the aryl azide was reached in every experiment (the reaction was considered to be finished when azide absorbance was below 0.006 using a 0.1 mm thick cell). The yield in the desired product was evaluated by ^{1}H NMR analysis using 2,4-dinitrotoluene as the internal standard unless "isolated yield" is clearly specified. In case the organic product was a new compound, it was isolated by flash chromatography on silica gel using *n*-hexane/ethyl acetate as eluent mixture and fully characterised.

General experiment: In a typical run, the catalyst and the substrate were suspended/dissolved in the solvent and a blank IR spectrum of the mixture was recorded. The organic azide was added and the initial absorbance value of the characteristic IR signal of the azide was registered. The mixture was heated to the desired temperature (generally solvent boiling temperature) by using a preheated oil bath. The organic azide conversion was monitored by IR spectroscopy and the reaction was followed by TLC and GC-MS analysis. Finally, the solution was concentrated to dryness and the residue was analysed by ^{1}H NMR spectroscopy.

3.7. Dihydronaphthalene amination catalysed by Co-porphyrins
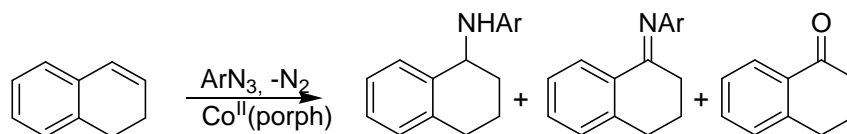
3.7.1. Catalytic Reaction Conditions: The general procedure for amination reactions was followed. Catalyst amount = 1.1×10^{-2} mmol, azide amount = 1.3×10^{-1} mmol, substrate: dihydronaphthalene (2.5 mL, 19 mmol), catalyst/azide ratio = 4:50, solvent: dihydronaphthalene (2,5 mL) and 1,2-dichloroethane (2.5 mL). T = 75°C.

Chromatographic purification conditions: silica gel, *n*-hexane/ethyl acetate = 50:1

3.7.2. Blank Reaction: *p*-Nitrophenyl azide (22 mg, 134 mmol) was dissolved in a dihydronaphthalene/1,2-dichloroethane 1:1 mixture (5 mL). The solution was heated at 75°C for 4 hours. The solvent was evaporated to dryness and the crude was purified by flash chromatography using *n*-hexane/ethyl acetate = 50:1 as eluent.

3.7.3. Characterisation for new compounds

a) 4-(1,2,3,4-tetrahydronaphthalen-1-ylamino)benzonitrile
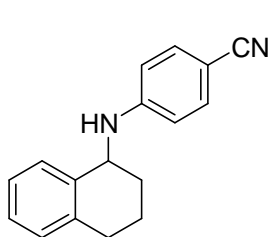
^{1}H NMR (400 MHz, CDCl$_3$): δ 7.46 (d, 2H, *J* = 8.7 Hz), 7.33 (dphic , 1H, *J* = 7.6 Hz), 7.27-7.17 (m, 3H,), 6.66 (d, 2H, *J* = 8.7 Hz), 4.73-4.68 (m, 1H), 4.66 (d, 1H, *J* = 6.4 Hz, N*H*), 2.93-2.77 (m, 2H), 2.07-1.96 (m, 2H,), 1.94-1.85 (m, 2H). ^{13}C NMR (100 MHz; CDCl$_3$) δ: 150.4 (CN), 137.7 (C), 136.6 (C), 133.9 (2 CH), 129.3 (CH), 129.0 (CH), 127.7 (CH), 126.3 (CH), 120.4 (C), 112.3 (2 CH), 98.6 (C), 50.7 (CH), 29.1 (CH$_2$), 28.6 (CH$_2$), 19.4 (CH$_2$). Anal. Calcd for C$_{17}$H$_{16}$N$_2$ C, 82.22; H, 6.49; N, 11.28. Found C, 82.30; H, 6.54; N, 10.97

b) *N*-(3,4-dihydronaphthalen-4(1*H*)-ylidene)-4-nitrobenzenamine
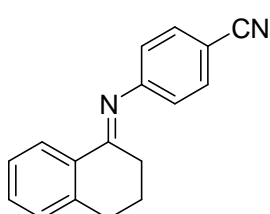
^{1}H NMR (300 MHz, CDCl$_3$): δ 8.28 (d, 1H, *J* = 7.6 Hz), 7.64 (d, 2H, *J* = 8.6 Hz), 7.45-7.40 (m, 1H), 7.34 (d, 1H, *J* = 7.6 Hz), 7.26-7.23 (m, 1H), 6.88 (d, 2H, *J* = 8.6 Hz), 2.94 (pst, 2H, *J* = 6.1 Hz), 2.49 (pst, 2H, *J* = 6.1 Hz), 2.01-1.93 (m, 2H). ^{13}C NMR (75 MHz; CDCl$_3$) δ: 166.7 (C), 156.4 (CN), 142.1

(C), 133.7 (2 CH), 133.4 (C), 131.7 (CH), 129.3 (CH), 127.0 (CH), 126.9 (CH), 120.5 (2 CH), 119.8 (C), 106.6 (C), 30.7 (CH$_2$), 30.2 (CH$_2$), 23.6 (CH$_2$). Anal. Calcd for C$_{17}$H$_{14}$N$_2$ C, 82.90; H, 5.73; N, 11.37. Found C, 83.15; H, 5.85; N, 10.95

c) *N*-(4-tert-butylphenyl)-1,2,3,4-tetrahydronaphthalen-1-amine
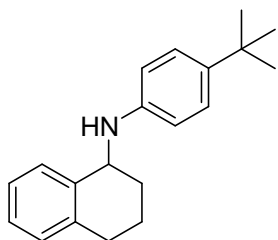
^{1}H NMR (400 MHz, CDCl$_3$): δ 7.47 (d, 1H, *J* = 6.8 Hz), 7.30 (d, 2H, *J* = 8.7 Hz), 7.25-7.22 (m, 2H), 7.20-7.18 (m, 1H), 6.70 (d, 2H, *J* = 8.7 Hz), 4.67 (m, 1H), 3.85 (bs, 1H, N*H*), 2.94-2.78 (m, 2H), 2.05-1.82 (m, 4H), 1.37 (s, 9H, ^{t}Bu). ^{13}C NMR (100 MHz; CDCl$_3$) δ: 145.1 (C), 139.9 (C), 138.4 (C), 137.7 (C), 129.4 (CH), 129.0 (CH), 127.1 (CH), 126.2 (2 CH), 126.1 (CH), 112.5 (2 CH), 51.2 (CH), 31.6 (CH$_3$), 29.4 (CH$_2$), 28.8 (CH$_2$),19.4 (CH$_2$). Anal. Calcd for C$_{20}$H$_{25}$N C, 85.97; H, 9.02; N, 5.01. Found C, 86.21; H, 9.17; N, 5.31.

d) 3,5-*bis*(trifluoromethyl)-*N*-(2,3-dihydronaphthalen-4(1*H*)-ylidene)benzenamine
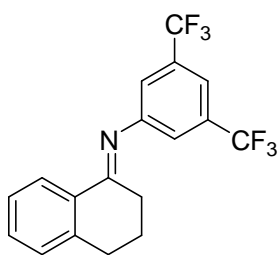
^{1}H NMR (400 MHz, CDCl$_3$): δ 8.29 (d, 1H, *J* = 7.9 Hz), 7.60 (s, 1H), 7.46-7.42 (m, 1H), 7.36-7.32 (m, 1H), 7.26-7.25 (m, 3H), 2.96 (pst, 2H, *J* = 6.1 Hz), 2.52 (pst, 2H, *J* = 6.1 Hz), 2.03-1.96 (m, 2H). ^{13}C NMR (100 MHz; CDCl$_3$) δ: 167.8 (C), 152.9 (C), 141.8 (C), 132.9 (C), 132.4 (q, *J* = 131 Hz, 2 *C*CF$_3$), 131.5 (CH), 128.9 (CH), 126.7 (CH), 126.6 (CH), 123.5 (*J* = 270 Hz, q, 2 CF$_3$), 119.9 (2 CH), 116.5 (CH), 30.3 (CH$_2$), 29.8 (CH$_2$), 22.8 (CH$_2$). ^{19}F NMR (282 MHz, CDCl$_3$) δ: -63.2. Anal. Calcd for C$_{18}$H$_{13}$F$_6$N C, 60.51; H, 3.67; N, 3.92. Found C, 60.87; H, 3.91; N, 3.78.

e) 3,4-dihydro-*N*-4-nosylnaphthalen-1(2*H*)-imine
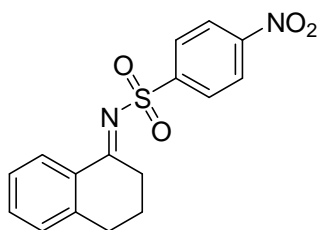
^{1}H NMR (300 MHz, CDCl$_3$): δ 8.42 (d, 2H, *J* = 8.9 Hz), 8.26 (d, 2H, *J* = 8.9 Hz), 8.04 (d, 1H, *J* = 7.3 Hz), 7.51 (pst, 1H, *J* = 7.3 Hz), 7.28-7.24 (m, 2H), 3.46 (pst, 2H, *J* = 6.1 Hz), 2.95 (pst, 2H, *J* = 6.1 Hz), 2.19-2.06 (m, 2H). ^{13}C NMR (100 MHz; CDCl$_3$) δ: 134.8 (CH), 129.6 (CH), 128.6 (2 CH), 128.1 (CH), 127.3 (CH), 124.5 (2 CH), 34.1 (CH$_2$), 29.7 (CH$_2$), 22.8 (CH$_2$), (quaternary carbons were not detected). Anal. Calcd for C$_{16}$H$_{14}$N$_2$O$_4$S C, 58.17; H, 4.27; N, 8.48. Found C, 58.44; H, 4.42; N, 8.22.

f) 3,4-dihydro-*N*-tosylnaphthalen-1(2*H*)-imine
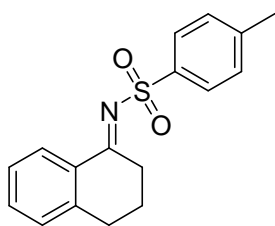
^{1}H NMR (300 MHz, C$_6$D$_6$) δ: 7.88 (d, 2H, *J* = 9.0 Hz), 7.16-7.00 (m, 9H), 5.83 (d, 2H, *J* = 9.0 Hz), 4.56 (s, 1H, N*H*), 2.70-2.64 (m, 2H), 2.03-1.97 (m, 2H), 1.47-1.34 (m, 2H). ^{13}C NMR (75 MHz, C$_6$D$_6$) δ: 150.7 (C), 146.9 (C), 139.1 (C), 139.0 (C), 137.9 (C), 63.3 (C), 129.8 (CH), 129.5 (CH), 129.1 (CH), 128.9 (CH), 128.1 (CH), 127.7 (CH), 127.1 (CH), 126.9 (CH), 126.8 (CH), 125.7 (2 CH), 114.4 (2 CH), 42.1 (CH$_2$), 30.3 (CH$_2$), 20.0 (CH$_2$). Anal. Calcd for C$_{22}$H$_{20}$N$_2$O$_2$ C, 76.72; H, 5.85; N, 8.13. Found C, 76.98; H, 6.03; N, 7.94.

3.8. Resonance Raman Mechanistic Study of Allylic Amination Catalysed by Ruthenium-Porphyrins

3.8.1. General Conditions

All the Raman experiments were performed using the instrumental set showed in *Figure 33*. A laser source of 405 nm was chosen since its frequency is close to the Soret band of ruthenium porphyrin complexes (λ_{max} = 418 nm in the case of Ru(TPP)CO). An etalon filter was placed after the laser source to get a sharp laser beam with a 1 nm width at half maximum. This was necessary in order to avoid broad peaks in the final spectrum, however it caused a slight shift of the laser maximum frequency, which had to be measured every time before starting the experiment. The laser power was reduced to 4 mV through a 0.3A filter to prevent decomposition of sample at high laser power (e.g. photolysis of the ruthenium-carbonyl bond[120]). The diameter of the laser beam was expanded using a Keplerian telescope and directed toward the cell which contained the sample.

Figure 33. Instrument scheme.

An objective lens focused the radiation into the cell, than the Raman scattered radiation was isolated using a series of dichroic mirrors and sent to a Czerny Turner Spectrograph. A charge-coupled device (CCD) was used as detector, it was cooled to about -80°C to minimize the instrument noise. The spectra were recorded as function of wavelength (nm), the conversion of the wavelength in the Raman shift (cm^{-1}) was performed using the following formula:

$$\Delta\tilde{\upsilon}(cm^{-1}) = 10^7 \times \left(\frac{1}{laser\ frequency(nm)} + \frac{1}{\lambda(nm)} \right)$$

The cell used in each experiment was an aluminum vessel with a window over which a cover glass could be placed and used to ensure an optical contact with the objective lens. This cell could be opened to load the sample and hermetically closed using a Viton o-ring as gasket. The cell was tested and showed itself to be resistant when it was charged with benzene and heated up to 80°C (nominal temperature) on a heating plate.

Reference spectra of Ru(TPP)CO, *bis*-imido complex **10** and [Ru(TPP)(OCH$_3$)]$_2$O were recorded from freshly prepared solutions in benzene (10^{-3} M).

3.8.2. Aniline coordination experiment

Ru(TPP)CO (5.0 mg, 6.7×10^{-3} mmol) was suspended in benzene (5 mL) and 3,5-*bis*(trifluoromethyl)aniline (**37**) (4.2 µL, 2.7×10^{-2} mmol) were added. The mixture was stirred until it turned into a red solution, then a sample (cca 0.5 mL) was placed in the cell and analysed by Raman spectroscopy. The spectrum was compatible with the one obtained by dissolving the aniline complex [Ru(TPP)CO(**37**)] in benzene. The latter complex was synthesised by using a known procedure.[66]

3.8.3. Azide coordination experiment

Under nitrogen atmosphere, Ru(TPP)CO (1.8 mg, 6.7×10^{-3} mmol) was suspended in benzene (2 mL) then 3,5-*bis*(trifluoromethyl)phenyl azide (**38**) (12.6 mg, 4.9×10^{-2} mmol) was added noticing a slight color change from orange/red to red-brown. A sample (about 0.5 mL) of the mixture was loaded in the cell and the Raman spectrum of the resulting mixture was recorded.

3.8.4. Spectra of the allylic amine(103):
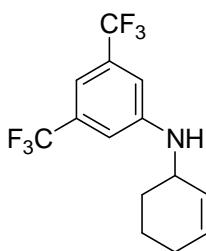
Figure 34. *Allylic amine 103.*

Compound **103** is the product of the Ru(TPP)CO allylic amination of cyclohexene using aryl azide **38**. This experiment proved that this compound is responsible for the increasing fluorescence observed in the catalytic reaction spectra. The Raman spectrum of a 5×10^{-3} M benzene solution of **103** was recorded but no signal was detected. The spectrum was recorded again in the presence of a small amount of Ru(TPP)CO (cca 10^{-3} M) and a strong fluorescence centered around 440 nm appeared beside the porphyrin complex signals.

/

3.8.5. General procedure for catalytic experiments.

A 2.5×10^{-4} M Ru(TPP)CO solution in a cyclohexene/benzene mixture (in which [cyclohexene] = 0.125 M) or in cyclohexene was prepared under nitrogen atmosphere. Then the flask was moved into a dry box were aryl azide **38** (13 mg, 5.0×10^{-2} mmol) was added to the reaction mixture and a small amount (0.5 mL) of the resulting solution was transferred into the cell. The cell was closed, removed from the drybox and placed on a heating plate (pre-heated at 70°C, nominal temperature) where the cover glass was in optical contact with the objective lens of the instrument.

The acquisition was performed by continuously recording the Raman spectra of the catalytic mixture for 2-4 hours using an integration time of 30 seconds.

Complex	Oxidation marker band (cm^{-1})	Coordinated aryl band (cm^{-1})
Ru(TPP)CO	1355	-
Ru(TPP)(NAr) (**10**)	1359	1023
[Ru(TPP)(OCH3)]$_2$O (**92)**	1362	-
[Ru(TPP)CO(**37**)]	1351	1015
Ru(TPP)CO + **38**	1351	-

Table 11. *Raman shift f the main signal of the employed Ru(porph complexes.)*

3.9. Mechanistic Insights of the Ru(Porph)-Catalysed Aziridination of α-Methyl Styrene by Aryl Azides

General procedure for the kinetic experiments: the catalyst (0.012 mmol, 2% with respect to aryl azide), the aryl azide (0.60 mmol) and α-methylstyrene were added to benzene in a Schlenk flask (total volume = 30 mL) under N_2. The resulting solution was immediately placed in a preheated oil bath at 75 °C. The solution was stirred for one minute to completely dissolve all reagents and then 0.2 mL were withdrawn for IR analysis at regular time intervals. The consumption of the azide was then followed by measuring the absorbance (A) of the $\nu_{(N=N)}$ signal at 2150-2100 cm^{-1}. Rate constants with respect to the aryl azide for each catalyst were determined from the specific variation of A with respect to time.

3.9.1. Determination of the kinetic order in 4-nitrophenyl azide concentration using different Ru(T(*p*-X)PP)CO catalysts.
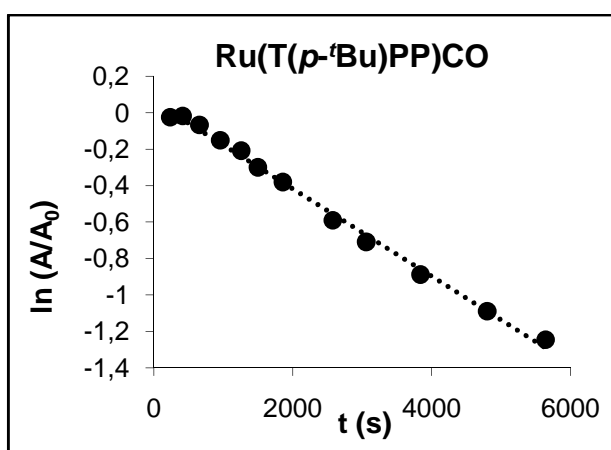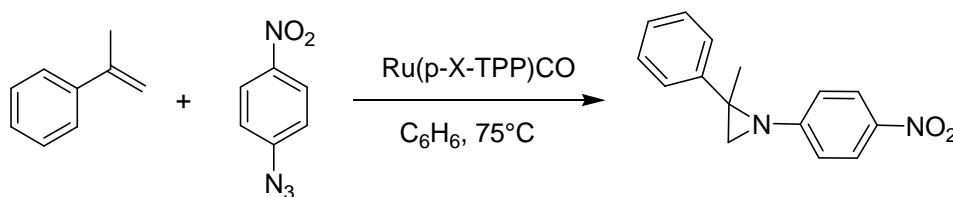
First order kinetic, $k = 2{,}42\times10^{-4}$ s^{-1}
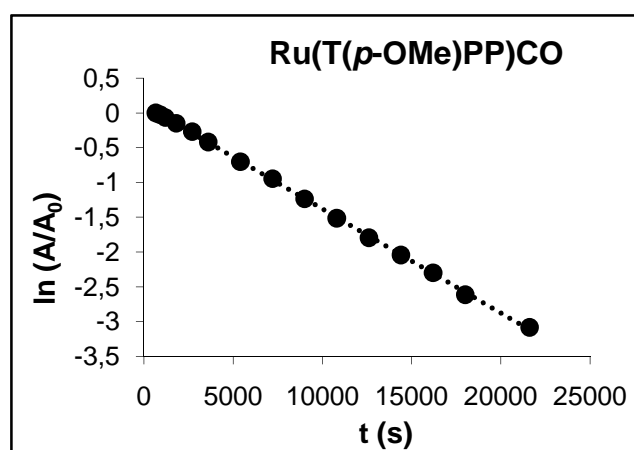
First order kinetic, $k = 1{,}50\times10^{-4}$ s^{-1}
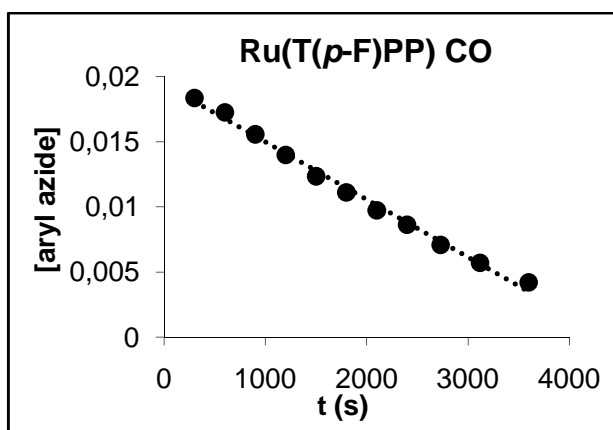
Zero order kinetic, $k = 4{,}42 \times 10^{-6}$ M s^{-1}
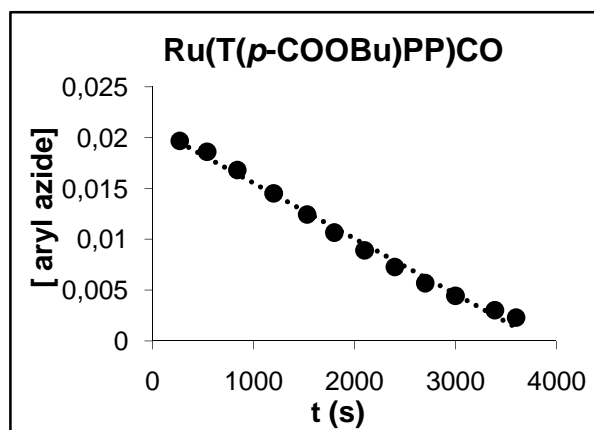
Zero order kinetic, $k = 5{,}46 \times 10^{-6}$ M s^{-1}
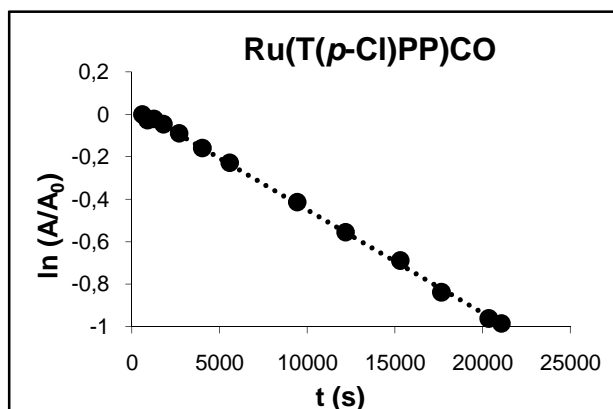
First order kinetic, $k = 4.86 \times 10^{-5}$ s^{-1}
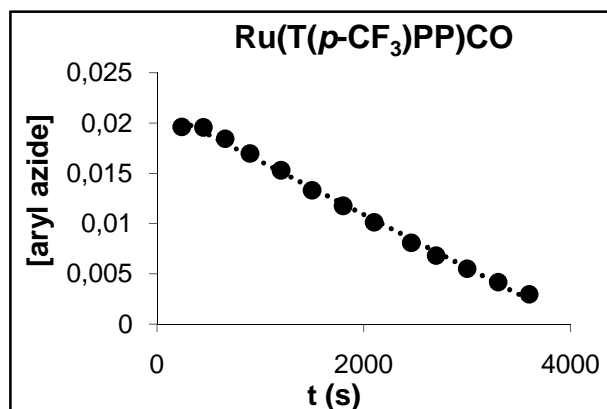
Zero order kinetic, $k = 5{,}30 \times 10^{-6}$ M s^{-1}
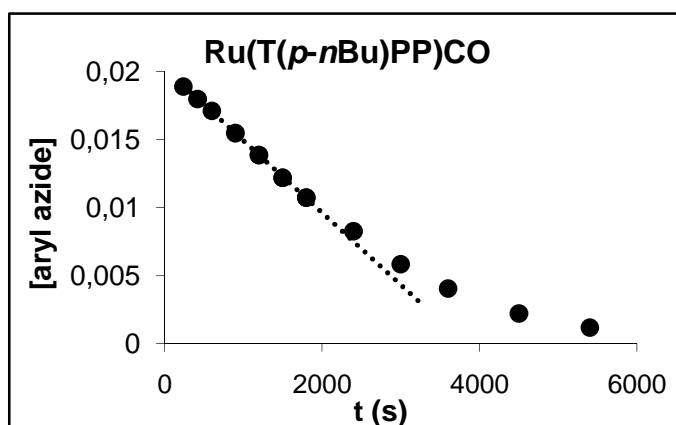
Mixed zero/first order

3.9.2. Kinetic experiment at different substrate concentrations
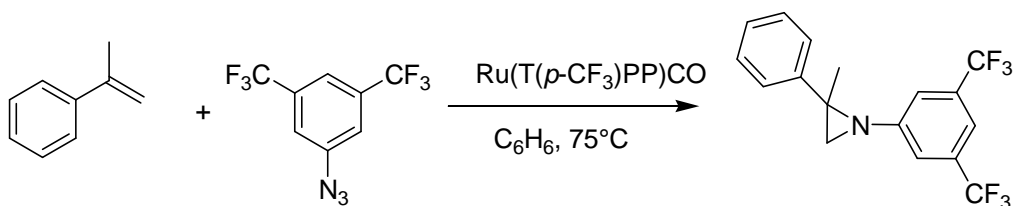
Table 12. *Kinetic constants with respect to 3,5-bis(trifluoromethyl)phenyl azide at different α-methylstyrene concentration using Ru(T(p-CF$_3$)PP)CO as the catalyst.*

Molar Ratio Catalyst/azide/substrate	[α-methylstyrene] (M)	k	Reaction Rate ΔM/Δt (M s^{-1})
1:50:250	0.10	1.66×10^{-5} M s^{-1}	1.66×10^{-5}
1:50 :1000	0.77	2.44×10^{-5} M s^{-1}	2.44×10^{-5}
1:50:2000	0.38	2.94×10^{-5} M s^{-1}	2.94×10^{-5}
1:50: 3750	1.50	3.40×10^{-3} M s^{-1}	2.90×10^{-5}
1:50:5128	2.05	mixed order	2.51×10^{-5}
1:50:7692	3.08	2.94×10^{-3} s^{-1}	2.01×10^{-5}
1:50:10916	4.37	2.76×10^{-3} s^{-1}	1.94×10^{-5}

Catalyst: Ru(T(p-CF$_3$)PP)CO (12.5 mg, 0.012 mmol), azide = 3,5-bis(trifluoromethyl)phenyl azide (153 mg, 0.60 mmol), the reaction rate was calculated at 90% conversion.
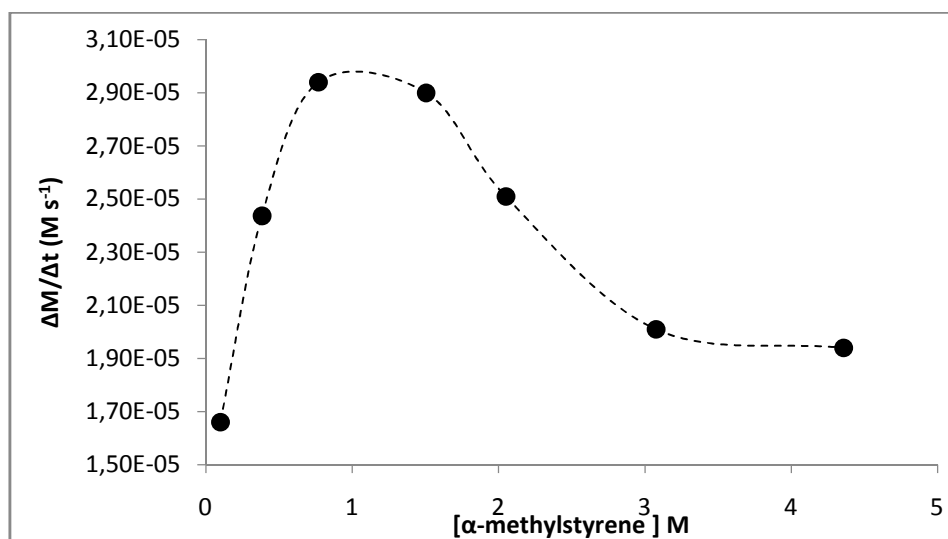
Figure 35. *Plot of the reaction rate versus styrene concentration.*

Table 13. *Kinetic constants with respect to 3,5-bis(trifluoromethyl)phenyl azide at different α-methylstyrene concentration using complex **42** as the catalyst.*
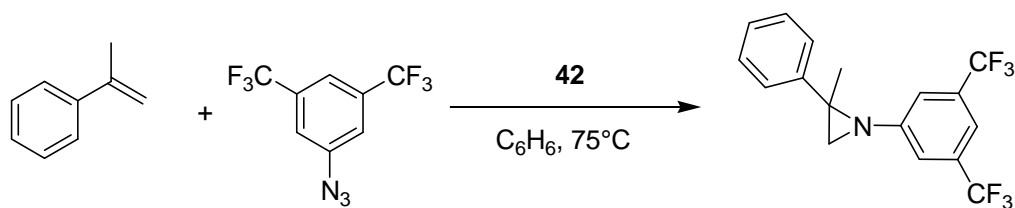
Molar Ratio Catalyst/azide/substrate	[α-methyl styrene] (M)	k
1:50:250	0.10	1.13×10^{-4} s^{-1}
1:50 :641	0.26	1.97×10^{-4} s^{-1}
1:50:961	0.38	2.03×10^{-5} s^{-1}

*Catalyst: complex **42** (16.7 mg, 0.012 mmol), azide = 3,5-bis(trifluoromethyl)phenyl azide (0.60 mmol).*

3.10. Synthesis of Amino esters by Ruthenium Porphyrin-Catalysed Amination of C-H Bonds

3.10.1. Model reaction
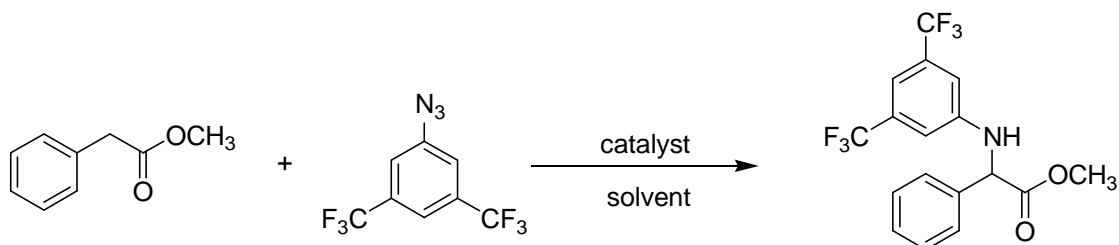
Table 14. *Catalyst screening*

Catalyst	Yield (%)	Reaction Time (h)
Ru(TPP)CO	64	8
Ru(T(*p*-CF$_3$)PP)CO	60	10
Ru(T(*p*-CF$_3$)PP)(NAr)$_2$ (**50**)	51	22
Co(TPP)	51	3

Experimental Conditions: molar ratio catalyst/azide/substrate = 1:10:50, catalyst = 6.0×10^{-2} mmol, 3,5-*bis*(trifluoromethyl)phenyl azide = 153 mg (6.0×10^{-1} mmol), methyl phenylacetate = 430 µL (3.0 mmol). Solvent: benzene (30 mL), T = 80°C.

Table 15. *Solvent screening*

Solvent	Yield (%)	Reaction Time (h)
1,2-dichloroethane[a]	30	21
benzene[a]	64	8
methyl phenylacetate[b]	70	3
acetonitrile[a]	40	31

Experimental Conditions: molar ratio Ru(TPP)CO/azide/substrate = 1:10:50, catalyst = Ru(TPP)CO (44.5 mg, 6.0×10^{-2} mmol), 3,5-*bis*(trifluoromethyl)phenyl azide = 153 mg (6.0×10^{-1} mmol), methyl phenylacetate = 430 µL (3.0 mmol). Solvent volume = 30 mL. [a]T = refluxing solvent, [b]T = 80°C.

Table 16. *Catalytic outcomes with different molar ratios*

Molar Ratio Ru/azide/substrate	Conversion	Yield(%)	Reaction Time (h)
1:20:50[a]	80	29	3
1:50 solvent[b]	100	72	6
1:50:1000[a]	44	32	5

Experimental Conditions: Catalyst = Ru(TPP)CO (8.1 mg, 1.1×10^{-2} mmol), azide = 3,5-*bis*(trifluoromethyl)phenyl azide, substrate = methyl phenylacetate. Solvent volume = 10 mL. [a]Solvent = benzene, T = 80°C; incomplete conversion due to the complete transformation of Ru(TPP)CO into the corresponding **49**-type *bis*-amido complex. [b]Solvent = methyl phenylacetate, T = 100°C.

Kinetics of the reaction between 3,5-*bis*(trifluoromethyl)phenyl azide and methyl phenylacetate catalysed by Ru(TPP)CO.

Kinetic Measurements: The catalyst, benzene (when required), methyl phenylacetate and 3,5-*bis*(trifluoromethyl)phenyl azide were added in this order to a Schlenk flask. A low azide/catalyst ratio was chosen in order to avoid the competitive catalytic cycle (cycle 2 in ***Scheme 64***) and the consequent formation of the inert *bis*-amido complex **49**.

The flask was capped with a rubber septum and immediately placed in an oil bath preheated to 75 °C. The solution was stirred for two minutes to dissolve all reagents, then the consumption of the aryl azide was followed by IR spectroscopy by withdrawing samples of the solution at regular time intervals and measuring the ν(N=N) absorbance values. The apparent zero-order with respect to the aryl azide was observed in the range of A/Ao between 1 and 0,3-0,4; the linearity was lost at higher conversion of the aryl azide. The rate constants were fitted to the equation $-d[\text{ArN}_3]/dt = k_{\text{observed}}[\text{Ru(TTP)CO}]/[\text{methyl phenylacetate}]$. The concentration of catalyst was calculated by the exact amount of catalyst weighed in each run and was considered to remain constant during the reaction.

Kinetic order of the aryl azide: The measurements were performed using benzene as reaction solvent (7 mL). The employed catalyst/azide/substrate ratio was 1:5:869 (Ru(TPP)CO = 16.6 mg

(2.2×10^{-2} mmol), 3,5-*bis*(trifluoromethyl)phenyl azide = 28.1 mg (1.1×10^{-1} mmol), methyl phenylacetate = 2.8 mL).
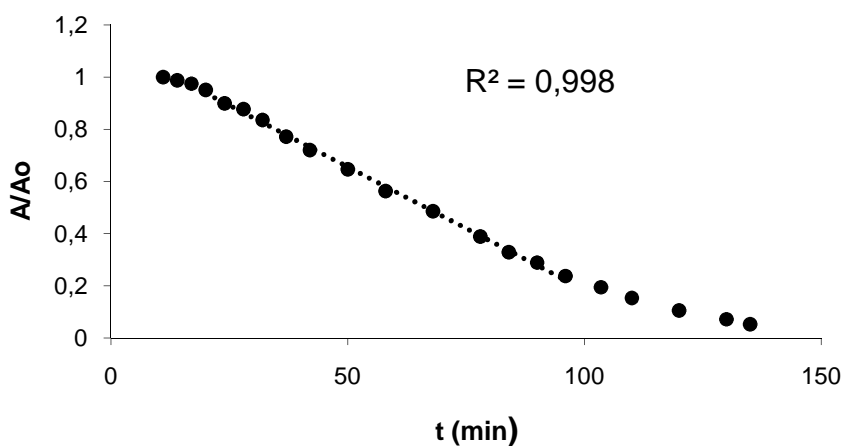
Figure 36. *Zero-order kinetic with respect to the aryl azide in the range of A/Ao between 1 and 0.3.*

Kinetic order of Ru(TPP)CO: The measurements were performed using methyl phenylacetate as reaction solvent (10 mL) and 3,5-*bis*(trifluoromethyl)phenyl azide (28.1 mg, 1.1×10^{-1} mmol) as aryl azide.

Ru(TPP)CO (mg)	[Ru(TPP)CO]	k_{obs} (M/s)	k_{obs}*[subs] (M/s^2)
6.0	0,000809	6.45×10^{-7}	7,64×10^{-8}
8.2	0,00111	6.69×10^{-7}	7,91×10^{-8}
10.4	0,00140	7.51×10^{-7}	8,89×10^{-8}
16.6	0,00224	9.32×10^{-7}	1,10×10^{-7}
21.0	0,00283	1.02×10^{-6}	1,21×10^{-7}
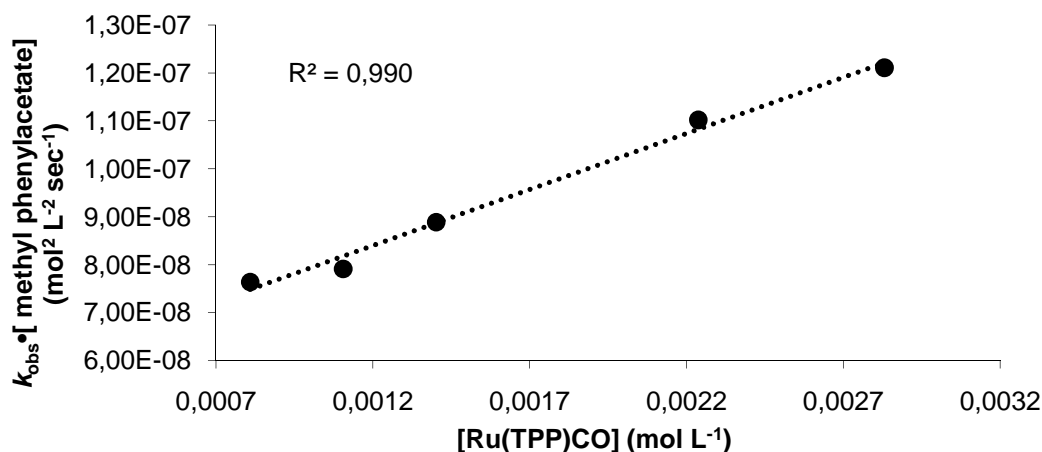
Figure 37. *First-order kinetic with respect to Ru(TPP)CO concentration.*

Kinetic order of methyl phenyl acetate: The measurements were performed using Ru(TPP)CO (16.6 mg, 2.2×10^{-2}), 3,5-*bis*(trifluoromethyl)phenyl azide (28.1 mg, 1.1×10^{-2}) and benzene/methyl phenylacetate mixture as solvent (benzene volume was calculated in order to reach a total volume of 10 mL). The kinetic order with respect to the aryl azide changed from apparent zero order at high methyl phenylacetate concentration (7.0 - 1.0 M) to apparent first order in the aryl azide at low methyl phenylacetate concentration (1.0 - 0.1 M). For this reason in the graph reported in ***Figure 39***, the reaction rate ($\Delta M/\Delta t$) was plotted at the Y-axis instead of the observed kinetic constants.

V substrate (mL)	M	1/M	k_{obs} (M/s)	k_{obs}/[Ru(TPP)CO] (min^{-1})
10	7,01	0,141	$9,32 \times 10^{-7}$	$4,16 \times 10^{-4}$
5	3,55	0,282	$1,08 \times 10^{-6}$	$4,82 \times 10^{-4}$
3	2,13	0,470	$1,13 \times 10^{-6}$	$5,20 \times 10^{-4}$
2	1,42	0,704	$1,57 \times 10^{-6}$	$7,00 \times 10^{-4}$
1,4	0,96	1,05	$1,90 \times 10^{-6}$	$8,50 \times 10^{-4}$
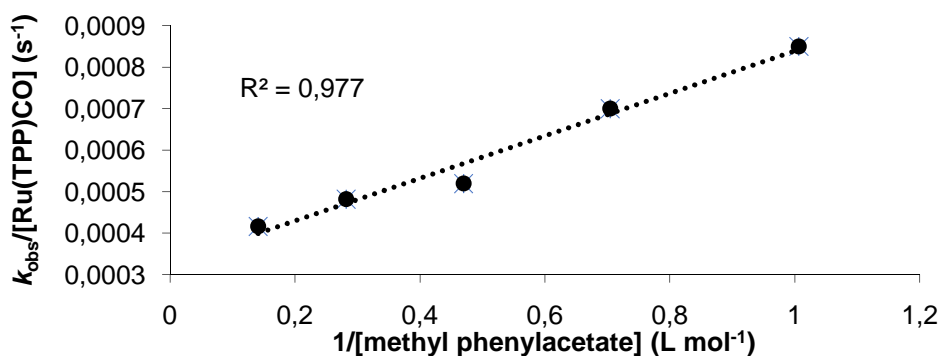
Figure 38. *Inverse dependence of the observed kinetic constant with respect to the substrate concentration in the [methyl phenylacetate] range of 7.0-1.0 M.*

V substrate (mL)c	M	$v(mol\ s^{-1}) \times 10^6$
10,0	7,10	0,931
5,0	3,55	1,08
3,0	2,13	1,16
2,0	1,42	1,57
1,400	0,99	1,90
0,800	0,57	2,07
0,400	0,28	1,72
0,140	0,10	1,44
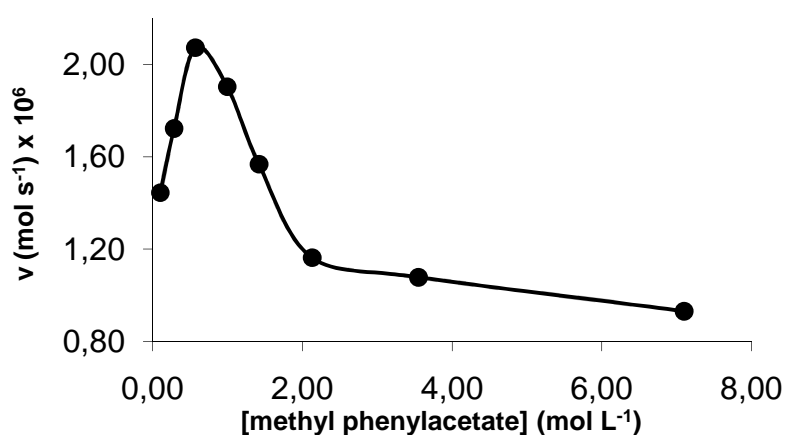
Figure 39. *Dependence of the reaction rate with respect to the substrate concentration. Reaction rate was calculated at 80% conversion of the aryl azide.*

3.10.2. α-Amino ester synthesis

3.10.2.1. Methyl (3,5-*bis*(trifluoromethyl)phenylamino)phenylacetate (48).
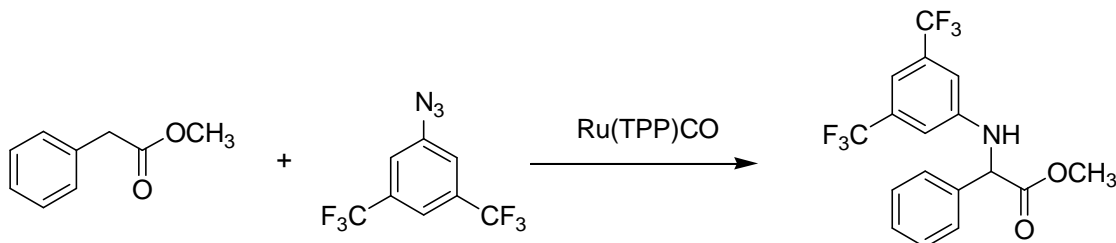
Method A: The general procedure for amination reactions was followed, a mixture of Ru(TPP)CO (46.3 mg, 6.2×10^{-2} mmol), 3,5-*bis*(trifluoromethyl)phenyl azide (161 mg, 6.3×10^{-1} mmol) and methyl phenylacetate (478 mg, 3.2 mmol) in benzene (30 mL) was heated to reflux for 8 hours. Yield = 64%.

Method B: The general procedure for amination reactions was followed, a mixture of Ru(TPP)CO (23.9 mg, 3.2×10^{-2} mmol), 3,5-*bis*(trifluoromethyl)phenyl azide (386.7 mg, 1.5 mmol) in methyl phenylacetate (15 mL) was heated to 100°C for 6 hours. Yield = 80%.

Characterisation for 48: ^{1}H NMR (300 MHz; CDCl$_3$): δ 7.48-7.34 (5H, m, H$_{Ar}$), 7.15 (1H, s, H$_{Ar}$), 6.90 (2H, s, H$_{Ar}$), 5.48 (1H, br, NH), 5.09 (1H, s, CH(NH$_{Ar}$)), 3.76 (3H, s, OCH$_3$).
^{13}C (75 MHz; CDCl$_3$) δ: 171.5 (C=O), 146.5 (C$_{Ar}$), 136.2 (C$_{Ar}$), 132.6 (CF$_3$, q, J = 32.7 Hz), 129.4 (CH$_{Ar}$), 129.0 (CH$_{Ar}$), 127.3 (CH$_{Ar}$), 125.3 (C$_{Ar}$), 121.7 (C$_{Ar}$), 112.8 (CH$_{Ar}$), 111.3 (CH$_{Ar}$), 60.3 (CH), 53.3 (OCH$_3$). ^{19}F-NMR (282 MHz; CDCl$_3$) -63.62 (CF$_3$). EI-MS: m/z = 377 [M]$^+$. IR (ATR): 3377 cm^{-1} (ν_{N-H}), 1733 cm^{-1} ($\nu_{C=O}$). X-ray quality crystals were obtained by slow evaporation of a compound **48** pentane solution at room temperature.

3.10.2.2. Methyl (4-nitrophenylamino)phenylacetate (52).
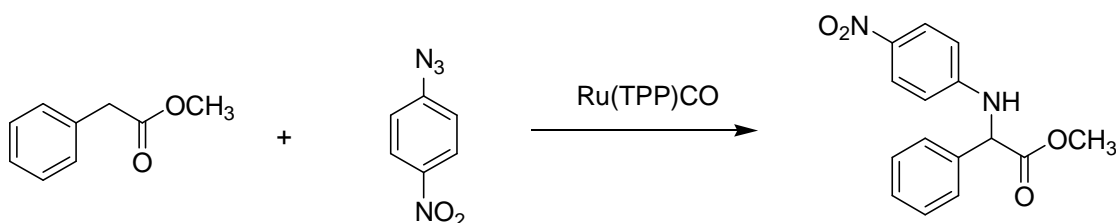
Method A: The general procedure for amination reactions was followed, a mixture of Ru(TPP)CO (46.3 mg, 6.2×10^{-2} mmol), 4-nitrophenyl azide (101 mg, 6.1×10^{-1} mmol) and methyl phenylacetate (456 mg, 3.0 mmol) in benzene (30 mL) was heated to reflux for 7.5 hours. Yield = traces.

Method B: The general procedure for amination reactions was followed, a mixture of Ru(TPP)CO (20.8 mg, 2.8×10^{-2} mmol), 4-nitrophenyl azide (225 mg, 1.4 mmol) in methyl phenylacetate (15 mL) was heated to 100°C for 8 hours. Yield = 32%.

Characterisation for 52: ^{1}H NMR (300 MHz, CDCl3): δ 8.05 (2H,d , J = 8.1 Hz, H_{Ar}), 7.35 (5H, m, H_{Ar}), 6.54 (2H, d, J = 8.1 Hz, H_{Ar}), 5.30 (1H, br, NH), 5.15 (1H, s, CH), 3.78 (3H, s, OCH_3).

3.10.2.3 Methyl (4-(trifluoromethyl)phenylamino)phenylacetate (51).
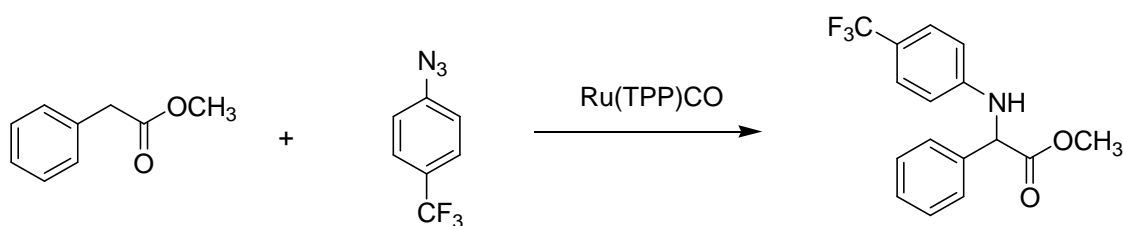
Method A: The general procedure for amination reactions was followed, a mixture of Ru(TPP)CO (22.4 mg, 3.0×10^{-2} mmol), 4-(trifluoromethyl)phenyl azide (56.4 mg, 3.0×10^{-1} mmol) and methyl phenylacetate (228 mg, 1.5 mmol) in benzene (30 mL) was heated to reflux for 2 hours. Yield = traces.

Method B: The general procedure for amination reactions was followed, a mixture of Ru(TPP)CO (22.7 mg, 3.1×10^{-2} mmol), 4-(trifluoromethyl)phenyl azide (282 mg, 1.5 mmol) in methyl phenylacetate (15 mL) was heated to 100°C for 5 hours. Yield = 26%.

Characterisation for 51: ^{1}H NMR (300 MHz, CDCl$_3$): δ 7.59 (2H, d, J = 8.5 Hz, H$_{Ar}$), 7.35 (5H, m, H$_{Ar}$), 6.57 (2H, d, J = 8.5 Hz, H$_{Ar}$), 5.31 (1H, br, NH), 5.12 (1H, s, CH), 3.77 (3H, s, OCH$_3$).

3.10.2.4. Methyl (4-*tert*-butylphenylamino)phenylacetate (53).
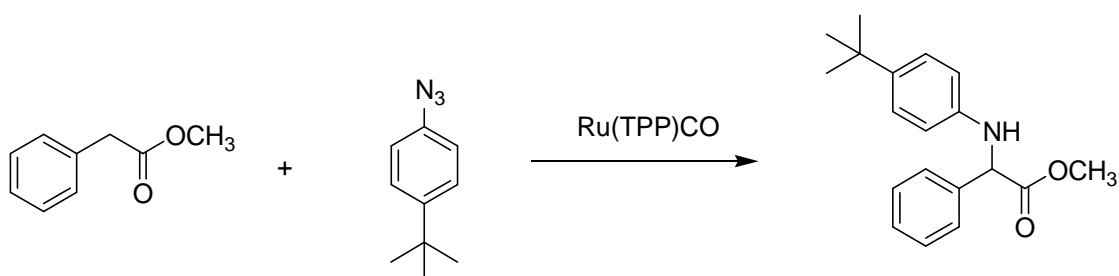
Method A: The general procedure for amination reactions was followed, a mixture of Ru(TPP)CO (23.0 mg, 3.1×10^{-2} mmol), 4-*tert*-butylphenyl azide (56.2 mg, 3.2×10^{-1} mmol) and methyl phenylacetate (228 mg, 1.5 mmol) in benzene (30 mL) was heated to reflux for 6.5 hours. Yield = traces.

Method B: The general procedure for amination reactions was followed, a mixture of Ru(TPP)CO (20.2 mg, 2.7×10^{-2} mmol), 4-*tert*-butylphenyl azide (234 mg, 1.3 mmol) in methyl phenylacetate (15 mL) was heated to 100°C for 5 hours. Yield = 20%.

Characterisation for 53: ^{1}H NMR (300 MHz, CDCl$_3$): δ 7.34 (7H, m, H$_{Ar}$), 6.56 (2H, d, J = 8.8 Hz, H$_{Ar}$), 5.13 (1H, br, NH), 5.11 (1H, s, CH), 3.75 (3H, s, OCH$_3$), 1.39 (9H, s, [t]Bu).

3.10.3. Synthesis of β-amino esters using methyl dihydrocinnamate as substrate

3.10.3.1. Methyl 3-(3,5-*bis*(trifluoromethyl)phenylamino)-3-phenylpropanoate (54a).
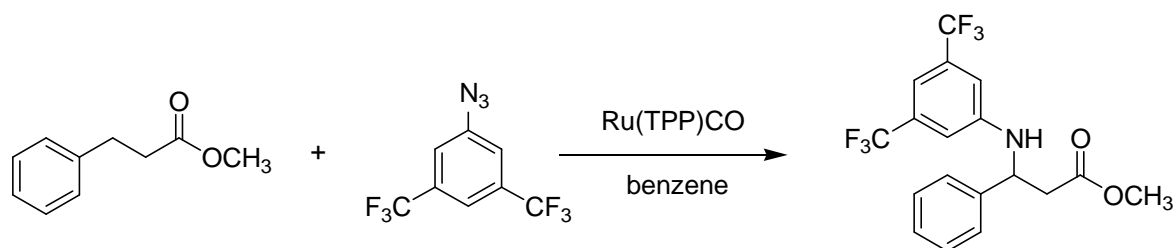
Method A: The general procedure for amination reactions was followed, a mixture of Ru(TPP)CO (9.1 mg, 1.2×10^{-2} mmol), 3,5-*bis*(trifluoromethyl)phenyl azide (30.8 mg, 1.2×10^{-1} mmol) and methyl dihydrocinnammate (102 mg, 6.2×10^{-1} mmol) in benzene (30 mL) was heated to reflux for 7 hours. Yield = traces.

Method B: The general procedure for amination reactions was followed, a mixture of Ru(TPP)CO (7.5 mg, 1.0×10^{-2} mmol), 3,5-*bis*(trifluoromethyl)phenyl azide (40.3 mg, 1.6×10^{-1} mmol) and methyl dihydrocinnammate (1.6 ml, 10 mmol) in benzene (7.0 mL) was heated to reflux for 2.25 hours. Benzene was evaporated and methyl dihydrocinnamate excess was removed by high vacuum distillation. Yield = 81%.

Method C: The general procedure for amination reactions was followed, a mixture of Ru(TPP)CO (7.4 mg, 1.0×10^{-2} mmol), 3,5-*bis*(trifluoromethyl)phenyl azide (132 mg, 5.2×10^{-1} mmol) and methyl dihydrocinnammate (1.6 ml, 10 mmol) in benzene (7.0 mL) was heated to reflux for 10.5 hours. Benzene was evaporated and methyl dihydrocinnamate excess was removed by high vacuum distillation. Yield = 77%.

3.10.3.2. Reaction between methyl phenylacetate and 4-nitrophenylazide in the presence of Ru(TPP)CO
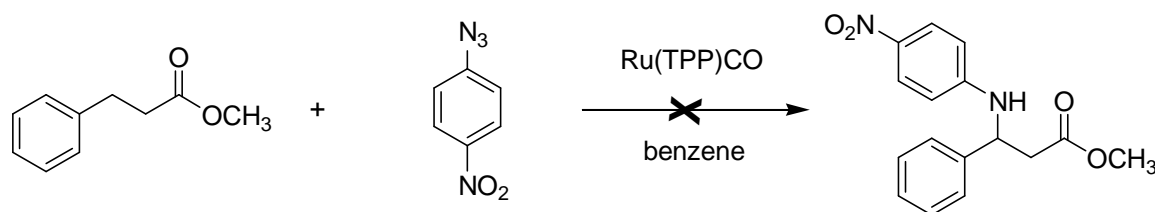

**Method B:** The general procedure for amination reactions was followed, a mixture of Ru(TPP)CO (7.5 mg, 1.0×10^{-2} mmol), 4-nitrophenyl azide (24.6 mg, 1.5×10^{-1} mmol) and methyl dihydrocinnamate (1.6 ml, 10 mmol) in benzene (7.0 mL) was heated to reflux for 1.5 hours. Benzene was evaporated and methyl dihydrocinnamate excess was removed by high vacuum distillation. Yield = traces, evidences of the β-amino ester formation were obtained by GC-MS analysis.

3.10.3.2. Reaction between methyl phenylacetate and 4-(trifluoromethyl)phenyl azide in the presence of Ru(TPP)CO
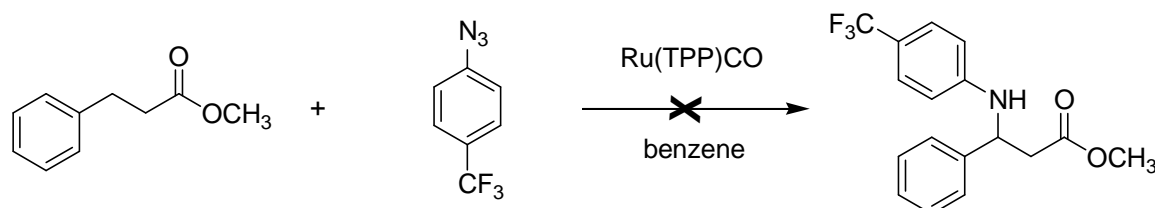
Method B: The general procedure for amination reactions was followed, a mixture of Ru(TPP)CO (7.5 mg, 1.0×10^{-2} mmol), 4-(trifluoromethyl)phenyl azide (30.8 mg, 1.7×10^{-1} mmol) and methyl dihydrocinnammate (1.6 ml, 10 mmol) in benzene (7.0 mL) was heated to reflux for 1.5 hours. Benzene was evaporated and methyl dihydrocinnamate excess was removed by high vacuum distillation. Yield = traces, evidences of the β-amino ester formation were obtained by GC-MS analysis.

3.10.3.3. Reaction between methyl phenylacetate and 4-(trifluoromethyl) phenyl azide in the presence of Ru (TPP) CO
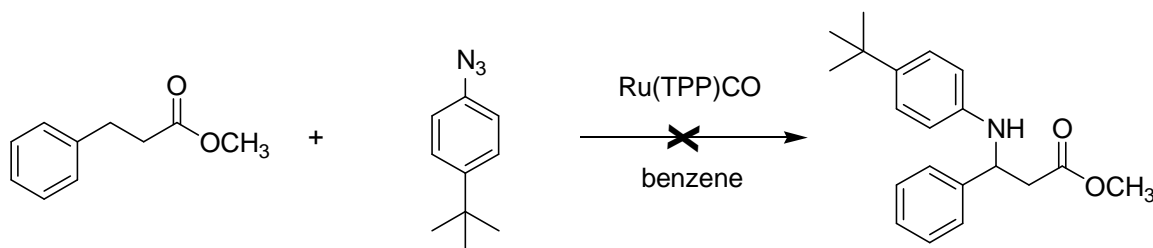

Method B: The general procedure for amination reactions was followed, a mixture of Ru(TPP)CO (7.4 mg, 1.0×10^{-2} mmol), 4-*tert*-butylphenyl azide (30.0 mg, 1.7×10^{-1} mmol) and methyl dihydrocinnamate (1.6 ml, 10.3 mmol) in benzene (7.0 mL) was heated to reflux for 2 hours. Benzene was evaporated and methyl dihydrocinnamate excess was removed by high vacuum distillation. Yield = traces, evidences of the β-amino ester formation were obtained by GC-MS analysis.

3.10.4 Synthesis of α- and β-amino esters using silyl ketene acetal 61 as substrate
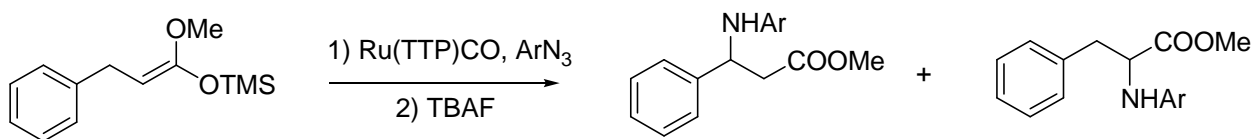

Experimental Procedure: The general procedure for amination reactions was followed, a mixture of Ru(TPP)CO, the aryl azide and the silyl ketene acetal **61** in benzene was heated to reflux.

Work-up: benzene was evaporated to dryness and THF (25 mL) was added to the residue, the resulting solution was placed in an ice bath before adding a THF solution of tetra-*n*-butylammonium fluoride (TBAF) (1.0 mol×L^{-1}, 3.0 mL). The solution was stirred for 15 minutes at 0°C, poured into a saturated aqueous NH$_4$Cl solution (200 mL), extracted with AcOEt (50 mL x 3), dried with Na$_2$SO$_4$ and the solvent was evaporated to dryness. The crude was then purified by flash chromatography (silica gel, *n*-hexane/ethyl acetate as eluent. Yields are reported as isolated yields.

3.10.4.1 Reaction between 3,5-*bis*(trifluoromethyl)phenyl azide and silyl ketene acetal 61 in the presence of Ru(TPP)CO.
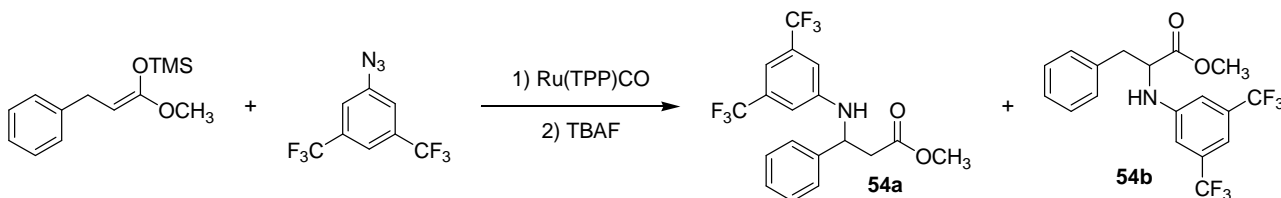
Ru(TPP)CO = 7.6 mg (1.0×10^{-2} mmol), 3,5-*bis*(trifluoromethyl)phenyl azide = 133 mg (5.2×10^{-1} mmol), silyl ketene acetal = 625 mg (2.7 mmol), benzene = 11 mL. Reaction time = 0.25 hours. Purification conditions = gradient elution from *n*-hexane/AcOEt 9.5:0.5 to *n*-hexane/AcOEt 9:1. Yield (**54a**) = 65%, yield (**54b**) =12%.

Characterisation for methyl 3-(3,5-*bis*(trifluoromethyl)phenylamino)-3-phenylpropanoate (54a): ^{1}H NMR (300 MHz, CDCl$_3$): δ 7.38-7.27 (5H, m, H$_{Ar}$), 7.12 (1H, s, H$_{Ar}$), 6.90 (2H, s, H$_{Ar}$), 5.17 (1H, br, NH), 4.85 (1H, dd, J = 7.7 Hz, J = 5.3 Hz, C*H*(NHAr)), 3.67 (3H, s, OCH$_3$), 2.90 (1H, dd, J = 15.2, 5.2 Hz, C*H*H), 2.82 (1H, dd, J = 15.2, 7.8 Hz, CH*H*). ^{13}C NMR (75 MHz, CDCl$_3$): δ 171.4 (C=O), 147.5 (C$_{Ar}$), 140.6 (C$_{Ar}$), 132.5 (*C*-CF$_3$, q, J = 32.9 Hz), 129.3 (CH$_{Ar}$), 128.2 (CH$_{Ar}$),

126.2 (CH$_{Ar}$), 123.6 (CF$_3$, q, J = 272.5 Hz, 113.0 (CH$_{Ar}$), 111.0 (CH$_{Ar}$), 54.9 (CH), 52.2 (OCH$_3$), 42.3 (CH$_2$). ^{19}F NMR (282 MHz, CDCl$_3$): δ (282 MHz, CDCl$_3$) -63.58 (CF$_3$). IR (ATR): 3396 cm^{-1} (v_{N-H}), 1727 cm^{-1} ($v_{C=O}$). EI-MS: m/z = 391 [M]$^+$.

Characterisation for methyl 2-(3,5-*bis*(trifluoromethyl)phenylamino)-3-phenylpropanoate (54b): ^{1}H NMR (300 MHz, CDCl$_3$): δ 7.35-7.23 (3H, m, H$_{Ar}$), 7.20-7.12 (3H, m, H$_{Ar}$), 6.88 (2H, s, H$_{Ar}$), 4.63 (1H, br, NH), 4.40 (1H, t, J = 5.3 Hz, CH(NHAr)), 3.74 (3H, s, OCH$_3$), 3.21 (1H, dd, J = 13.7, 5.6 Hz, CHH), 3.11 (1H, dd, J = 13.7, 5.6 Hz, CHH. ^{13}C NMR (75 MHz, CDCl$_3$): δ 172.7 (C=O), 147.3 (C$_{Ar}$), 135.7 (C$_{Ar}$), 132.7 (C-CF$_3$, q, J = 32.8 Hz), 129.4 (CH$_{Ar}$), 128.9 (CH$_{Ar}$), 127.6 (CH$_{Ar}$), 123.5 (CF$_3$, q, J = 272.7 Hz), 112.7 (CH$_{Ar}$), 111.5 (CH$_{Ar}$), 57.4 (CH), 52.6 (OCH$_3$), 38.7 (CH$_2$). ^{19}F NMR (282 MHz, CDCl$_3$): δ -63.54 (CF$_3$). EI-MS: m/z = 391 [M]$^+$.

3.10.4.2 Reaction between 4-(trifluoromethyl)phenyl azide and silyl ketene acetal 61 in the presence of Ru(TPP)CO.
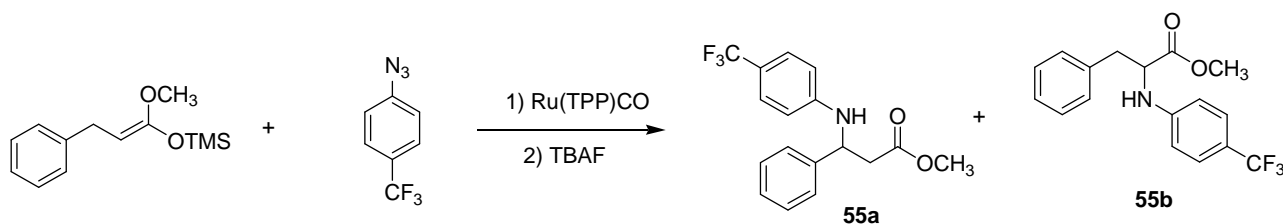
Ru(TPP)CO = 7.8 mg (1.1×10^{-2}mmol), 4-(trifluoromethyl)phenyl azide = 106 mg (5.7×10^{-1} mmol), silyl ketene acetal = 629 mg (2.7 mmol), benzene = 10 mL. Reaction time = 2 hours. Purification conditions = gradient elution from *n*-hexane/AcOEt 9.5:0.5 to *n*-hexane/AcOEt 9:1.

Yield (**55a**) = 38%, yield (**55b**) =14%.

Characterisation for methyl 3-(4-(trifluoromethyl)phenylamino)-3-phenylpropanoate (55a): ^{1}H NMR (400 MHz, CDCl$_3$): δ 7.39-7.24 (7H, m, H$_{Ar}$), 6.58 (2H, d, J = 8.4 Hz, H$_{Ar}$), 4.86 (1H, m, CH(NHAr)), 3.66 (3H, s, OCH$_3$), 2.85 (2H, m, CH$_2$), NH signal was not detected. ^{13}C NMR (100 MHz, CDCl$_3$): δ 171.5 (C=O), 149.3 (C$_{Ar}$), 141.3 (C$_{Ar}$), 129.1 (CH$_{Ar}$), 128.0 (CH$_{Ar}$), 126.7 (CH$_{Ar}$), 126.3 (CH$_{Ar}$), 122.3 (CF$_3$, q, J = 272.7 Hz), 119.7 (C-CF$_3$, q, J = 32.0 Hz), 113.1 (CH$_{Ar}$), 54.8 (CH), 52.1 (OCH$_3$), 42.5 (CH$_2$). ^{19}F NMR (282 MHz, CDCl$_3$): δ -61.48 (CF$_3$). EI-MS: m/z = 323 [M]$^+$.

Characterisation for methyl 2-(4(trifluoromethyl)phenylamino)-3-phenylpropanoate (55b): ^{1}H NMR (300 MHz, CDCl$_3$): δ 7.40 (2H, d, J = 8.5 Hz, H$_{Ar}$), 7.29 (3H, m, H$_{Ar}$), 7.14 (2H, m, H$_{Ar}$),

6.60 (2H, d, J = 8.5 Hz, H_{Ar}), 4.41 (1H, t, J = 6.1 Hz, CH), 3.71 (3H, s, OCH$_3$), 3.11 (1H, dd, J = 13.7, 6.3 Hz, CHH), (1H, dd, J = 13.7, 5.9 Hz, CHH), NH signal was not detected. ^{13}C NMR (75 MHz, CDCl$_3$): δ 173.0 (C=O), 149.0 (C$_{Ar}$), 136.0 (C$_{Ar}$), 129.4 (CH$_{Ar}$), 128.8 (CH$_{Ar}$), 127.4 (CH$_{Ar}$), 126.9 (CH$_{Ar}$), 121.3 (CF$_3$, q, J = 276.3 Hz), 120.1 (*C*-CF$_3$, q, J = 32.7 Hz), 112.8 (CH$_{Ar}$), 57.2 (CH), 52.4 (OCH$_3$), 38.5 (CH$_2$). ^{19}F NMR (282 MHz, CDCl$_3$): δ -61.53 (CF$_3$). EI-MS: m/z = 323 [M]$^+$.

3.10.4.3 Reaction between 4-nitrophenyl azide and silyl ketene acetal 61 in the presence of Ru(TPP)CO.
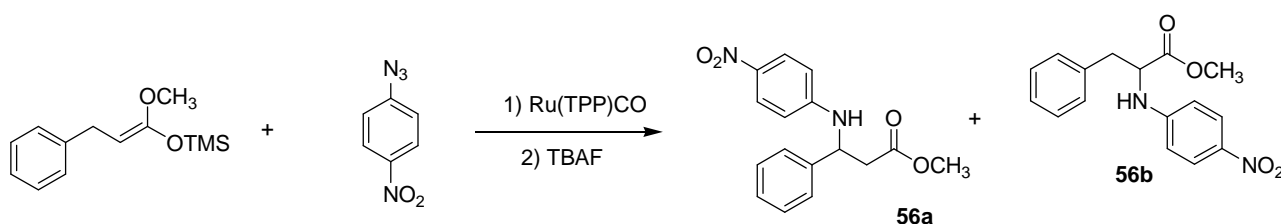
Ru(TPP)CO = 7.6 mg (1.1×10^{-2} mmol), 4-nitrophenyl azide = 85.0 mg (5.2×10^{-1} mmol), silyl ketene acetal = 606 mg (2.6 mmol), benzene = 10 mL. Reaction time = 0.75 hours. Purification conditions = gradient elution from n-hexane/AcOEt 9:1 to n-hexane/AcOEt 7:3).

Yield (**56a**) = 55%, yield (**56b**) =21%.

Characterisation for methyl 3-(4-nitrophenylamino)-3-phenylpropanoate (56a): ^{1}H NMR (300 MHz, CDCl$_3$): δ 8.00 (2H, d, J = 9.1 Hz, H_{Ar}), 7.38-7.24 (5H, m, H_{Ar}), 6.51 (2H, d, J = 9.1 Hz, H_{Ar}), 5.63 (1H, d, J = 6.5 Hz, NH), 4.92 (1H, dd, J = 12.7, 6.7 Hz, CH(NHAr)), 3.65 (3H, s, OCH$_3$), 2.98-2.79 (2H, m, CH$_2$). ^{13}C NMR (75 MHz, CDCl$_3$): δ 171.3 (C=O), 152.2 (C$_{Ar}$), 140.5 (C$_{Ar}$), 138.6 (C$_{Ar}$), 129.2 (CH$_{Ar}$), 128.2 (CH$_{Ar}$), 126.3 (CH$_{Ar}$), 126.1 (CH$_{Ar}$), 112.3 (CH$_{Ar}$), 54.5 (CH), 52.2 (OCH$_3$), 42.1 (CH$_2$). EI-MS: m/z = 300 [M]$^+$.

Characterisation for methyl 2-(4-nitrophenylamino)-3-phenylpropanoate (56b): ^{1}H NMR (300 MHz, CDCl$_3$): δ 8.07 (2H, d, J = 9.2 Hz, H_{Ar}), 7.33-7.22 (3H, m, H_{Ar}), 7.16-7.09 (2H, m, H_{Ar}), 6.52 (2H, d, J = 9.2 Hz, H_{Ar}), 4.97 (1H, d, J = 8.0 Hz, NH), 4.47 (1H, dt, J = 8.0, 6.0 Hz, CH(NHAr)), 3.74 (3H, s, OCH$_3$), 3.23 (1H, dd, J = 13.8, 6.0 Hz, CHH), 3.14 (1H, dd, J = 13.8, 6.2 Hz, CHH). ^{13}C NMR (75 MHz, CDCl$_3$): δ 172.2 (C=O), 151.6 (C$_{Ar}$), 139.1 (C$_{Ar}$), 135.4 (C$_{Ar}$), 129.3 (CH$_{Ar}$), 128.9 (CH$_{Ar}$), 127.6 (CH$_{Ar}$), 126.5 (CH$_{Ar}$), 112.0 (CH$_{Ar}$), 56.9 (CH), 52.7 (OCH$_3$), 38.3 (CH$_2$). EI-MS: m/z = 300 [M]$^+$.

**3.10.4.4 Reaction between 3,5-dichlorophenyl azide and silyl ketene acetal 61 in the presence of Ru(TPP)CO.**
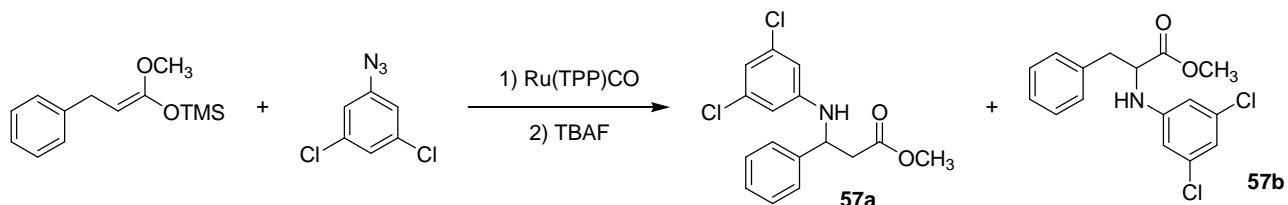
Ru(TPP)CO = 7.9 mg (1.1×10^{-2} mmol), 3,5-dichlorophenyl azide = 107 mg (5.7×10^{-1} mmol), silyl ketene acetal = 629 mg (2.7 mmol), benzene = 10 mL. Reaction time = 1.25 hours. Purification conditions = gradient elution from *n*-hexane/AcOEt 9.5:0.5 to *n*-hexane/AcOEt 9:1).

Yield (**57a**) = 65%, yield (**57b**) =8%.

Characterisation for methyl 3-(3,5-dichlorophenylamino)-3-phenylpropanoate (57a): ^{1}H NMR (400 MHz, CDCl$_3$): δ 7.45-7.22 (5H, m, H$_{Ar}$), 6.64 (1H, brs, H$_{Ar}$), 6.43 (2H, d, *J* = 1.6 Hz, H$_{Ar}$), 4.78 (2H, m, C*H*(NHAr) and NH), 3.66 (3H, s, OCH$_3$), 2.85 (1H, dd, *J* = 15.1, 5.3 Hz, C*H*H), 2.85 (1H, dd, *J* = 15.1, 5.3 Hz, C*H*H), 2.78 (1H, dd, *J* = 15.1, 7.8 Hz, C*H*H). ^{13}C NMR (100 MHz, CDCl$_3$): δ 171.4 (C=O), 148.5 (C$_{Ar}$), 141.0 (C$_{Ar}$), 135.5 (C$_{Ar}$), 129.1 (CH$_{Ar}$), 128.0 (CH$_{Ar}$), 126.2 (CH$_{Ar}$), 117.7 (CH$_{Ar}$), 112.0 (CH$_{Ar}$), 54.7 (CH), 52.1 (OCH$_3$), 42.4 (CH$_2$). EI-MS: *m/z* = 323 [M]$^+$.

Characterisation for methyl 2-(3,5-dichlorophenylamino)-3-phenylpropanoate (57b): ^{1}H NMR (400 MHz, CDCl$_3$): δ 7.34-7.23 (3H, m, H$_{Ar}$), 7.13 (2H, d, *J* = 6.8 Hz, H$_{Ar}$), 6.70 (1H, pst, H$_{Ar}$), 6.43 (2H, d, *J* = 1.6 Hz, H$_{Ar}$), 4.30 (2H, m, C*H*(NHAr) and NH), 3.72 (3H, s, OCH$_3$), 3.17 (1H, dd, *J* = 13.7, 5.4 Hz, C*H*H), 3.08 (1H, dd, *J* = 13.7, 5.9 Hz, CH*H*). ^{13}C NMR (100 MHz, CDCl$_3$): δ 172.8 (C=O), 148.1 (C$_{Ar}$), 135.82 (C$_{Ar}$), 135.76 (C$_{Ar}$), 129.4 (CH$_{Ar}$), 128.8 (CH$_{Ar}$), 127.4 (CH$_{Ar}$), 118.3 (CH$_{Ar}$), 111.8 (CH$_{Ar}$), 57.3 (CH), 52.5 (OCH$_3$), 38.5 (CH$_2$). EI-MS: *m/z* = 323 [M]$^+$.

3.10.4.5. ^{1}H-NMR spectrum of the crude of the reaction between ketene silyl acetal and 3,5-*bis*(trifluoromethyl)phenyl azide (see Section 3.10.4.1) before desilylation with TBAF.
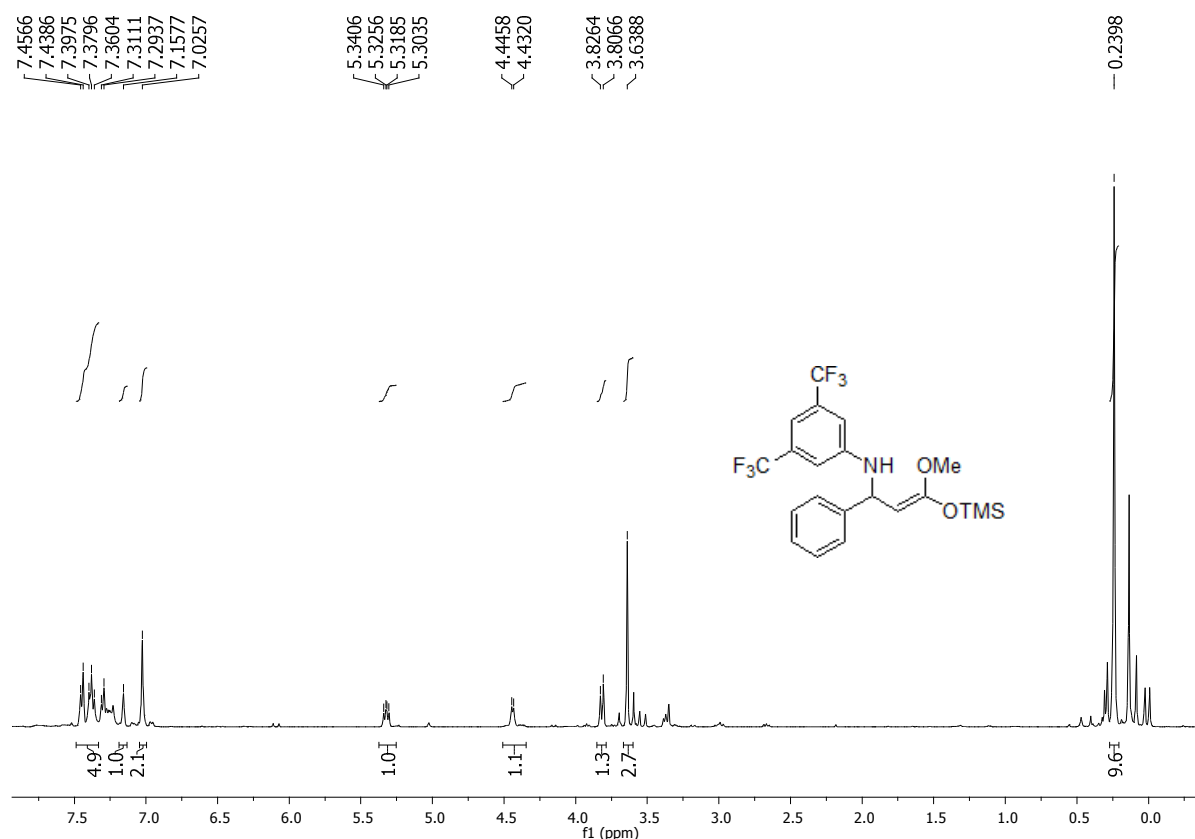
Experiment Conditions: 3,5-*bis*(trifluoromethyl)phenyl azide (150 mg, 5.9×10^{-1} mmol) was added to a benzene (12 mL) suspension of Ru(TPP)CO (8.9 mg, 1.2×10^{-2} mmol) and ketene silyl acetal (168 mg, 7.1×10^{-1} mmol). The resulting mixture was refluxed using a preheated oil bath until the complete consumption of the azide (50 min) and then the solvent was evaporated to dryness. The sample for NMR spectroscopy was prepared dissolving the crude in anhydrous CDCl$_3$.

^{1}H-NMR (300 MHz; CDCl$_3$) δ 7.48-7.32 (5H, m, H$_{Ar}$), 7.16 (1H, s, H$_{Ar}$), 7.03 (2H, s, H$_{Ar}$), 5.32 (1H, dd, J = 8.9 Hz, 6.0 Hz, CH(NHAr)), 4.44 (1H, d, J = 5.5 Hz, NH), 3.82 (1H, d, J = 7.9 Hz), 3.64 (3H, s, CH$_3$), 0.24 (9H, s, TMS).

We obtained a NMR spectrum suitable with the product of benzylic amination of **61**. We tried to isolate this compound through chromatography (silica gel, n-hexane with 3% TEA) but only compound **54b** beside unidentified decomposition products were recovered.

3.10.5. Synthesis of α-oxy-β-amino esters using methyl L-3-phenyllactate derivatives as substrates.

3.10.5.1. Reaction between methyl L-3-phenyllactate and 3,5-*bis*(trifluoromethyl)phenyl azide in the presence of Ru(TPP)CO.
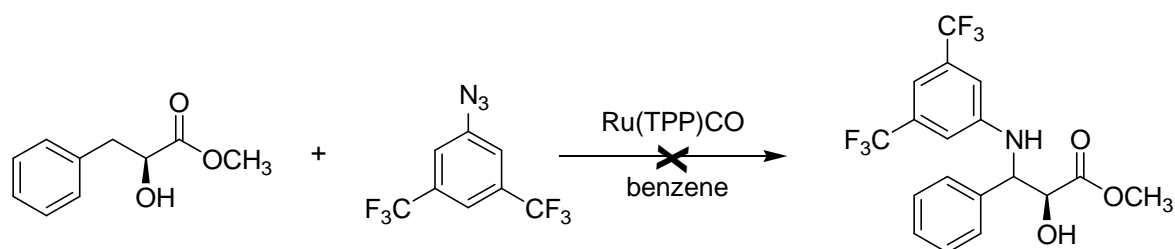
Method A: The general procedure for amination reactions was followed, a mixture of Ru(TPP)CO (7.9 mg, 1.1×10^{-2} mmol), 3,5-*bis*(trifluoromethyl)phenyl azide (44.1 mg, 1.7×10^{-1} mmol) and methyl L-3-phenyllactate (958 mg ml, 5.3 mmol) in benzene (12 mL) was heated to reflux for 19 hours, reaching a 90% conversion of the aryl azide. Benzene was evaporated and methyl L-3-phenyllactate excess was removed by high vacuum distillation. The desired product was observed in the crude.

3.10.5.2. Synthesis of (2*S*)-methyl 2-acetoxy-3-(3,5-*bis*(trifluoromethyl)phenylamino)-3-phenylpropanoate (58).
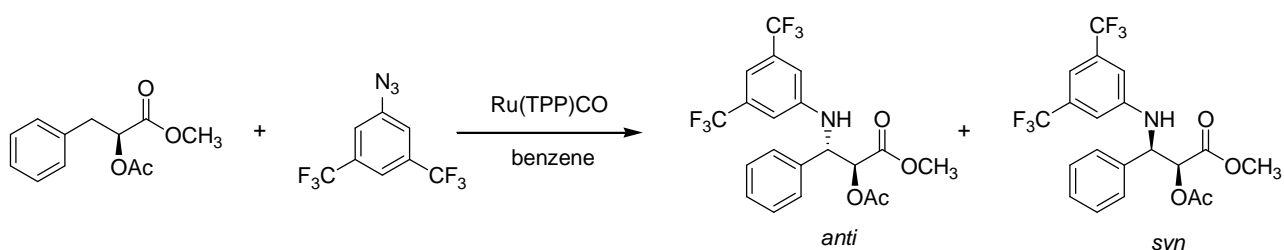
Method A: The general procedure for amination reactions was followed, a mixture of Ru(TPP)CO (13.9 mg, 1.9×10^{-2} mmol), 3,5-*bis*(trifluoromethyl)phenyl azide (90.1 mg, 3.5×10^{-1} mmol) and (2*S*)-methyl 3-phenyl-2-acetoxy-propanoate (5.4 mL, 19 mmol) in benzene (13 mL) was heated to reflux for 5 hours. Benzene was evaporated and the substrate excess was removed by high vacuum distillation. Yield =23%, *sin/anti* ratio = 1:3.5.

Method B: The general procedure for amination reactions was followed, a mixture of Ru(TPP)CO (7.7 mg, 1.0×10^{-2} mmol), 3,5-*bis*(trifluoromethyl)phenyl azide (132 mg, 5.2×10^{-1} mmol) and (2*S*)-methyl 3-phenyl-2-acetoxy-propanoate (3.0 mL, 10 mmol) in benzene (7.0 mL) was heated to reflux for 23 hours. Benzene was evaporated and the substrate excess was removed by high vacuum distillation. Yield =35%, *sin*/*anti* ratio = 1:3.5.

Characterisation for 58: *Syn/anti* assignment was performed on the basis of chemical shifts and coupling constant trends reported in the literature[151]. ^{1}H NMR (400 MHz, CDCl$_3$) major isomer (*anti*): δ 7.38-7.30 (5H, m, H$_{Ar}$), 7.15 (1H, s, H$_{Ar}$), 6.91 (2H, s, H$_{Ar}$), 5.35 (1H, d, *J* = 4.9 Hz, C*H*(OAc)), 5.20 (1H, m, NH), 4.95 (1H, br, C*H*(NHAr)), 3.64 (3H, s, OCH$_3$), 2.15 (3H, s, CH$_3$ acetoxy). *Minor isomer* (syn): δ 7.38-7.30 (5H, m, H$_{Ar}$), 7.15 (1H, s, H$_{Ar}$), 6.91 (2H, s, H$_{Ar}$), 5.41 (1H, d, *J* = 2.6 Hz, C*H*(OAc)), 5.16-5.05 (2H, m, NH and C*H*(NHAr)), 3.75 (3H, s, OCH$_3$), 2.11 (3H, s, CH$_3$ acetoxy).

^{13}C NMR (100 MHz, CDCl$_3$) major isomer (*anti*): δ 170.2 (C=O acetoxy), 168.4 (C=O methyl ester), 147.1 (C$_{Ar}$), 136.8 (C$_{Ar}$), 132.6 (*C*-CF$_3$, q, *J* = 33.1 Hz), 129.1 (CH$_{Ar}$), 127.2 (CH$_{Ar}$), 126.8 (CH$_{Ar}$), 123.5 (CF$_3$, q, *J* = 272.8 Hz), 113.0 (CH$_{Ar}$), 111.4 (CH$_{Ar}$), 74.7 (*C*H(OAc)), 58.4 (*C*H(NHAr)), 52.6 (OCH$_3$ methoxy), 20.7 (CH$_3$ acetoxy). *Minor isomer* (syn): δ 169.7 (C=O acetoxy), 168.4 (C=O methyl ester), 147.0 (C$_{Ar}$), 136.1 (C$_{Ar}$), 132.6 (*C*-CF$_3$, q, *J* = 33.1 Hz), 129.2 (CH$_{Ar}$), 128.9 (CH$_{Ar}$), 128.7 (CH$_{Ar}$), 123.5 (CF$_3$, q, *J* = 272.8 Hz), 113.0 (CH$_{Ar}$), 111.4 (CH$_{Ar}$), 75.3 (*C*H(OAc)), 58.0 (*C*H(NHAr)), 53.1 (OCH$_3$ methoxy), 20.5 (CH$_3$ acetoxy).

^{19}F NMR (282 MHz, CDCl$_3$) -63.24 (CF$_3$ minor isomer), -63.25 (CF$_3$ major isomer). EI-MS: *m/z* = 449 [M]$^{+}$

3.10.5.2. Synthesis of (2*S*)-methyl 2-methoxy-3-(3,5-*bis*(trifluoromethyl)phenylamino)-3-phenylpropanoate (59).
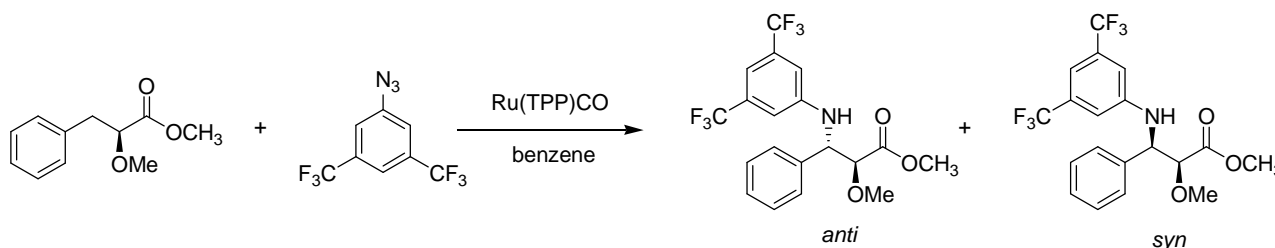
Method A: The general procedure for amination reactions was followed, a mixture of Ru(TPP)CO (7.4 mg, 1.0×10^{-2} mmol), 3,5-*bis*(trifluoromethyl)phenyl azide (39.2 mg, 1.5×10^{-1} mmol) and (2*S*)-

methyl 3-phenyl-2-methoxy-propanoate (1.91 g, 9.8 mmol) in benzene (8 mL) was heated to reflux for 2 hours. Benzene was evaporated and the substrate excess was removed by high vacuum distillation. Yield =43%, *sin/anti* ratio = 1:1.2.

Method B: The general procedure for amination reactions was followed, a mixture of Ru(TPP)CO (11.4 mg, 1.5×10^{-2} mmol), 3,5-*bis*(trifluoromethyl)phenyl azide (196 mg, 7.7×10^{-1} mmol) and (2*S*)-methyl 3-phenyl-2-methoxy-propanoate (2.97 g, 15 mmol) in benzene (12 mL) was heated to reflux for 6.5 hours. Benzene was evaporated and the substrate excess was removed by high vacuum distillation. Yield =53%, *sin/anti* ratio = 1:1.05.

Characterisation for 59: *Syn/anti* assignment was done on the basis of chemical shift and coupling constants trends reported in the literature.[151] ^{1}H NMR (400 MHz, CDCl$_3$) major isomer (*anti*): δ 7.37-7.27 (5H, m, H$_{Ar}$), 7.11 (1H, s, H$_{Ar}$), 6.91 (2H, s, H$_{Ar}$), 5.37 (1H, d, *J* = 7.3 Hz, NH), 4.85 (1H, m, C*H*(NHAr)), 4.20 (1H, d, *J* = 4.7 Hz, C*H*(OMe)), 3.62 (3H, s, OCH$_3$ ester), 3.48 (3H, s, OCH$_3$ ether). Minor isomer (*syn*): δ 7.37-7.27 (5H, m, H$_{Ar}$), 7.09 (1H, s, H$_{Ar}$), 6.87 (2H, s, H$_{Ar}$), 5.27 (1H, d, *J* = 7.6 Hz, NH), 4.85 (1H, m, C*H*(NHAr)), 4.05 (1H, d, *J* = 3.0 Hz, C*H*(OMe)), 3.75 (3H, s, OCH$_3$ ester), 3.36 (3H, s, OCH$_3$ ether).

^{13}C NMR (75 MHz, CDCl$_3$) major isomer (*anti*): δ 170.8 (C=O), 147.4 (C$_{Ar}$), 136.6 (C$_{Ar}$), 132.4 (CF$_3$, q, *J* = 32.8 Hz), 128.9 (CH$_{Ar}$), 128.6 (CH$_{Ar}$), 127.3 (CH$_{Ar}$), 123.6 (CF$_3$, q, *J* = 272.6 Hz), 113.0 (CH$_{Ar}$), 110.9 (CH$_{Ar}$), 83.2 (*C*H(OMe)), 59.3 (OCH$_3$ ether), 59.1 (*C*H(NHAr)), 52.1 (OCH$_3$ ester). Minor isomer (*syn*): δ 170.2 (C=O), 147.5 (C$_{Ar}$), 138.2 (C$_{Ar}$), 132.4 (CF$_3$, q, *J* = 32.8 Hz), 129.0 (CH$_{Ar}$), 128.3 (CH$_{Ar}$), 127.1 (CH$_{Ar}$), 123.6 (CF$_3$, q, *J* = 272.6 Hz), 113.0 (CH$_{Ar}$), 110.9 (CH$_{Ar}$), 83.7 (*C*H(OMe), 59.6 (OCH$_3$ ether), 59.1 (*C*H(NHAr)), 52.5 (OCH$_3$ ester).

^{19}F NMR (282 MHz, CDCl$_3$) -63.59 (CF$_3$). EI-MS: 421 [M]$^+$.
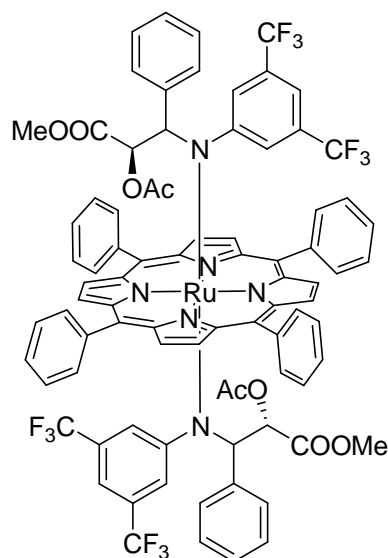
*Figure 40. Complex **104**.*

A porphyrin complex was isolated in the chromatographic purification of the reaction crude as a dark violet solid. MS (ESI+) analysis was suitable with the *bis*-amido complex **104** reported in ***Figure 40***. MS (ESI+) $m/z = 1633$ $[M+23]^+$ (M = $C_{84}H_{60}F_{12}N_6O_8Ru$).

3.10.6 Synthesis of β-lactam 64
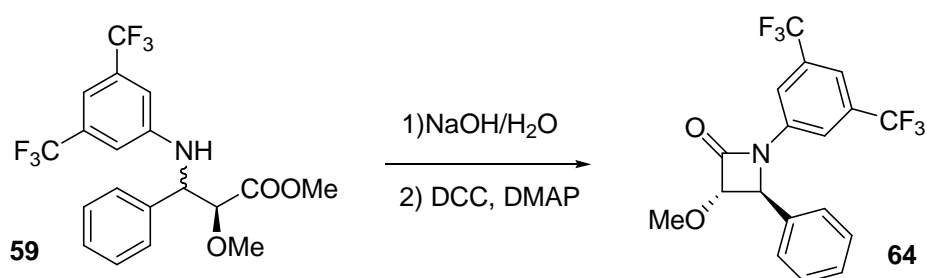
Amino ester **59** (189 mg, 4.5×10^{-1} mmol) was dissolved in THF (35 mL) and water (6.0 mL). NaOH was added (93 mg, 2.3 mmol). The solution was refluxed for 8 hours, then CH_2Cl_2 (60 mL) was added HCl 2M was added until an acidic pH was reached. The organic phase was washed with brine (50 mL × 3), dried over Na_2SO_4 and evaporated to dryness. The so-obtained crude was dissolved in CH_2Cl_2 (23 mL), *N,N'*-dicyclohexylcarbodiimide (DCC) (157 mg, 7.6×10^{-1} mmol) and dimethylaminopyridines (DMAP) (9.4 mg, 0.077 mmol) were added. The solution was stirred for 2 days at RT, then it was washed with H_2O (10 mL), AcOH(5%) (10 mL) and H_2O again (10 mL),

then it was dried over Na_2SO_4 and evaporated to dryness. Chromatographic purification (SiO2, n-hexane/AcOEt 8:2) gave pure **64** and unidentified side-products. Only one β-lactam diastereoisomer was formed in 30% yield, it was identified as the *trans* isomer because of the small coupling constant between the protons of the lactam backbone.

Characterisation for 64: ^{1}H NMR (300 MHz; CDCl$_3$) δ 7.70 (2H, s, H$_{Ar}$), 7.55 (1H, s, H$_{Ar}$), 7.44-7.30 (5H, m, H$_{Ar}$), 4.99 (1H, d, J = 1.9 Hz, CH(Ph)), 4.53 (1H, d, J = 1.9 Hz, CH(OMe)), 3.60 (3H, s, OCH$_3$ methoxy). ^{13}C NMR (75 MHz, CDCl$_3$) δ 164.8 (C=O), 138.5 (C$_{Ar}$), 135.0 (C$_{Ar}$), 132.8 (*C*-CF$_3$, q, J = 33.7 Hz), 129.8 (CH$_{Ar}$), 129.6 (CH$_{Ar}$), 126.1 (CH$_{Ar}$), 122.9 (CF$_3$, q, J = 273.1 Hz), 117.7 (CH$_{Ar}$), 117.3 (CH$_{Ar}$), 91.8 (*C*H(OMe)), 64.1 (*C*H(Ph)), 58.6 (OCH$_3$ methoxy). ^{19}F NMR(282 MHz, CDCl$_3$) δ -63.53 (CF$_3$). EI-MS: m/z = 389 [M]$^+$.

3.11. Ruthenium Porphyrin-Catalysed Synthesis of Indoles by the Reaction between Aryl Azides and Alkynes

3.11.1. Catalyst-free reaction of 3,5-*bis*(trifluoromethyl)phenyl azide (38) with phenylacetylene.
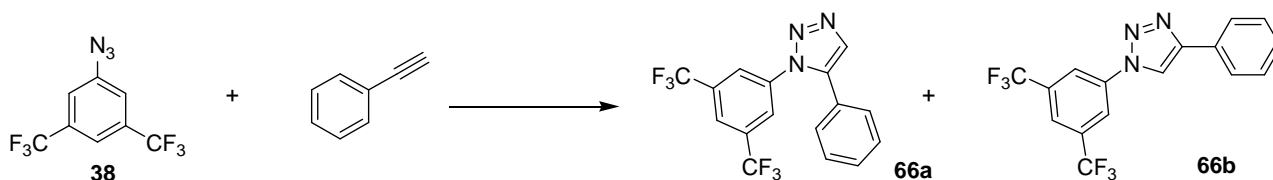
Experiment A: 3,5-*bis*(trifluoromethyl)phenyl azide (100.0 mg, 3.9×10^{-1} mmol) and phenylacetylene (0.21 mL, 1.9 mmol) were dissolved in decalin (7.0 mL) and stirred at 120°C for 4 hours. The solvent was evaporated to dryness and the crude was purified by flash chromatography (SiO$_2$, gradient elution from *n*-hexane/AcOEt = 19:1 to *n*-hexane/AcOEt = 9:1). Compounds **66b** (27.0 mg, 18%) and **66a** (118.0 mg, 80%) were both obtained as white solids.

Experiment B: The same reaction described above was performed by using refluxing benzene as the solvent (T = 80°C). After 5 hours only 12% of azide conversion was observed by measuring the absorbance value of the ν(N=N) signal (2116 cm^{-1}). GC-MS analysis revealed the presence of triazoles **66a** and **66b** beside the unreacted aryl azide.

1-(3,5-*bis*(trifluoromethyl)phenyl)-5-phenyl-1,2,3-triazole (66a): ^{1}H NMR (300 MHz, CDCl$_3$): δ 7.92 (1H, s, H$_{Ar\,para}$), 7.90 (1H, s, H$_{triazole}$), 7.86 (2H, s, H$_{Ar\,ortho}$), 7.52-7.35 (3H, m, H$_{Ph\,meta}$ and H$_{Ph\,para}$), 7.24 (2H, dd, $^2J_{HH}$ = 8.1 Hz, $^3J_{HH}$ = 1.6 Hz, H$_{Ph\,ortho}$). ^{13}C NMR (75 MHz, CDCl$_3$) 138.2 (C), 137.9 (C), 134.3 (CH$_{triazole}$), 133.2 (C-CF$_3$, q, $^2J_{CF}$ = 34.4 Hz), 130.3 (CH$_{Ph\,para}$), 129.5 (CH$_{Ph\,meta}$), 128.9 (CH$_{Ph\,ortho}$), 124.9 (CH$_{Ar\,ortho}$, q, $^3J_{CF}$ = 2.8 Hz) 122.7 (CH$_{Ar\,para}$, m), 122.6 (CF$_3$, q, $^1J_{CF}$ = 273.1 Hz). ^{19}F NMR (282 MHz, CDCl$_3$) -63.52 (CF$_3$). Anal. Calcd. for C$_{16}$H$_9$N$_3$F$_6$: C, 53.79; H, 2.54; N, 11.76. Found: C, 53.61; H, 2.49; N, 11.54. EI-MS: *m/z* = 357 [M]$^+$.

1-(3,5-*bis*(trifluoromethyl)phenyl)-4-phenyl-1,2,3-triazole (66b): ^{1}H NMR (300 MHz, CDCl$_3$): δ 8.31 (3H, m, H$_{Ar\,ortho}$ and H$_{triazole}$), 7.97 (1H, s, H$_{Ar\,para}$), 7.95 (2H, m, H$_{Ph\,ortho}$), 7.49 (2H, t, $^2J_{HH}$ = 7.3 Hz, H$_{Ph\,meta}$), 7.41 (1H, t, $^2J_{HH}$ = 7.3 Hz, H$_{Ph\,para}$). ^{13}C NMR (75 MHz, CDCl$_3$) 149.6 (C4$_{triazole}$), 138.2 (C$_{Ar}$), 133.9 (C-CF$_3$, q, $^2J_{CF}$ = 34.4 Hz), 129.6 (C$_{Ph}$), 129.23 (CH$_{Ph\,meta}$), 129.18 (CH$_{Ph\,para}$), 126.2 (CH$_{Ph\,ortho}$), 122.8 (CF$_3$, q, $^1J_{CF}$ = 273.1 Hz), 122.3 (CH$_{Ar\,para}$, m), 120.5 (CH$_{Ar\,ortho}$, q, $^3J_{CF}$ = 2.8 Hz), 117.3 (CH$_{triazole}$). ^{19}F NMR (282 MHz, CDCl$_3$) -63.31 (CF$_3$). Anal. Calcd. for C$_{16}$H$_9$N$_3$F$_6$: C, 53.79; H, 2.54; N, 11.76. Found: C, 53.66; H, 2.54; N, 11.41. EI-MS: *m/z* = 357 [M]$^+$.

3.11.2. Indole Synthesis

3.11.2. 1. Synthesis of 4,6-*bis*(trifluoromethyl)-3-phenylindole (65).
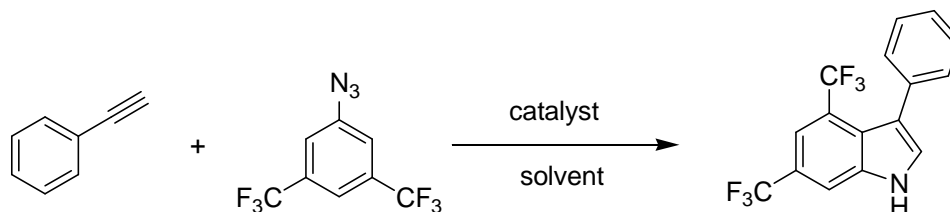
Method A: The general procedure for amination reactions was followed, a mixture of complex **10** (13.7 mg, 12×10^{-2} mmol), 3,5-*bis*(trifluoromethyl)phenyl azide (148 mg, 5.8×10^{-1} mmol) and phenylacetylene (320 µL, 2.9 mmol) in benzene (12 mL) was heated to reflux for 1 hour. Yield = 86%.

Purification conditions: *n*-hexane/AcOEt = 9:1

Catalyst and solvent screening using Method A: Ru(TPP)CO as the catalyst, yield = 65%, reaction time = 6 h; **92** as the catalyst, yield = 60%, reaction time = 14.5h; 1,2-dichloroethane as the solvent, yield = 73%, reaction time = 2.5h; *n*-hexane as the solvent, yield = 19%, reaction time = 12.5h; decalin as the solvent, T= 80°C, Yield = 36%, reaction time =12h.

Method A with additives: **a) Methanol**: The general procedure for amination reactions was followed, a mixture of complex **10** (13.0 mg, 1.1×10^{-2} mmol), 3,5-*bis*(trifluoromethyl)phenyl azide (135 mg, 5.3×10^{-1} mmol), phenylacetylene (290 µL, 2.6 mmol) and methanol (30 µL, 7.2×10^{-1} mmol) in benzene (12 mL) was heated to reflux for 1 hours. Yield = 90%.

b) Cyclohexene: The general procedure for amination reactions was followed, a mixture of complex **10** (13.5 mg, 1.2×10^{-2} mmol), 3,5-*bis*(trifluoromethyl)phenyl azide (150 mg, 5.9×10^{-1} mmol), phenylacetylene (310 µL, 2.8 mmol) and cyclohexene (290 µL, 1.0×10^{-1} mmol) in benzene (11 mL) was heated to reflux for 11 hours, when a 92% conversion in the aryl azide was reached. Yield (**65**) = 65%, yield(allylic amine **103**) = 8%. Complex **16** was detected by TLC analysis.

c) Triethylamine (TEA): The general procedure for amination reactions was followed, a mixture of complex **10** (9.9 mg, 8.4×10^{-3} mmol), 3,5-*bis*(trifluoromethyl)phenyl azide (107 mg, 4.2×10^{-1} mmol), phenylacetylene (230 µL, 2.1 mmol) and TEA (120 µL, 0.86 mmol) in benzene (11 mL) was heated to reflux for 6 hours. Yield = 10%.

Method B (*bis*-imido formation *in-situ*): 3,5-*bis*(trifluoromethyl)phenyl azide (5.8 mg, 2.3×10^{-2} mmol) was added to a benzene (8.0 mL) suspension of Ru(TPP)CO (5.6 mg, 7.6×10^{-3} mmol). The mixture was refluxed for 30 minutes, when the complete consumption of Ru(TPP)CO was observed (TLC monitoring, Al_2O_3, *n*-hexane/CH_2Cl_2 = 1:1). Then, phenylacetylene (208 µL, 1.9 mmol) and 3,5-*bis*(trifluoromethyl)phenyl azide (96.8 mg, 3.8×10^{-1} mmol) were added to the mixture and the general procedure for amination reactions for catalytic aminations was followed. The solution was refluxed for 5 h. Yield = 81%.
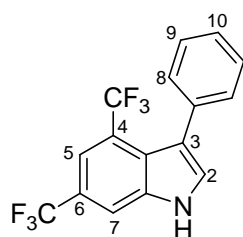
Characterisation for 4,6-*bis*(trifluoromethyl)-3-phenylindole: ^{1}H NMR (400 MHz, $CDCl_3$): δ 8.70 (1H, br, NH), 7.92 (1H, s, H7), 7.73 (1H, s, H5), 7.41 (1H, d, [3]J_{HH} = 2.6 Hz, H2), 7.39 (5H, m, H_{Ph}). ^{13}C-NMR (75 MHz, $CDCl_3$): δ 136.3 (C7-*C*-NH), 134.9 (C8-*C*-C3), 131.0 (C8-H), 128.6 (C2-H), 127.7 (C9-H), 127.5 (C10-H), 124.9 (C4-*C*-C3), 124.5(CF_3, q, [1]J_{CF} = 271.4 Hz), 123.8 (CF_3, q, [1]J_{CF} = 272.9 Hz), 123.7 (*C*-CF_3, q, [2]J_{CF} = 33.2 Hz), 122.9 (*C*-CF_3, q, [2]J_{CF} = 33.7 Hz), 119.6 (C3), 115.8 (C5-H, m), 112.7 (C7-H, q, [3]J_{CF} = 3.9 Hz). ^{19}F NMR (376 MHz, $CDCl_3$): δ -58.16 (CF_3), -61.03 (CF_3). Anal. Calcd. for $C_{16}H_9NF_6$: C, 58.37; H, 2.76; N, 4.25. Found: C, 58.60; H, 2.71; N, 4.33. EI-MS: *m/z* = 329 [M][+].

3.11.2. 2. Synthesis of 4,6-*bis*(trifluoromethyl)-3-*p*-tolylindole (72).
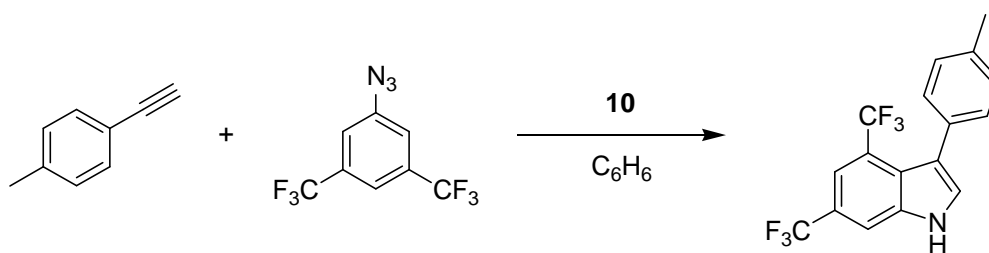
Method A: The general procedure for amination reactions was followed, a mixture of complex **10** (10.5 mg, 9.0×10^{-3} mmol), 3,5-*bis*(trifluoromethyl)phenyl azide (118 mg, 4.6×10^{-1} mmol) and 4-ethynyltoluene (280 µL, 2.5 mmol) in benzene (9.0 mL) was heated to reflux for 0.75 hours. Yield = 75%.

Purification conditions: *n*-hexane/AcOEt = 9:1.

Characterisation for 4,6-*bis*(trifluoromethyl)-3-*p*-tolylindole: ^{1}H NMR (300 MHz, CDCl$_3$): δ 8.67 (1H, br, NH), 7.91 (1H, s, H7), 7.72 (1H, s, H5), 7.38 (1H, d, $^3J_{HH}$ = 1.9 Hz, H2), 7.27 (2H, d, $^3J_{HH}$ = 8.6 Hz, H8), 7.21 (2H, d, $^3J_{HH}$ = 8.0 Hz, H9), 2.43 (3H, s, CH$_3$). ^{13}C-NMR (75 MHz, CDCl$_3$): δ 137.2 (C8-*C*-C3), 136.3 (C7-*C*-NH), 131.8 (C10), 130.8 (C8-H), 128.6 (C2-H), 128.4 (C9-H), 125.0 (C4-*C*-C3), 124.6 (CF$_3$, q, $^1J_{CF}$ = 271.6 Hz), 123.8 (CF$_3$, q, $^1J_{CF}$ = 272.9 Hz), 123.7 (*C*-CF$_3$, q, $^2J_{CF}$ = 33.2 Hz), 122.9 (*C*-CF$_3$, q, $^2J_{CF}$ = 33.7 Hz), 119.5 (C3), 115.7 (C5-H, m), 112.7 (C7-H, q, $^3J_{CF}$ = 3.9 Hz), 21.4 (CH$_3$). ^{19}F NMR (282 MHz, CDCl$_3$): δ -58.38 (CF$_3$), -61.34 (CF$_3$). Anal. Calcd. for C$_{17}$H$_{11}$NF$_6$: C, 59.31; H, 3.51; N, 4.07. Found: C, 59.10; H, 3.33; N, 4.10. EI-MS: *m/z* = 343 [M]$^+$.
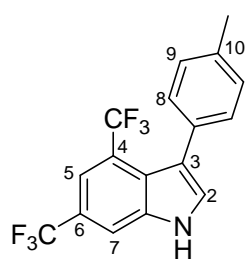
3.11.2. 3. Synthesis of 4,6-*bis*(trifluoromethyl)-3-(4-(trifluoromethyl)phenyl)indole (73).
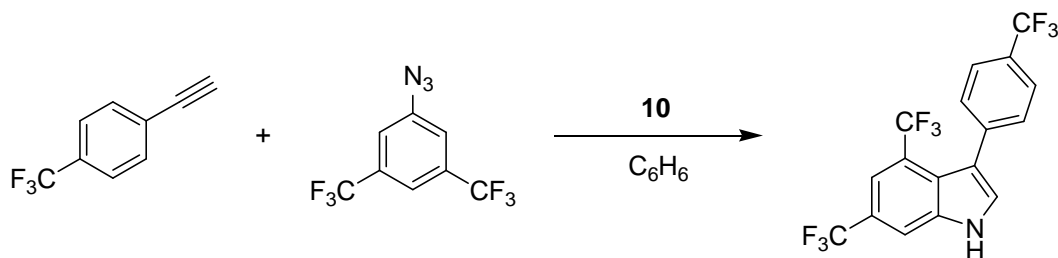
Method A: The general procedure for amination reactions was followed, a mixture of complex **10** (10.0 mg, 8.6×10^{-3} mmol), 3,5-*bis*(trifluoromethyl)phenyl azide (118 mg, 4.6×10^{-1} mmol) and 4-(trifluoromethyl)phenylacetylene (350 µL, 2.1 mmol) in benzene (9.0 mL) was heated to reflux for 14.5 hours, when an 83% conversion of the aryl azide was reached. Yield = 70%.
Purification conditions: *n*-hexane/AcOEt = 9:1).
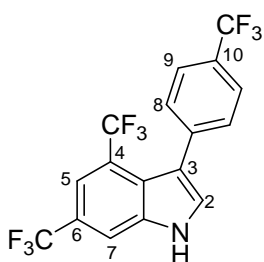
Characterisation for 4,6-*bis*(trifluoromethyl)-3-(4-(trifluoromethyl)phenyl)indole ^{1}H NMR (300 MHz, CDCl$_3$): δ 8.77 (1H, br, NH), 7.95 (1H, s, H7), 7.75 (1H, s, H5), 7.65 (2H, d, $^3J_{HH}$ = 8.2 Hz, H9), 7.50 (2H, d, $^3J_{HH}$ = 8.0 Hz, H8), 7.43 (1H, d, $^3J_{HH}$ = 2.6 Hz, H2). ^{13}C-NMR (75 MHz, CDCl$_3$): δ 138.8 (C3-*C*-C8), 136.3 (C7-*C*-NH), 131.2 (C8-H, q, $^4J_{CF}$ = 1.5 Hz), 128.7 (C2-H), 126.2 (C4-*C*-C3), 124.7 (C9-H, q, $^3J_{CF}$ = 3.7 Hz), 124.5 (CF$_3$, q, $^1J_{CF}$ = 272.1 Hz), 124.4 (CF$_3$, q, $^1J_{CF}$ = 271.6 Hz), 123.8 (*C*-CF$_3$, q, $^2J_{CF}$ = 33.5 Hz), 123.7 (CF$_3$, q, $^1J_{CF}$ = 272.7 Hz), 122.9 (*C*-CF$_3$, q, $^2J_{CF}$ = 33.6 Hz), 118.2 (C3), 116.1 (C5-H, m), 112.9 (C7-H, q, $^3J_{CF}$ = 3.8 Hz); one *C*-CF$_3$

signal was not detected. ^{19}F NMR (282 MHz, CDCl$_3$): δ -58.43 (C4-CF_3), -61.47 (C6-CF_3), -62.74 (C10-CF_3). Anal. Calcd. for C$_{17}$H$_8$NF$_9$: C, 51.27; H, 2.28; N, 3.52. Found: C, 51.44; H, 2.10; N, 3.61. EI-MS: m/z = 397 [M]$^+$.

3.11.2. 4. Synthesis of 4,6-*bis*(trifluoromethyl)-3-(4-methoxyphenyl) indole (74).
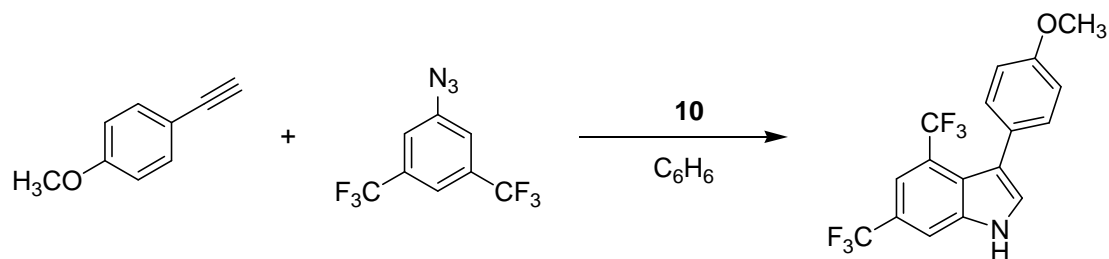
Method A: The general procedure for amination reactions was followed, a mixture of complex **10** (9.3 mg, 7.9×10^{-3} mmol), 3,5-*bis*(trifluoromethyl)phenyl azide (99.5 mg, 3.9×10^{-1} mmol) and 4-ethynylanisole (258 mg, 2.0 mmol) in benzene (9.0 mL) with 3Å molecular sieves (130 mg) with was heated to reflux for 0.5 hours. Yield = 95%.

Purification conditions: *n*-hexane/AcOEt = 9:1).

**Characterisation for4,6-*bis*(trifluoromethyl)-3-(4-methoxyphenyl)indole:** ^{1}H NMR (300 MHz, CDCl$_3$): δ 8.70 (1H, br, NH), 7.91 (1H, s, H7), 7.72 (1H, s, H5), 7.38 (1H, d, $^3J_{HH}$ = 2.8 Hz, H2), 7.29 (2H, d, $^3J_{HH}$ = 8.3 Hz, H8), 6.93 (2H, d, $^3J_{HH}$ = 8.8 Hz, H9), 3.87 (3H, s, CH$_3$). ^{13}C-NMR (75 MHz, CDCl$_3$): δ 159.2 (C10), 136.3 (C7-*C*-NH), 132.0 (C8-H), 128.7 (C2-H), 127.1 (C8-*C*-C3), 125.2 (C4-*C*-C3), 124.5 (CF$_3$ q, $^1J_{CF}$ = 271.8 Hz), 123.8 (CF$_3$, q, $^1J_{CF}$ = 273.2 Hz), 123.6 (*C*-CF$_3$, q, $^2J_{CF}$ = 33.4 Hz), 122.9 (*C*-CF$_3$, q, $^2J_{CF}$ = 33.2 Hz), 119.1(C3), 115.6 (C5-H, m), 113.1 (C9-H), 112.7 (C7-H, q, $^3J_{CF}$ = 4.2 Hz), 55.4 (OCH$_3$). ^{19}F NMR (282 MHz, CDCl$_3$): δ -58.42 (CF$_3$), -61.33 (CF$_3$). Anal. Calcd. for C$_{17}$H$_{11}$NOF$_6$: C, 56.83; H, 3.09; N, 3.90. Found: C, .02; H, 2.85; N, 3.52. EI-MS: m/z = 359 [M]$^+$.
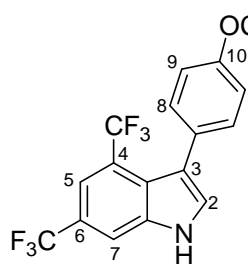
3.11.2.5. Synthesis of 4,6-*bis*(trifluoromethyl)-3-(4-fluorophenyl)indole (75).
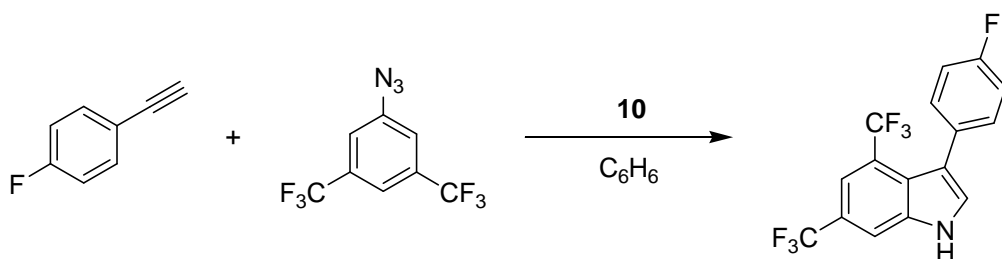
Method A: The general procedure for amination reactions was followed, a mixture of complex **10** (4.9 mg, 4.1×10^{-3} mmol), 3,5-*bis*(trifluoromethyl)phenyl azide (54.0 mg, 2.1×10^{-1} mmol) and 4-fluorophenylacetylene (120 µL, 1.1 mmol) in benzene (4 mL) with 3Å molecular sieves (37 mg) with was heated to reflux for 1.25 hours. Yield = 90%.

Purification conditions: gradient elution from *n*-hexane/AcOEt = 9:1 to *n*-hexane/AcOEt = 8:2.

Characterisation for 4,6-*bis*(trifluoromethyl)-3-(4-fluorophenyl)indole: ^{1}H NMR (400 MHz, CDCl$_3$): δ 8.72 (1H, br, NH), 7.92 (1H, s, H7), 7.73 (1H, s, H5), 7.40 (1H, d, $^3J_{HH}$ = 2.4 Hz, H2), 7.33 (2H, m, H8), 7.08 (2H, t, $^3J_{HH}$ = 8.7 Hz, H9). ^{13}C-NMR (100 MHz, CDCl$_3$): δ 162.6 (C10-F, d, $^1J_{CF}$ = 245.5 Hz), 136.2 (C7-*C*-NH), 132.6 (C8-H, d, $^3J_{CF}$ = 8.8 Hz), 130.6 (C8-*C*-C3), 125.0 (C4-*C*-C3), 124.5 (CF$_3$ q, $^1J_{CF}$ = 271.5 Hz), 123.9 (*C*-CF$_3$, q, $^2J_{CF}$ = 32.9 Hz), 123.7 (CF$_3$, q, $^1J_{CF}$ = 272.9 Hz), 122.9 (*C*-CF$_3$, q, $^2J_{CF}$ = 33.6 Hz), 118.4 (C3), 115.8 (C5-H, m), 114.6 (C9-H, d, $^2J_{CF}$ = 20.5 Hz), 112.8 (C7-H, q, $^3J_{CF}$ = 4.0 Hz). ^{19}F NMR (282 MHz, CDCl$_3$): δ -58.45 (CF$_3$), -61.40 (CF$_3$), -115.59 (F). Anal. Calcd. for C$_{16}$H$_8$NF$_7$: C, 55.34; H, 2.32; N, 4.03. Found: C, 55.36; H, 2.40; N, 3.80. EI-MS: *m/z* = 347 [M]$^+$.

3.11.2.6. Synthesis of 4,6-*bis*(trifluoromethyl)-3-(4-bromophenyl)indole (76).
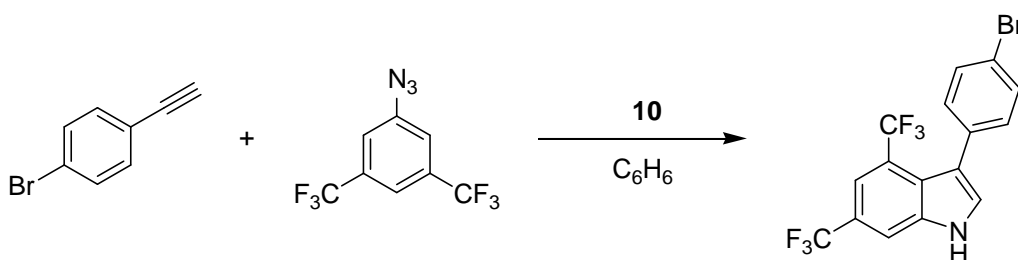
Method A: The general procedure for amination reactions was followed, a mixture of complex **10** (9 mg, 8.4×10^{-3} mmol), 3,5-*bis*(trifluoromethyl)phenyl azide (105 mg, 4.1×10^{-1} mmol) and 4-

bromophenylacetylene (374 mg, 2.1 mmol) in benzene (9.0 mL) was heated to reflux for 4.5 hours. Yield = 65%.

Purification conditions: *n*-hexane/AcOEt = 9:1).
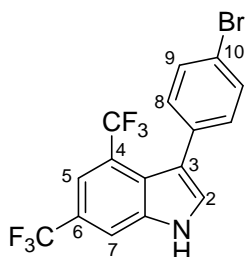
Characterisation for 4,6-*bis*(trifluoromethyl)-3-(4-fluorophenyl)indole: ^{1}H NMR (300 MHz, CDCl$_3$): δ 8.73 (1H, br, NH), 7.92 (1H, s, H7), 7.73 (1H, s, H5), 7.52 (1H, d, $^3J_{HH}$ = 8.3 Hz, H9), 7.39 (1H, d, $^3J_{HH}$ = 2.5 Hz, H2), 7.25 (2H, d, $^3J_{HH}$ = 8.0 Hz, H8). ^{13}C-NMR (75 MHz, CDCl$_3$): δ 136.3 (C7-*C*-NH), 133.8 (C10-Br), 132.6 (C8-H), 130.9 (CH-9), 128.6 (C2-H), 124.7 (C4-C-C3), 124.4 (CF$_3$, q, $^1J_{CF}$ = 271.4 Hz), 124.0 (*C*-CF$_3$, q, $^2J_{CF}$ = 33.4 Hz), 123.7 (CF$_3$,

q, $^1J_{CF}$ = 273.0 Hz), 121.8 (C3-*C*-C8), 122.9 (*C*-CF$_3$, q, $^2J_{CF}$ = 33.4 Hz), 118.3 (C3), 115.9 (C5-H, m), 112.8 (C7-H, q, $^3J_{CF}$ = 4.0 Hz). ^{19}F NMR (282 MHz, CDCl$_3$): δ -58.36 (CF$_3$), -61.41 (CF$_3$). Anal. Calcd. for C$_{16}$H$_8$NF$_6$Br: C, 47.09; H, 1.98; N, 3.43. Found: C, 47.22; H, 1.93; N, 3.35. EI-MS: *m/z* = 407 [M]$^+$.

3.11.2.7. Synthesis of 4,6-*bis*(trifluoromethyl)-3-(4-biphenyl)indole (77).
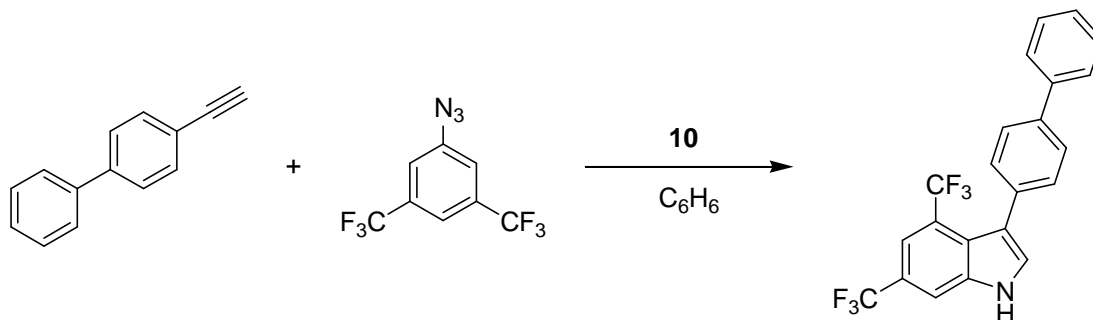

Method A: The general procedure for amination reactions was followed, a mixture of complex **10** (12.5 mg, 1.1×10^{-2} mmol), 3,5-*bis*(trifluoromethyl)phenyl azide (133 mg, 5.2×10^{-1} mmol) and 4-biphenylacetylene (470 mg, 2.6 mmol) in benzene (8.0 mL) was heated to reflux for 1 hour. Yield = 95%.

Purification conditions: *n*-hexane/AcOEt = 9:1) in order to obtain the pure indole product.

Characterisation for 4,6-*bis*(trifluoromethyl)-3-(4-biphenyl)indole: ^{1}H NMR (400 MHz, CDCl$_3$): δ 8.71 (1H, br, NH), 7.93 (1H, s, H7), 7.75 (1H, s, H5), 7.69 (2H, d, $^3J_{HH}$ = 7.2 Hz, H11), 7.65 (2H, d, $^3J_{HH}$ = 8.2 Hz, H9), 7.52-7.41 (4H, m, H12 and H8), 7.46 (1H, d, $^3J_{HH}$ = 2.2 Hz, H2), 7.37 (1H, t, $^3J_{HH}$ = 7.4 Hz, H13). ^{13}C-NMR (100 MHz, CDCl$_3$): δ 141.0 (*C*-C9), 140.2 (*C*-C11), 136.4 (C7-*C*-NH), 133.9 (C3-*C*-C8), 131.3 (C8-H), 128.9 (C12-H), 128.7 (C2-H), 127.4 (C13-H),
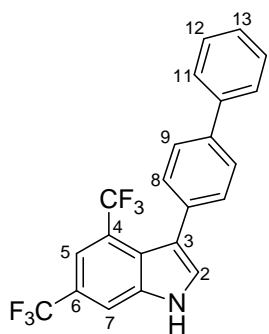
127.3 (C11-H), 126.4 (C9-H), 124.9 (C3-C-C4), 124.5 (CF$_3$, q, $^1J_{CF}$ = 271.7 Hz), 123.81 (CF$_3$, q, $^1J_{CF}$ = 272.9 Hz), 123.77 (C-CF$_3$, q, $^2J_{CF}$ = 33.2 Hz), 123.0 (C-CF$_3$, q, $^2J_{CF}$ = 33.7 Hz), 119.1 (C3), 115.8 (C5-H), 112.8 (C7-H, d, $^3J_{CF}$ = 3.8 Hz). ^{19}F NMR (282 MHz, CDCl$_3$): δ -58.30 (CF$_3$), -61.35 (CF$_3$). Anal. Calcd. for C$_{22}$H$_{13}$NF$_6$: C, 65.19; H, 3.23; N, 3.46. Found: C, 65.10; H, 3.32; N, 3.34. EI-MS: m/z = 405 [M]$^+$.

3.11.2.8. Synthesis of 4,6-*bis*(trifluoromethyl)-2,3-diphenylindole (79).
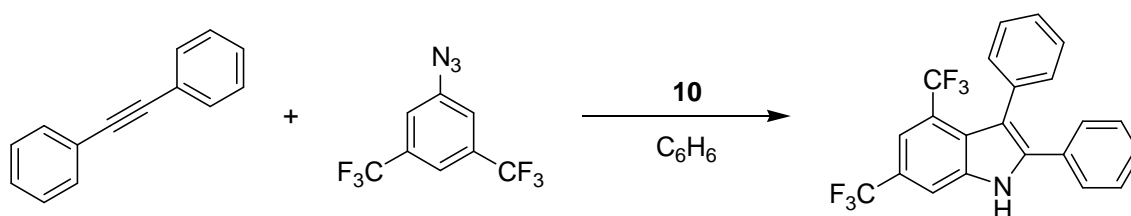
Method A: The general procedure for amination reactions was followed, a mixture of complex **10** (12.1 mg, 1.0×10^{-2} mmol), 3,5-*bis*(trifluoromethyl)phenyl azide (133 mg, 5.2×10^{-1} mmol) and diphenylacetylene (455 mg, 2.6 mmol) in benzene (9.0 mL) was heated to reflux for 15 hours, when a 88% conversion of the aryl azide was reached. Yield = 37%.

Purification conditions: *n*-hexane/AcOEt = 9:1.

Method B: The general procedure for amination reactions was followed, a mixture of complex **10** (11.0 mg, 9.4×10^{-3} mmol), 3,5-*bis*(trifluoromethyl)phenyl azide (112 mg, 4.4×10^{-1} mmol) and diphenylacetylene (1.42 g, 8.0 mmol) in benzene (9.0 mL) was heated to reflux for 29 hours, when a 95% conversion of the aryl azide was reached. Benzene was evaporated, the crude was filtrated over a short silica gel pad using *n*-hexane as eluent to recover the alkyne excess, the subsequent elution with *n*-hexane/AcOEt 6:4 gave the rest of the crude, which was analysed by ^{1}H-NMR. Yield = 40%.
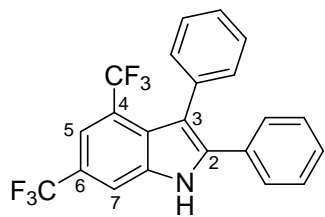
Characterisation for 4,6-*bis*(trifluoromethyl)-2,3-diphenylindole ^{1}H NMR (300 MHz, CDCl$_3$): δ 8.81 (1H, br, NH), 7.92 (1H, s, H7), 7.73 (1H, s, H5), 7.41-7.25 (10H, m, H$_{Ph}$). ^{13}C-NMR (75 MHz, CDCl$_3$): δ 139.9 (C), 135.8 (C), 134.5 (C), 132.1 (CH), 131.4 (C), 128.9 (CH), 128.7 (CH), 128.0 (CH), 127.6 (CH), 127.0 (C4-*C*-C3), 124.6 (CF$_3$, q, [1]J_{CF} = 271.7 Hz), 123.7 (CF$_3$, q, [1]J_{CF} = 272.9 Hz), 123.5 (*C*-CF$_3$, q, [2]J_{CF} = 33.1 Hz), 122.7 (*C*-CF$_3$, q, [2]J_{CF} = 33.6 Hz), 118.2 (C), 116.0 (C5-H, m), 112.2 (C7-H, q, [3]J_{CF} = 4.0 Hz). ^{19}F NMR (282 MHz, CDCl$_3$): δ -58.09 (CF$_3$), -61.34 (CF$_3$). Anal. Calcd. for C$_{22}$H$_{13}$NF$_6$: C, 65.19; H, 3.23; N, 3.46. Found: C, 64.91; H, 3.15; N, 3.54. EI-MS: *m/z* = 405 [M]$^+$.

3.11.2.9. Synthesis of 4,6-*bis*(trifluoromethyl)-2-methyl-3-phenylindole (78).
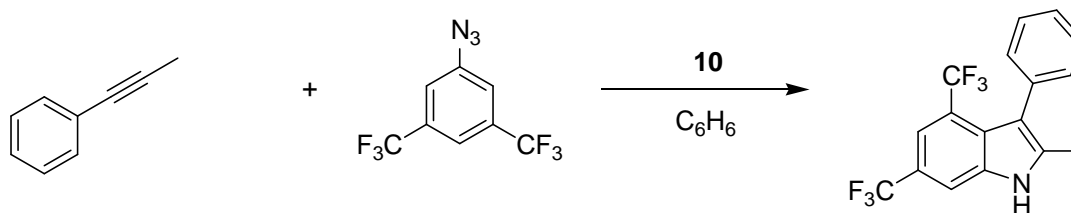
Method A: The general procedure for amination reactions was followed, a mixture of complex **10** (11.1 mg, 9.4×10^{-3} mmol), 3,5-*bis*(trifluoromethyl)phenyl azide (120 mg, 4.7×10^{-1} mmol) and 1-phenylpropyne (269 mg, 2.3 mmol) in benzene (9.0 mL) was heated to reflux for 28.5 hours, when a 99% conversion of the aryl azide was reached. Yield = 30%.

Purification conditions: *n*-hexane/AcOEt = 9:1.
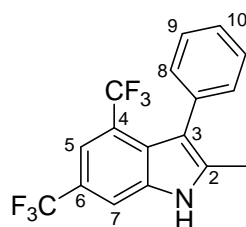
Characterisation for 4,6-*bis*(trifluoromethyl)-2-methyl-3-phenylindole ^{1}H NMR (400 MHz, CDCl$_3$): δ 8.49 (1H, br, NH), 7.78 (1H, s, H7), 7.67(1H, s, H5), 7.45-7.36 (3H, m, H9 and H10), 7.29 (2H, d, [3]J_{HH} = 7.4 Hz, H8), 2.29 (3H, s, CH$_3$). ^{13}C-NMR (100 MHz, CDCl$_3$): δ 138.6 (C2), 135.3 (C7-*C*-NH), 134.9 (C3-*C*-C8), 131.5 (C8-H), 127.9 (C9-H), 127.4 (C10-H), 126.5 (C4-*C*-C3), 124.7 (CF$_3$, q, [1]J_{CF} = 271.3 Hz), 123.8 (CF$_3$, q, [1]J_{CF} = 272.8 Hz), 122.4 (*C*-CF$_3$, q, [2]J_{CF} = 33.3 Hz), 121.5 (*C*-CF$_3$, q, [2]J_{CF} = 33.6 Hz), 115.8 (C3), 115.4 (C5-H, m), 111.5 (C7-H, q, [3]J_{CF} = 3.1 Hz), 12.6 (CH$_3$). ^{19}F NMR (282 MHz, CDCl$_3$): δ -58.06 (CF$_3$), -60.77 (CF$_3$). Anal. Calcd. for C$_{17}$H$_{11}$NF$_6$: C, 59.48; H, 3.23; N, 4.08. Found: C, 59.13; H, 3.24; N, 4.08. EI-MS: *m/z* = 343 [M]$^+$.

3.11.2.10 Synthesis of 4,6-dinitro-3-phenylindole (80).
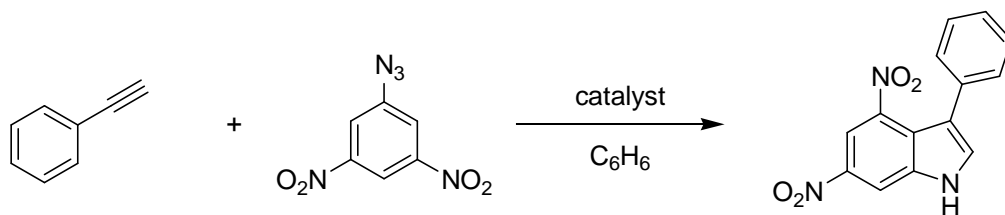
**Method A:** The general procedure for amination reactions was followed, a mixture of complex **10** (10.0 mg, 8.6×10^{-3} mmol), 3,5-dinitrophenyl azide (88 mg, 4.7×10^{-1} mmol) and phenylacetylene (230 µL, 2.1 mmol) in benzene (9.0 mL) was heated to reflux for 0.5 hours during which the formation of a yellow precipitate was observed. Benzene was evaporated, the crude was washed with dichloromethane (2.5 mL×2) obtaining a yellow solid (98 mg). Isolated yield = 82%

Reactions run using "modified Method A": complex **81** as the catalyst, yield = 75%, reaction time = 0.4h; Ru(TPP)CO as the catalyst, yield = 80%, reaction time = 0.6h.

Method B (*bis* imido formation *in-situ*): 3,5-dinitrophenyl azide (7.7 mg, 3.7×10^{-2} mmol) was added to a benzene (8.0 mL) suspension of Ru(TPP)CO (8.5 mg, 1.1×10^{-3} mmol). The mixture was refluxed for 5 minutes, when the complete consumption of Ru(TPP)CO was observed (TLC monitoring, Al_2O_3, *n*-hexane/CH_2Cl_2 = 1:1). Then, phenylacetylene (320 µL, 2.9 mmol) and 3,5-dinitrophenyl azide (121 mg, 5.8×10^{-1} mmol) were added to the mixture and the general procedure for amination reactions for catalytic aminations was followed. The solution was refluxed for 0.8 h, benzene was evaporated, the crude was washed with dichloromethane (2.5 mL×2) obtaining a yellow solid (138 mg). Isolated yield = 79%.

Characterisation for 4,6-dinitro-3-phenylindole: ^{1}H NMR (400 MHz, DMSO): δ 12.89 (1H, br, NH), 8.72 (1H, d, $^4J_{HH}$ = 1.0 Hz, H7), 8.54 (1H, d, $^4J_{HH}$ = 0.9 Hz, H5), 8.23 (1H, s, H2), 7.39 (2H, m, H9), 7.33 (1H, t, $^3J_{HH}$ = 7.1 Hz, H10), 7.23 (2H, d, $^3J_{HH}$ = 7.2Hz, H8). ^{13}C-NMR (75 MHz, DMSO) 140.8 (C5-NO_2), 140.1 (C7-NO_2), 137.4 (C7-*C*-NH), 136.0 (C2-H), 134.0 (C3-*C*-C8), 128.2 (C8-H), 127.8 (C9-H), 126.6 (C10-H), 119.6 (C4-*C*-C3), 117.2 (C3), 113.3 (C7-H), 111.7 (C5-H). Anal. Calcd. for $C_{14}H_9N_3O_4$: C, 59.37; H, 3.20; N, 14.84. Found: C, 59.11; H, 2.94; N, 14.64. ESI-MS: *m/z* = 282 [M-1]⁻.
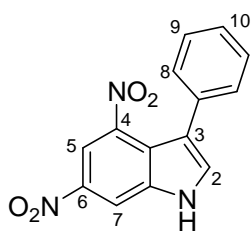
### 3.11.2.11 Synthesis of 4,6-dinitro-3-*p*-tolylindole (81).
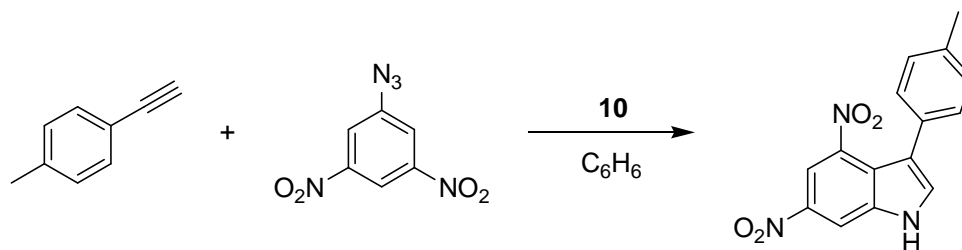
Method A: The general procedure for amination reactions was followed, a mixture of complex **10** (10.6 mg, 9.1×10^{-3} mmol), 3,5-dinitrophenyl azide (94.9 mg, 4.5×10^{-1} mmol) and *p*-tolylacetylene (0.280 µL, 2.2 mmol) in benzene (9.0 mL) with 3Å molecular sieves (90 mg) was heated to reflux for 0.5 hours. While the mixture was cooling at room temperature the formation of a yellow precipitate was observed. Benzene was evaporated, the crude was washed with dichloromethane (2.5 mL×2) obtaining a yellow solid (94 mg). Isolated yield = 70%

Characterisation for 4,6-dinitro-3-*p*-tolylindole: ^{1}H NMR (300 MHz, CD$_2$Cl$_2$) δ 12.85 (1H, s, NH), 8.71 (1H, d, $^4J_{HH}$ = 2.0 Hz, H7), 8.52 (1H, d, $^4J_{HH}$ = 2.0 Hz, H5), 8.19 (1H, s, H2), 7.20 (2H, d, $^3J_{HH}$ = 7.9 Hz, H9), 7.11 (2H, d, $^3J_{HH}$ = 8.0 Hz, H8), 2.35 (3H, s, CH$_3$). ^{13}C NMR (75 MHz, CDCl$_3$) δ 140.9 (C4), 140.0 (C6), 137.3 (C7-*C*-NH), 135.9 (C2-H), 135.8 (C10), 131.0 (C3-*C*-C8), 128.5 (C7-H), 128.1 (C5-H), 119.6 (C3-*C*-C4), 117.1 (C3), 113.2 (C8-H), 111.6 (C9-H), 20.7 (CH$_3$).
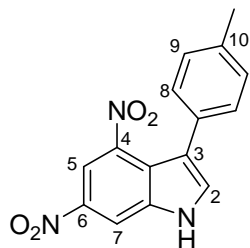
3.11.2.12 Synthesis of 4,6-dinitro-3- (4-(trifluoromethyl))phenylindole (82).
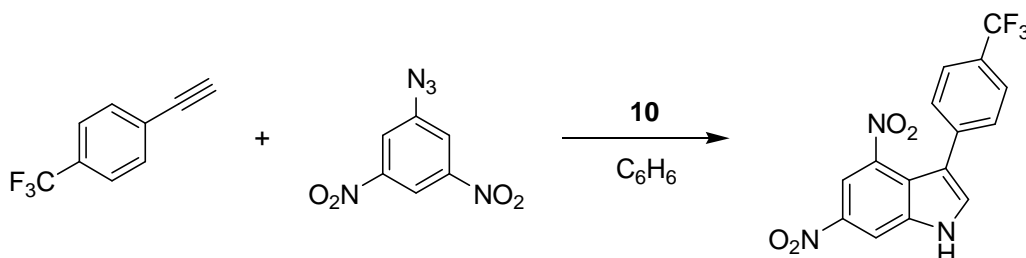
Method A: The general procedure for amination reactions was followed, a mixture of complex **10** (10.3 mg, 8.6×10^{-3} mmol), 3,5-dinitrophenyl azide (91.6 mg, 4.4×10^{-1} mmol) and 4-(trifluoromethyl)phenylacetylene (360 µL, 2.2 mmol) in benzene (9.0 mL) with 3Å molecular sieves (90 mg) was heated to reflux for 2.5 hours during which the formation of a yellow precipitate

was observed. Benzene was evaporated, the crude was washed with dichloromethane (2.5 mL×2) obtaining a yellow solid (98 mg). Isolated yield = 68%
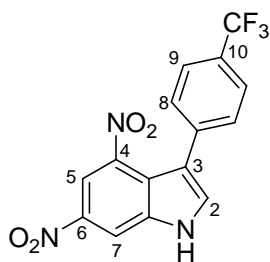

Characterisation for 4,6-dinitro-3-(4-(trifluoromethyl))phenylindole: ^{1}H NMR (300 MHz, DMSO) δ 13.04 (1H, s, NH), 8.76 (1H, s, H7), 8.61 (1H, s, H5), 8.35 (1H, s, H2), 7.76 (2H, d, $^3J_{HH}$ = 8.0 Hz, H9), 7.47 (2H, d, $^3J_{HH}$ = 8.0 Hz, H8). ^{13}C NMR (75 MHz, DMSO): δ 140.6 (C6), 140.3 (C4), 138.6 (C3-*C*-C8), 137.6 (C7-*C*-NH), 136.9 (C2-H), 129.1 (C8-H), 127.0 (q, $^3J_{CF}$= 31.8 Hz, C9-H), 124.62 (q, $^2J_{CF}$ = 3.6 Hz, *C*-CF₃), 124.43 (q, $^1J_{CF}$ = 271.8 Hz, CF₃), 119.7 (C3-*C*-C4), 115.8 (C3), 113.7 (C8-H), 112.3 (C9-H). ^{19}F NMR (282 MHz, DMSO): δ -61.02 (CF₃).

3.11.2.13 Synthesis of 4,6-dinitro-3-(4-byphenyl)indole (83).
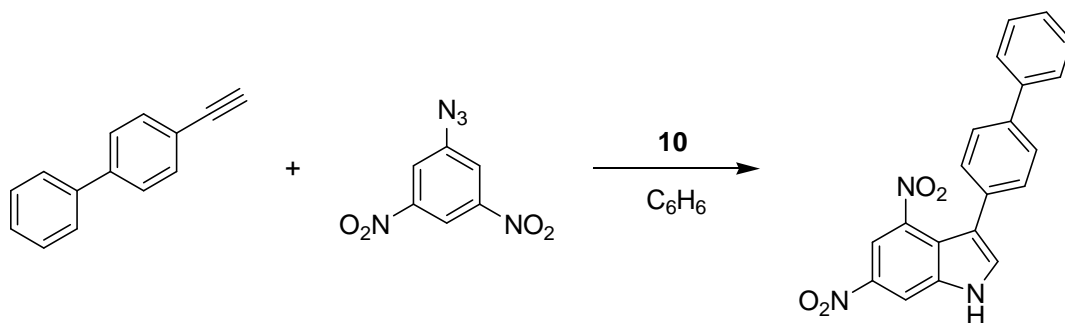
Method A: The general procedure for amination reactions was followed, a mixture of complex **10** (10.2 mg, 8.7×10⁻³ mmol), 3,5-dinitrophenyl azide (90.8 mg, 4.3×10⁻¹ mmol) and 4-biphenylacetylene (392 mg, 2.2 mmol) in benzene (9.0 mL) with 3Å molecular sieves (90 mg) was heated to reflux for 0.25 hours during which the formation of a yellow precipitate was observed. Benzene was evaporated, the crude was washed with *n*-hexane (7.5 mL×2) and dichloromethane (2.5 mL×2) obtaining a yellow solid (136 mg). Isolated yield = 87%
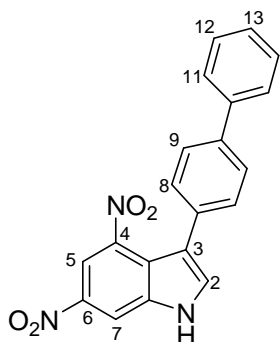
Characterisation for 4,6-dinitro-3-(4-byphenyl)indole: ^{1}H NMR (300 MHz, DMSO): δ 8.75 (1H, m, H7), 8.58 (1H, m, H5), 8.30 (1H, s, H2), 7.73 (4H, t, $^3J_{HH}$ = 8.1 Hz, H9 and H11), 7.49 (2H, t, $^3J_{HH}$ = 7.4 Hz, H12), 7.38 (1H, m, H13), 7.33 (2H, d, $^3J_{HH}$ = 8.4 Hz, H8), NH was not detected. ^{13}C NMR (75 MHz, CDCl3): δ 140.8 (C4), 140.1 (C6), 139.7 (*C*-C11), 138.3 (*C*-C9), 137.5 (C7-*C*-NH), 136.3 (C2-H), 133.3 (C3-*C*-C8), 129.0

(C12-H), 128.8 (C8-H), 127.4 (C13-H), 126.5 (C11-H), 126.0 (C9-H), 119.7 (C3-*C*-C4), 116.8 (C3), 113.5 (C7-H), 111.9 (C5-H).

3.11.2.14 Synthesis of 4,6-dinitro-3-(4-bromophenyl)indole (84).
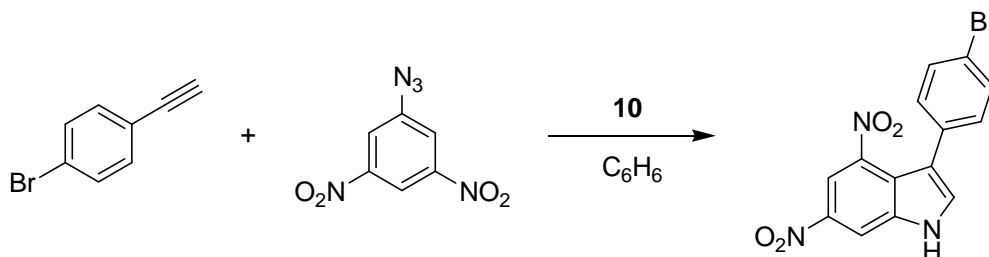
Method A: The general procedure for amination reactions was followed, a mixture of complex **10** (8.2 mg, 7.0×10^{-3} mmol), 3,5-dinitrophenyl azide (71.0 mg, 0.34 mmol) and 4-bromophenylacetylene (307 mg, 1.69 mmol) in benzene (7 mL) with 3Å molecular sieves (68 mg) was heated to reflux for 0.5 hours during which the formation of a yellow precipitate was observed. Benzene was evaporated, the crude was washed with *n*-hexane (2.5 mL×2) and dichloromethane (2.5 mL×2) obtaining a yellow solid (102 mg). Isolated yield = 83%

**Characterisation for 4,6-dinitro-3-(4-bromophenyl)indole** ^{1}H NMR (300 MHz, DMSO) δ 12.95 (1H, s, NH), 8.73 (1H, d, $^4J_{HH}$ = 1.5 Hz, H7), 8.57 (1H, d, $^4J_{HH}$ = 1.5 Hz, H5), 8.26 (1H, s, H2), 7.58 (2H, d, $^3J_{HH}$ = 8.2 Hz, H9), 7.19 (2H, d, $^3J_{HH}$ = 8.2 Hz, H8). ^{13}C NMR (75 MHz, DMSO) δ 140.63 (C6), 140.15 (C4), 137.45 (C7-*C*-NH), 136.36 (C2-H), 133.50 (C3-*C*-C8), 130.67 (C9-H), 130.42 (C8-H), 119.84 (C10), 119.63 (C3-*C*-C4), 115.93 (C3), 113.54 (C7-H), 112.01 (C5-H).
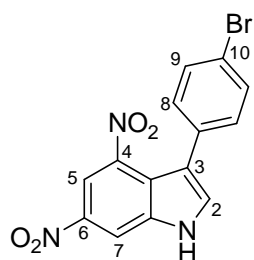
### 3.11.2.15 Synthesis of 4,6-dichloro-3-phenylindole (85).
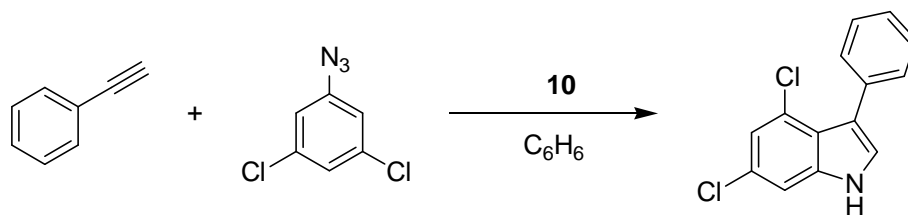
Method A: The general procedure for amination reactions was followed, a mixture of complex **10** (13 mg, 1.1×10^{-2} mmol), 3,5-dichlorophenyl azide (105 mg, 5.6×10^{-1} mmol) and phenylacetylene (300 µL, 2.7 mmol) in benzene (12 mL) was heated to reflux for 6 hours. Yield = 25%.

Method B: The general procedure for amination reactions was followed, a mixture of complex **10** (9.4 mg, 8.0×10^{-3} mmol), 3,5-dichlorophenyl azide (74.4 mg, 4.0×10^{-1} mmol) and phenylacetylene (880 µL, 8.0 mmol) in benzene (9.0 mL) was heated to reflux for 1.5 hours. The mixture was distilled and the benzene/phenylacetylene mixture was kept under nitrogen to be used as the solvent for the subsequent reaction. Yield = 60%.

Purification conditions: gradient elution from *n*-hexane/AcOEt = 9.5:0.5 to *n*-hexane/AcOEt = 9:1.

Method C (alkyne recycle): Complex **10** (9.3 mg, 7.8×10^{-3} mmol) and 3,5-dichlorophenyl azide (77.2 mg, 4.1×10^{-1} mmol) were added to the previously distilled benzene/phenylacetylene mixture (see ***Method B***), the general procedure for amination reactions for catalytic amination was followed the mixture was heated to reflux for 3.5 hours. Yield = 32%.
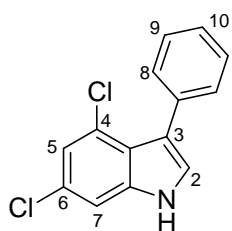
Characterisation for 4,6-dichloro-3-phenylindole. ^{1}H NMR (300 MHz, CDCl$_3$): δ 8.31 (1H, br, NH), 7.50 (2H, d, $^3J_{HH}$ = 6.9 Hz, H8), 7.46-7.34 (3H, m, H9 and H10), 7.32 (1H, d, $^4J_{HH}$ = 1.2 Hz, H7), 7.17 (1H, d, $^3J_{HH}$ = 2.2 Hz, H2), 7.16 (1H, d, $^4J_{HH}$ = 1.3 Hz, H5). ^{13}C NMR (100 MHz, CDCl$_3$) δ 137.5 (C7-*C*-NH), 134.6 (C3-*C*-C8), 131.0 (C8-H), 128.0 (C-Cl), 127.6 (C9-H), 127.2 (C-Cl), 126.9 (C10-H), 124.9 (C2-H), 122.2 (C3-*C*-C4), 121.8 (C5-H), 119.5 (C3), 110.1 (C7-H). EI-MS: 261 [M]$^+$.

**3.11.2.16 Synthesis of 4-(trifluoromethyl)-3-phenylindole (86a).**
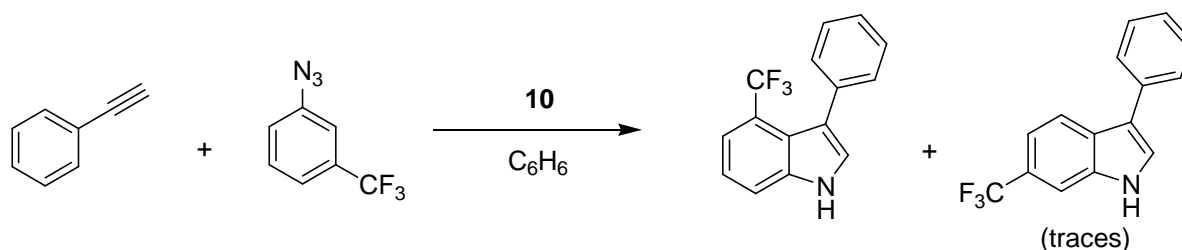
Method A: The general procedure for amination reactions was followed, a mixture of complex **10** (13 mg, 1.1×10^{-2} mmol), 3-(trifluoromethyl)phenyl azide (105 mg, 5.6×10^{-1} mmol) and phenylacetylene (300 µL, 2.7 mmol) in benzene (12 mL) was heated to reflux for 11 hours, when a 67% conversion in the aryl azide was reached. Yield = 20%.

Method A with additives: **a) Ethanol**: The general procedure for amination reactions was followed, a mixture of complex **10** (13.8 mg, 1.2×10^{-2} mmol), 3-(trifluoromethyl)phenyl azide (112 mg, 6.0×10^{-1} mmol), phenylacetylene (320 µL, 2.9 mmol) and ethanol (68 µL, 1.2 mmol) in benzene (12 mL) with 3Å molecular sieves (118 mg) was heated to reflux for 14 hours, when a 91% conversion in the aryl azide was reached. Yield (**86a**) = 24%

b) Benzoic Acid: The general procedure for amination reactions was followed, a mixture of complex **10** (11.5 mg, 9.8×10^{-3} mmol), 3-(trifluoromethyl)phenyl azide (98 mg, 5.2×10^{-1} mmol), phenylacetylene (270 µL, 2.5 mmol) and benzoic acid (12.7 mg, 1.0×10^{-1} mmol) in benzene (10 mL) was heated to reflux for 6 hours, when a 91% conversion in the aryl azide was reached.
Yield (**86a**) = 35%

Method B: The general procedure for amination reactions was followed, a mixture of complex **10** (8.4 mg, 8.0×10^{-3} mmol), 3-(trifluoromethyl)phenyl azide (78.1 mg, 4.2×10^{-1} mmol) and phenylacetylene (925 µL, 8.4 mmol) in benzene (9.0 mL) was heated to reflux for 6 hours.
Purification conditions: *n*-hexane/AcOEt = 9:1. The product was isolated as a mixture of **86a/86b** (as detected by GC-MS analysis, ***Figure 41***) in a 16:1 ratio (evaluated by ^{19}F NMR).
Isolated yield = 88%.
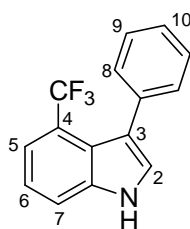
Characterisation for 4-(trifluoromethyl)-3-phenylindole: ^{1}H NMR (300 MHz, CDCl$_3$): δ 8.46 (1H, br, NH), 7.62 (1H, d, $^3J_{HH}$ = 8.2 Hz, H7), 7.50 (1H, d, $^3J_{HH}$ = 7.4 Hz, H5), 7.46-7.34 (5H, m, H$_{Ph}$), 7.29 (1H, m, H6), 7.24 (1H, d, $^3J_{HH}$

= 2.4 Hz, H2). ^{19}F NMR (282 MHz, CDCl$_3$) -57.99 (CF$_3$ $_{86a}$), -58.45 (CF$_3$ $_{86b}$). ^{13}C NMR (75 MHz, CDCl$_3$) δ 137.16 (C7-*C*-NH), 135.97 (C3-*C*-C8), 130.98 (C8-H), 127.54 (C9-H), 127.05 (C10-H), 125.89 (C2-H), 124.54 (q, $^1J_{CF}$ = 272.6 Hz, CF$_3$), 122.6 (C3-*C*-C4), 122.16 (q, $^2J_{CF}$ = 32.7 Hz, C4), 121.28 (C6-H), 119.0 (C3), 118.92 (q, $^3J_{CF}$ = 6.2 Hz, C5-H), 115.33 (C7-H). EI-MS: 261 [M]$^+$.
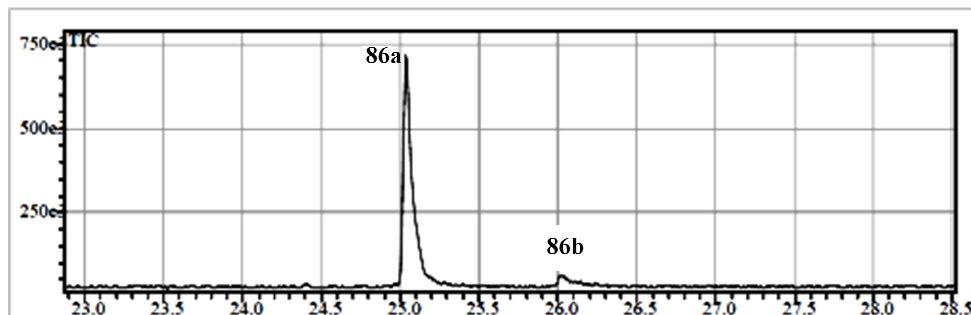
Figure 41. GC-MS *chromatogram of the* **86a/86b** *mixture*

### 3.11.2.17 Synthesis of 4-nitro-3-phenylindole (87a) and 6-nitro-3-phenylindole (87b).
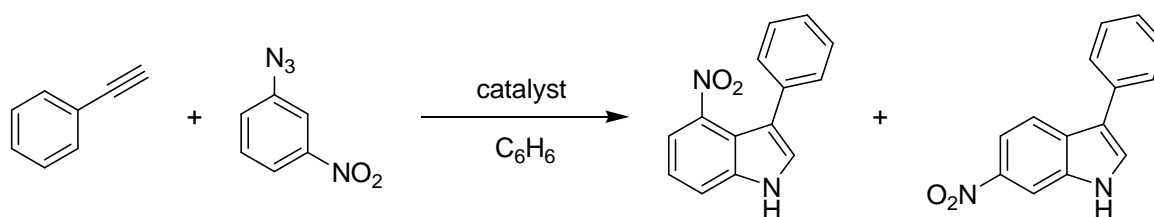
Method A: The general procedure for amination reactions was followed, a mixture of complex **10** (10.0 mg, 8.6×10^{-3} mmol), 3-nitrophenyl azide (69.2 mg, 4.2×10^{-1} mmol) and phenylacetylene (230 µL, 2.1 mmol) in benzene (9.0 mL) with 3Å molecular sieves (133 mg) was heated to reflux for 3.5 hours.

Yield (**79a**) = 27%, yield (**79b**) = 13%.

Method A using Ru(TPP)CO as the catalyst: reaction time = 12h (91% conversion). Yield (**79a**) = 21%, yield (**79b**) = 8%.

Method B (*bis*-imido formation *in-situ*): 3-nitrophenyl azide (5.4 mg, 3.3×10^{-2} mmol) was added to a benzene (11 mL) suspension of Ru(TPP)CO (8.1 mg, 1.1×10^{-2} mmol) with 3Å molecular sieves (85 mg). The mixture was refluxed for 20 minutes, when an almost complete consumption of Ru(TPP)CO was observed (TLC monitoring, Al$_2$O$_3$, *n*-hexane/CH$_2$Cl$_2$ = 1:1). Then, phenylacetylene (300 µL, 2.7 mmol) and 3-nitrophenyl azide (84.4 mg, 5.1×10^{-1} mmol) were added

to the mixture and the general procedure for amination reactions for catalytic aminations was followed. The solution was refluxed for 12 h. Yield (**79a**) = 22%, yield (**79b**) = 8%.

Method C: The general procedure for amination reactions was followed, a mixture of complex **10** (10.9 mg, 9.2×10^{-3} mmol), 3-nitrophenyl azide (76.7 mg, 4.7×10^{-1} mmol) and phenylacetylene (1.0 mL, 9.1 mmol) in benzene (8.0 mL) was heated to reflux for 4.5 hours. Yield (**79a**) = 45%, yield (**79b**) = 15%.

Purification conditions: *n*-hexane/AcOEt = 8:2.

Characterisation for 4-nitro-3-phenylindole: ^{1}H NMR (300 MHz, DMSO): δ 12.20 (1H, br, NH), 7.88 (1H, d, $^{3}J_{HH}$ = 8.0 Hz, H7), 7.80 (1H, s, H2), 7.78 (1H, d, $^{3}J_{HH}$ = 8.1 Hz, H5), 7.39-7.31 (3H, m, H9 + H6), 7.26 (1H, t, $^{3}J_{HH}$ = 7.3 Hz, H10), 7.18 (2H, d, $^{3}J_{HH}$ *J* = 7.0 Hz, H8). ^{13}C-NMR (75 MHz, DMSO) 142.2 (C4), 138.8 (C7-*C*-NH), 135.4 (C8-*C*-C3), 129.5 (C2-H), 128.0 (C8-H), 127.6 (C9-H), 125.9 (C10-H), 120.5 (C6-H), 117.9 (C7-H), 116.6 (C5-H), 116.1 (C3-*C*-C4), 115.8 (C3). Anal. Calcd. for $C_{14}H_{10}N_2O_2$: C, 70.58; H, 4.23; N, 11.76. Found: C, 70.21; H, 3.99; N, 11.87. ESI-MS: *m/z* = 237 [M-1]$^-$.
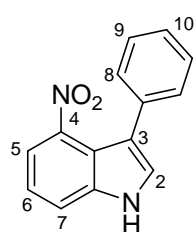
Characterisation for 6-nitro-3-phenylindole ^{1}H NMR (400 MHz, DMSO): δ ^{1}H NMR (300 MHz, DMSO): δ 12.13 (1H, br, NH), 8.40 (1H, d, $^{4}J_{HH}$ = 2.0 Hz, H7), 8.14 (1H, d, $^{3}J_{HH}$ = 2.2 Hz, H2), 8.03 (1H, d, $^{3}J_{HH}$ = 8.9 Hz, H4), 7.97 (1H, dd, $^{3}J_{HH}$ = 8.7 Hz, ^{4}J = 1.7 Hz, H5), 7.72 (2H, d, $^{3}J_{HH}$ = 7.5 Hz, H8), 7.48 (2H, t, $^{3}J_{HH}$ = 7.7 Hz, H9), 7.31 (1H, t, $^{3}J_{HH}$ = 7.4 Hz, H10). ^{13}C-NMR (100 MHz, DMSO) 142.0 (C6-NO_2), 135.3 (C7-*C*-NH), 134.2 (C3-*C*-C8), 130.3 (C2-H), 129.5 (C3-*C*-C4), 128.9 (C9-H), 126.8 (C8-H), 126.2 (C10-H), 119.3 (C4-H), 116.9 (C3), 114.7 (C5-H), 108.7 (C6-H). Anal. Calcd. for $C_{14}H_{10}N_2O_2$: C, 70.58; H, 4.23; N, 11.76. Found: C, 70.23; H, 4.49; N, 11.52. ESI-MS: *m/z* = 237 [M-1]$^-$.
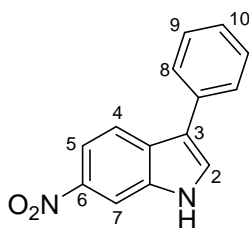
3.11.2.18 Synthesis of 5-methyl-4-nitro-3-phenylindole (80a) and 5-methyl-6-nitro-3-phenylindole (80b).
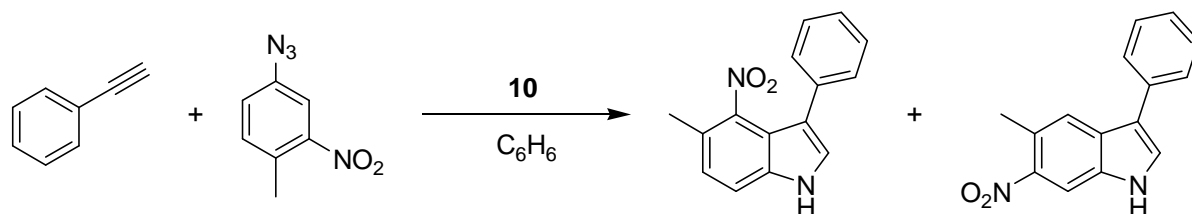
Method A: The general procedure for amination reactions was followed, a mixture of complex **10** (10.0 mg, 8.6×10^{-3} mmol), 4-methyl-3-nitrophenyl azide (75.1 mg, 4.2×10^{-1} mmol) and phenylacetylene (230 µL, 2.1 mmol) in benzene (9.0 mL) with 3Å molecular sieves (133 mg) was heated to reflux for 4.5 hours.

Yield (**80a**) = 24%, yield (**80b**) = traces

Method B: The general procedure for amination reactions was followed, a mixture of complex **10** (10.0 mg, 8.8×10^{-3} mmol), 4-methyl-3-nitrophenyl azide (77.3 mg, 4.3×10^{-1} mmol) and phenylacetylene (950 µL, 8.7 mmol) in benzene (9.0 mL) with 3Å molecular sieves (130 mg) was heated to reflux for 6 hours. Yield (**80a**) = 35%, yield (**80b**) = 6%.

Purification conditions: *n*-hexane/AcOEt = 8:2.
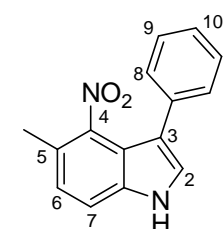
Characterisation for 5-methyl-4-nitro-3-phenylindole: ^{1}H NMR (300 MHz, CDCl$_3$): δ 8.49 (1H, br, NH), 7.46 (1H, d, $^3J_{HH}$ = 8.3 Hz, H7), 7.42-7.25 (5H, m, H$_{Ph}$), 7.28 (1H, s, H2), 7.12 (1H, d, $^3J_{HH}$ = 8.4 Hz, H6), 2.46 (3H, s, CH$_3$). ^{13}C-NMR (75 MHz, CDCl$_3$): δ 143.3 (C4-NO$_2$), 136.6 (C7-*C*-NH), 134.1 (C3-*C*-C8), 128.4(CH$_{Ph}$), 128.3(CH$_{Ph}$), 127.1 (C10-H), 125.8 (C2-H), 125.1 (C6-H), 122.5 (*C*5-CH$_3$), 117.5 (C3), 117.4 (C4-*C*-C3), 114.2 (C7-H), 17.8 (CH$_3$). Anal. Calcd. for C$_{15}$H$_{12}$N$_2$O$_2$: C, 71.42; H, 4.79; N, 11.10. Found: C, 71.33; H, 4.59; N, 10.85. ESI-MS: *m/z* = 252 [M]$^+$.
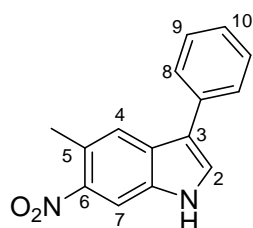
Characterisation for 5-methyl-6-nitro-3-phenylindole: ^{1}H NMR (300 MHz, CDCl$_3$): δ 8.57 (1H, br, NH), 8.25 (1H, s, H7), 7.78 (1H, s, H4), 7.63 (2H, m, H$_{Ph}$), 7.59 (1H, d, $^3J_{HH}$ = 2.6 Hz, H2), 7.49 (2H, t, $^3J_{HH}$ = 7.7 Hz, H$_{Ph}$), 7.36 (1H, m, H$_{Ph}$), 2.73 (3H, s, CH$_3$). ESI-MS: *m/z* = 252 [M]$^+$.

3.11.2.19. Synthesis of 4,6-*bis*(trifluoromethyl)-2-carboxyethylindole (105).
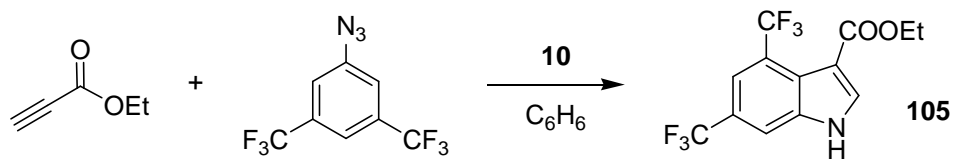
Method A: The general procedure for amination reactions was followed, a mixture of complex **10** (11.3 mg, 9.5×10^{-3} mmol), 3,5-*bis*(trifluoromethyl)phenyl azide (121.6 mg, 4.8×10^{-1} mmol) and phenylacetylene (240 µL, 2.4 mmol) in benzene (9.0 mL) with 3Å molecular sieves (130 mg) was heated to reflux for 13 hours reaching a 98% conversion. The corresponding triazole species were detected in the reaction crude by ^{1}H NMR analysis as the major products. Yield (**105**) = 13%. Purification conditions: *n*-hexane/AcOEt = 8:2.

Characterisation for 4,6-*bis*(trifluoromethyl)-2-carboxyethylindole: ^{1}H NMR (400 MHz, CDCl$_3$) δ 9.26 (1H, s, NH), 8.10 (1H, s, H7), 7.91 (1H, s, H5), 7.87 (1H, s, H2), 4.38 (2H, q, *J* = 7.1 Hz, O-CH$_2$), 1.39 (3H, t, *J* = 7.1 Hz, CH$_2$-C*H$_3$*).

3.11.3. Reaction of 9a/9b mixture with Ru(TPP)CO.
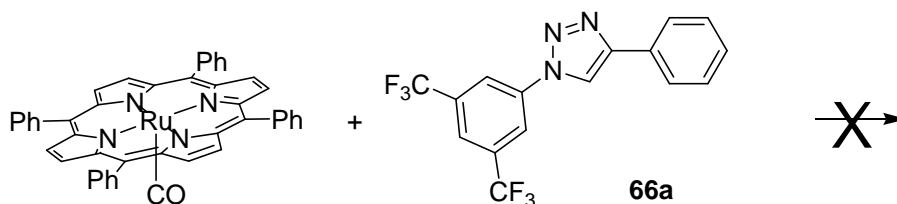
Ru(TPP)CO (4.4 mg, 5.9×10^{-3} mmol) was suspended in benzene (10.0 mL) and the triazole **66a** (39.7 mg, 1.1×10^{-1} mmol) was added. The red solution was refluxed for 6 h, no reaction was observed by TLC monitoring.

3.11.4. Reaction between Ru(TPP)(NAr)$_2$ (Ar = 3,5-(CF$_3$)$_2$C$_6$H$_3$) (6) and phenylacetylene (2a).
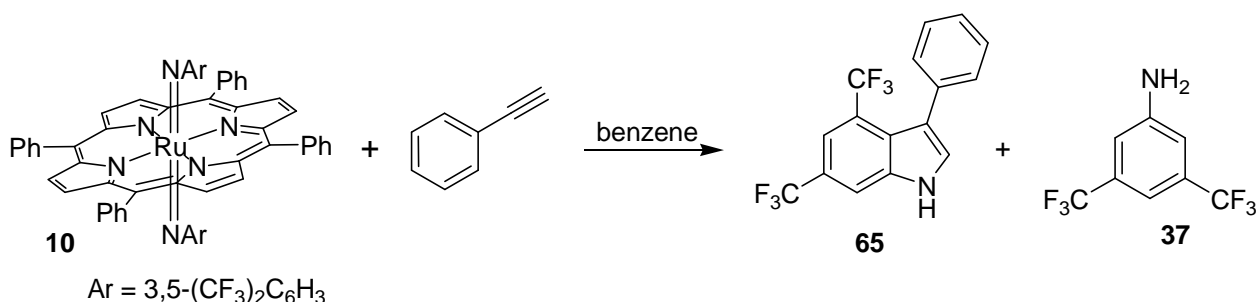
Complex **10** (57.4 mg, 4.9×10^{-2} mmol) was dissolved in benzene (30 mL) and phenylacetylene (27 µL, 2.4×10^{-1} mmol) was added. The solution was refluxed till the complete disappearance of **10** (TLC monitoring, Al$_2$O$_3$, *n*-hexane/CH$_2$Cl$_2$ = 9:1). GC-MS analysis revealed the formation of indole **65** and 3,5-*bis*(trifluoromethyl)aniline. The solvent was evaporated to dryness and the crude was purified by flash chromatography (silica gel, *n*-hexane/AcOEt = 9:1) obtaining 7.0 mg of **65**, (44% yield, considering the transfer of only one nitrene functionality from **10** to phenylacetylene). The yield was confirmed also by quantitative GC analysis (46% considering the transfer of only one nitrene functionality from **10** to phenylacetylene**).

3.11.5 Synthesis of 65 in the presence of TEMPO.
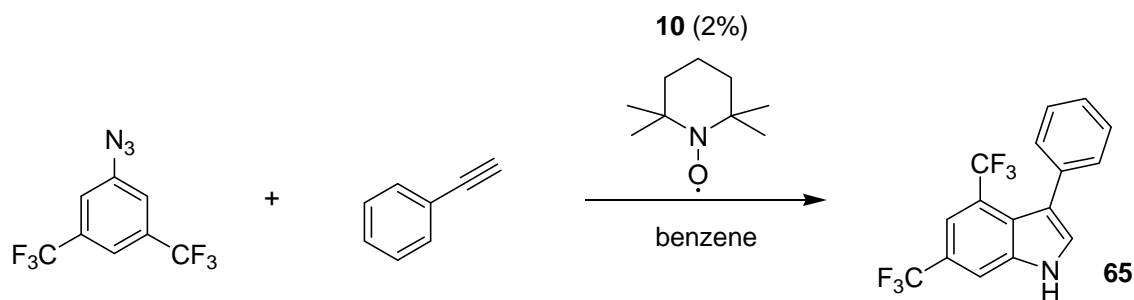
The general procedure for amination reactions was followed, a solution of complex **10** (11.7 mg, 1.0×10^{-2} mmol), 3,5- *bis*(trifluoromethyl)phenyl azide (86 µL, 5.0×10^{-1} mmol), phenylacetylene (275 µL, 2.5 mmol) and TEMPO (21.0 mg, 1.3×10^{-1} mmol) in benzene (10.0 mL) was refluxed for 1.3 h. Yield = 76%.

3.11.6 Isotope Tracing Experiment using phenylacetylene-d_1
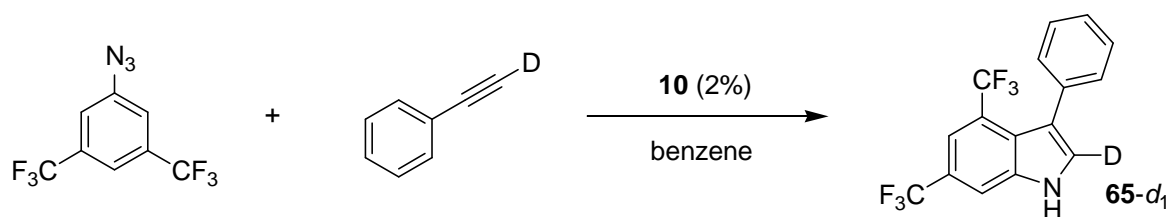
The general procedure for amination reactions was followed, a solution of complex **6** (11.7 mg, 1.0×10^{-2} mmol), 3,5-*bis*(trifluoromethyl)phenyl azide (86 µL, 5.0×10^{-1} mmol) and phenylacetylene-d_1 (99 atom % D) (275 µL, 2.5 mmol) in benzene (10 mL) was refluxed for 1.0 h. The pure product **65**-d_1 was obtained by washing the crude with a few millilitres of *n*-pentane. ^{1}H-NMR (400 MHz, CDCl$_3$) spectrum of the purified indole showed the absence of H2 signal.

3.11.7 Kinetic Isotope Effect (KIE) Experiment

3.11.7.1. Determination by NMR analysis.
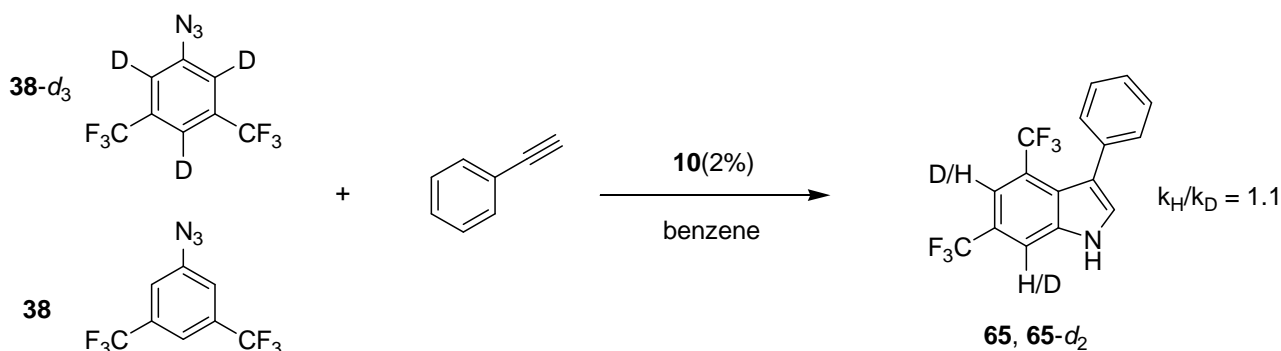
The general procedure for amination reactions was followed, phenylacetylene (275 μL, 2.5 mmol) and an equimolar mixture of 3,5-*bis*(trifluoromethyl)phenyl azide (**38**) (64.6 mg, 2.5×10^{-1} mmol) and 3,5-*bis*(trifluoromethyl)phenyl azide-d_3 (94 atom % D) (**38**-d_3) (65.3 mg, 2.5×10^{-1} mmol) were added to a benzene (10.0 mL) solution of complex **10** (12.0 mg, 1.0×10^{-2} mmol). The solution was refluxed for 15 minutes until an azide conversion of 39% was reached. The solvent was evaporated to dryness and the crude was purified by flash chromatography (silica gel, *n*-hexane/AcOEt = 9:1) to give a mixture of **65** and **65**-d_2 (the labile D of the N-D bond was replaced by H during the purification). The k_H/k_D ratio of 1.1 was determined by ^{1}H-NMR spectroscopy (300 MHz, CDCl$_3$) (***Figure 42***).
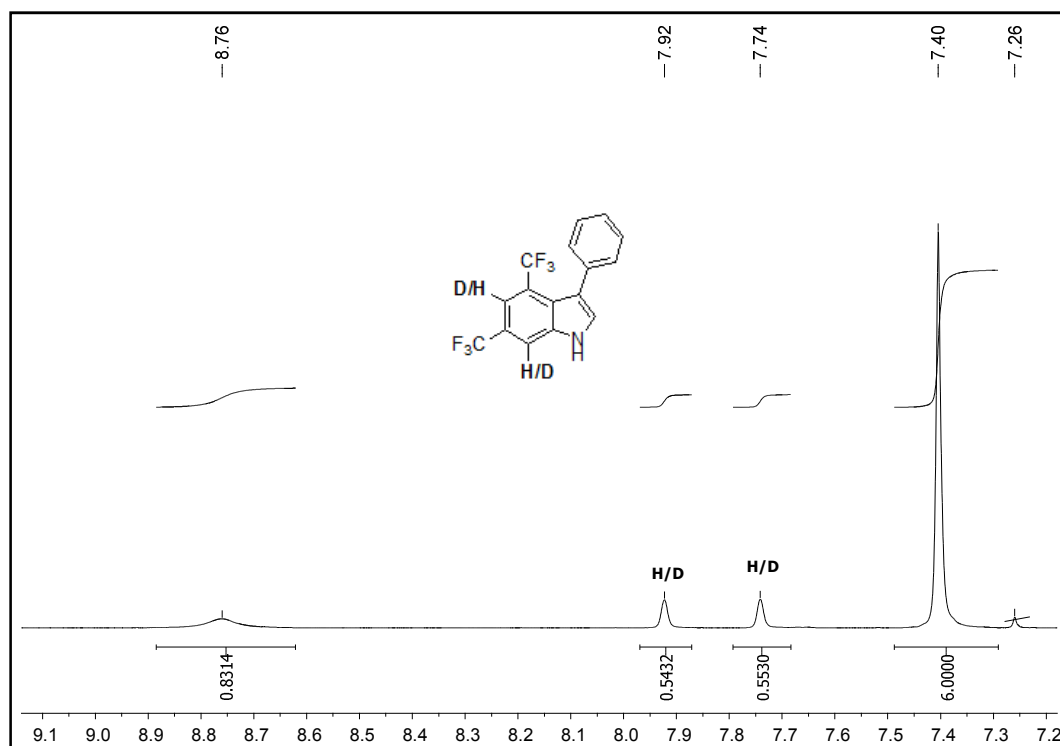
Figure 42. *^{1}H NMR spectrum of indole products obtained from the KIE experiment*

3.11.7.2. Determination by evaluation of the single kinetic constants
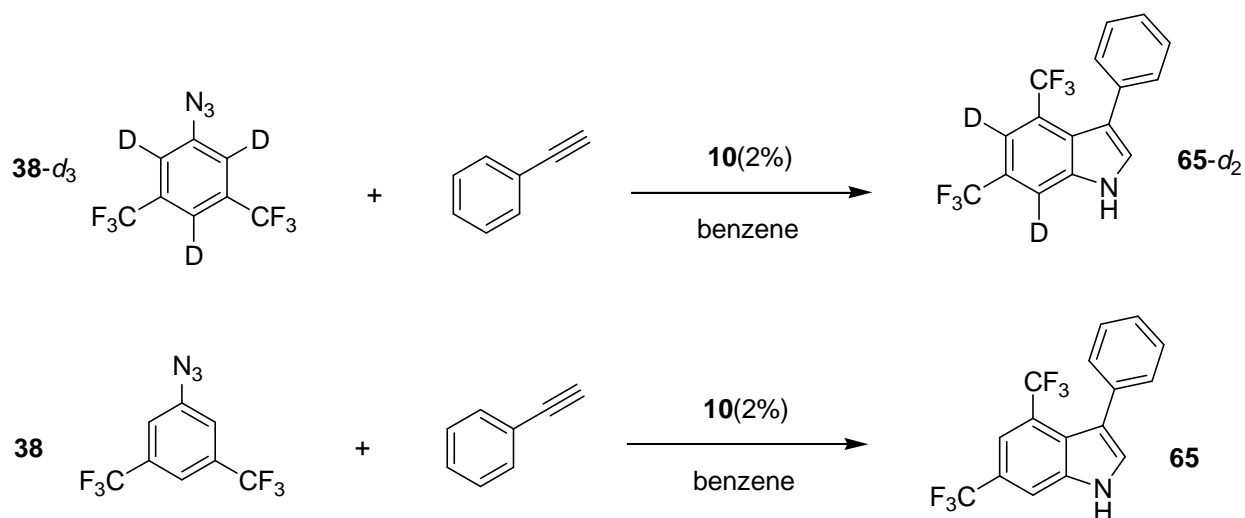
General procedure for the kinetic experiments: the catalyst (9.9 mg, 8.5×10^{-3} mmol), the aryl azide (4.1×10^{-1} mmol) and phenylacetylene (230 µL, 2.1 mmol) were added to 9 mL of benzene in a Schlenk flask under N_2. The resulting solution was immediately placed in a preheated oil bath at 75 °C and stirred for one minute to completely dissolve all the reagents. The consumption of the azide was then followed by IR spectroscopy withdrawing samples of the solution at regular time intervals and measuring the absorbance value (A) of the $\nu(N=N)$ band at 2116 cm^{-1}. Two runs were performed, one using **38** (for k_H) and the other using **38-d_3** (for k_D) as the aryl azide. First order rate constants with respect to the aryl azide concentration were determined (***Figure 43***).

$$k_H = 1.66 \times 10^{-4}\,\text{s}^{-1} \qquad k_D = 1.04 \times 10^{-4}\,\text{s}^{-1}$$

$$k_H/k_D = 1.6$$
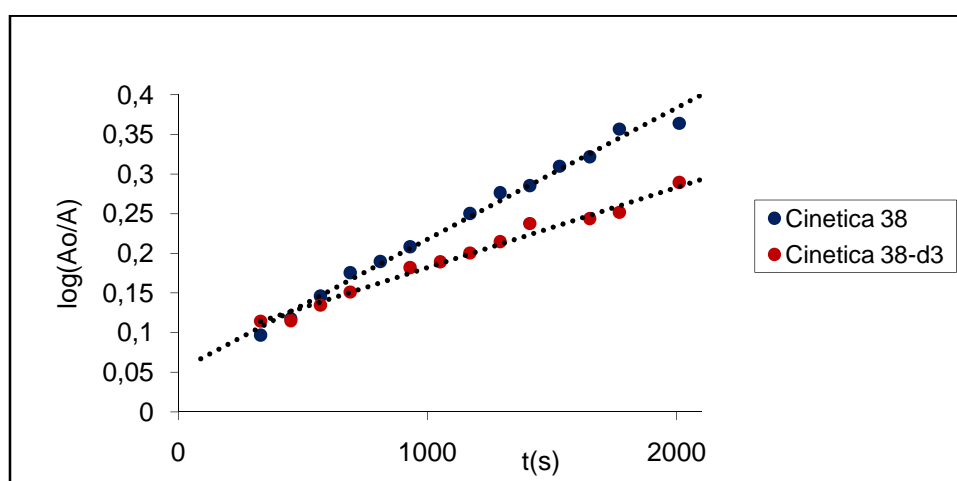
Figure 43.

3.12. Amination reactions using [Ru(TPP)(OCH₃)]₂O (92) as the catalyst

All the following reactions were carried out using the general procedure for amination reactions for catalytic aminations (**Section 3.6**).

Table 17 . Allylic amination of cyclohexene using 3,5-bis(trifluoromethyl)phenyl azide
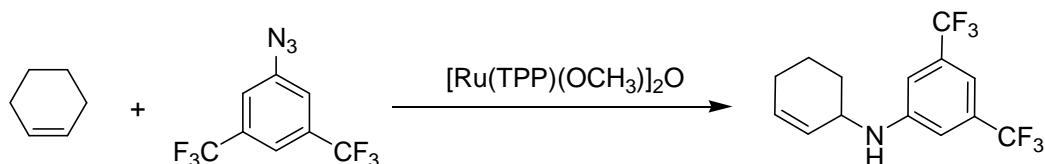
Compound	PM	mass (mg)	mmol	Molar Ratio	V (mL)
[Ru(TPP)(OCH₃)]₂O	1505.65	22.7	0.015	1	
3,5-(CF₃)₂C₆H₃-N₃	255.12	19.6	0.77	51	
Cyclohexene					30

Reaction conditions: cyclohexene as solvent, T = 83°C (refluxing hydrocarbon).

Yield: 65%   **Reaction Time:** 0.75 h

Table 18. Allylic amination of cyclohexene using 4-tert-butylphenyl azide
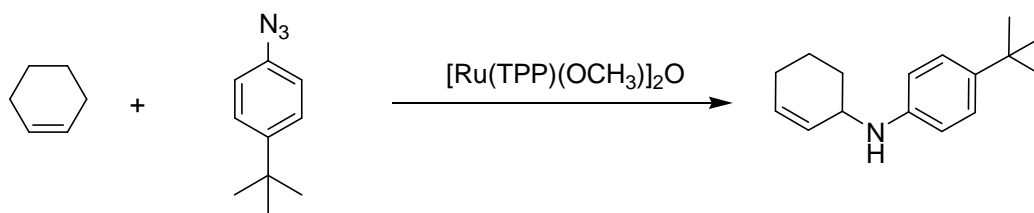
Compound	PM	mass (mg)	mmol	Molar Ratio	V (mL)
[Ru(TPP)(OCH₃)]₂O	1505.65	10.7	7.1×10^{-3}	1	
ᵗBuC₆H₄-N₃	175.23	121.8	0.77	108	
Cyclohexene					30

Reaction conditions: cyclohexene as solvent, T = 83°C (refluxing hydrocarbon).

Yield: 57%   **Reaction Time:** 3 h

Table 19. *Allylic amination of cyclohexene using 4-anisyl azide*
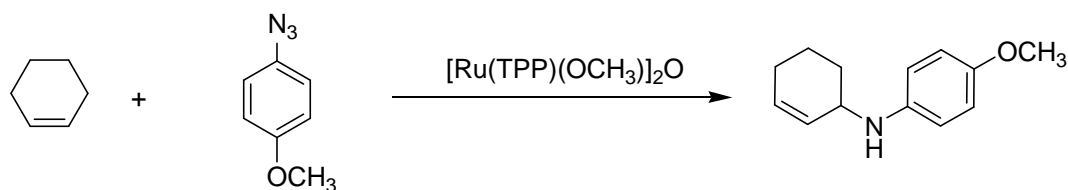
Compound	PM	mass (mg)	mmol	Molar Ratio	V (mL)
[Ru(TPP)(OCH$_3$)]$_2$O	1505.65	10.3	6.8×10^{-3}	1	
CH$_3$O-C$_6$H$_4$-N$_3$	149.15	103.8	0.70	102	
Cyclohexene					30

Reaction conditions: cyclohexene as solvent, T = 83°C (refluxing hydrocarbon).

Yield: 20%   **Reaction Time:** 1.5 h

Table 20. *Benzylic amination of cumene*
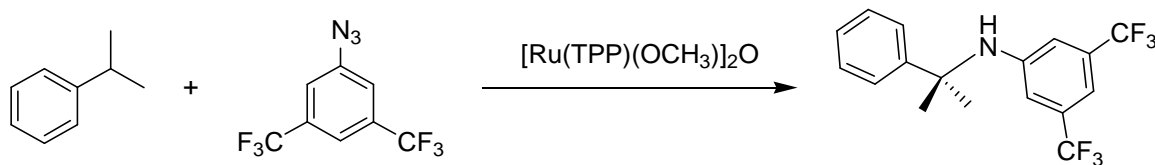
Compound	PM	mass (mg)	mmol	Molar Ratio	V (mL)	d (g/mL)
[Ru(TPP)(OCH$_3$)]$_2$O	1505.65	4.3	2.86×10^{-3}	1		
3,5-(CF$_3$)$_2$C$_6$H$_3$-N$_3$	255.12	72.9	0.286	100		
Cumene					10	

Reaction conditions: cumene as solvent, T = 152°C (refluxing hydrocarbon).

Yield: 58%   **Reaction Time:** 0.2 h

Table 21. Benzylic amination of methyl acetate
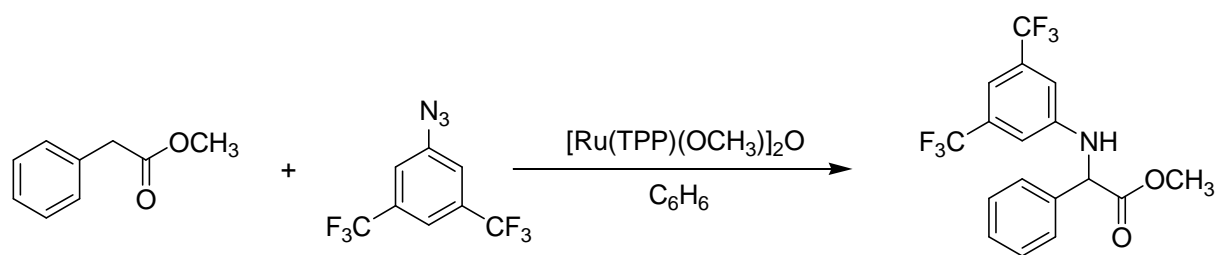
Compound	PM	mass (mg)	Mmol	Molar Ratio	V (mL)	d (g/mL)
[Ru(TPP)(OCH$_3$)]$_2$O	1505.65	47.3	0.031	1		
3,5-(CF$_3$)$_2$C$_6$H$_3$-N$_3$	255.12	161.2	0.63	20		
methyl phenylacetate	150.18	470	3.1	100	0.450	1.044

Reaction conditions: benzene as solvent (30 mL). T = 80°C

Conversion: 98%   **Yield:** 44%   **Reaction Time:** 8 h

Table 22. Benzylic amination of methyl dihydrocinnamate
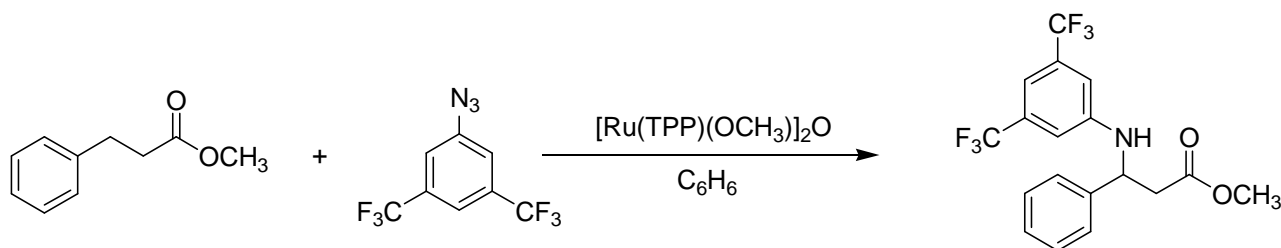
Compound	PM	mass (mg)	Mmol	Molar Ratio	V (mL)	d (g/mL)
[Ru(TPP)(OCH$_3$)]$_2$O	1505.65	7.7	5.1×10^{-3}	1		
3,5-(CF$_3$)$_2$C$_6$H$_3$-N$_3$	255.12	42.9	0.17	33		
methyl dihydrocinnamate	164.20	1696	10	2016	1.6	1.06

Reaction conditions: benzene as solvent (6.5 mL). T = 80°C.

Yield: 70%   **Reaction Time:** 4.5 h

Table 23. *Aziridination of α-methyl styrene*
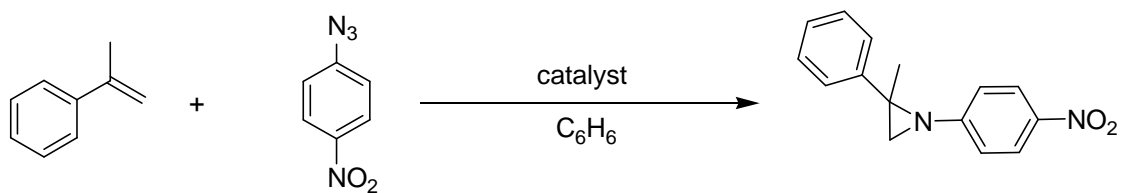
Compound	PM	mass (mg)	mmol	Molar Ratio	V (mL)	d (g/mL)
[Ru(TPP)(OCH$_3$)]$_2$O	1505.65	10.2	6.8×10^{-3}	1		
4-(NO$_2$)-C$_6$H$_4$-N$_3$	164.12	108.4	0.660	97		
α-methyl styrene	118.18	0.400	3.4	500	0.440	0.909

Reaction conditions: benzene as solvent (33 mL). T = 80°C.

Yield: 99%　　　　**Reaction Time:** 1.0 h

3.13. Amination reactions using glycoporphyrin complexes as catalysts

All the following reactions were carried out using the general procedure for amination reactions (**Section 3.6**).

3.13.1. Benzylic amination of ethyl benzene
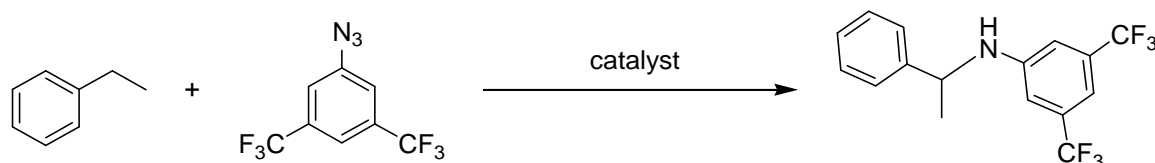
*Table 24. Benzylic amination of ethyl benzene catalysed by **Co-98** as the catalyst.*

Compound	PM	mass (mg)	mmol	Molar Ratio	V (mL)
Co-98	2809.64	6.0	2.2×10^{-3}	1	
$3,5\text{-}(CF_3)_2C_6H_3\text{-}N_3$	255.12	36.0	0.14	65	
ethylbenzene					5.0

Reaction conditions: ethylbenzene as solvent (5.0 mL), T = 136°C (refluxing hydrocarbon).

Yield: 56%   **Reaction Time:** 4.0 h

*Table 25. Benzylic amination of ethyl benzene catalysed by **Fe-98** as the catalyst.*

Compound	PM	mass (mg)	mmol	Molar Ratio	V (mL)
Fe-98	2837.58	5.0	1.8×10^{-3}	1	
$3,5\text{-}(CF_3)_2C_6H_3\text{-}N_3$	255.12	22.2	0.087	49	
ethylbenzene					5.0

Reaction conditions: ethylbenzene as solvent (5.0 mL), T = 136°C (refluxing hydrocarbon).

Yield: 60%   **Reaction Time:** 1.5 h

Table 26. *Benzylic amination of ethyl benzene catalysed by **Fe-101** as the catalyst.*

Compound	PM	mass (mg)	mmol	Molar Ratio	V (mL)
Fe-**101**	2817.93	5.0	1.7×10^{-3}	1	
3,5-$(CF_3)_2C_6H_3$-N_3	255.12	22.2	0.087	50	
ethylbenzene					5.0

Reaction conditions: ethylbenzene as solvent (5.0 mL), T = 136°C (refluxing hydrocarbon).

Yield: 14%   **Reaction Time:** 30 h

Table 27. *Benzylic amination of ethyl benzene catalysed by **Ru-98** as the catalyst.*

Compound	PM	mass (mg)	mmol	Molar Ratio	V (mL)
Ru-98	2879.78	10.1	3.52×10^{-3}	1	
3,5-$(CF_3)_2C_6H_3$-N_3	255.12	45.0	0.176	50	
ethylbenzene					10

Reaction conditions: ethylbenzene as solvent (10 mL), T = 136°C (refluxing hydrocarbon).

Yield: 92%   **Reaction Time:** 1 h

Compound	PM	mass (mg)	mmol	Molar Ratio	V (mL)
Ru-102	1798.31	6.4	3.6×10^{-3}	1	
3,5-$(CF_3)_2C_6H_3$-N_3	255.12	45.0	0.18	50	
ethylbenzene					10

Reaction conditions: ethylbenzene as solvent (10 mL), T = 136°C (refluxing hydrocarbon).

Yield: 78%   **Reaction Time:** 1 h

At the end of the reaction the precipitation of a dark solid was observed. Ethylbenzene was evaporated and CH_2Cl_2 was added to separate the organic product form the dark precipitate, which

was recovered by filtration. NMR analyses of the solid were compatible with those obtained in the characterization of **Ru-102** (recovery yield = 78%).

3.13.2. Benzylic amination of methyl phenylacetate
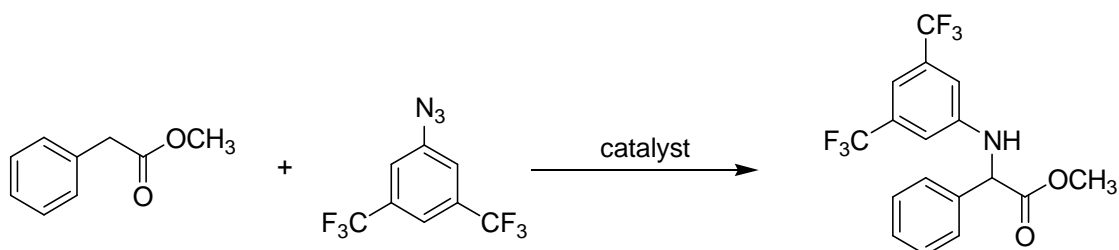
*Table 28. Benzylic amination of methyl phenylacetate catalysed by **Fe-98** as the catalyst.*

Compound	PM	mass (mg)	mmol	Molar Ratio	V (mL)
Fe-98	2837.58	5.0	1.8×10^{-3}	1	
$3,5\text{-}(CF_3)_2C_6H_3\text{-}N_3$	255.12	22.2	0.0870	49	
methyl phenylacetate					5.0

Reaction conditions: methyl phenylacetate as solvent (5.0 mL), T = 100°C

Conversion: 80%   **Yield:** traces   **Reaction Time:** 19 h

*Table 29. Benzylic amination of methyl phenylacetate catalysed by **Fe-98** as the catalyst.*

Compound	PM	mass (mg)	mmol	Molar Ratio	V (mL)
Ru-98	2879.78	5.1	1.8×10^{-3}	1	
$3,5\text{-}(CF_3)_2C_6H_3\text{-}N_3$	255.12	22.2	0.087	49	
methyl phenylacetate					5.0

Reaction conditions: methyl phenylacetate as solvent (5.0 mL), T = 100°C

Yield: 68%   **Reaction Time:** 0.5 h

3.13.3. Cyclopropanation of α-methyl styrene

The general procedure for amination reactions was followed using ethyl diazoacetate (EDA) instead of the aryl azide. When specified, the diazoalkane solution was slowly added using a syringe pump. The EDA consumption was monitored by IR spectroscopy ($v_{N=N} = 2114$ cm^{-1}) if not specified a 100% conversion of the diazoalkane was reached. Yield and diastereoselectivity were evaluated by ^{1}H NMR.
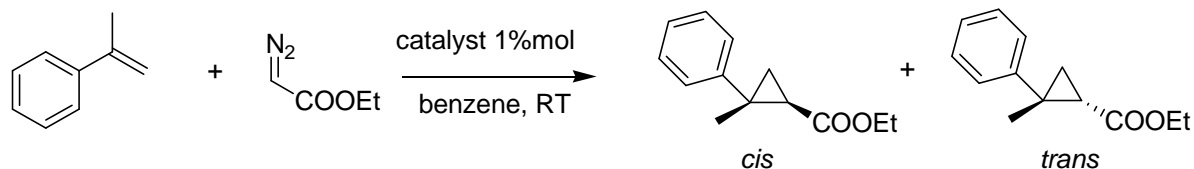
Table 30. *Cyclopropanation of α-methyl styrene catalysed by* **Co-98**.

Compound	PM	mass (mg)	mmol	Molar Ratio	V (mL)	d (g/mL)
Co-98	2809.64	7.0	2.5×10^{-3}	1		
ethyl diazoacetate	114.11	28.2	0.25	99	0.026	1.085
α-methyl styrene	118.18	295	2.5	1000	0.325	0.909

Reaction conditions: benzene as solvent (10 mL). An EDA solution in benzene (1 mL was added at RT in 100 minutes using a syringe pump. After the slow addition the solution was stirred at 50°C for 2 hours. Complete conversion was not reached.

Yield: 14%   *Syn/trans* **ratio:** 1:1   **Reaction Time:** 220 min.

Table 31. *Cyclopropanation of α-methyl styrene catalysed by* **Fe-98**.

Compound	PM	mass (mg)	mmol	Molar Ratio	V (mL)	d (g/mL)
Fe-98	2837.58	5.0	1.8×10^{-3}	1		
ethyl diazoacetate	114.11	21.7	0.19	108	0.020	1.085
α-methyl styrene	118.18	52.7	0.45	253	0.058	0.909

Reaction conditions: benzene as solvent (5.0 mL). T = RT

Yield: 75%   *Syn/trans* **ratio:** 1:1.1   **Reaction Time:** 1.5 h.

Table 32. Cyclopropanation of α-methyl styrene catalysed by Ru-98.

Compound	PM	mass (mg)	mmol	Molar Ratio	V (mL)	d (g/mL)
Ru-98	2879.78	5.1	1.8×10^{-3}	1		
ethyl diazoacetate	114.11	195	1.7	970	180	1.085
α-methyl styrene	118.18	418	3.5	2010	460	0.909

Reaction conditions: benzene as solvent (4.5 mL). An EDA solution in benzene (1 mL) was added at RT in 100 minutes using a syringe pump. EDA was completely consumed at the end of the addition.

Yield: 69%   *Syn/trans* **ratio:** 2:1   **Reaction Time:** 100 minutes.

3.13.4. Other amination reactions catalysed by Ru-98.

Table 33. *Allylic amination of cyclohexene*
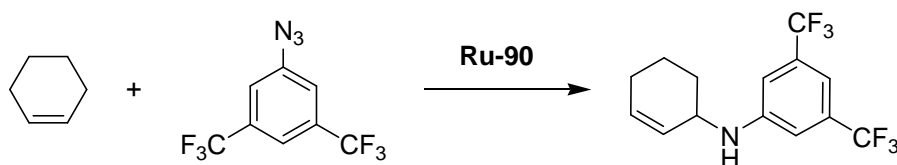
Compound	PM	mass (mg)	mmol	Molar Ratio	V (mL)
Ru-98	2879.78	5.1	1.8×10^{-3}	1	
$3,5\text{-}(CF_3)_2C_6H_3\text{-}N_3$	255.12	22.2	0.087	49	
cyclohexene					5.0

Reaction conditions: cyclohexene as solvent, T = 83°C (refluxing hydrocarbon).

Yield: 65%   **Reaction Time:** 2 h

Table 34. *Aziridination of α-methyl styrene.*
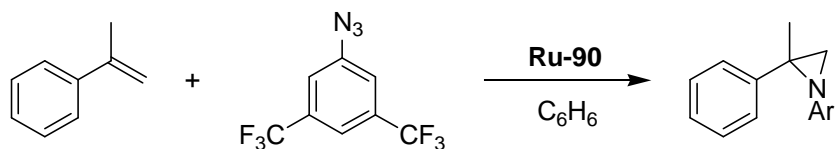
Compound	PM	mass (mg)	mmol	Molar Ratio	V (mL)	d (g/mL)
Ru-98	2879.78	5.1	1.8×10^{-3}	1		
$3,5\text{-}(CF_3)_2C_6H_3\text{-}N_3$	255.12	44.4	0.17	99		
α-methyl styrene	118.18	109	0.92	520	0.12	0.909

Reaction conditions: benzene as solvent (5.0 mL). T = 80°C.

Yield: 87%   **Reaction Time:** 0.5 h

References

[1]   J. Juselius, D. Sundholm, *Phys. Chem. Chem. Phys.* **2000**, *2*, 2145-2151.

[2]   A. Battersby, *Science* **1994**, *264*, 1551-1557.

[3]   H. Fischer, B. Walach, *Justus Liebigs Annalen der Chemie* **1926**, *450*, 164-181.

[4]   P. Rothemund, *J. Am. Chem. Soc.* **1935**, *57*, 2010-2011; P. Rothemund, A. R. Menotti, *J. Am. Chem. Soc.* **1941**, *63*, 267-270.

[5]   A. D. Adler, F. R. Longo, J. D. Finarelli, J. Goldmacher, J. Assour, L. Korsakoff, *J. Org. Chem.* **1967**, *32*, 476.

[6]   M. O. Liu, C.-H. Tai, W.-Y. Wang, J.-R. Chen, A. T. Hu, T.-H. Wei, *J. Organomet. Chem.* **2004**, *689*, 1078-1084.

[7]   J. S. Lindsey, I. C. Schreiman, H. C. Hsu, P. C. Kearney, A. M. Marguerettaz, *J. Org. Chem.* **1987**, *52*, 827-836.

[8]   A. D. Adler, F. R. Longo, F. Kampas, J. Kim, *J. Inorg. Nucl. Chem.* **1970**, *32*, 2443-2445.

[9]   M. Tsutsui, D. Ostfeld, L. M. Hoffman, *J. Am. Chem. Soc.* **1971**, *93*, 1820-1823; D. P. Rillema, J. K. Nagle, L. F. Barringer, Jr., T. J. Meyer, *J. Am. Chem. Soc.* **1981**, *103*, 56-62.

[10]   I. Schlichting, J. Berendzen, K. Chu, A. M. Stock, S. A. Maves, D. E. Benson, R. M. Sweet, D. Ringe, G. A. Petsko, S. G. Sligar, *Science* **2000**, *287*, 1615-1622.

[11]   B. Meunier, S. P. de Visser, S. Shaik, *Chem. Rev.* **2004**, *104*, 3947-3980.

[12]   J. T. Groves, T. E. Nemo, R. S. Myers, *J. Am. Chem. Soc.* **1979**, *101*, 1032-1033.

[13]   P. S. Traylor, D. Dolphin, T. G. Traylor, *J. Chem. Soc, Chem. Comm.* **1984**, 279-280.

[14]   J. P. Collman, R. R. Gagne, C. Reed, T. R. Halbert, G. Lang, W. T. Robinson, *J. Am. Chem. Soc.* **1975**, *97*, 1427-1439.

[15]   E. Rose, A. Kossanyi, M. Quelquejeu, M. Soleilhavoup, F. Duwavran, N. Bernard, A. Lecas, *J. Am. Chem. Soc.* **1996**, *118*, 1567-1568.

[16]   J. T. Groves, R. Quinn, *J. Am. Chem. Soc.* **1985**, *107*, 5790-5792.

[17]   J. T. Groves, R. Quinn, *Inorg. Chem.* **1984**, *23*, 3844-3846.

[18]   R. Zhang, W.-Y. Yu, H.-Z. Sun, W.-S. Liu, C.-M. Che, *Chem. Eur. J.* **2002**, *8*, 2495-2507; T.-S. Lai, R. Zhang, K.-K. Cheung, C.-M. Che, T.-S. Lai, H.-L. Kwong, *Chem Commun* **1998**, 1583-1584.

[19]   J.-L. Zhang, C.-M. Che, *Chem. Eur. J.* **2005**, *11*, 3899-3914; H. Ohtake, T. Higuchi, M. Hirobe, *J. Am. Chem. Soc.* **1992**, *114*, 10660-10662.

[20]   C. Wang, K. V. Shalyaev, M. Bonchio, T. Carofiglio, J. T. Groves, *Inorg. Chem.* **2006**, *45*, 4769-4782.

[21]   E. Gallo, A. Caselli, F. Ragaini, S. Fantauzzi, N. Masciocchi, A. Sironi, S. Cenini, *Inorg. Chem.* **2005**, *44*, 2039-2049; C. Ho, W.-H. Leung, C.-M. Che, *J. Chem. Soc, Dalton Trans.* **1991**, 2933-2939.

[22]   H. Sugimoto, T. Higashi, M. Mori, M. Nagano, Z.-i. Yoshida, H. Ogoshi, *Bull. Chem. Soc. Jpn.* **1982**, *55*, 822-828.

[23]   J. P. Collman, C. E. Barnes, P. J. Brothers, T. J. Collins, T. Ozawa, J. C. Gallucci, J. A. Ibers, *J. Am. Chem. Soc.* **1984**, *106*, 5151-5163.

[24]   E. Vanover, Y. Huang, L. Xu, M. Newcomb, R. Zhang, *Org. Lett.* **2010**, *12*, 2246-2249.

[25]   R. Zhang, E. Vanover, W. Luo, M. Newcomb, *Dalton Trans.* **2014**, *43*, 8749-8756.

[26]   H. M. L. Davies, J. R. Manning, *Nature* **2008**, *451*, 417-424; M. M. Diaz-Requejo, P. J. Perez, *Chem. Rev.* **2008**, *108*, 3379-3394; S. Fantauzzi, A. Caselli, E. Gallo, *Dalton Trans* **2009**, 5434-5443; D. Intrieri, P. Zardi, A. Caselli, E. Gallo, *Chem. Commun.* **2014**.

[27]   P. Müller, C. Fruit, *Chem. Rev.* **2003**, *103*, 2905-2920.

[28]   Y. Yamada, T. Yamamoto, M. Okawara, *Chem. Lett.* **1975**, 361-362.

[29]   D. A. Evans, M. M. Faul, M. T. Bilodeau, *J. Org. Chem.* **1991**, *56*, 6744-6746.

[30]   R. Breslow, S. H. Gellman, *J. Chem. Soc., Chem. Commun.* **1982**, 1400-1401.

[31]   J. P. Mahy, G. Bedi, P. Battioni, D. Mansuy, *Tetrahedron Lett.* **1988**, *29*, 1927-1930.

[32] J. Yang, R. Weinberg, R. Breslow, *Chem. Commun.* **2000**, 531-532.

[33] J. P. Mahy, G. Bedi, P. Battioni, D. Mansuy, *New J. Chem.* **1989**, *13*, 651-657.

[34] J. P. Mahy, P. Battioni, D. Mansuy, *J. Am. Chem. Soc.* **1986**, *108*, 1079-1080.

[35] J.-L. Liang, J.-S. Huang, X.-Q. Yu, N. Zhu, C.-M. Che, *Chem. Eur. J.* **2002**, *8*, 1563-1572; X.-G. Zhou, X.-Q. Yu, J.-S. Huang, C.-M. Che, *Chem. Commun.* **1999**, 2377-2378; X. Q. Yu, J. S. Huang, X. G. Zhou, C. M. Che, *Org. Lett.* **2000**, *2*, 2233-2236.

[36] S.-M. Au, W.-H. Fung, M.-C. Cheng, C.-M. Che, S.-M. Peng, *Chem. Commun.* **1997**, 1655-1656.

[37] S.-M. Au, J.-S. Huang, W.-Y. Yu, W.-H. Fung, C.-M. Che, *J. Am. Chem. Soc.* **1999**, *121*, 9120-9132.

[38] C.-M. Che, W.-Y. Yu, *Pure Appl. Chem.* **1999**, *71*, 281-288.

[39] Z. Guo, X. Guan, J.-S. Huang, W.-M. Tsui, Z. Lin, C.-M. Che, *Chem. Eur. J.* **2013**, *19*, 11320-11331.

[40] J. B. Sweeney, *Chemical Society Reviews* **2002**, *31*, 247-258.

[41] D. Mansuy, J. P. Mahy, A. Dureault, G. Bedi, P. Battioni, *J. Chem. Soc., Chem. Commun.* **1984**, 1161-1163; J. P. Mahy, G. Bedi, P. Battioni, D. Mansuy, *J. Chem. Soc., Perkin Trans. 2* **1988**, 1517-1524.

[42] J.-P. Simonato, J. Pecaut, J.-C. Marchon, W. Robert Scheidt, *Chem. Commun.* **1999**, 989-990; T.-S. Lai, C.-M. Che, H.-L. Kwong, S.-M. Peng, *Chem Commun* **1997**, 2373-2374.

[43] J.-L. Liang, S.-X. Yuan, J.-S. Huang, W.-Y. Yu, C.-M. Che, *Angew. Chem. Int. Ed.* **2002**, *41*, 3465-3468.

[44] X. Lin, C.-M. Che, D. L. Phillips, *J. Org. Chem.* **2008**, *73*, 529-537.

[45] D. H. R. Barton, R. S. Hay-Motherwell, W. B. Motherwell, *J. Chem. Soc., Perkin Trans. 1* **1983**, 445-451.

[46] R. Fructos Manuel, S. Trofimenko, M. M. Diaz-Requejo, J. Perez Pedro, *J. Am. Chem. Soc.* **2006**, *128*, 11784-11791; D. P. Albone, S. Challenger, A. M. Derrick, S. M. Fillery, J. L. Irwin, C. M. Parsons, H. Takada, P. C. Taylor, D. J. Wilson, *Org. Biomol. Chem.* **2005**, *3*, 107-111; H. Wu, L.-W. Xu, C.-G. Xia, J. Ge, W. Zhou, L. Yang, *Cat. Commun.* **2005**, *6*, 221-223; J. U. Jeong, B. Tao, I. Sagasser, H. Henniges, K. B. Sharpless, *J. Am. Chem. Soc.* **1998**, *120*, 6844-6845.

[47] S. Cenini, A. Penoni, S. Tollari, *J. Mol. Catal. A: Chem.* **1997**, *124*, 109-113.

[48] R. Vyas, G.-Y. Gao, J. D. Harden, X. P. Zhang, *Org. Lett.* **2004**, *6*, 1907-1910; G.-Y. Gao, J. D. Harden, X. P. Zhang, *Org. Lett.* **2005**, *7*, 3191-3193; J. D. Harden, J. V. Ruppel, G.-Y. Gao, X. P. Zhang, *Chem. Commun.* **2007**, 4644-4646.

[49] S. Braese, C. Gil, K. Knepper, V. Zimmermann, *Angew. Chem., Int. Ed.* **2005**, *44*, 5188-5240.

[50] K. R. Henery-Logan, R. A. Clark, *Tetrahedron Lett.* **1968**, *9*, 801-806.

[51] B. C. G. Soderberg, *Current Organic Chemistry* **2000**, *4*, 727-764.

[52] H. Kwart, A. A. Khan, *J. Am. Chem. Soc.* **1967**, *89*, 1950-1951.

[53] J. T. Groves, T. Takahashi, *J. Am. Chem. Soc.* **1983**, *105*, 2073-2074.

[54] G.-Y. Gao, J. E. Jones, R. Vyas, J. D. Harden, X. P. Zhang, *J. Org. Chem.* **2006**, *71*, 6655-6658.

[55] W. Xiao, J. Wei, C.-Y. Zhou, C.-M. Che, *Chem Commun* **2013**, *49*, 4619-4621.

[56] J. V. Ruppel, J. E. Jones, C. A. Huff, R. M. Kamble, Y. Chen, X. P. Zhang, *Org. Lett. FIELD Full Journal Title:Organic Letters* **2008**, *10*, 1995-1998.

[57] Y. Liu, C.-M. Che, *Chem. Eur. J.* **2010**, *16*, 10494-10501.

[58] S. Fantauzzi, E. Gallo, A. Caselli, C. Piangiolino, F. Ragaini, S. Cenini, *Eur. J. Org. Chem.* **2007**, 6053-6059.

[59] S. Fantauzzi, E. Gallo, A. Caselli, F. Ragaini, P. Macchi, N. Casati, S. Cenini, *Organometallics* **2005**, *24*, 4710-4713.

[60] F. Ragaini, A. Penoni, E. Gallo, S. Tollari, C. Li Gotti, M. Lapadula, E. Mangioni, S. Cenini, *Chem. Eur. J.* **2003**, *9*, 249-259.

[61] H. Lu, V. Subbarayan, J. Tao, X. P. Zhang, *Organometallics* **2009**, *29*, 389-393.

[62] V. Lyaskovskyy, A. I. O. Suarez, H. Lu, H. Jiang, X. P. Zhang, B. de Bruin, *J. Am. Chem. Soc.* **2011**, *133*, 12264-12273.

[63] A. I. Olivos Suarez, H. Jiang, X. P. Zhang, B. de Bruin, *Dalton Trans.* **2011**, *40*, 5697-5705.

[64] A. Caselli, E. Gallo, S. Fantauzzi, S. Morlacchi, F. Ragaini, S. Cenini, *Eur. J. Inorg. Chem.* **2008**, 3009-3019.

[65] D. Intrieri, A. Caselli, F. Ragaini, S. Cenini, E. Gallo, *J. Porphyrins Phthalocyanines* **2010**, *14*, 732-740.

[66] D. Intrieri, A. Caselli, F. Ragaini, P. Macchi, N. Casati, E. Gallo, *Eur. J. Inorg. Chem.* **2012**, 569-580.

[67] K. H. Chan, X. Guan, V. K. Lo, C. M. Che, *Angew Chem Int Ed Engl* **2014**, *53*, 2982-2987.

[68] S. Fantauzzi, E. Gallo, A. Caselli, F. Ragaini, N. Casati, P. Macchi, S. Cenini, *Chem. Commun.* **2009**, 3952-3954.

[69] G. Manca, E. Gallo, D. Intrieri, C. Mealli, *ACS Catal.* **2014**, *4*, 823-832.

[70] U. Kazmaier, *Angew. Chem. Int. Ed.* **2005**, *44*, 2186-2188; E. R. Jarvo, S. J. Miller, *Tetrahedron* **2002**, *58*, 2481-2495.

[71] A. Mori, H. Abet, S. Inoue, *Applied Organometallic Chemistry* **1995**, *9*, 189-197; B. Castano, S. Guidone, E. Gallo, F. Ragaini, N. Casati, P. Macchi, M. Sisti, A. Caselli, *Dalton Trans.* **2013**, *42*, 2451-2462.

[72] F. J. Sardina, H. Rapoport, *Chem. Rev.* **1996**, *96*, 1825-1872; J. Kaiser, S. S. Kinderman, B. C. J. van Esseveldt, F. L. van Delft, H. E. Schoemaker, R. H. Blaauw, F. P. J. T. Rutjes, *Organic & Biomolecular Chemistry* **2005**, *3*, 3435-3467.

[73] B. D. Vineyard, W. S. Knowles, M. J. Sabacky, G. L. Bachman, D. J. Weinkauff, *J. Am. Chem. Soc.* **1977**, *99*, 5946-5952.

[74] H.-J. Drexler, J. You, S. Zhang, C. Fischer, W. Baumann, A. Spannenberg, D. Heller, *Organic Process Research & Development* **2003**, *7*, 355-361; S. Lühr, J. Holz, O. Zayas, V. Wendisch, A. Börner, *Tetrahedron: Asymmetry* **2012**, *23*, 1301-1319; C. Nájera, J. M. Sansano, *Chem. Rev.* **2007**, *107*, 4584-4671.

[75] L.-W. Xu, C.-G. Xia, *Eur. J. Org. Chem.* **2005**, *2005*, 633-639; B. Weiner, W. Szymanski, D. B. Janssen, A. J. Minnaard, B. L. Feringa, *Chemical Society Reviews* **2010**, *39*, 1656-1691.

[76] A. P. Patwardhan, V. R. Pulgam, Y. Zhang, W. D. Wulff, *Angew. Chem. Int. Ed.* **2005**, *44*, 6169-6172.

[77] D. A. Evans, S. G. Nelson, *J. Am. Chem. Soc.* **1997**, *119*, 6452-6453; M. Marigo, K. Juhl, K. A. Jørgensen, *Angew. Chem. Int. Ed.* **2003**, *42*, 1367-1369.

[78] S. Mukherjee, J. W. Yang, S. Hoffmann, B. List, *Chem. Rev.* **2007**, *107*, 5471-5569.

[79] J.-L. Liang, X.-Q. Yu, C.-M. Che, *Chem Commun* **2002**, 124-125.

[80] T. Baumann, M. Bächle, S. Bräse, *Org. Lett.* **2006**, *8*, 3797-3800.

[81] N. Matsuda, K. Hirano, T. Satoh, M. Miura, *Angew. Chem. Int. Ed.* **2012**, *51*, 11827-11831.

[82] S.-F. Zhu, Q.-L. Zhou, *Accounts of Chemical Research* **2012**, *45*, 1365-1377.

[83] H. E. Bartrum, D. C. Blakemore, C. J. Moody, C. J. Hayes, *Chem. Eur. J.* **2011**, *17*, 9586-9589.

[84] S. S. So, A. E. Mattson, *J. Am. Chem. Soc.* **2012**, *134*, 8798-8801; T. Yang, H. Zhuang, X. Lin, J.-N. Xiang, J. D. Elliott, L. Liu, F. Ren, *Tetrahedron Lett.* **2013**, *54*, 4159-4163.

[85] S.-F. Zhu, B. Xu, G.-P. Wang, Q.-L. Zhou, *J. Am. Chem. Soc.* **2011**, *134*, 436-442.

[86] L. K. Baumann, H. M. Mbuvi, G. Du, L. K. Woo, *Organometallics* **2007**, *26*, 3995-4002.

[87] Q.-H. Deng, H.-W. Xu, A. W.-H. Yuen, Z.-J. Xu, C.-M. Che, *Org. Lett.* **2008**, *10*, 1529-1532.

[88] H. Lu, Y. Hu, H. Jiang, L. Wojtas, X. P. Zhang, *Org. Lett.* **2012**, *14*, 5158-5161.

[89] N. Kaushik, N. Kaushik, P. Attri, N. Kumar, C. Kim, A. Verma, E. Choi, *Molecules* **2013**, *18*, 6620-6662.

[90] G. R. Humphrey, J. T. Kuethe, *Chem. Rev.* **2006**, *106*, 2875-2911.

[91] P. J. Walsh, M. J. Carney, R. G. Bergman, *J. Am. Chem. Soc.* **1991**, *113*, 6343-6345.

[92] C. Cao, Y. Shi, A. L. Odom, *Org. Lett.* **2002**, *4*, 2853-2856.

[93] N. Schwarz, K. Alex, I. A. Sayyed, V. Khedkar, A. Tillack, M. Beller, *Synlett* **2007**, *2007*, 1091-1095.

[94] K. Alex, A. Tillack, N. Schwarz, M. Beller, *Angew. Chem. Int. Ed.* **2008**, *47*, 2304-2307.

[95] M. Tokunaga, M. Ota, M.-a. Haga, Y. Wakatsuki, *Tetrahedron Lett.* **2001**, *42*, 3865-3868.

[96] M. P. Kumar, R.-S. Liu, *J. Org. Chem.* **2006**, *71*, 4951-4955.

[97] R. C. Larock, E. K. Yum, *J. Am. Chem. Soc.* **1991**, *113*, 6689-6690.

[98] L. Ackermann, L. T. Kaspar, C. J. Gschrei, *Chem Commun* **2004**, 2824-2825.

[99] J. Barluenga, M. A. Fernández, F. Aznar, C. Valdés, *Chem. Eur. J.* **2005**, *11*, 2276-2283.

[100] K. Krüger, A. Tillack, M. Beller, *Advanced Synthesis & Catalysis* **2008**, *350*, 2153-2167.

[101] S. Cacchi, G. Fabrizi, A. Goggiamani, *Advanced Synthesis & Catalysis* **2006**, *348*, 1301-1305.

[102] X. Han, X. Lu, *Org. Lett.* **2010**, *12*, 3336-3339.

[103] B. Z. Lu, W. Zhao, H.-X. Wei, M. Dufour, V. Farina, C. H. Senanayake, *Org. Lett.* **2006**, *8*, 3271-3274.

[104] B. Lu, Y. Luo, L. Liu, L. Ye, Y. Wang, L. Zhang, *Angew. Chem. Int. Ed.* **2011**, *50*, 8358-8362.

[105] D. F. Taber, W. Tian, *J. Am. Chem. Soc.* **2006**, *128*, 1058-1059.

[106] X. Li, Y. Du, Z. Liang, X. Li, Y. Pan, K. Zhao, *Org. Lett.* **2009**, *11*, 2643-2646.

[107] K. Isomura, K. Uto, H. Taniguchi, *J. Chem. Soc, Chem. Comm.* **1977**, 664-665; S. Chiba, G. Hattori, K. Narasaka, *Chemistry Letters* **2007**, *36*, 52-53.

[108] S. Jana, M. D. Clements, B. K. Sharp, N. Zheng, *Org. Lett.* **2010**, *12*, 3736-3739.

[109] B. J. Stokes, H. Dong, B. E. Leslie, A. L. Pumphrey, T. G. Driver, *J. Am. Chem. Soc.* **2007**, *129*, 7500-7501.

[110] M. Shen, B. E. Leslie, T. G. Driver, *Angew. Chem. Int. Ed.* **2008**, *47*, 5056-5059.

[111] S. Würtz, S. Rakshit, J. J. Neumann, T. Dröge, F. Glorius, *Angew. Chem. Int. Ed.* **2008**, *47*, 7230-7233.

[112] Y. Tan, J. F. Hartwig, *J. Am. Chem. Soc.* **2010**, *132*, 3676-3677.

[113] D. R. Stuart, M. Bertrand-Laperle, K. M. N. Burgess, K. Fagnou, *J. Am. Chem. Soc.* **2008**, *130*, 16474-16475; D. R. Stuart, P. Alsabeh, M. Kuhn, K. Fagnou, *J Am Chem Soc* **2010**, *132*, 18326-18339.

[114] M. P. Huestis, L. Chan, D. R. Stuart, K. Fagnou, *Angew Chem Int Ed Engl* **2011**, *50*, 1338-1341.

[115] A. Penoni, K. M. Nicholas, *Chem Commun* **2002**, 484-485.

[116] F. Ragaini, A. Rapetti, E. Visentin, M. Monzani, A. Caselli, S. Cenini, *J. Org. Chem.* **2006**, *71*, 3748-3753.

[117] A. A. Lamar, K. M. Nicholas, *Tetrahedron* **2009**, *65*, 3829-3833.

[118] J. A. Franz, D. M. Camaioni, R. R. Beishline, D. K. Dalling, *J. Org. Chem.* **1984**, *49*, 3563-3570.

[119] J. Pajak, K. R. Brower, *J. Org. Chem.* **1985**, *50*, 2210-2216.

[120] D. Kim, Y. O. Su, T. G. Spiro, *Inorg. Chem.* **1986**, *25*, 3993-3997.

[121] S. Cenini, S. Tollari, A. Penoni, C. Cereda, *J. Mol. Catal. A: Chem.* **1999**, *137*, 135-146.

[122] J. A. S. Howell, P. M. Burkinshaw, *Chem. Rev.* **1983**, *83*, 557-599.

[123] P. Zardi, A. Caselli, P. Macchi, F. Ferretti, E. Gallo, *Organometallics* **2014**, *33*, 2210-2218.

[124] J.-S. Huang, X.-R. Sun, S. K.-Y. Leung, K.-K. Cheung, C.-M. Che, *Chem. Eur. J.* **2000**, *6*, 334-344.

[125] Y. Xu, S. Zhu, *Tetrahedron* **2001**, *57*, 3909-3913.

[126] F. A. Davis, H. Qiu, M. Song, N. V. Gaddiraju, *J. Org. Chem.* **2009**, *74*, 2798-2803.

[127] R. K. Mishra, C. M. Coates, K. D. Revell, E. Turos, *Org. Lett.* **2007**, *9*, 575-578.

[128] M. Zarei, *Tetrahedron* **2013**, *69*, 6620-6626.

[129] P. Zardi, A. Savoldelli, D. M. Carminati, A. Caselli, F. Ragaini, E. Gallo, *ACS Catal.* **2014**, *4*, 3820-3823.

[130] B. C. Boren, S. Narayan, L. K. Rasmussen, L. Zhang, H. Zhao, Z. Lin, G. Jia, V. V. Fokin, *J. Am. Chem. Soc.* **2008**, *130*, 8923-8930; M. Lamberti, G. C. Fortman, A. Poater, J. Broggi, A. M. Z. Slawin, L. Cavallo, S. P. Nolan, *Organometallics* **2012**, *31*, 756-767; M. M. Majireck, S. M. Weinreb, *J. Org. Chem.* **2006**, *71*, 8680-8683.

[131] G. Mitchell, C. W. Rees, *J. Che. Soc., Perkin Trans. 1* **1987**, 413-422.

[132] D. J. Anderson, T. L. Gilchrist, C. W. Rees, *J. Chem. Soc., Chem. Comm.* **1969**, 147-147.

[133] K. Banert, S. Bochmann, M. Hagedorn, F. Richter, *Tetrahedron Lett.* **2013**, *54*, 6185-6188.

[134] D. J. Anderson, T. L. Gilchrist, G. E. Gymer, C. W. Rees, *J. Che. Soc., Perkin Trans. 1* **1973**, 550-555; R. S. Atkinson, M. J. Grimshire, *J. Che. Soc., Perkin Trans. 1* **1986**, 1215-1224.

[135] W.-L. Man, J. Xie, P.-K. Lo, W. W. Y. Lam, S.-M. Yiu, K.-C. Lau, T.-C. Lau, *Angew. Chem. Int. Ed.* **2014**, *53*, 8463-8466.

[136] J. P. Collman, J. I. Brauman, J. P. Fitzgerald, J. W. Sparapany, J. A. Ibers, *J. Am. Chem. Soc.* **1988**, *110*, 3486-3495.

[137] C. M. Che, W. Y. Yu, in *Pure Appl. Chem., Vol. 71*, **1999**, p. 281.

[138] J. S. Cavaleiro, J. C. Tomé, M. F. Faustino, in *Heterocycles from Carbohydrate Precursors, Vol. 7* (Ed.: E. El Ashry), Springer Berlin Heidelberg, **2007**, pp. 179-248.

[139] I. Grossweiner Leonard, in *Porphyric Pesticides, Vol. 559*, American Chemical Society, **1994**, pp. 255-265.

[140] C.-M. Ho, J.-L. Zhang, C.-Y. Zhou, O.-Y. Chan, J. J. Yan, F.-Y. Zhang, J.-S. Huang, C.-M. Che, *J. Am. Chem. Soc.* **2010**, *132*, 1886-1894.

[141] J. P. C. Tomé, M. G. P. M. S. Neves, A. C. Tomé, J. A. S. Cavaleiro, A. F. Mendonça, I. N. Pegado, R. Duarte, M. L. Valdeira, *Bioorganic & Medicinal Chemistry* **2005**, *13*, 3878-3888.

[142] C.-H. Lee, S. Lee, H. Yoon, W.-D. Jang, *Chem. Eur. J.* **2011**, *17*, 13898-13903.

[143] S. Fantauzzi, E. Gallo, E. Rose, N. Raoul, A. Caselli, S. Issa, F. Ragaini, S. Cenini, *Organometallics* **2008**, *27*, 6143-6151.

[144] D. Intrieri, S. Le Gac, A. Caselli, E. Rose, B. Boitrel, E. Gallo, *Chem Commun* **2014**, *50*, 1811-1813.

[145] Z.-C. Sun, Y.-B. She, Y. Zhou, X.-F. Song, K. Li, *Molecules* **2011**, *16*, 2960-2970.

[146] D. Intrieri, A. Caselli, E. Gallo, *Eur. J. Inorg. Chem.* **2011**, *2011*, 5071-5081.

[147] S. P. Bew, G. D. Hiatt-Gipson, J. A. Lovell, C. Poullain, *Org. Lett.* **2012**, *14*, 456-459.

[148] O. Bortolini, S. Campestrini, F. Di Furia, G. Modena, *J. Org. Chem.* **1987**, *52*, 5093-5095.

[149] K. Oisaki, Y. Suto, M. Kanai, M. Shibasaki, *J. Am. Chem. Soc.* **2003**, *125*, 5644-5645.

[150] Y.-J. Yoon, M.-H. Chun, J.-E. Joo, Y.-H. Kim, C.-Y. Oh, K.-Y. Lee, Y.-S. Lee, W.-H. Ham, *Arch. Pharm. Res.* **2004**, *27*, 136-142.

[151] J. C. Adrian, J. L. Barkin, R. J. Fox, J. E. Chick, A. D. Hunter, R. A. Nicklow, *J. Org. Chem.* **2000**, *65*, 6264-6267.